

COMMENTARY AND WORKED EXAMPLES TO EN 1993-1-5 “PLATED STRUCTURAL ELEMENTS”

B. Johansson, R. Maquoi, G. Sedlacek, C. Müller, D. Beg

Background documents in support to the implementation, harmonization and
further development of the Eurocodes



Joint Report

Prepared under the JRC – ECCS cooperation agreement for the evolution of Eurocode 3
(programme of CEN / TC 250)

First Edition, October 2007

EUR 22898 EN - 2007



COMMENTARY AND WORKED EXAMPLES TO EN 1993-1-5 “PLATED STRUCTURAL ELEMENTS”

B. Johansson, R. Maquoi, G. Sedlacek, C. Müller, D. Beg

Background documents in support to the implementation, harmonization and
further development of the Eurocodes



Joint Report

Prepared under the JRC – ECCS cooperation agreement for the evolution of Eurocode 3
(programme of CEN / TC 250)

First Edition, October 2007

EUR 22898 EN - 2007

The mission of the JRC is to provide customer-driven scientific and technical support for the conception, development, implementation and monitoring of EU policies. As a service of the European Commission, the JRC functions as a reference centre of science and technology for the Union. Close to the policy-making process, it serves the common interest of the Member States, while being independent of special interests, whether private or national.

European Commission
Joint Research Centre

The European Convention for Constructional Steelwork (ECCS) is the federation of the National Associations of Steelwork industries and covers a worldwide network of Industrial Companies, Universities and Research Institutes.

<http://www.steelconstruct.com/>

Contact information

Address: Mies-van-der-Rohe-Straße 1, D-52074 Aachen
E-mail: sed@stb.rwth-aachen.de
Tel.: +49 241 80 25177
Fax: +49 241 80 22140
<http://www.stb.rwth-aachen.de>

Legal Notice

Neither the European Commission nor any person acting on behalf of the Commission is responsible for the use which might be made of this publication.

A great deal of additional information on the European Union is available on the Internet. It can be accessed through the Europa server
<http://europa.eu/>

JRC 38239

EUR 22898 EN
ISSN 1018-5593

Luxembourg: Office for Official Publications of the European Communities

© European Communities, 2007
Reproduction is authorised provided the source is acknowledged

Printed in Italy

Acknowledgements

Both ECCS and the JRC acknowledge the major contribution of the Coordinator of the works, Prof. Bernt Johansson, Division of Steel Structures, Luleå University of Technology, who succeeded in keeping the momentum from the Project Team works in CEN/TC250/SC3 to persuade Project Team members to write this commentary.

The contribution of the many international experts who have supported the works by their comments and reviews as stated in the introduction is also acknowledged.

Foreword

The EN Eurocodes are a series of European standards which provide a common series of methods for calculating the mechanical strength of elements playing a structural role in construction works, i.e. the structural construction products. They make it possible to design construction works, to check their stability and to give the necessary dimensions of the structural construction products.

They are the result of a long procedure of bringing together and harmonizing the different design traditions in the Member States. In the same time, the Member States keep exclusive competence and responsibility for the levels of safety of works.

According to the Commission Recommendation of 11 December 2003 on the implementation and use of Eurocodes for construction works and structural construction products, the Member States should take all necessary measures to ensure that structural construction products calculated in accordance with the Eurocodes may be used, and therefore they should refer to the Eurocodes in their national regulations on design.

The Member States may need using specific parameters in order to take into account specific geographical, geological or climatic conditions as well as specific levels of protection applicable in their territory. The Eurocodes contain thus 'nationally determined parameters', the so-called NDPs, and provide for each of them a recommended value. However, the Member States may give different values to the NDPs if they consider it necessary to ensure that building and civil engineering works are designed and executed in a way that fulfils the national requirements.

The so-called background documents on Eurocodes are established and collected to provide technical insight on the way the NDPs have been selected and may possibly be modified at the national level. In particular, they intend to justify:

- The theoretical origin of the technical rules,
- The code provisions through appropriate test evaluations whenever needed (e.g. EN 1990, Annex D),
- The recommendations for the NDPs,
- The country decisions on the choice of the NDPs.

Collecting and providing access to the background documents is essential to the Eurocodes implementation process since they are the main source of support to:

- The Member States, when choosing their NDPs,
- To the users of the Eurocodes where questions are expected,
- To provide information for the European Technical Approvals and Unique Verifications,
- To help reducing the NDPs in the Eurocodes when they result from different design cultures and procedures in structural analysis,
- To allow for a strict application of the Commission Recommendation of 11 December 2003,
- To gradually align the safety levels across Member States,
- To further harmonize the design rules across different materials,
- To further develop the Eurocodes.

This joint ECCS-JRC report is part of a series of background documents in support to the implementation of Eurocode 3. It provides background information on the specific issue of plated steel structures addressed in EN 1993-1-5.

For the design of plated steel structures, the rules for shear lag effects and plate buckling that have been specified in EN 1993-1-5 may look novel for many practitioners who so far have been

acquainted to traditional national rules. These rules draw their reliability and satisfactory applicability not so much from time-testing, but from systematic evaluations of test results to prove compliance with the European reliability requirements and from a certain amount of worked examples and more and more emerging successful practical applications.

This commentary is meant to provide the following:

- The background of the rules,
- Their reliability basis,
- Explanations on how they are meant to be used,
- Some key examples.

The European Convention for Constructional Steelwork (ECCS) has initiated the development of this commentary in the frame of the cooperation between the Commission (JRC) and the ECCS for works on the further evolution of the Eurocodes. It is therefore published as a Joint Commission (JRC)-ECCS report.

Aachen, Delft and Ispra, August 2007

Gerhard Sedlacek

Chairman of the ECCS Technical Management Board

Frans Bijlaard

Chairman of CEN/TC 250/SC 3

Michel Gérardin, Artur Pinto and Silvia Dimova

European Laboratory for Structural Assessment, IPSC, JRC

Content

1	Introduction	1
1.1	General	1
1.2	Calibration of the safety level	2
1.3	References	6
2	Design of plated members	7
2.1	General	7
2.2	Effective width models for global analysis	8
2.3	Plate buckling effects	9
2.3.1	General	9
2.3.2	Reduced stress method and effective width approach	10
2.3.3	Plate buckling verification methods	16
2.3.4	The general method	17
2.3.5	The component method	19
2.4	Serviceability limits	21
2.4.1	General	21
2.4.2	Rules to avoid excessive plate breathing	21
2.4.3	Comparison of SLS and ULS limit state verification	22
3	Effective width approaches in design	27
3.1	Contributory areas without shear lag effects	27
3.2	Shear lag effects	30
3.3	Basic situations	33
3.4	Conclusions	35
3.5	Symmetrical and asymmetrical loading	39
3.6	Effects at the ultimate limit state	39
4	Plate buckling effects due to direct stresses	41
4.1	Introduction	41
4.2	General verification procedures	42
4.3	Approach based on the reduced cross-section concept	45
4.3.1	General	45
4.3.2	Plate behaviour	46
4.3.3	Column behaviour	50
4.3.4	Interpolation between plate behaviour and column behaviour	54
4.3.5	Plate buckling check	55
4.3.6	Validation of plate buckling check procedure	56
4.4	References	57

5	Resistance to shear	59
5.1	Introduction	59
5.2	Design shear resistance according to EN 1993-1-5	61
5.2.1	General	61
5.2.2	Contribution from the web	63
5.2.3	Contribution from the flanges	69
5.2.4	Shear resistance check	71
5.2.5	Verification of the shear resistance formula	71
5.3	Conclusions	72
5.4	References	73
6	Resistance to transverse loads	74
6.1	Background	74
6.1.1	Buckling	74
6.1.2	Yielding	75
6.1.3	Combined models	76
6.2	Model for patch loading resistance	78
6.2.1	Plastic resistance	78
6.2.2	Critical force	80
6.2.3	Reduction factor	81
6.2.4	Influence of longitudinal stiffeners	85
6.3	Calibration of design rules versus test results	88
6.4	Outlook	90
6.5	References	91
7	Interaction	93
7.1	Interaction between shear force, bending moment and axial force	93
7.1.1	Plastic resistance	93
7.1.2	Buckling resistance	95
7.2	Interaction between transverse force, bending moment and axial force	98
7.3	References	99
8	Flange induced buckling	100
9	Stiffeners and detailing	103
9.1	Introduction	103
9.2	Direct stresses	104
9.2.1	Minimum requirements for transverse stiffeners	104
9.2.2	Minimum requirements for longitudinal stiffeners	115
9.2.3	Splices of plates	116

9.2.4	Cut-outs in stiffeners	117
9.3	Shear stresses	117
9.3.1	Rigid end post	117
9.3.2	Non-rigid end post	119
9.3.3	Intermediate transverse stiffeners	120
9.3.4	Longitudinal stiffeners	121
9.3.5	Welds	121
9.4	Transverse loads	122
9.5	References	122
10	The reduced stress method	123
10.1	Basic procedure	123
10.2	Modification of plate buckling curves	125
10.3	Justification of the procedure	127
10.3.1	Stiffened panels with a stress field $\sigma_{x,Ed}$	127
10.3.2	Unstiffened and stiffened panels with stress fields $\sigma_{x,Ed}$, $\sigma_{z,Ed}$ and τ_{Ed}	128
10.3.3	Unstiffened panels with stress fields from patch loading	129
10.3.4	Stiffened panels with stress field from patch loading	131
10.3.5	Unstiffened panels with stress field for patch loading, bending and shear	132
10.3.6	Concluding comparison of test and calculation results	134
11	Annex A to EN 1993-1-5 – Calculation of critical stresses for stiffened plates	136
11.1	Case of multiple stiffeners	136
11.2	Case of one or two stiffeners	137
12	Annex C to EN 1993-1-5 – Finite Element Methods of analysis (FEM)	142
12.1	Introduction	142
12.2	Modelling for FE-calculations	143
12.3	Choice of software and documentation	143
12.4	Use of imperfections	144
12.4.1	Geometrical imperfections	144
12.4.2	Residual stresses	146
12.4.3	Combination of imperfections	147
12.5	Material properties	149
12.6	Loads	150
12.7	Limit state criteria	150
12.8	Partial factors	150
12.9	References	151

13 Annex D to EN 1993-1-5 – Plate girders with corrugated webs	152
13.1 Background	152
13.2 Bending moment resistance	153
13.3 Shear resistance	156
13.3.1 Introduction	156
13.3.2 Model according to Leiva [5]	159
13.3.3 Model according to Lindner [6]	159
13.3.4 Model according to Johnson [8]	160
13.3.5 Combined model	161
13.3.6 Model according to EN 1993-1-5	162
13.3.7 Discussion	165
13.4 Patch loading	166
13.5 References	166
14 Annex E to EN 1993-1-5 – Refined methods for determining effective cross sections	168
14.1 Effective areas for stress levels below the yield strength	168
14.2 Effective areas for stiffness	170
14.3 References	171
15 Worked example – Launching of a box girder	172
15.1 Patch loading	173
15.2 Bending	174
16 Worked example – Orthotropic plate with trapezoid stiffeners	181
16.1 Data	181
16.2 Direct stresses	182
16.2.1 Subpanels – calculation of effective ^p areas of subpanels	182
16.2.2 Stiffened plate	183
16.2.3 Minimum requirements for longitudinal stiffeners	188
16.3 Resistance to shear	188
16.3.1 Stiffened plate	188
16.3.2 Subpanels	189
16.3.3 Shear buckling factor	190
16.3.4 Verification	190
16.4 Interaction M-V-N	191

17 Worked example – Plate girder	192
17.1 Data	192
17.2 Shear lag in the flanges	193
17.2.1 Elastic shear lag (serviceability, fatigue)	193
17.2.2 Elastic – plastic shear lag (ULS)	194
17.3 Panel I (at the exterior support)	194
17.3.1 Rigid end post	195
17.3.2 Shear resistance	195
17.3.3 Verification for shear resistance	196
17.3.4 Verification of bending resistance	197
17.3.5 Verification of interaction M-V	197
17.4 Panel II (at midspan)	197
17.4.1 Verification of shear resistance	197
17.4.2 Verification of bending resistance	197
17.4.3 Interaction M-V	197
17.5 Panel III (at the interior support)	197
17.5.1 Calculation of normal stresses	198
17.5.2 Local buckling of an individual web subpanel	199
17.5.3 Stiffened web	202
17.5.4 Plate type behaviour	206
17.5.5 Column type behaviour	207
17.5.6 Interaction between plate and column buckling	209
17.5.7 Calculation of effective geometric characteristics	209
17.5.8 Verification of bending resistance	210
17.5.9 Resistance to shear	211
17.5.10 Interaction M-V	214
17.5.11 Minimum requirements for longitudinal stiffeners	216
17.5.12 Intermediate transverse stiffeners	218
17.6 Web to flange weld	223
17.7 Flange induced buckling	224
17.8 Vertical stiffener above the interior support	224

1 Introduction

Bernt Johansson, Division of Steel Structures, Luleå University of Technology

Gerhard Sedlacek, Christian Müller, Lehrstuhl für Stahlbau und Leichtmetallbau, RWTH Aachen

1.1 General

New design rules for plated structures have been developed by CEN/TC250/SC3 by a project team consisting of

Professor Darko Beg, University of Ljubljana

Mr Bruno Chabrolin, CTICM

Mr Richard Craig, Atkins highways and transportation

Professor Bernt Johansson, Luleå University of Technology, convener

Professor René Maquoi, University of Liege

Dr. Christian Müller, RWTH

Professor Gerhard Sedlacek, RWTH

The result of the work is EN 1993-1-5:2004 with the full name **Eurocode 3 Design of Steel Structures. Part 1.5 Plated Structural Elements** [1]. It is based on the previous version ENV 1993-1-5:1997, which has been thoroughly updated and complemented according to requests from CEN members. It has been drafted in close co-operation with the project team preparing the steel bridge code and it contains rules for stiffened or unstiffened plated structures. The main theme is resistance to plate buckling and several other Eurocodes refer to these rules, not only the bridge code.

The objective of this commentary is to present the scientific background to the rules. The mechanical models behind the rules are presented and references to source documents are given. All such models include simplifications, which have to be justified by calibration of the rules against test results. Several models for each failure mode have been checked with calibrations according to Annex D of EN 1990 [2] and the ones included in EN 1993-1-5 are those giving the lowest scatter and the most uniform safety. The procedure for calibration will be summarised in section 1.2. It should be noted that EN 1993-1-5, being a generic code, does not suggest γ_M values. According to the Eurocode system these values depend on the specific application and should be given by application parts e.g. for buildings in EN 1993-1-1 [3] and bridges in EN 1993-2 [4].

Although the rules may look unfamiliar to many engineers they are in fact only a new combination of rules from different European countries. For the time being they represent a set of useful rules for common plated structures. The intention is to cover beam type of structures like I-girders and box-girders. There are also details that may be improved by further research and some indications are given in this commentary.

This commentary is organised mainly in the same way as the code. In the right hand margin of the pages there are references to the specific clause in the code that the text refers to. The section headings follow that of the code but sometimes

related rules from other sections are dealt with together with the main topic of the section. References to literature are given in the end of each section. Some sections go quite far into detail with the intention of documenting unpublished work with development of design rules during the drafting of the code.

This commentary is not an official document from CEN but a private initiative by the authors. The content of commentary expresses the opinion of the author of each section although the content has been reviewed within the group. This applies also to clarifications and interpretations of the code.

In addition to giving background information to the sections of EN 1993-1-5 this commentary also presents some worked examples in Section 15, 16 and 17. They show how the rules of the code can be applied in practical design.

1.2 Calibration of the safety level

Many of the design rules in EN 1993-1-5 have been calibrated versus test results by a statistical evaluation according to Annex D of EN 1990 [2]. This general description of the procedure is an updated version of the presentation in [5]. The procedure uses the following definitions and assumptions.

It is assumed that both the action effects E and the resistance R of a structure are subject to statistical normal distributions, which are characterized by mean values "m" and standard deviations "σ", see Figure 1.1.

To guarantee that the distribution of the action effects E and the resistance R have a sufficient safety distance a safety index β is defined in EN 1990 as follows:

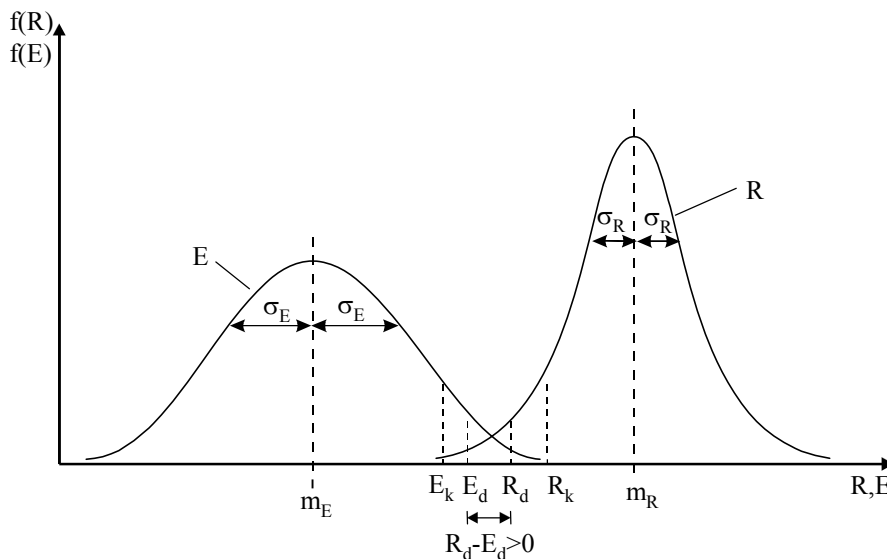


Figure 1.1: Statistical distribution of the action effects and the resistances

$$\beta = \frac{m_R - m_E}{\sqrt{\sigma_R^2 + \sigma_E^2}} \geq 3.8 \tag{1.1}$$

where:

m_E is the mean value of the action effects;

m_R is the mean value of the resistance;
 σ_E is the standard deviation of the action effects;
 σ_R is the standard deviation of the resistance.

The safety requirement for a structure is defined by the criterion

$$[R_d] - [E_d] > 0 \tag{1.2}$$

where $[R_d]$ and $[E_d]$ are design values.

To define the design values in equation (1.2), the equation (1.1) may be expressed by:

$$\left[m_R - \frac{\sigma_R}{\sqrt{\sigma_R^2 + \sigma_E^2}} \beta \sigma_R \right] - \left[m_E - \frac{-\sigma_E}{\sqrt{\sigma_R^2 + \sigma_E^2}} \beta \sigma_E \right] \geq 0 \tag{1.3}$$

With the notations:

$$\alpha_R = \frac{\sigma_R}{\sqrt{\sigma_R^2 + \sigma_E^2}}$$

$$\alpha_E = \frac{\sigma_E}{\sqrt{\sigma_R^2 + \sigma_E^2}}$$

it is possible to express the design values as:

$$R_d = m_R - \alpha_R \beta \sigma_R \tag{1.4}$$

$$E_d = m_E + \alpha_E \beta \sigma_E \tag{1.5}$$

With the approximations $\alpha_R = 0,8$ and $\alpha_E = 0,7$ (see EN 1990, C7, D.7.3 and D.8.3) the design values of the action effects and of the resistances can be described independently from each other and a more detailed investigation of the design value of the resistance can be carried out using the statistical procedure given in Annex D of EN 1990.

In a first step of this procedure a resistance function $r_t = g_R(\bar{x})$, the so called design model for the resistance, has to be established. This is an arithmetic expression describing the influence of all relevant parameters x on the resistance r which is investigated by tests. By comparing the strength values from the resistance function r_t with test results r_e , see Figure 1.2, the mean value correction factor \bar{b} for the resistance function r_t and the standard deviation s_δ for the deviation term δ can be determined. This gives the following formula describing the field:

$$R = \bar{b} r_t \delta \tag{1.6}$$

In most cases the probabilistic density distribution of the deviation term δ cannot be described by a single normal distribution as it is assumed in Figure 1.2. It may be represented by a non-normal distribution, which may be interpreted as a composition of two or more normal distributions. Therefore the density distribution for the resistance is checked by plotting the measured probability distribution on a Gaussian paper. If the plot shows a straight line, the actual distribution corresponds to a unimodal normal distribution as assumed and the statistical data (\bar{b} and S_δ) are determined with the standard formulas provided in

Annex D of EN 1990.

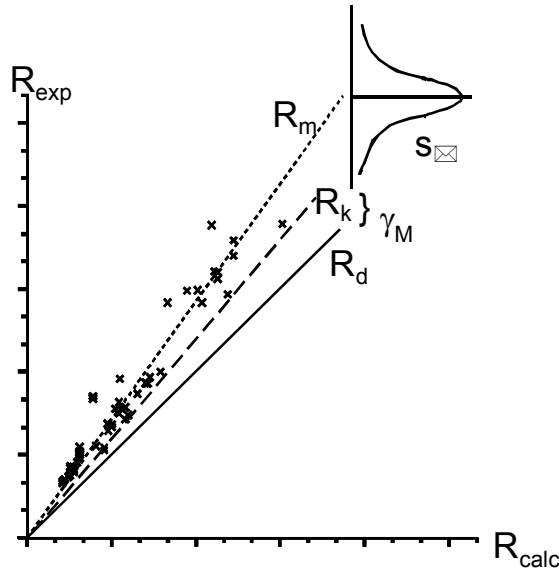


Figure 1.2: Plot of $r_e - r_t$ values, mean value correction \bar{b} and standard deviation s_δ of the deviation term δ

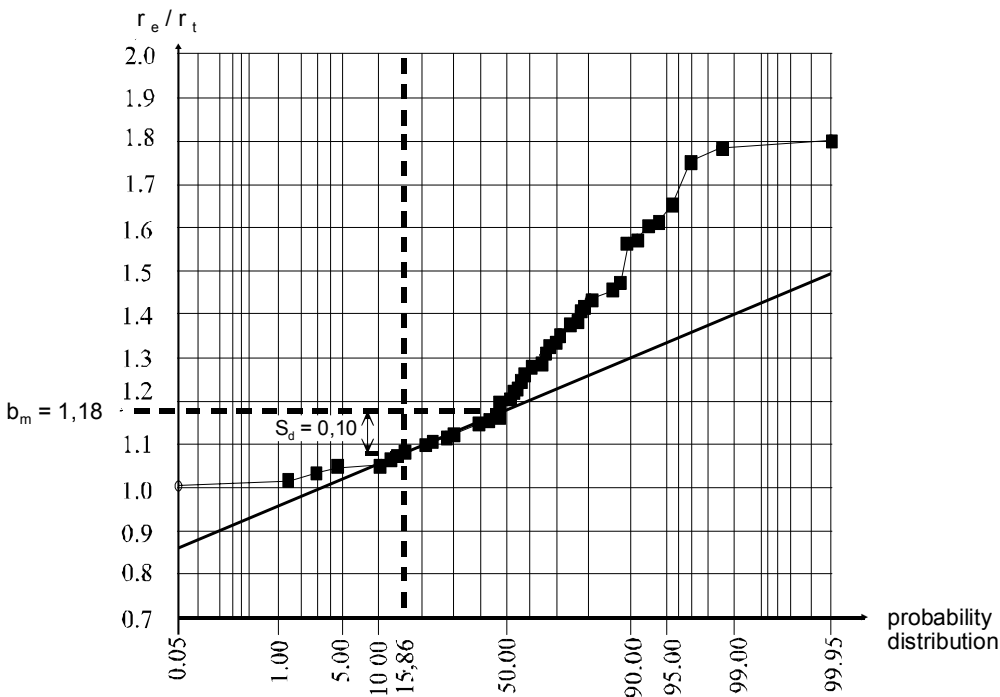


Figure 1.3: Plot of r_{ei}/r_{ti} – values on Gaussian paper and definition of the relevant normal distribution at the design point

For the case that the plot shows a curved line the relevant normal distribution at the design point is determined by a tangent to the lower tail of the measured distribution, see Figure 1.3.

The statistical data \bar{b} and s_δ of the relevant normal distribution are then determined from the tangent approach to the actual distribution.

In general the test population is not representative for the total population of structures and therefore is only used to determine the mean value deviation \bar{b} and

the scatter value S_δ of the design model. To consider scatter effects of parameters not sufficiently represented by the test population the standard deviation of the resistance has to be increased. To this end in addition to the standard deviation S_δ , the following variation coefficients are taken into account for the yield strength and geometrical values (see Table 1.1).

Table 1.1: Variation coefficients

	Mean	Coeff. of variation
Yield strength f_y	$1,14f_{y,nom}$	0,07
Thickness t	t_{nom}	0,05 (0,03)
Plate width b	b_{nom}	0,005 (0,01)

These coefficients of variation are combined with the standard deviation s_δ according to eq. (1.7):

$$\sigma_R = \sqrt{\sum \sigma_{R_i}^2 + s_\delta^2} \tag{1.7}$$

Using a log normal distribution for R the characteristic value R_k of the resistance function may be represented by the 5% fractile value and can be obtained from eq. (1.8):

$$R_k = \bar{b} m_R \exp(-1,64 \sigma_R - 0,5 \sigma_R^2) \tag{1.8}$$

Also, the design value R_d of the resistance function may be defined by:

$$R_d = \bar{b} m_R \exp(-\alpha_R \beta \sigma_R - 0,5 \sigma_R^2) \tag{1.9}$$

where $\alpha_R \beta = +0,8 \cdot 3,8 = +3,04$

The γ_M - value of the resistance function is obtained from the ratio of the characteristic value to the design value:

$$\gamma_M = \frac{R_k}{R_d} \tag{1.10}$$

In most cases instead of a 5% fractile value R_k a value R_{nom} with nominal values for the input parameters is used as characteristic value. To consider R_{nom} instead of R_k a modified partial safety factor γ_M^* is used from:

$$\gamma_M^* = \Delta k \gamma_M \tag{1.11}$$

where $\Delta k = R_{nom}/R_k$.

For the resistance functions for plate buckling Δk may be expressed by:

$$\Delta k = \frac{\exp(-2,0 \sigma_{fy} - 0,5 \sigma_{fy}^2)}{\bar{b} \exp(-1,64 \sigma_R - 0,5 \sigma_R^2)} = \frac{0,867}{\bar{b} \exp(-1,64 \sigma_R - 0,5 \sigma_R^2)} \tag{1.12}$$

where the nominal yield strength is considered as the mean minus 2 standard deviations of the yield strength distribution.

The procedure explained above is used in the following to determine the γ_M^* values for the resistance functions for plate buckling due to compressive stresses,

shear buckling and buckling due to patch loading. Where γ_M^* is not in compliance with the target value $\gamma_M^* = 1,00$ to $1,10$ used for stability checks, the function R_{nom} is subsequently modified by a factor to reach the target value γ_M^* .

1.3 References

- [1] Eurocode 3 EN 1993-1-5:2004: Design of Steel Structures. Part 1.5 Plated Structural Elements,
- [2] Eurocode EN 1990:2003: Basis of structural design
- [3] Eurocode 3 EN 1993-1-1:2004: Design of Steel Structures. Part 1.1 General rules and rules for buildings
- [4] Eurocode 3 EN 1993-2:2004: Design of Steel Structures. Part 2 Bridges
- [5] Johansson B., Maquoi R., Sedlacek G., New design rules for plated structures in Eurocode 3, Journal of Constructional Steel Research 57, 2001, pp 279-311.

2 Design of plated members

Gerhard Sedlacek, Christian Müller, Lehrstuhl für Stahlbau und Leichtmetallbau, RWTH Aachen

2.1 General

- (1) In general bar structures are designed using the hypothesis of linear strain distributions for a cross section:

$$\varepsilon(z) = z \eta'' \quad (2.1)$$

where ε is the strain,

z is the distance of the point considered from the neutral axis,

η'' is the curvature for the deformation η .

- (2) Using a linear material law for the elastic range:

$$\sigma = E \varepsilon \quad (2.2)$$

where σ is the stress,

E is the modulus of elasticity.

The stress distribution is also linear.

- (3) In consequence there is an easy way to determine cross sectional properties as:

I second moment of area,

W elastic section modulus,

and to determine stresses from action effects.

- (4) There are three causes for deviations from this linear stress distributions:

a) by exceeding the elastic range, where strain distributions are still linear but stress responses are not because of exceedance of yield;

b) by local buckling where strain distributions along the original plane elements are considered to be linear but stress responses are not because of the stiffness reduction due to out of plane local buckling;

c) by shear deformations in the plane elements where the strain distributions deviate from linear distributions and cause a non linear stress distribution with shear lag.

All these effects may interact and are the more pronounced the more the strain situation approaches the limit states.

- (5) By using the concept of effective widths the non linear effects from shear lag, plate buckling and the combination of both may be modelled keeping the hypothesis of linear strain distributions and the easy way to determine cross sectional properties and stresses.

EN 1993-1-5
§2.1

- (6) There are three effective widths distinguished according to their cause:
- effective^s width from shear lag;
 - effective^p width from local plate buckling;
 - effective width from interaction of effective^s width and effective^p width.

NOTE The single terminology in English (effective) needs a reference to either shear lag or to plate buckling or to both together while these separate effects are sometimes clearly distinguished in other languages.

- (7) In general these effective widths apply to the cross section at the location in the structure, for which they are determined, to calculate the stress distributions at that location. They also govern the stiffness of the cross section for the curvature at that location. As however the distribution of action effects along a structure is governed by the integral of stiffness along the length and not so much by local stiffness reduction when local buckling occurs, there is a variation of the strains along the supported edges that leads to an increased stiffness compared to the lowest local value that corresponds to effective areas for resistance valid at the peak of the buckles, see section 14. The effective width for the integral stiffness is larger than that for local stresses so that different indications are made for effective widths for:
- global analysis (see section 2.2);
 - local assessments (see section 2.3).

2.2 Effective width models for global analysis

- (1) The effects of shear lag (see section 3) and of plate buckling (see section 4) on the stiffness of members and joints should be taken into account in the global analysis.
- (2) The effects of shear lag in flanges on the global analysis may be taken into account by the use of an effective^s width. For simplicity this effective^s width may be assumed to be uniform over the length of the span. For each span of a member the effective^s width of flanges should be taken as the lesser of the full width and $L/8$ per side of the web, where L is the span or twice the distance from the support to the end of a cantilever.
- (3) The effects of plate buckling in elastic global analysis may be taken into account by effective^p cross sectional areas of the elements in compression, see EN 1993-1-5, 4.3. For global analysis the effect of plate buckling on the stiffness may be ignored when the effective^p cross-sectional area of an element in compression is not less than $\rho_{\text{lim}} = 0,5$ - times the gross cross-sectional area of the same element. When the latter condition is not fulfilled EN 1993-1-5, Annex E applies.

2.3 Plate buckling effects

2.3.1 General

- (1) EN 1993-1-5 provides two methods for considering plate buckling effects:
 1. a method to determine the resistance of a cross section by "effective widths" of its various plate elements in compression, where the reduction of stiffness and strength due to local plate buckling is reflected by a reduced section with "holes" in the cross sectional area, which is supposed to be stressed until the flanges reach yielding;
 2. a method to determine the resistance of a cross section by limiting the stresses in its various plate elements without considering "holes" by using "reduced stress limits" due to local buckling.

The most cautious way in this method is to limit the linear stress distribution of the cross section to the stress limit of the plate element that buckles first. This may be very conservative because it does not consider load-shedding e.g. from webs to flanges due to first plate buckling in the web, as the reduced section method does.

Less conservative approaches for the "reduced stress method" are to consider further straining of the cross section after the first plate buckling of the weakest part up to attaining the "stress limit" of the strongest plate element or even the yielding strain. These approaches are not yet explicitly specified in EN 1993-1-5, however they may be used where appropriate.
- (2) The "reduced section" method with effective width and the "reduced stress method" are different methods and as such they are specified in EN 1993-1-5 in separate sections:
 1. The "reduced section" method is specified in section 4, 5, 6, and 7, where section 4, 5 and 6 are related to the various stress components, for which separate plate buckling checks are performed to combine their effects with interaction formulae in section 7.
 2. The "reduced stress" method is specified in section 10. It generally works with the full stress field without separating it to stress components and therefore is particularly suitable for FE-calculations.
- (3) Though these two methods look quite different, it can be demonstrated that if they are used to solve the same problem of ultimate resistance of a section, they give in all cases of longitudinal stresses the same, in cases of combined stresses about the same results.
- (4) In order to guide the user of EN 1993-1-5 to a choice of the method appropriate for his problem in the following an explanation of the equivalence of the two methods and of their differences is given, whereby also some fundamentals are given where necessary.

2.3.2 Reduced stress method and effective width approach

Cross-section in compression

- (1) Cross-sections of prismatic members in compression may be modelled as a set of separate plate elements that are subject to compression, see Figure 2.1.

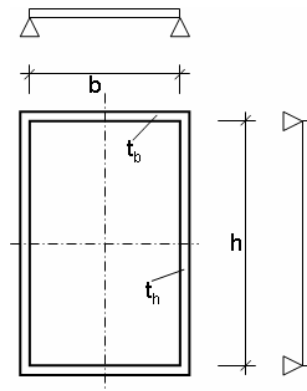


Figure 2.1: Cross-section composed of separate linear plate elements

- (2) Each of the plate elements may have a buckling strength

$$\sigma_{\text{limit}} = \rho \cdot f_y \tag{2.3}$$

where

ρ is the plate buckling reduction factor depending on the plate slenderness $\bar{\lambda}_p = \sqrt{\frac{f_y}{\sigma_{\text{crit}}}}$

f_y is the yield strength;

σ_{limit} is the mean value of a stress distribution resulting from local buckling of the plate element, see Figure 2.2.

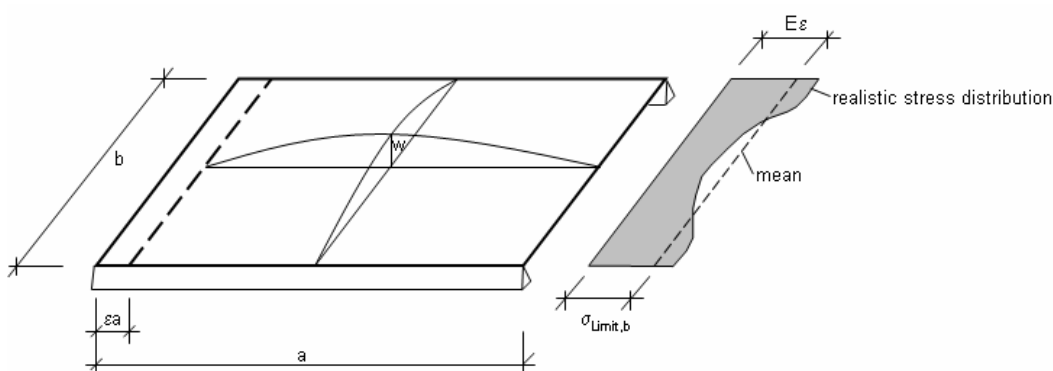


Figure 2.2: Distribution of stress σ caused by local buckling w of a plate element (a , b) subjected to the compression strain ϵ

- (3) This leads to a distribution of buckling strength as given in Figure 2.3 for the case of a doubly symmetrical cross-section with the consequence that the cross-section behaves as that of a hybrid column.

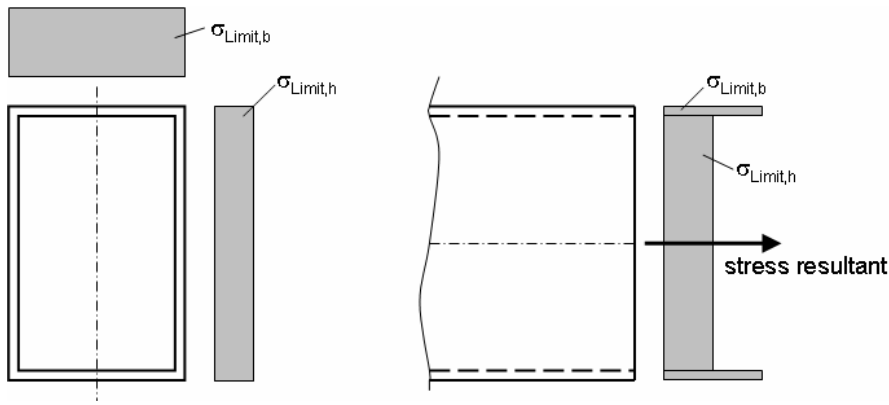


Figure 2.3: Distribution of plate buckling strength along the contour of a doubly symmetrical cross-section

- (4) In assuming, that the stress-strain curve of a single plate element subject to plate buckling can be modelled as a bilinear function, see Figure 2.4.

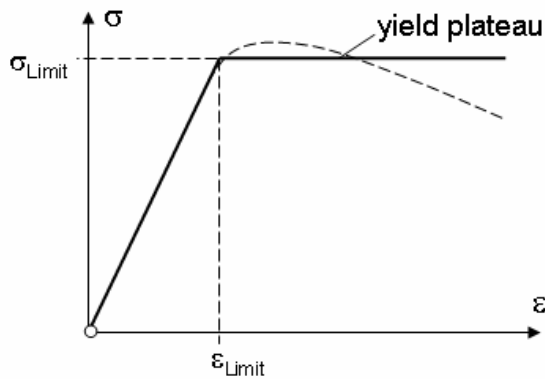


Figure 2.4: Modelling of the stress-strain relationship for plate buckling as a bilinear function

the stress-strain characteristic of the full cross-section in Figure 2.3 looks like as given in Figure 2.5.

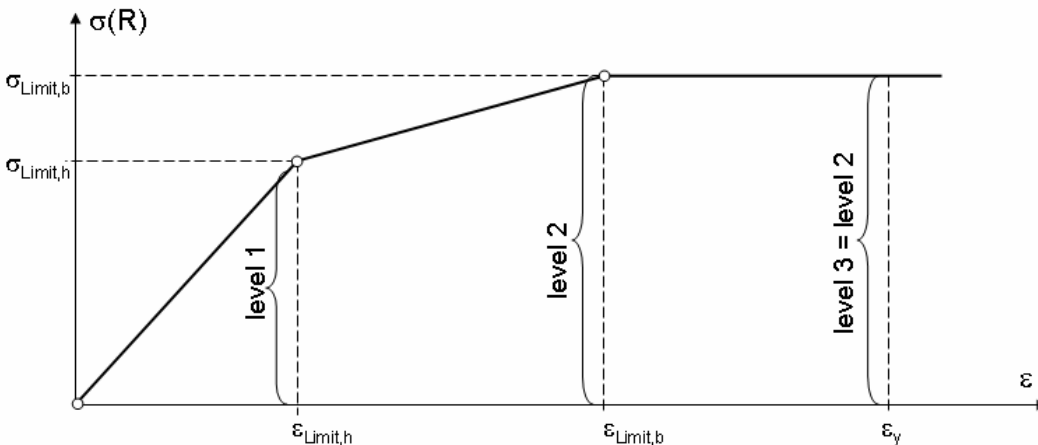


Figure 2.5: Stress-strain function for a cross-section

- (5) The resistance of the cross-section to plate buckling may be expressed by three levels:

Level 1: $R_{ult} = (h \cdot t_h + b \cdot t_b) \sigma_{limit, h} = \left(\sum A_i \right) \cdot \sigma_{limit, min}$ (2.4)

where $\sigma_{limit, h}$ is the plate buckling strength of the weakest plated element.

Level 2: $R_{ult} = h \cdot t_h \cdot \sigma_{limit, h} + b \cdot t_b \cdot \sigma_{limit, b} = \sum A_i \cdot \sigma_{limit, i}$ (2.5)

where the “straining capacities” of the weakest plate elements are exploited until the plate buckling strength of the strongest plate element is reached.

Level 3: $R_{ult} = \sum A_i \cdot \sigma_{limit, i}$ (2.6)

where the “straining capacities” of the weakest and the strongest parts are exploited to reach a strain ϵ_y (equivalent to yielding f_y).

- (6) For each plate element "i" there is an equivalence between the resistance calculated with the reduced stress $\sigma_{limit, i}$ or calculated with the reduced section $A_{eff, i}$:

$R_{ult, i} = b_i \cdot t_i \cdot \sigma_{limit, i} = b_{eff, i} \cdot t_i \cdot f_y$ (2.7)

$= A_{cross, i} \cdot \sigma_{limit, i} = A_{eff, i} \cdot f_y$

see Figure 2.6, if an increase of strains to ϵ_y is accepted, see Figure 2.5.

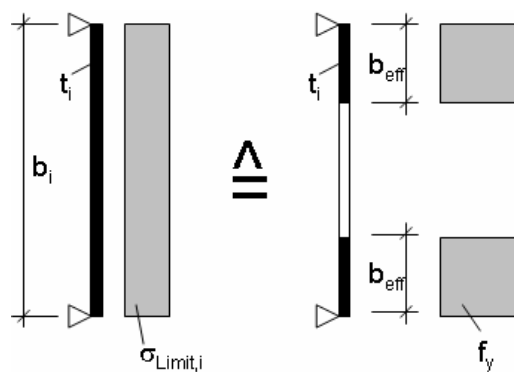


Figure 2.6: Equivalence of R_{ult}

- (7) Though in the case of symmetrical cross-sections in compression only the resistances R_{ult} for level 2 and level 3 are the same, the acceptance of strains exceeding the maximum strains for plate-buckling of the strongest plate-element may lead to a level 3 larger than level 2 for cross-sections in bending.
- (8) The equivalence leads to the concept of effective widths b_{eff} or effective cross-sections A_{eff} with a relation to the stress-strain curve of the cross-section as demonstrated in Figure 2.7.

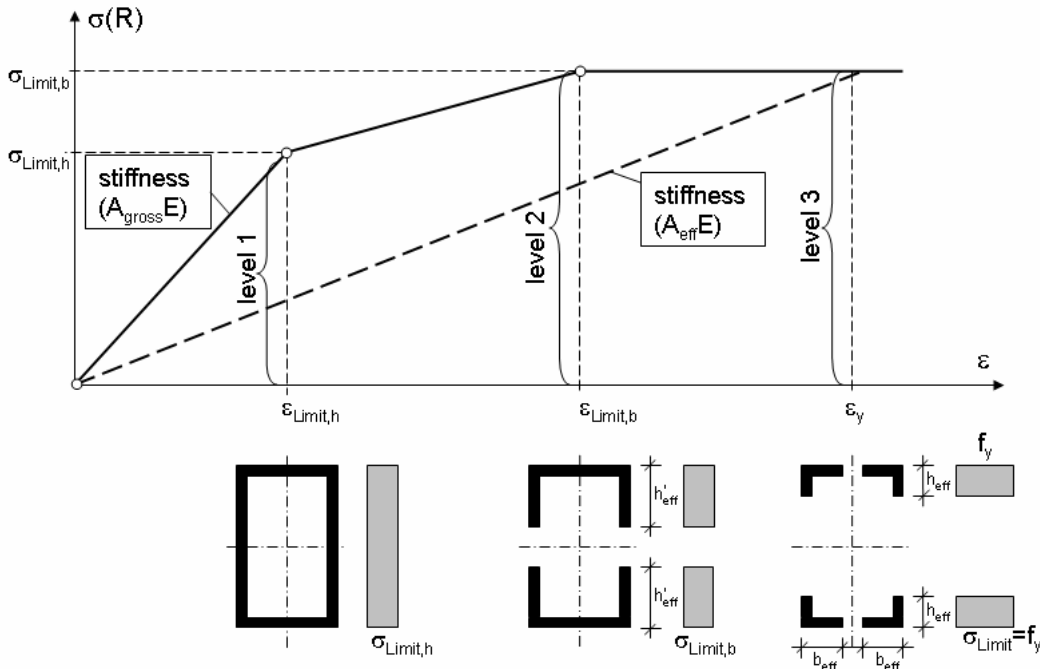


Figure 2.7: Development of effective cross-sections versus the strains ϵ

- (9) In case of singly symmetrical cross-sections with compression, see Figure 2.8, the stress resultant R_{ult}^* has an eccentricity Δe_N .

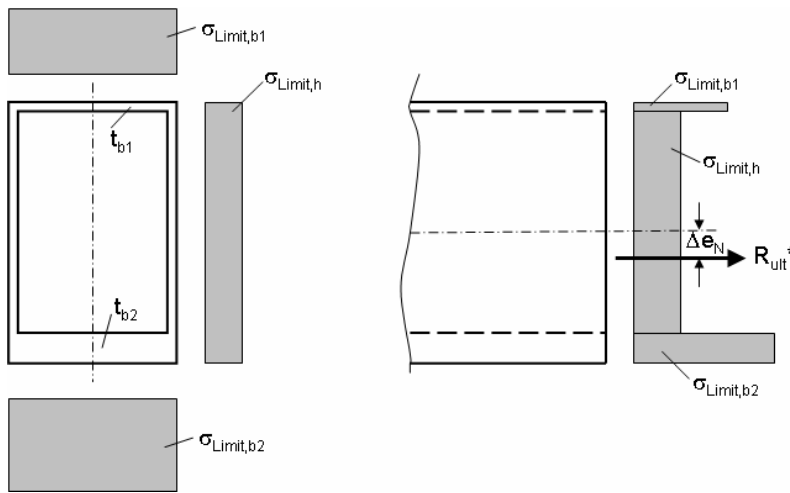


Figure 2.8: Singly symmetrical cross-section in compression

- (10) Figure 2.9 gives the relationship between the eccentricity Δe_N and the level of strength.

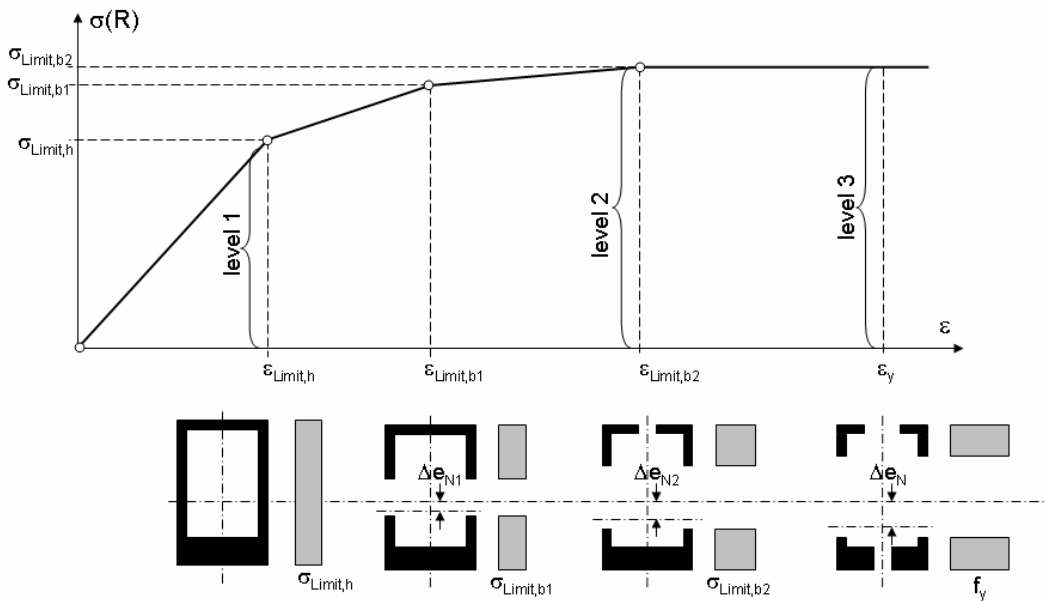


Figure 2.9: Development of eccentricity of neutral elastic axis versus the strain ϵ

- (11) It is apparent, that the effective area A_{eff} depends on the stresses/strains to which it refers.

Cross-section in bending

- (1) As for cross-sections in compression the development of plate buckling resistance starts with the stress distribution obtained from the gross cross-section, Figure 2.10.

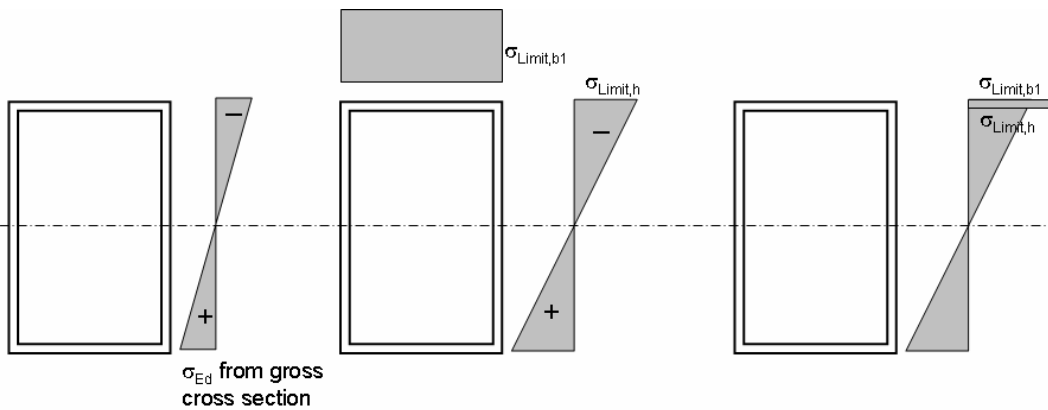


Figure 2.10: Distribution of plate buckling strength for bending

- (2) The development of the various strength levels and eccentricities Δe_M versus the strain in the compression flange may be taken from Figure 2.11.

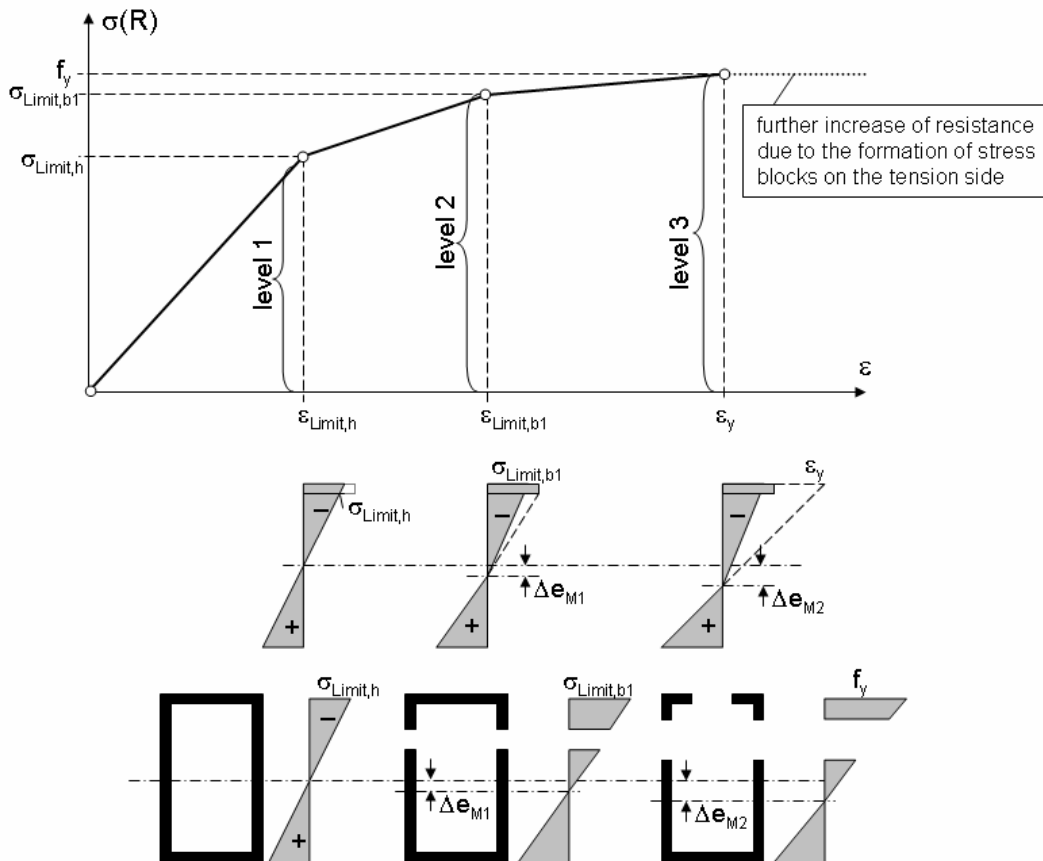


Figure 2.11: Development of strength and eccentricity versus the compression strain in the compression flange

- (3) Whereas the eccentricity Δe_N for columns in compression results in an additional bending moment $\Delta M = N_{Ed} \cdot \Delta e_N$ to be considered in design if the axial force retains its original position, the eccentricity Δe_M for beams in bending resulting from the equilibrium of stress distributions in the cross-section leads to an iterative procedure for determining the final elastic neutral axis of the cross-section. The use of effective widths instead of the plate buckling strength distributions is helpful for these iterations and also allows to determine the local stiffnesses.
- (4) It is evident, that for bending the resistance R_{ult} for level 3 is higher than the resistance for level 2 and that the resistance for level 3 defined for the maximum strain ϵ_{fy} could be further increased, if the strain limitation ϵ_y in the tension flange and the compression flange would be abandoned. This would asymptotically lead to stress block distributions as illustrated in Figure 2.12. Under certain stabilizing aspects, see EN 1993-1-1 such stress block distributions can be used.

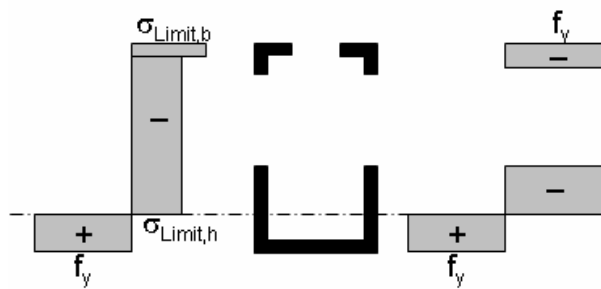


Figure 2.12: Maximum bending resistance for large compression strains

Conclusions

- (1) Depending on the strain accepted for the extreme plate element in compression of a cross-section the reduced stress method provides different resistances with the following three resistance levels:
 - level 1 limits the exploitation of the cross-section to the plate buckling resistance of the weakest plate element
 - level 2 allows for stress redistribution up to the plate buckling resistance of the strongest plate element
 - level 3 allows to straining the extreme plate elements in compression to the yield strain (equivalent to the yield strength of the material) with the possibility of exploiting further reserves.
- (2) The application of the reduced stress-method allowing for stress redistribution in the cross-section on one hand and the effective width approach on the other hand are fully equivalent with respect to the ultimate resistance of the cross section.
- (3) The effective width approach is advantageous because of easier iterations for determining the actual elastic neutral axis and because of determining the local stiffness.
- (4) Longitudinal stiffeners can be included in the effective width-approach, due to the limited yield plateau associated with the column-buckling-resistances.

2.3.3 Plate buckling verification methods

- (1) There are in principle two verification methods for the plate buckling of plated members, that are supposed to exhibit a stress-field E_d (σ_x , σ_z , τ) caused by the design loads:
 1. the general method using a global slenderness,
 2. the component method using different slendernesses for each stress component σ_x , σ_z , τ .

2.3.4 The general method

- (1) The general method is based on the definition of a global slenderness $\bar{\lambda}$, that is obtained from:

$$\bar{\lambda} = \sqrt{\frac{R_k}{R_{crit}}} = \sqrt{\frac{\alpha_{ult,k} \cdot E_d}{\alpha_{crit} \cdot E_d}} \quad (2.8)$$

where:

$\alpha_{ult,k}$ is the amplifier to the design load E_d to obtain the characteristic resistance R_k of the member without out-of-plane displacements;

α_{crit} is the amplifier to the design load E_d to obtain the elastic critical load R_{crit} of the member related to out-of-plane displacements.

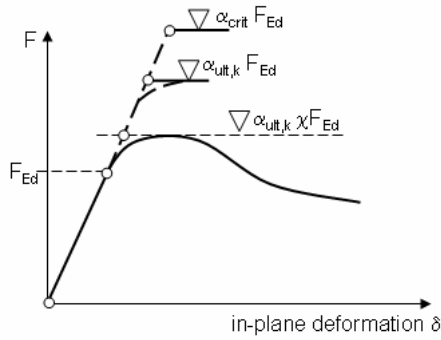
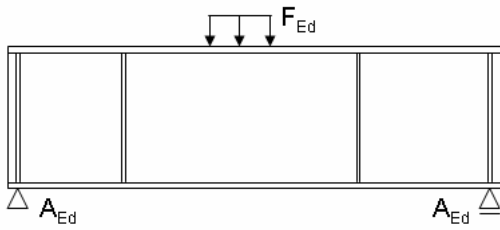
- (2) This method is consistent with the global method used for shell buckling verifications and also with the general method used for flexural and lateral-torsional buckling of members. It works with the verification format:

$$\alpha_{R,d} = \frac{\chi \alpha_{ult,k}}{\gamma_{M1}} \geq 1,0 \quad (2.9)$$

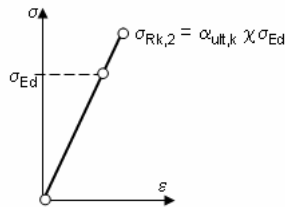
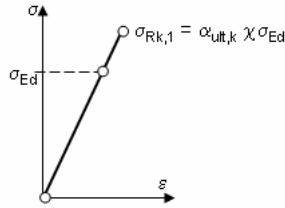
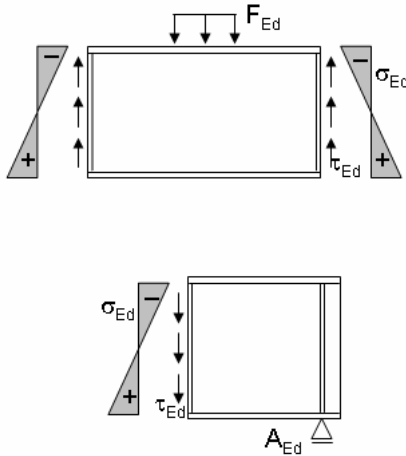
where χ is an appropriate reduction factor depending on $\bar{\lambda}$, see also (9) for patch loading.

- (3) For determining the amplifiers $\alpha_{ult,k}$ and α_{crit} Finite-Element calculations can be used.
- (4) The applicability of the method is not limited to certain types of members, loading or support conditions.
- (5) The method can be used for verifying the plate buckling stability of a member under the design load in a single step (Figure 2.13a) or of parts of the full member (assembly of plate fields or only single plates) (Figure 2.13b).

a) Full member



b) Several plate field assemblies of full members



$$\sigma_{Rk} = \text{Min} [\sigma_{Rk,1} ; \sigma_{Rk,2}]$$

Figure 2.13: Verification of a full member or of various parts of a full member

- (6) In case the verification is performed with individual plates the procedure with different levels as given in Figure 2.11 can be applied, see Figure 2.14.

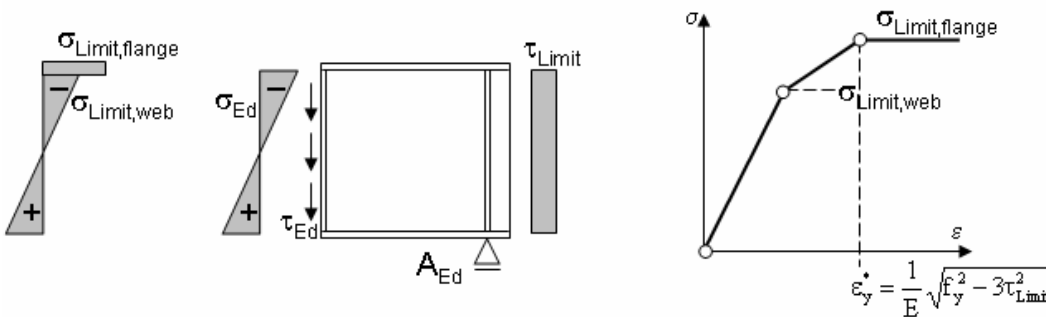


Figure 2.14: Verification of an assembly of plates with checks of individual plates

NOTE Section 10 of EN 1993-1-5 does not yet specify the procedure with different levels according to Figure 2.11.

- (7) The general method can utilize the beneficial effect of the continuity between the plate elements of the cross section.

2.3.5 The component method

- (1) The component method requires to approximate the behaviour of a part of the full member by the behaviour of a set of basic component fields each of which is loaded by either σ_x or σ_y or τ , see Figure 2.15.

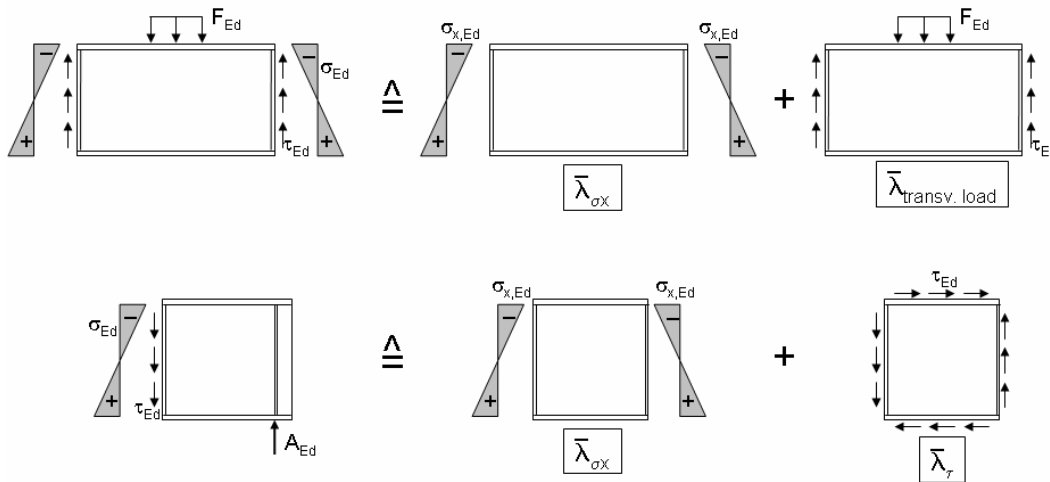


Figure 2.15: Breakdown of full stress fields to basic stress components

- (2) To each of these basic component fields the slendernesses $\bar{\lambda}_{\sigma_x}$, $\bar{\lambda}_{\sigma_z}$, $\bar{\lambda}_{\tau}$ are determined to perform individual checks, see Figure 2.15.
- (3) For the component $\sigma_{x,Ed}$ effective cross-sectional properties may be applied without considering any interaction with other stress components, see Figure 2.16.

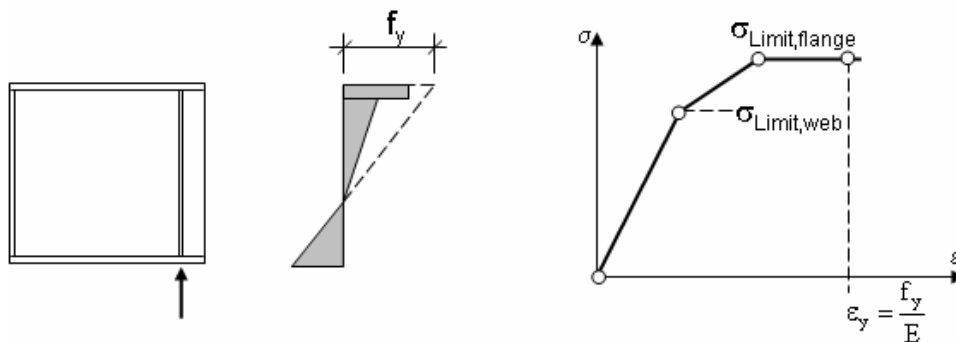


Figure 2.16: Effective cross-section based on f_y

- (4) Figure 2.17 illustrates the procedure for the different stress components of a box girder and the eventual interaction formulae used to verify the interactive behaviour of the components at the limit state.

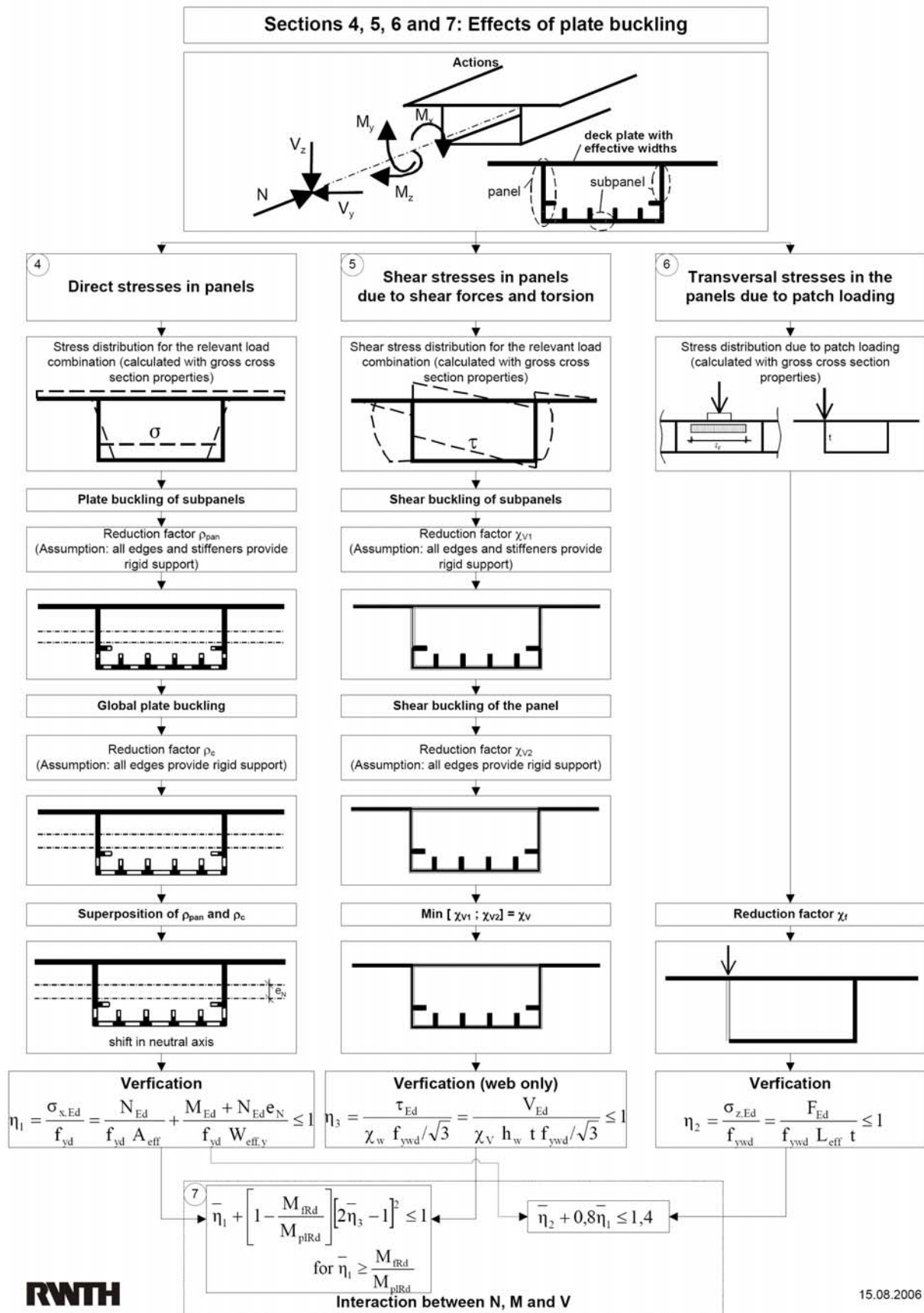


Figure 2.17: Independent verifications for σ_x , τ and σ_z and interaction formulae

- (5) This component method is preferable where hand calculations are applied, as critical stresses for the different stress components are available in handbooks.
- (6) The disadvantage is that the applicability of the method is limited to the geometrical, loading and support conditions, for which the method has been proven by tests and handbooks are available.
- (7) EN 1993-1-5 deals with the component method in its sections 4, 5, 6 and 7.
- (8) The section 4 gives fully identical results both for the individual steps $\alpha_{ult,k}$, α_{crit} , $\bar{\lambda}$ and ρ and for the final verification when compared with the general method when for this the particular loading condition and support conditions as in section 4 are applied. Section 5 give gives about the same results as the general method; small differences originate from the different treatment of stiffeners
- (9) The verification method in section 6 for patch loading uses particular tools that give about the same results as the general method when using their tools (i.e. $\alpha_{ult,k}$, α_{crit} , $\bar{\lambda}$ and ρ). A mixture of the tools is not allowed.

2.4 Serviceability limits

2.4.1 General

- (1) EN 1993-1-5 does not specify any serviceability limits for plate buckling, however there are rules in 2.2 (5) and Annex E that refer to effective areas and stiffnesses of members subject to stress levels below the yield strength, that allow to determine plate buckling effects in the serviceability limit state.
- (2) Also 3.1(2) opens the door for effective widths for elastic shear lag in 3.2 applicable for serviceability and fatigue limit state verifications.
- (3) Serviceability limits are only specified in the application parts of EN 1993, e.g. for the plate buckling of steel bridges in 7.4 (3) of EN 1993-2. The rules given there refer to the limitation of breathing of plated elements of members and aim at avoiding cracks from fatigue. Therefore these rules are also applicable to other structures subject to fatigue load.
- (4) The plate buckling rules in 7.4 of EN 1993-2 for serviceability may be relevant for the design of plated elements. Therefore in the following some SLS criteria are used to identify where limits to ULS-criteria may be.

2.4.2 Rules to avoid excessive plate breathing

- (1) The rules in 7.4(3) of EN 1993-2 give the following general limitations for web breathing for panels assumed to have hinged edges:

$$\sqrt{\left(\frac{\sigma_{x,Ed,ser}}{\sigma_{x,crit}}\right)^2 + \left(\frac{1,1 \cdot \tau_{Ed,ser}}{\tau_{crit}}\right)^2} \leq 1,1 \quad (2.10)$$

where $\sigma_{x,Ed,ser}$ and $\tau_{Ed,ser}$ are the stresses for the frequent load combination.

- (2) In the following a comparison between this serviceability limit and the plate buckling verification for the ultimate limit state is performed to identify what limit state is relevant.

2.4.3 Comparison of SLS and ULS limit state verification

- (1) For plates under compression and for plates under shear load the following limits apply:

SLS:

$$\frac{\sigma_{x,Ed,ser}}{\sigma_{x,crit}} \leq 1,1 \text{ and } \frac{1,1 \cdot \tau_{Ed,ser}}{\tau_{crit}} \leq 1,1 \quad (2.11)$$

ULS:

$$\frac{\sigma_{x,Ed}}{\rho_x f_y / \gamma_{M1}} \leq 1 \text{ and } \frac{\tau_{Ed,ser} \cdot \sqrt{3}}{\chi_\tau f_y / \gamma_{M1}} \leq 1 \quad (2.12)$$

- (2) The working stresses $\sigma_{Ed,ser}$ and $\tau_{Ed,ser}$ may be taken as

$$\sigma_{x,Ed,ser} = \left\{ \frac{\mu}{\gamma_G} + \frac{\psi_1}{\gamma_Q} (1 - \mu) \right\} \sigma_{x,Ed} \quad (2.13)$$

$$\tau_{Ed,ser} = \left\{ \frac{\mu}{\gamma_G} + \frac{\psi_1}{\gamma_Q} (1 - \mu) \right\} \tau_{Ed} \quad (2.14)$$

where

ψ_1 is the combination factor for frequent loads

γ_G, γ_Q are partial factors for permanent and variable loads

μ is ratio $\mu = \frac{G}{G + Q}$.

- (3) For the example of road bridges the following assumptions are used:

$$\mu = 0,5$$

$$\gamma_G = \gamma_Q = \gamma_F = 1,35$$

$$\psi_1 = 0,75 \text{ for small spans}$$

$$\psi_1 = 0,40 \text{ for large spans}$$

$$\rho = \frac{\bar{\lambda}_p - 0,22}{\bar{\lambda}_p^2} = \frac{1}{\bar{\lambda}_p} - \frac{0,22}{\bar{\lambda}_p^2}$$

$$\chi_\tau = \frac{0,83}{\bar{\lambda}_w}$$

$$\gamma_{M1} = 1,10$$

(4) The limit state checks then read:

SLS:

$$\frac{\sigma_{x,Ed,ser}}{1,10 \cdot \sigma_{x,crit}} \leq 1 \text{ and } \frac{\tau_{Ed,ser}}{\tau_{crit}} \leq 1 \quad (2.15)$$

ULS:

$$\frac{\sigma_{x,Ed,ser}}{\left\{ \frac{\mu}{\gamma_G} + \frac{\psi_1}{\gamma_Q} (1 - \mu) \right\} \left\{ \frac{1}{\bar{\lambda}_p} - \frac{0,22}{\bar{\lambda}_{p^2}} \right\} \frac{f_y}{\gamma_{M1}}} = \varepsilon_\sigma \frac{\sigma_{x,Ed,ser}}{1,10 \cdot \sigma_{x,crit}} \leq 1 \quad (2.16)$$

where

$$\varepsilon_\sigma = \frac{1,10 \cdot \gamma_{M1}}{\left\{ \frac{\mu}{\gamma_G} + \frac{\psi_1}{\gamma_Q} (1 - \mu) \right\} \left\{ \frac{1}{\bar{\lambda}_p} - \frac{0,22}{\bar{\lambda}_{p^2}} \right\} \frac{f_y}{\sigma_{x,crit}}} = \frac{2 \cdot 1,10^2 \cdot 1,35}{[1 + \psi_1][\bar{\lambda}_p - 0,22]} = \frac{3,27}{[1 + \psi_1] + [\bar{\lambda}_p - 0,22]}$$

and

$$\frac{\tau_{x,Ed,ser} \cdot \sqrt{3}}{\left\{ \frac{\mu}{\gamma_G} + \frac{\psi_1}{\gamma_Q} (1 - \mu) \right\} \left\{ \frac{0,83}{\bar{\lambda}_w} \right\} \frac{f_y}{\gamma_{M1}}} = \varepsilon_\tau \frac{\tau_{Ed,ser}}{\tau_{crit}} \leq 1$$

where

$$\varepsilon_\tau = \frac{\sqrt{3} \cdot \gamma_{M1}}{\left\{ \frac{\mu}{\gamma_G} + \frac{\psi_1}{\gamma_Q} (1 - \mu) \right\} \left\{ \frac{0,83}{\bar{\lambda}_w} \right\} \tau_{crit}} = \frac{2 \cdot \sqrt{3} \cdot 1,10 \cdot 1,35}{[1 + \psi_1] \cdot 0,83 \cdot \bar{\lambda}_w \cdot \sqrt{3}} = \frac{2,97}{[1 + \psi_1] \cdot 0,83 \cdot \bar{\lambda}_w}$$

(5) For $\varepsilon \geq 1$ the ULS-check is relevant, whereas for $\varepsilon < 1$ the SLS check governs the design.

(6) The limit criterion $\varepsilon = 1$ leads to the following slenderness limits:

for small spans: $\bar{\lambda}_p = \frac{3,267}{1,75} + 0,22 = \underline{2,09}$

$$\bar{\lambda}_w = \frac{2,97}{1,75} + 0,83 = \underline{2,045}$$

for large spans: $\bar{\lambda}_p = \frac{3,267}{1,4} + 0,22 = \underline{2,55}$

$$\bar{\lambda}_w = \frac{2,97}{1,4 \cdot 0,83} = \underline{2,56}$$

(7) Figure 2.18 illustrates the limits.

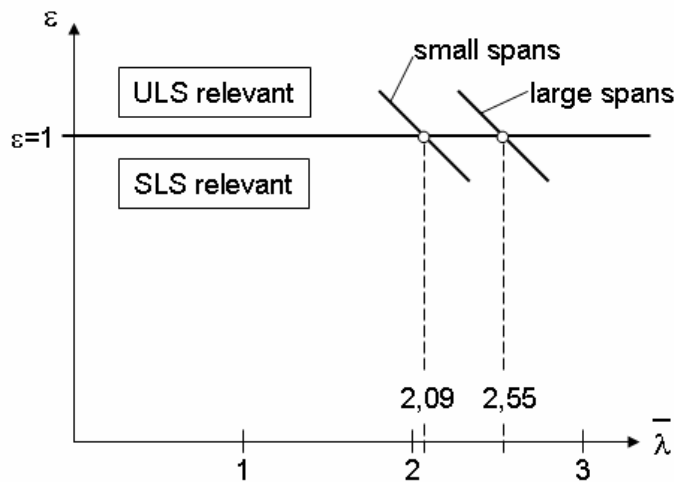


Figure 2.18: Slenderness limits for SLS-checks

(8) There is another limit state criterion in 7.4 (2) of EN 1993-2 related specially to road bridges, that takes realistic bridge weights and fatigue loads depending on the span lengths L into account (μ, ψ_1). This criterion reads:

$$b/t \leq 30 + 4,0 L \leq 300 \tag{2.17}$$

where L is the span length, but not less than 20 m.

This criterion results in a $\bar{\lambda}_p = \frac{30 + 4,0 L}{\sqrt{\frac{k_\sigma \cdot 190.000}{f_y}}}$.

It gives for

$$k_\sigma = 4$$

$$f_y = 355 \text{ N/mm}^2$$

$$L = 20 \text{ m}$$

$$\bar{\lambda}_{p,\min} = \frac{30 + 80}{\sqrt{\frac{4 \cdot 190.000}{355}}} = 2,38$$

which is about the mean between $\bar{\lambda}_p = 2,09$ and $\bar{\lambda}_p = 2,55$.

(9) As the assumption for the rules for web breathing is that stresses are in the linear elastic range, see Figure 2.19, there is a relationship between the first occurrence of plate buckling in the weakest plate-panel of the member and the overall resistance.

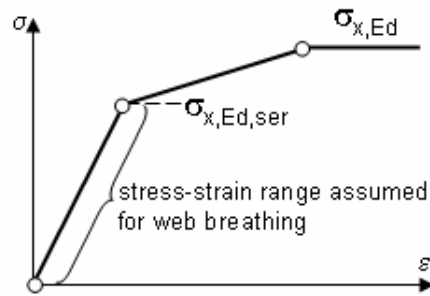


Figure 2.19: Stress-strain curve with linear-elastic range for web-breathing

(10) The verification formulae for the level $\sigma_{x,Ed}$ and $\sigma_{x,Ed,ser}$ of direct stresses read:

$$\text{ULS: } \frac{N_{x,Ed}}{\sum \rho_i A_i f_y / \gamma_{M1}} \leq 1 \tag{2.18}$$

$$\text{where } \rho_i = \frac{1}{\bar{\lambda}} + \frac{0,22}{\bar{\lambda}_{p^2}}$$

$$\text{SLS: } \frac{N_{Ed,ser}}{\rho_{min} \cdot \sum A_i f_y / \gamma_{M,ser}} \leq 1 \tag{2.19}$$

$$\text{where } \rho_{min} = \frac{1}{\bar{\lambda}_{p,ser}} + \frac{0,22}{\bar{\lambda}_{p,ser}^2}$$

$$\bar{\lambda}_{p,ser} = \bar{\lambda}_p \cdot \sqrt{\frac{N_{Ed,ser}}{N_{pl}} \cdot \gamma_{M1}}$$

(11) In assuming

$$N_{d,ser} = \left(\frac{\mu}{\gamma_G} + \frac{\Psi_1}{\gamma_Q} (1 - \mu) \right) N_{x,Ed} \tag{2.20}$$

the following criterion can be drawn for the limit slenderness

$$\frac{\left\{ \frac{\mu}{\gamma_G} + \frac{\Psi_1}{\gamma_Q} (1 - \mu) \right\}}{\rho_{min} \sum A_i} = \frac{1}{\sum \rho_i A_i} \tag{2.21}$$

(12) On the safe side the minimum reduction factor for the slenderness is

$$\rho_{min} = \left\{ \frac{\mu}{\gamma_G} + \frac{\Psi_1}{\gamma_Q} (1 - \mu) \right\} \rho_{max} \tag{2.22}$$

or

$$\rho_{min} = \left\{ \frac{\mu}{\gamma_G} + \frac{\Psi_1}{\gamma_Q} (1 - \mu) \right\} \cdot 1,0 \tag{2.23}$$

(13) For shear stresses the stress-strain curve in general is bilinear, so that no slenderness limit from two levels $\tau_{Ed,ser}$ and τ_{Ed} exists.

(14) From the assumptions

$$\mu = 0,5$$

$$\gamma_G = \gamma_Q = 1,35$$

$$\psi_1 = 0,75 \text{ for small spans}$$

follows

$$\rho_{min} = \frac{1}{2} \frac{1 + 0,75}{1,35} = \frac{1}{1,543} = 0,65$$

$$\frac{\sqrt{1,543}}{\bar{\lambda}_{p,min}} \left[1 + \frac{0,22 \sqrt{1,543}}{\bar{\lambda}_{p,min}} \right] = 0,65$$

$$\bar{\lambda}_{p,min} = \frac{\sqrt{1,543}}{0,65} \left[1 + \frac{0,22 \sqrt{1,543}}{\bar{\lambda}_{p,min}} \right] = \underline{2,15}$$

(15) This value calculated for small spans and also the value $\bar{\lambda}_{p,min} = \underline{2,95}$ calculated for large spans ($\psi_1 = 0,4$) are larger than the associated minimum values for breathing ($\bar{\lambda}_{p,min} = 2,09$ and $2,55$ respectively in (6)). Therefore the assumption made in (9) applies.

3 Effective width approaches in design

EN 1993-1-5
§3

Gerhard Sedlacek, Christian Müller, Lehrstuhl für Stahlbau und Leichtmetallbau, RWTH Aachen

3.1 Contributory areas without shear lag effects

- (1) Regularly stiffened structures as orthotropic plates, see Figure 3.1, may be analysed either by smearing the stiffeners to a continuum or by separating individual stiffeners with effective widths to obtain a grid with discrete beams.

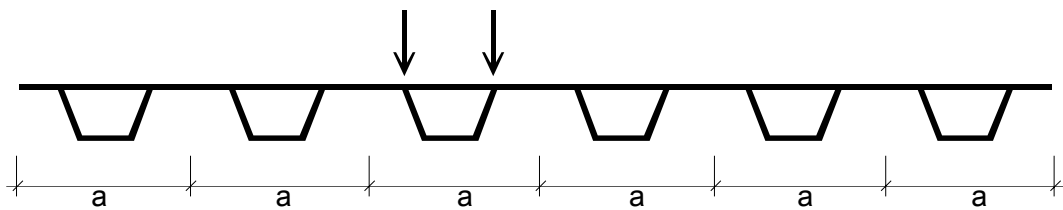


Figure 3.1: Orthotropic plate

NOTE In such separations the shear effect of the continuous deck plate is neglected. Depending on the loading situation the shear effect would lead to a distribution of normal forces and bending moments in the stiffeners as given in Figure 3.2. These distributions would effect smaller stresses in the deckplate and hence be equivalent to a larger effective width a_{eff} for the stringer loaded. However the effects on the bottom flange of the stringers are small so that these effects are normally neglected.

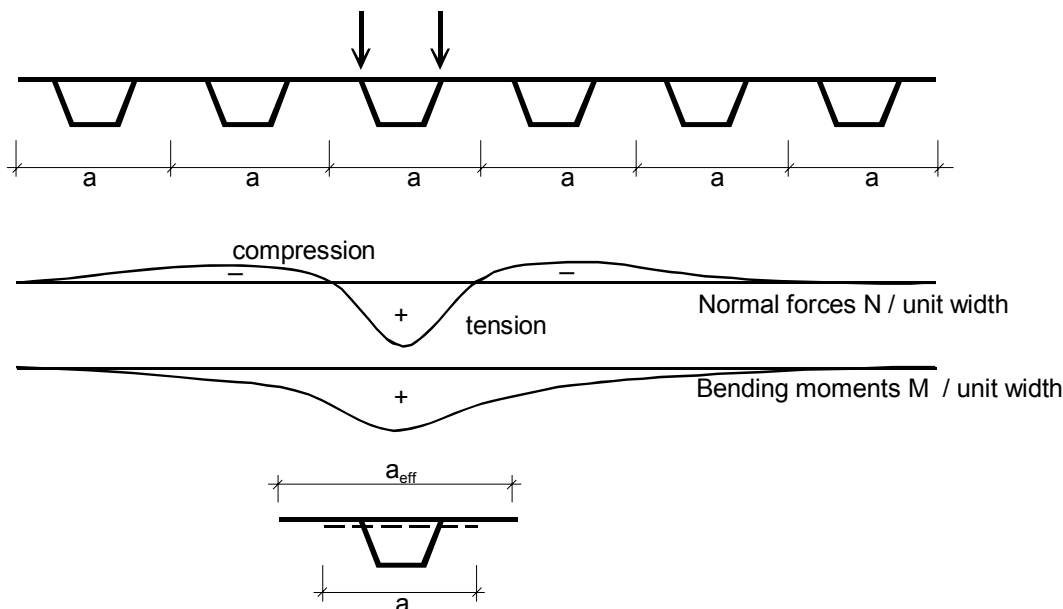


Figure 3.2: Distribution of normal forces and bending moments in a stiffened plate with eccentric deckplate (results based on continuum theory)

- (2) Similar attributions of effective widths as for stiffeners may also be carried out for double bay bridge sections, see Figure 3.3, for which a separation into two beams for symmetrical loading because of the symmetry conditions is logical.

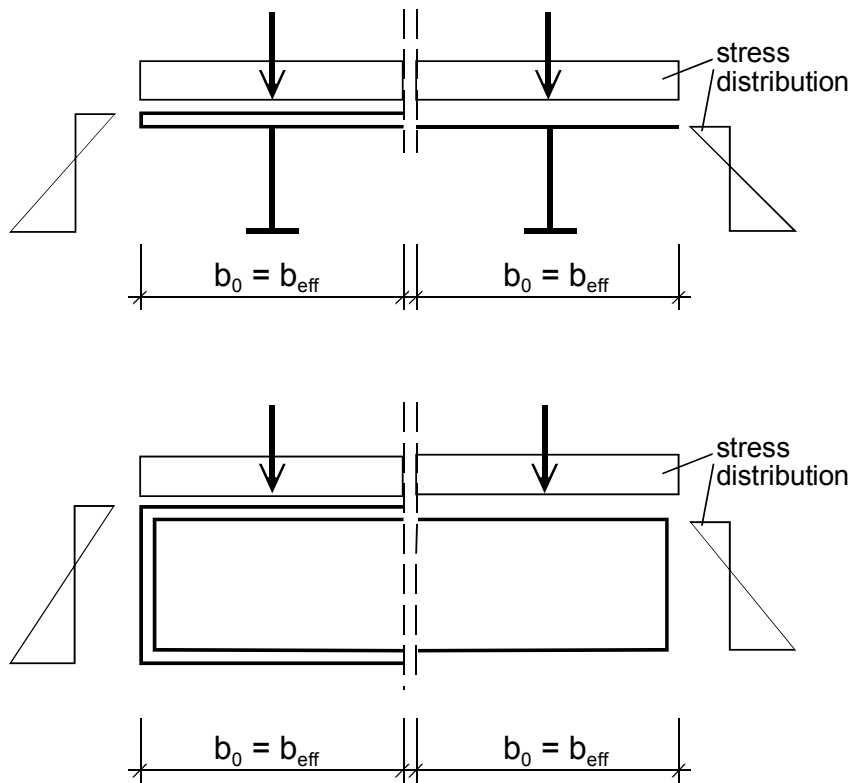


Figure 3.3: Effective widths of a double bay bridge under symmetric loading

- (3) For asymmetrical loading conditions however stress distributions require different effective widths as given in Figure 3.4.

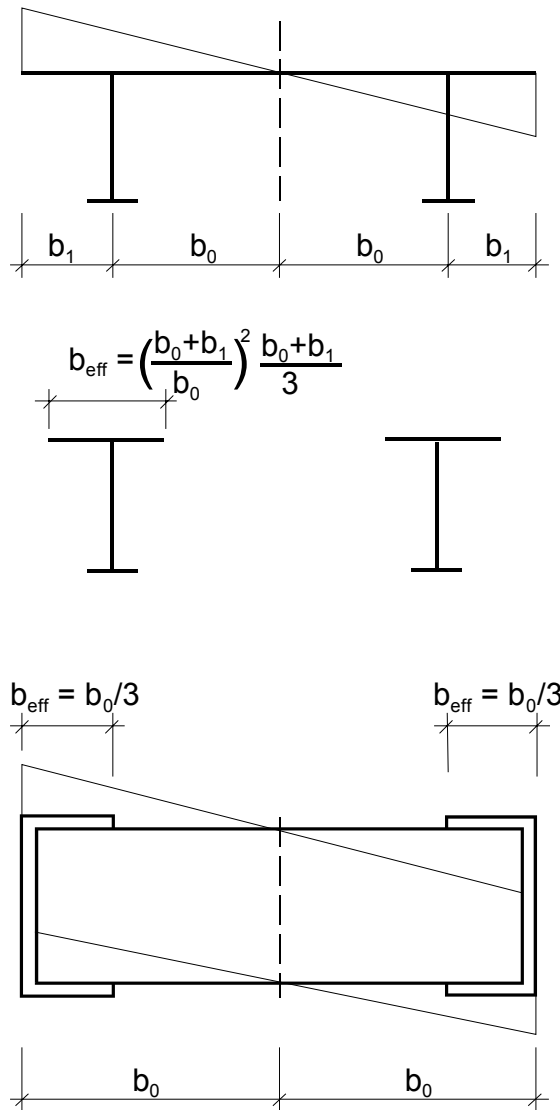


Figure 3.4: Effective widths under asymmetric loading

- (4) This distinction between symmetrical and asymmetrical loading cases normally leads to a modelling of box girders with discrete diaphragms as given in Figure 3.5.

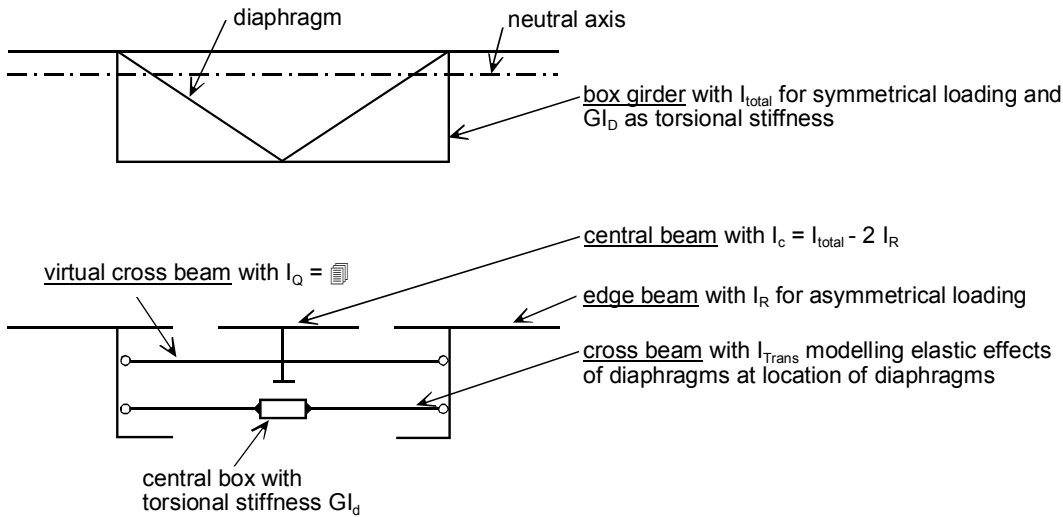


Figure 3.5: Modelling of box girders by a central beam (I_c) and two edge beams (I_R)

3.2 Shear lag effects

(1) Shear deformation in plates follow the compatibility rule:

$$\varepsilon_x'' - \gamma'^{\bullet} + \varepsilon_y'' = 0 \tag{3.1}$$

where ε_x is the strain in the longitudinal direction and ε_x'' is $\frac{\partial^2 \varepsilon_x}{\partial y^2}$;

ε_y is the strain in the transverse direction and ε_y'' is $\frac{\partial^2 \varepsilon_y}{\partial x^2}$;

γ is the shear strain and γ'^{\bullet} is $\frac{\partial^2 \gamma}{\partial x \partial y}$.

(2) In order to simplify the solution an infinite transverse stiffness conforming to the usual bending theory is assumed, so that $\varepsilon_y = 0$ and hence it reads:

$$\varepsilon_x^{\bullet} - \gamma' = 0 \tag{3.2}$$

(3) This allows to define warping functions w_s to model shear lag effects, so that:

$$\varepsilon_x = -w_s v_s'' \tag{3.3}$$

$$\gamma = -w_s^{\bullet} v_s' \tag{3.4}$$

and

$$\sigma_x = E \varepsilon_x \tag{3.5}$$

$$\tau = G \gamma \tag{3.6}$$

EN 1993-1-5
§3.2

The derivatives $w_s^{\bullet} = \frac{\partial w}{\partial s}$ of these warping functions w_s should be proportional to the τ distribution in the flange from the variation of bending and hence have a linear characteristic, whereas $w_s = \int w_s^{\bullet} ds$ gets a parabolic shape, see Figure 3.6.

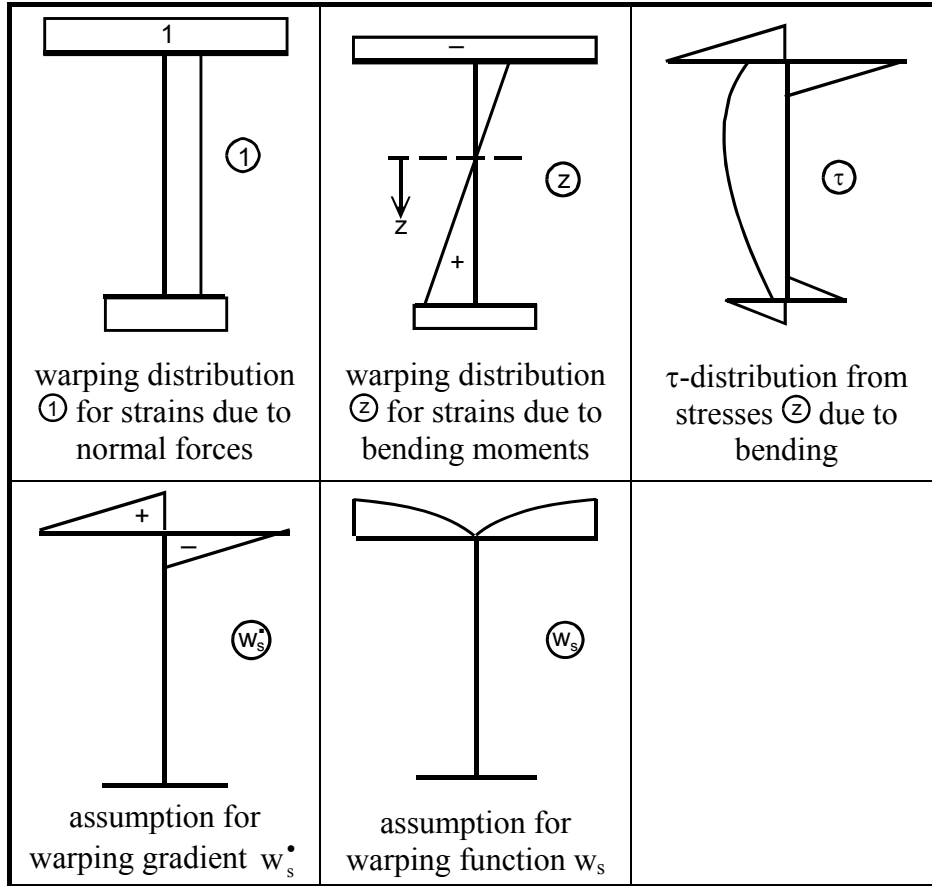


Figure 3.6: Elementary stress distributions

- (4) For making w_s independent of the warping distributions ① and ② a linear combination \tilde{w} is assumed:

$$\tilde{w}_s = w_s + k_{1w} \textcircled{1} + k_{zw} \textcircled{2} \tag{3.7}$$

with the conditions for orthogonality of $A_{\tilde{w}\tilde{w}} = \int \tilde{w}_s^2 dA$ (main axes):

$$A_{1w_s} = \int \textcircled{1} \tilde{w}_s dA = 0 \tag{3.8}$$

$$A_{zw_s} = \int \textcircled{2} \tilde{w}_s dA = 0 \tag{3.9}$$

These conditions lead to the factors k_{1w} and k_{zw} and also to the final function \tilde{w}_s as given in Figure 3.7.

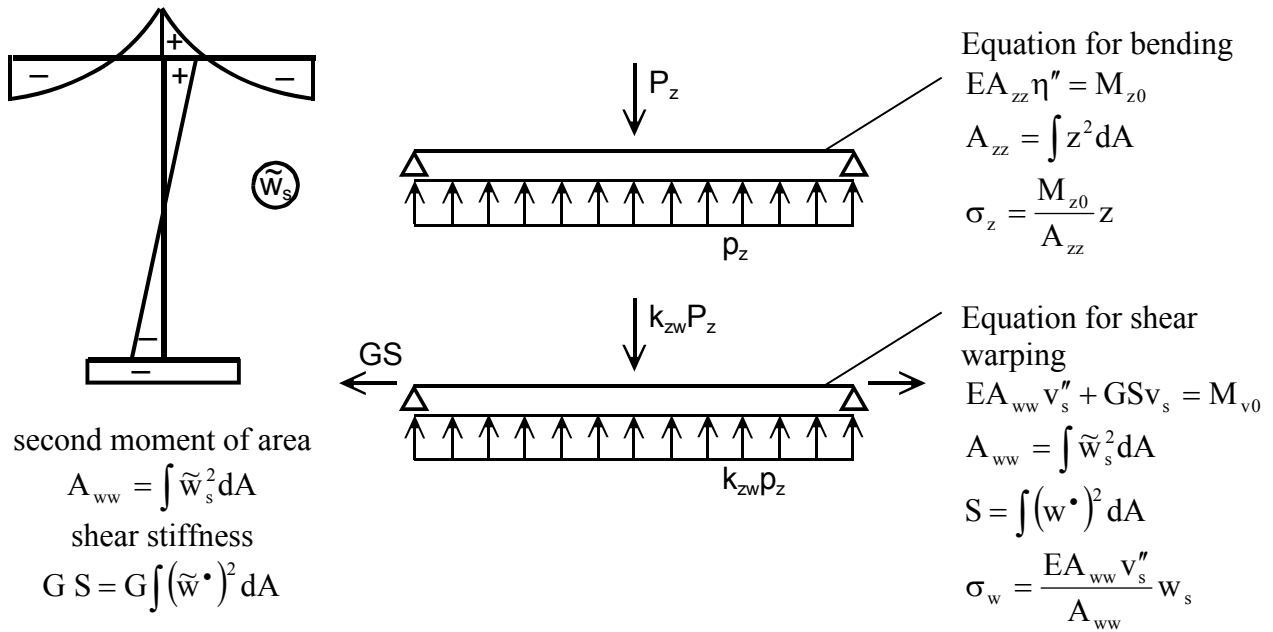


Figure 3.7: Final warping function

(5) This orthogonalised warping function allows to determine a stress pattern:

$$\sigma_w = -E \tilde{w}_s v_s'' = \frac{M_v}{A_{ww}} \tilde{w}_s \tag{3.10}$$

from the solution of the differential equation, see Figure 3.7:

$$EA_{ww} v_s'' + GS v_s = M_{v0} \tag{3.11}$$

This stress pattern can be superimposed on the stress pattern from M_z that is based on a full effective width and then gives a realistic picture of the stress distribution with shear lag effects, see Figure 3.8.

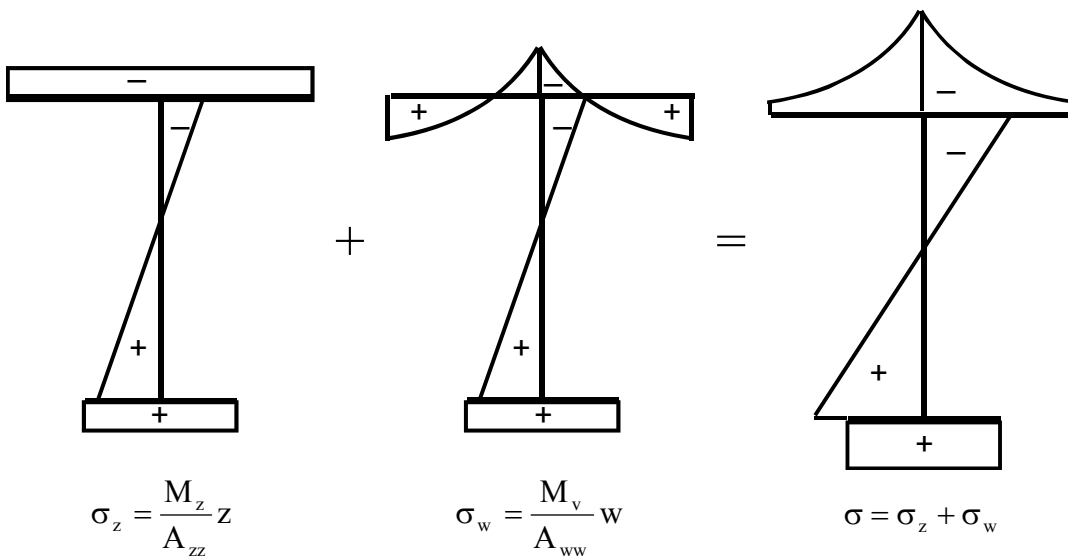


Figure 3.8: Stress distribution with shear lag effects

- (6) This approach is the basis for specifying a formula for determining shear lag effects in the elastic range.

3.3 Basic situations

- (1) To determine a formula for effective widths due to shear lag the distribution of bending moments along a continuous beams subjected to a uniformly distributed load is separated into modules separated by the counterflexure points, see Figure 3.9. These modules represent simply supported beams the moment distributions of which can be determined as effects from a uniformly distributed load and a concentrated load, see Figure 3.10.

EN 1993-1-5
§3.2.1

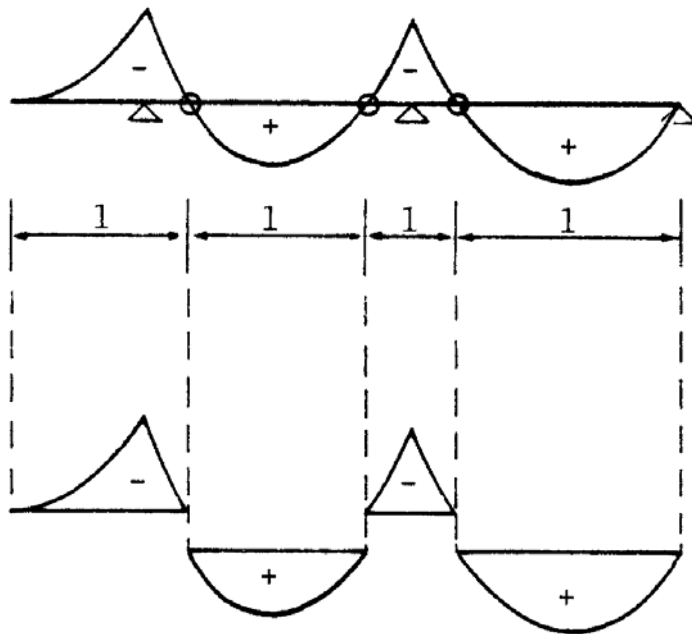


Figure 3.9: Separated modules

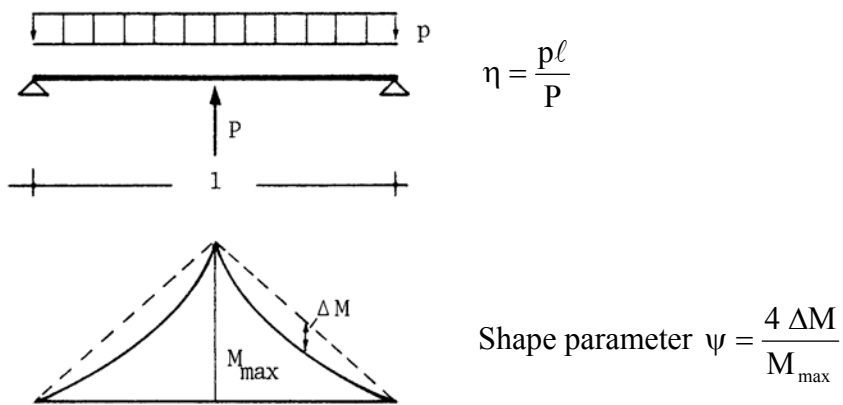


Figure 3.10: Modules representing simply supported beams

- (2) By the shape factor ψ , see Figure 3.10, various shapes of the moments can be modelled, see Figure 3.11.

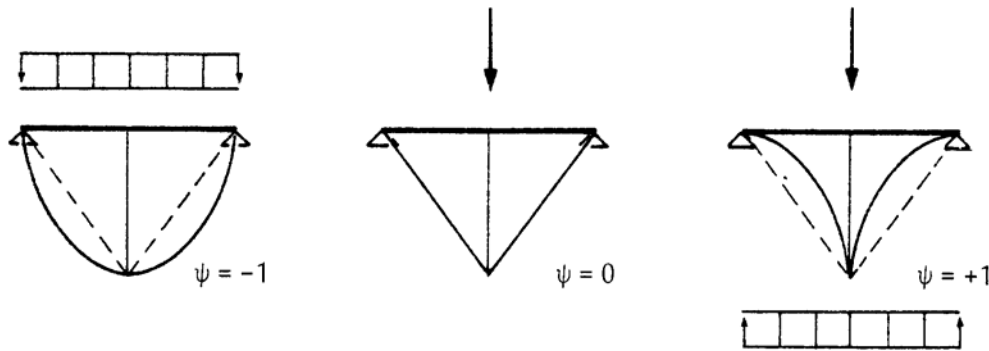


Figure 3.11: Modelling of various shapes of moment distribution

- (3) For simplifying the situation further a doubly symmetrical cross section is assumed as given in Figure 3.12.

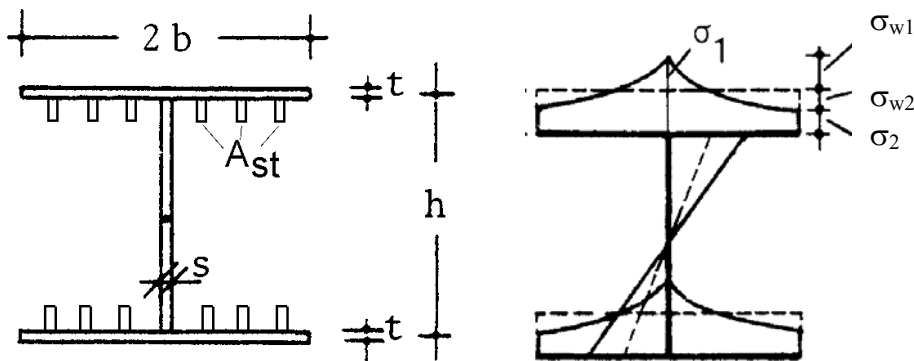


Figure 3.12: Doubly symmetrical cross section

- (4) In this cross section the flange area consists of $(2bt)$ for shear and $(2bt + \Sigma A_{st})$ for direct stresses, where ΣA_{st} is the area of all stringers, so that the orthotropy factor

$$k = \sqrt{\frac{E(2bt + \Sigma A_{st})}{G(2bt)}} = \sqrt{\frac{E}{G}} \alpha_0 \tag{3.12}$$

with

$$\alpha_0 = \sqrt{1 + \frac{\Sigma A_{st}}{2bt}} \tag{3.13}$$

can be defined.

- (5) The effective width is given by:

$$b_{eff} = \beta b \tag{3.14}$$

and due to the parabolic stress distribution in the flange:

$$\beta = \frac{1}{3} + \frac{2}{3} \frac{\sigma_2}{\sigma_1} \tag{3.15}$$

- (6) After solving the differential equation (3.1) and further simplifications the reduction factor β is eventually as given in Figure 3.13.

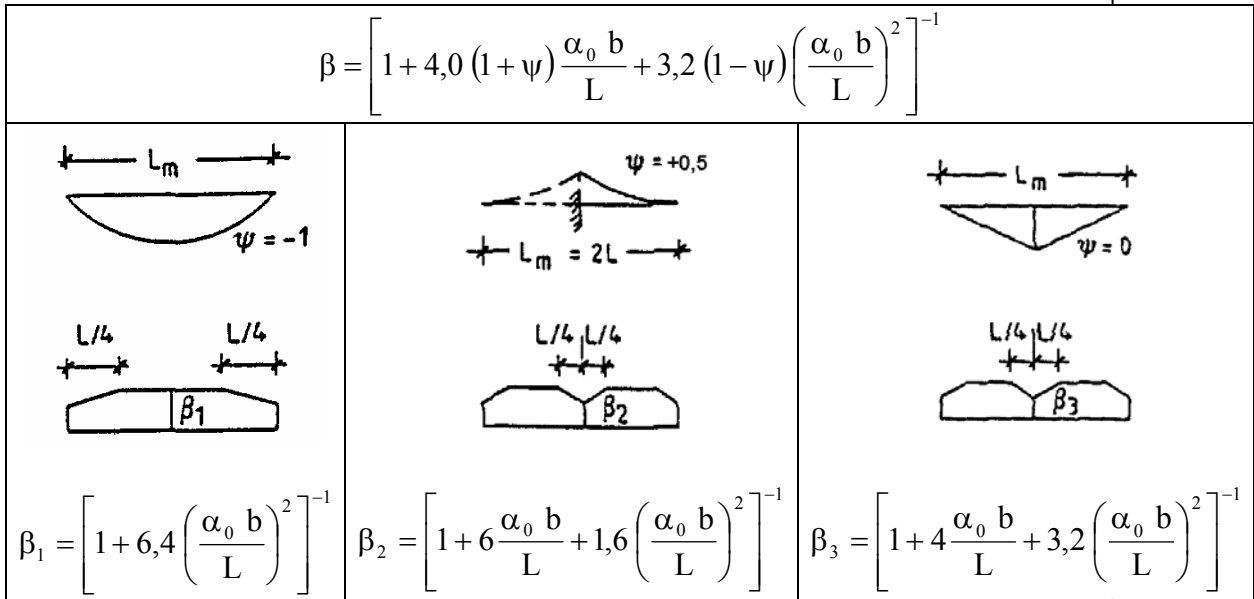


Figure 3.13: Solution for β

EN 1993-1-5
§3.2.1

3.4 Conclusions

- (1) There are two cases where the effective width due to shear lag is needed:
 1. A moment distribution is given for a certain load case.
 2. A distribution of a moment envelope is given representing extreme values of moments.
- (2) In case 1 the separation of modules according to Figure 3.9 is needed and effective widths can be determined according to Figure 3.13.
- (3) In case of distribution of bending moments that cannot be directly attributed to the standard cases in Figure 3.11, e.g. for continuous beams on elastic springs, see Figure 3.14, the basic modules $M_{\psi=-1}$ and $M_{\psi=0}$ must be determined indirectly.

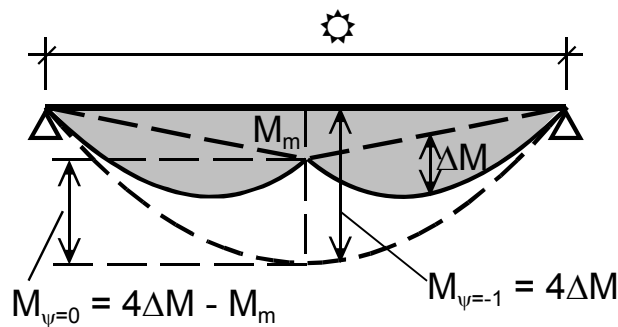


Figure 3.14: Continuous beam on elastic springs

(4) For the case in Figure 3.14 the stress distribution is determined as

$$\sigma = \sigma(4\Delta M) + \sigma(4\Delta M - M_m) \tag{3.16}$$

and may be shaped as given in Figure 3.15.

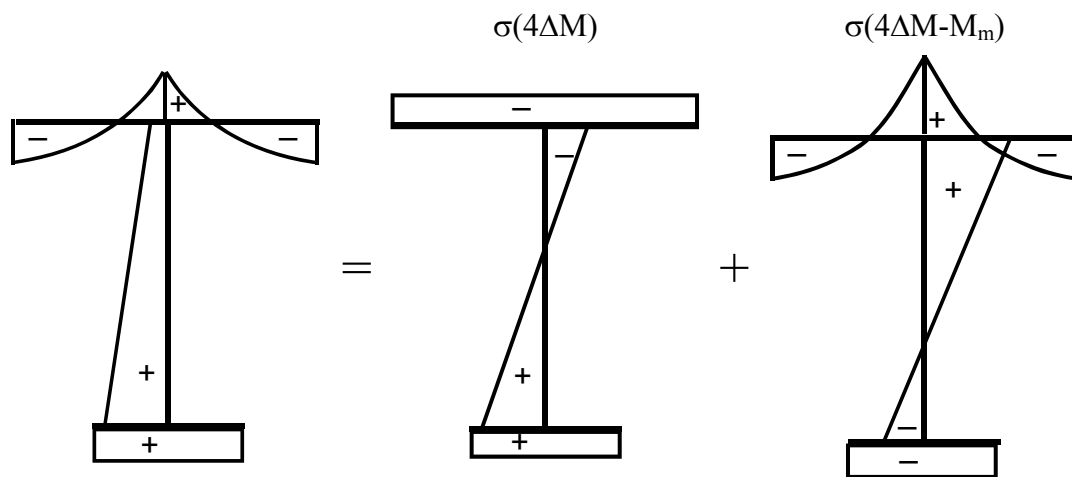
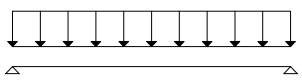
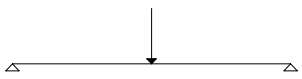
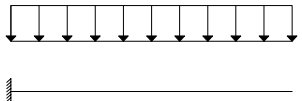


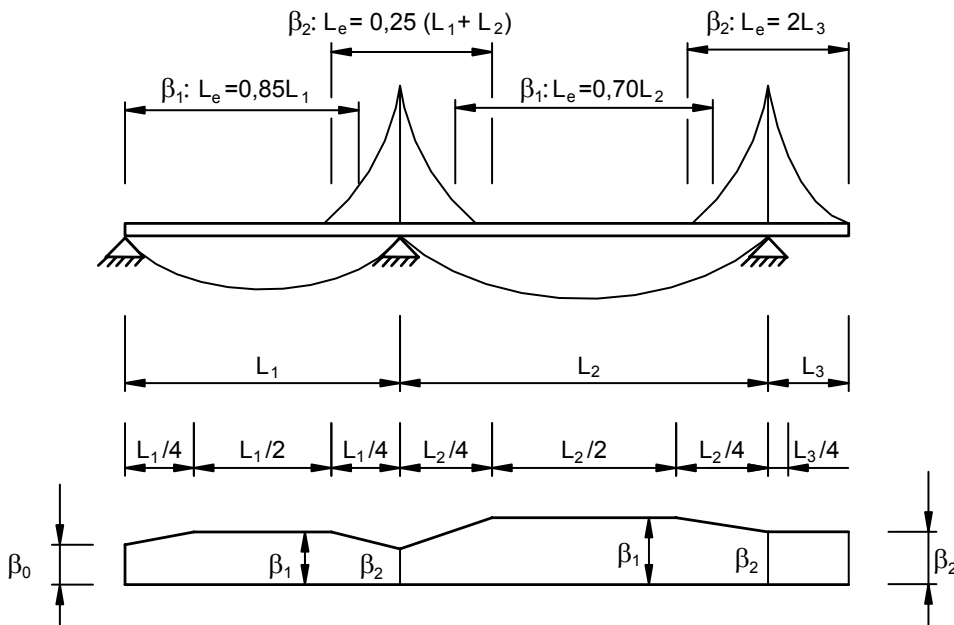
Figure 3.15: Stress distribution

- (5) Table 3.1 gives a comparison of β -values determined according to various codes.

Table 3.1: Comparison of β -values

β -values	b/l	$k = \frac{A_{st}}{2bt} = 0$		$k = \frac{A_{st}}{2bt} = 1$	
		BS 5400	EC 3	BS 5400	EC 3
 <p style="text-align: center;">$\psi = -1$</p>	0	1	1	1	1
	0,05	0,98	0,98	0,97	0,97
	0,1	0,95	0,94	0,89	0,88
	0,2	0,81	0,78	0,67	0,64
	0,3	0,66	0,62	0,47	0,44
	0,4	0,50	0,47	0,35	0,31
	0,5	0,38	0,37	0,28	0,22
	0,6	0,32	0,29	0,24	0,17
	0,8	0,21	0,18	0,16	0,10
	1	0,16	0,13	0,12	0,07
 <p style="text-align: center;">$\psi = 0$</p>	0	1	1	1	1
	0,05	0,80	0,82	0,75	0,76
	0,1	0,67	0,69	0,59	0,60
	0,2	0,49	0,51	0,40	0,41
	0,3	0,38	0,39	0,30	0,30
	0,4	0,30	0,31	0,23	0,22
	0,5	0,24	0,25	0,17	0,18
	0,6	0,20	0,21	0,15	0,14
	0,8	0,14	0,15	0,10	0,08
	1	0,12	0,12	0,08	0,07
 <p style="text-align: center;">$\psi = +1$</p>	0	1	1	1	1
	0,05	0,68	0,71	0,61	0,63
	0,1	0,52	0,55	0,44	0,46
	0,2	0,35	0,38	0,28	0,30
	0,3	0,27	0,29	0,22	0,22
	0,4	0,21	0,23	0,17	0,18
	0,5	0,18	0,19	0,14	0,15
	0,6	-	0,17	-	0,12
	0,8	-	0,13	-	0,10
	1	-	0,11	-	0,08

- (6) For moment envelopes according to Figure 3.16 equivalent lengths ℓ_0 for the various β -factors may be determined. Sagging moment areas may be treated with $\psi = -1$, hogging moment areas with $\psi = +0,5$. The formulae are given in Table 3.2.



EN 1993-1-5
§3.2.1, Fig. 3.1

Figure 3.16: Moment envelopes

Table 3.2: Effective^s width factor β

κ	location for verification	β – value
$\kappa \leq 0,02$		$\beta = 1,0$
$0,02 < \kappa \leq 0,70$	sagging bending	$\beta = \beta_1 = \frac{1}{1 + 6,4 \kappa^2}$
	hogging bending	$\beta = \beta_2 = \frac{1}{1 + 6,0 \left(\kappa - \frac{1}{2500 \kappa} \right) + 1,6 \kappa^2}$
$> 0,70$	sagging bending	$\beta = \beta_1 = \frac{1}{5,9 \kappa}$
	hogging bending	$\beta = \beta_2 = \frac{1}{8,6 \kappa}$
all κ	end support	$\beta_0 = (0,55 + 0,025 / \kappa) \beta_1$, but $\beta_0 < \beta_1$
all κ	cantilever	$\beta = \beta_2$ at support and at the end
$\kappa = \alpha_0 b_0 / L_e \quad \text{with} \quad \alpha_0 = \sqrt{1 + \frac{A_{sl}}{b_0 t}}$ <p>in which A_{sl} is the area of all longitudinal stiffeners within the width b_0.</p>		

EN 1993-1-5
§3.2.1, Tab. 3.1

3.5 Symmetrical and asymmetrical loading

EN 1993-1-5
§3.2.2

- (1) Where two girder cross sections are subjected to symmetrical and asymmetrical loading, the concluding stress distributions using the warping theory as given in section 3.2 may result in stress distributions as given in Figure 3.17.

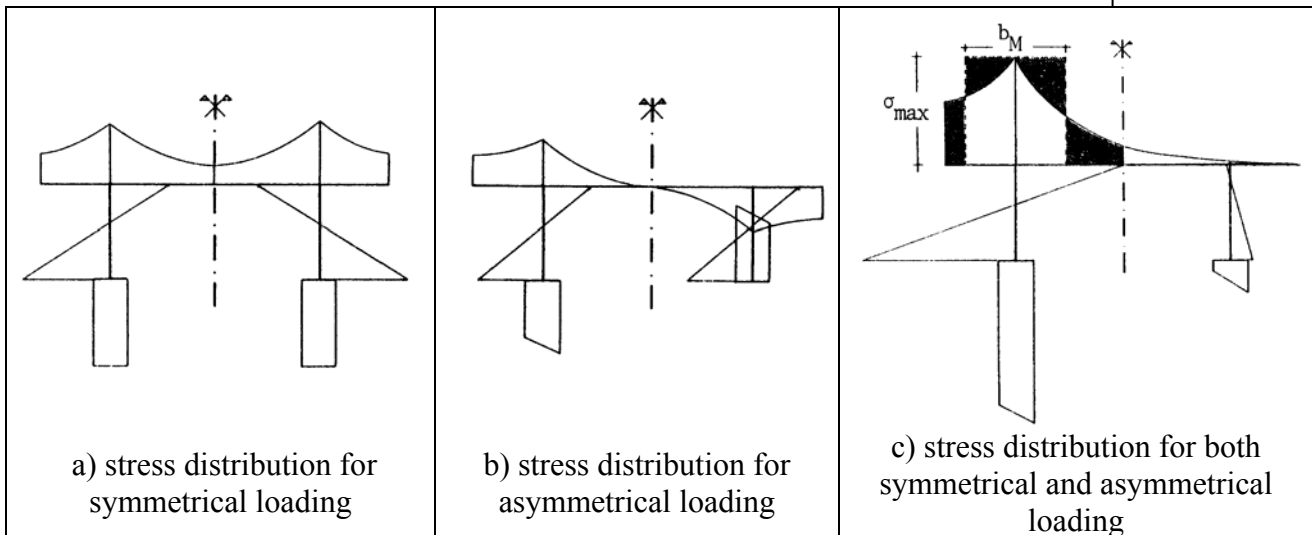


Figure 3.17: Stress distribution of two girder cross section

- (2) As the differences between β -values as given in Figure 3.13 and Table 3.2 determined for the symmetric case, see Figure 3.17a), and those for the asymmetric case, see Figure 3.17b), are small, it is sufficient to use the β -values from Figure 3.13 and Table 3.2 for both the symmetrical case, see Figure 3.3, and the asymmetrical case, see Figure 3.4.

Normally it is sufficient to refer to the symmetrical case only, see Figure 3.17c).

3.6 Effects at the ultimate limit state

EN 1993-1-5
§3.3

- (1) At the ultimate limit state the elastic stress distribution from shear lag may be modified by the following effects:
1. Exceedance of yield strain ϵ_y .
 2. Change of orthotropy factor by reduction of longitudinal stiffness, e.g. by
 - cracking of concrete slab in tension;
 - local plate buckling of a steel flange in compression.
- (2) For the exceedance of the yield strength to the limit $\epsilon_{max} = 1,5 \epsilon_y$ (to keep stresses in the serviceability limit state in the elastic range) the strain distribution for ϵ_{max} can be assumed to be proportional to the one obtained in the elastic range, see Figure 3.18.

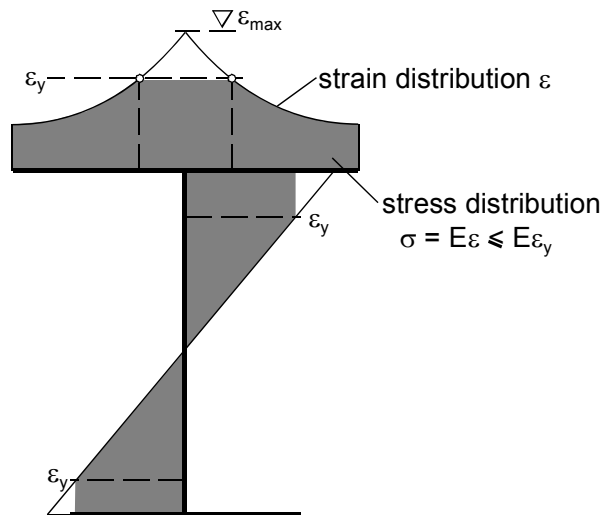


Figure 3.18: Stress and strain distribution at ultimate limit state

- (4) As a consequence larger β^* -values are obtained, see Figure 3.19, that can be approximated by:

$$\beta^* = \beta^k \tag{3.17}$$

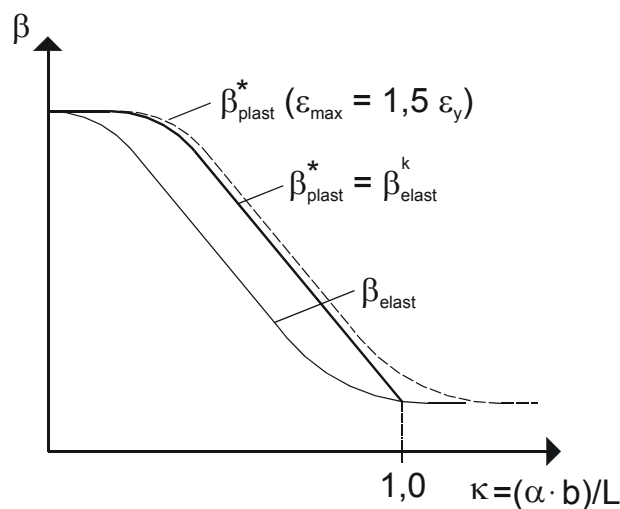


Figure 3.19: β^* -values at ultimate limit states

- (5) The reduction of the longitudinal stiffness can be modelled by the orthotropy factor:

$$\alpha_0 = \sqrt{1 + \frac{A_{st}}{2 b_0 t}} = \sqrt{\frac{2 b_0 t + A_{st}}{2 b_0 t}} \tag{3.18}$$

where b_0 is the gross width b , see Figure 3.12, and A_{st} may be negative. Instead of the area composed of the plate and the longitudinal stiffeners ($2b_0t + A_{st}$) a reduced area A_{eff} may be used to model stiffness reduction in the case of plate buckling. For cracking of the concrete the stiffness of the cracked slab in tension including tension stiffening by the concrete should be considered.

- (6) For bridges where plate buckling is based on an elastic stress distribution in the cross section however these reduction effects should only be taken into account when justified by subsequent assessments.

4 Plate buckling effects due to direct stresses

René Maquoi, Department M&S, Université de Liège

4.1 Introduction

(1) The general principles governing the determination of the cross section resistance of all classes of sections are given in *EN 1993-1-1*. More specifically:

EN 1993-1-1
§5.5.2

- For a *Class 3* section subjected to direct stresses, only an *elastic* stress distribution over the *fully effective cross-section* is permitted and the section resistance is governed by the onset of yielding in the most compressed fibre¹ of the *fully effective cross-section*.
- For a *Class 4* section subjected to direct stresses, an *elastic* stress distribution over the so-called *reduced cross-section* is likely to take place and the section resistance is governed by the onset of the yielding in the most compressed fibre of the *reduced cross-section*.

In EN 1993-1-5, the "most compressed fibre" is taken in the mid-plane of the unstiffened plating of the stiffened compressed flange.

(2) However, according to *EN 1993-1-1*, a *Class 4* section may be treated as an *equivalent Class 3* section when the maximum design compressive stress is substantially below the yield strength. Then, the maximum compressive direct stress cannot exceed a *reduced strength* compared to the yield strength..

EN 1993-1-1
§5.5.2(9)

(3) Often the *reduced cross-section* is designated as the *effective cross-section* because it is based on the concept of *effective width/cross-sectional area*, according to which possible plate buckling in the compression zone of the section makes part of this zone non efficient for transmitting direct stresses. The wording *effective* may be questionable because it is given different meanings in the literature².

(4) Whatever the method referring either to a reduced cross-section or to a reduced strength, the use of the rules given in *EN 1993-1-5* for plate buckling effects due to direct stresses *at the ultimate limit state* is subordinated to the fulfilment with the following criteria:

EN 1993-1-5
§2.3(1)
§4.1(1)

¹ For the sake of simplicity, it is assumed that the maximum tensile stress is not governing the section resistance.

² It is necessary to clearly distinguish amongst them. In the German literature, the situation is much better because the wording "*wirksame Breite/Querschnitt*" corresponds to effects of local plate buckling only, the one "*mittragende Breite/Querschnitt*" to shear-lag effects only, while the one "*effective breite/querschnitt*" results from the interaction between both plate buckling and shear-lag effects. In the English literature, there is no such well established delicate distinction so that "*effective width*" will be fitted with the index *p* when only local plate buckling effects are concerned and with the index *s* when only shear lag effects are considered; the absence of index means implicitly that the interaction between plate buckling and shear lag is concerned.

- The individual plate elements or sub-elements are *quasi rectangular*³, i.e. with their longitudinal edges within an angle not greater than 10°;
- Stiffeners, if any, are provided in the direction of the longitudinal direct stresses (*longitudinal stiffeners*) and/or in the direction perpendicular to the previous one (*transverse stiffeners*);
- Openings or cut outs, if any, are small⁴;
- Members are supposed to be of uniform cross-section;
- Flange induced web buckling is prevented by appropriate proportioning of the web h_w/t ratio (see Section 1.4) or sufficient and appropriate stiffening.

4.2 General verification procedures

- (1) The rules for the determination of the effects due to shear lag are given in another chapter (see Section 3). Herein only those relative to plate buckling are discussed; it is referred to the interaction between both – respectively shear-lag and plate buckling - when necessary.
- (2) Plate buckling may be accounted for by referring to anyone of the two following procedures:
 - The *reduced cross- section approach*:
 First, a separate check is made for the cross-section of the member subjected to longitudinal direct stresses, shear stresses or concentrated transverse edge loads, respectively. Then, an additional check is conducted for the actual combined loading by means of a so-called interaction formula involving the results of the separate checks. The design is governed by the onset of the *yield strength* (see § 4.1(1)) in the most compressed fibre of the *reduced cross-section* of the member. As far as longitudinal stresses are concerned, the concept of effective^p width/cross-sectional area is thus referred to.
 - The *reduced strength approach*:
 Plate buckling is no more accounted for through a loss in efficiency of the cross-sectional properties; it is indeed referred to the individual plate elements of the cross-section and each of them is involved with its *fully effective cross-section*. In contrast with the previous approach, the maximum compressive/shear stress in each plate element shall not exceed a so-called *reduced strength* (less than the design yield strength/shear yield strength) and the check of coincident stresses shall be conducted through the *von Mises* yield criterion. The reduced strength method is described in section 10

EN 1993-1-5
§3

EN 1993-1-5
§4

EN 1993-1-5
§10

³ For angles greater than 10°, panels may conservatively be checked assuming a notional rectangular panel having the largest dimensions a and b of the actual panel.

⁴ In *EN1993-1-5*, only round holes are covered; their diameter d shall be such that $d \leq 0,05 b$ where b is the width of the plate element.

- (3) Both *reduced strength approach* and *reduced cross-section approach* will be equivalent for single plate elements; they will generally not be equivalent in a section composed of several plate elements.
- (4) Compared to the *reduced strength approach*, the *reduced cross-section approach* allows the use of more slender structural plate elements in a cross-section with the result that serviceability limit states may become more determinative.

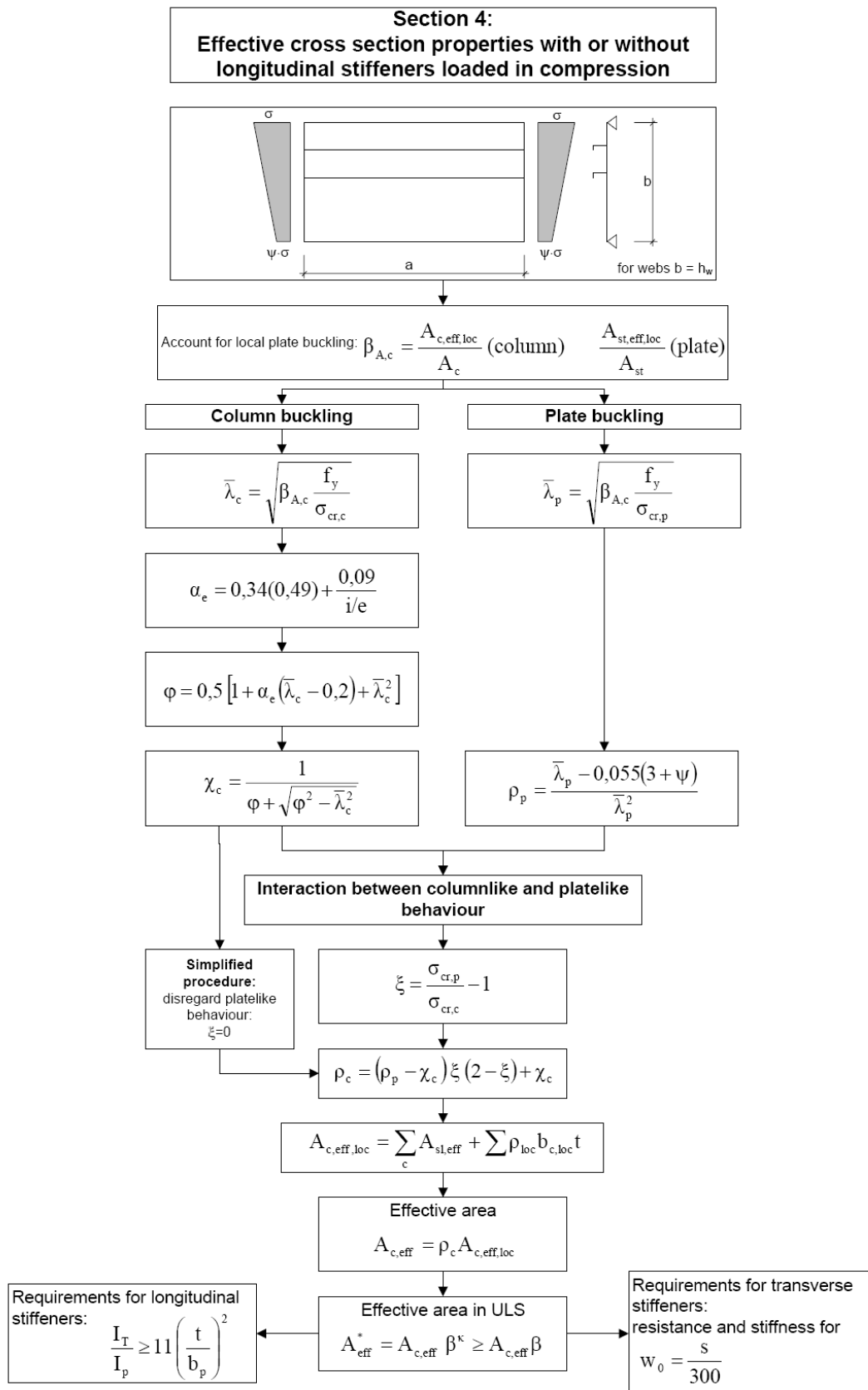


Figure 4.1: Determination of the reduced section of a Class 4 stiffened plate element

4.3 Approach based on the reduced cross-section concept

EN 1993-1-5
§4.3(1)

4.3.1 General

- (1) In the approach based on the *reduced cross-section concept*, the buckling verification of a longitudinally stiffened girder is conducted according to the following steps:
 - a) Determination of the stress distribution computed based on the assumption of a fully effective cross-section;
 - b) From this stress distribution, determination of the reduced cross-section of each individual plate element composing the section;
 - c) Determination of the stress distribution computed based on the properties of the reduced cross-section of the member, the latter being composed of the reduced sections of all the plate elements composing this cross-section;
 - d) Refinement of the reduced cross-section of each of the individual plate elements computed based on the stress distribution obtained in Step c), when the stress distributions obtained in Step a) and Step c) are significantly different;
 - e) The above process is repeated till the stress distribution is consistent with the properties of the reduced cross-section.
- (2) When the maximum compressive stress in the reduced cross-section of the member is supposed to reach the material yield strength, the steps d) and e) may be omitted. If the design stress σ_{xEd} lower than the yield strength is being calculated, iterations according to steps d) and e) are needed.
- (3) There is no limitation in the stress due to local plate buckling; the latter effect is accounted for by means of the concept of effective^p width (section) applied to any (unstiffened) plate element composing the plating and longitudinal stiffeners, with the following consequences:
 - Both stiffness and resistance of the longitudinal stiffeners shall be determined based on the fact that an effective^p width of plating is properly associated to the stiffener;
 - The buckling coefficient k_{σ} of a longitudinally stiffened plate element shall not be limited by local plate buckling of the unstiffened plate subpanels, so that reference shall be made to a so-called equivalent orthotropic plate element.
- (4) The procedure relative to the above Step b) is illustrated in Figure 4.2 for the case of an individual longitudinally stiffened plate element.
- (5) For a given loading, the amount of post-buckling strength reserve is highly dependent of the aspect ratio of the plate element under consideration; it depends moreover on the orthotropy degree when this plate element is longitudinally stiffened. Therefore due attention shall be paid to both influences by computing reduction factors relative to two extreme situations - the so-called *plate type behaviour* and *column type behaviour* (see Sections 4.3.2 and 4.3.3) - and then interpolating between both (see Section 4.3.4) with regards to the characteristics of the plate element in consideration.

4.3.2 Plate behaviour

(1) The elastic critical plate buckling stress may always be determined by means of any appropriate software. Alternatively, for that purpose, the code provides two simple approaches according to the number of longitudinal stiffeners located *in the compression zone* of the plate element :

- At least 3 longitudinal stiffeners, in which case it is referred to so-called *multiple stiffeners*;
- *One or two* longitudinal stiffeners.

(2) When *multiple stiffeners*, the stiffened plate element may be treated as an *orthotropic plate*, i.e. a plating no more fitted with discretely located stiffeners - as it is really the case - but with *smearred stiffeners*. The latter wording means that the total rigidity of all the stiffeners is distributed across the plate width so as to transform the actual plate into a fictitious one where the concept of subpanels is irrelevant. Plate buckling of the stiffened plate element reduces to global buckling of the *equivalent orthotropic plate element*. The elastic critical plate buckling stress $\sigma_{cr,p}$ is computed accordingly.

EN 1993-1-5
§A.1

(3) When the plate is longitudinally stiffened by *one or two stiffeners*, then a simplified specific procedure is used. The elastic critical plate buckling stress $\sigma_{cr,p}$ is deduced (see Section 11.2(6)) from the elastic critical column stress $\sigma_{cr,sl}$ of the stiffener closest to the edge with the highest compressive stress. This stiffener is supposed to be axially loaded and supported by an *elastic foundation*; the latter aims at reflecting the stabilising effects caused by bending of the plating, in the direction perpendicular to the stiffeners, when the compressed stiffeners are prone to buckle.

EN 1993-1-5
§A.2

(4) The effective^p width $b_{c,eff}$ of the compression zone of an *unstiffened plate element* is a proportion ρ of the actual geometric width b_c of the compression zone of this plate element. This proportion is seen as a reduction factor; it depends on the direct stress distribution ψ across the geometric width b of the plate element and on the support conditions along the longitudinal edges:

EN 1993-1-5
§4.5.2

- For internal compression plate elements (two longitudinal edges supported) [1]:

$$\rho = \frac{1}{\bar{\lambda}_p} - \frac{0,055(3 + \psi)}{\bar{\lambda}_p^2} \leq 1 \tag{4.1}$$

EN 1993-1-5
§4.4.2

- For outstand compression plate elements (one longitudinal edge supported and the other free)⁵ [2]:

$$\rho = \frac{1}{\bar{\lambda}_p} - \frac{0,188}{\bar{\lambda}_p^2} \leq 1 \tag{4.2}$$

EN 1993-1-5
§4.4.2

where $\bar{\lambda}_p$ is the *relative plate slenderness*. The latter is defined, similarly as for column slenderness, as the square root of the ratio between the squash

⁵ Distinction between internal element and outstand was not made in *ENV 1993-1-1*.

load and the elastic critical load of the sole compression zone of the plating in consideration:

$$\bar{\lambda}_p = \sqrt{\frac{A_c f_y}{A_c \sigma_{cr,p}}} = \sqrt{\frac{f_y}{\sigma_{cr,p}}} \quad (4.3)$$

EN 1993-1-5
§4.4.2

Taking into account that the elastic critical plate buckling stress $\sigma_{cr,p}$ is given as:

$$\sigma_{cr,p} = k_\sigma \sigma_E = k_\sigma \frac{\pi^2 E}{12(1-\nu^2)} \left(\frac{t}{b}\right)^2 \quad (4.4)$$

EN 1993-1-5
§A.1(2)

where k_σ is the buckling coefficient, the relative plate slenderness $\bar{\lambda}_p$ writes more explicitly (with $E = 210000 \text{ N/mm}^2$, $\nu=0,3$ and the yield factor $\varepsilon = \sqrt{235/f_y}$):

$$\bar{\lambda}_p = \frac{\left(\frac{b}{t}\right)}{28,4 \varepsilon \sqrt{k_\sigma}} \quad (4.5)$$

EN 1993-1-5
§4.4.2

In both above expressions of ρ , the first term is the well-known *von Karman* contribution, which, accounting for post-buckling strength reserve, is supposed to provide the behaviour of an ideally elastic perfectly flat plate; the second term is a penalty which was calibrated against test results so as to account for the detrimental effects of out-of-plane imperfections of the plate element, residual stresses and interaction between material yielding and plate buckling. The reduction factor ρ depends on the stress ratio ψ in such a way that, with some approximations, a full efficiency ($\rho=1$) is consistent with the b/t limits relative to *Class 3* plate elements⁶.

- (5) Similarly, the effective^p width $b_{c,eff}$ of the compression zone of a *longitudinally stiffened plate element* is a proportion ρ_{loc} of the actual width b_c of this zone. The expression of the relevant reduction factor ρ_{loc} is the same as for the unstiffened plate element⁷:

EN 1993-1-5
§4.5(2)

$$\rho_{loc} = \frac{1}{\bar{\lambda}_p} - \frac{0,055(3+\psi)}{\bar{\lambda}_p^2} \leq 1 \quad (4.6)$$

However the relative plate slenderness $\bar{\lambda}_p$ needs to be modified so as to pay due account for possible local plate buckling (in the plating between the longitudinal stiffeners and/or in the wall elements composing the section of the longitudinal stiffeners). The squash load then results from the yield strength applied on a reduced cross-sectional area $A_{c,eff,loc}$ because of the local plate buckling effects. This slenderness $\bar{\lambda}_p$ then writes:

$$\bar{\lambda}_p = \sqrt{\frac{A_{c,eff,loc} f_y}{A_c \sigma_{cr,p}}} = \sqrt{\frac{\beta A_c f_y}{\sigma_{cr,p}}} \quad (4.7)$$

EN 1993-1-5
§4.5.2(1)

where:

⁶ Formerly, some discrepancies in this respect did exist in *ENV 1993-1-1*.

⁷ Only the expression for internal elements is written because compression longitudinally stiffened outstands are rarely met in practice.

$$\beta_{A,c} = \frac{A_{c,eff.loc}}{A_c} \tag{4.8}$$

The elastic critical plate buckling stress is computed based on an *equivalent orthotropic plate*, i.e. a plate with *smear*ed” stiffeners⁸, so that local plate buckling is here irrelevant.

- (6) When computing $\beta_{A,c}$, the cross-sectional areas A_c and $A_{c,eff.loc}$ of the compression zone refer to a width, which is simply the superimposition of the respective influence zones of the individual stiffeners. This width differs from the actual width by the part of the width of the plating subpanel(s) which is (are) supported by an adjacent other plate element. If so, and for the sake of consistency, the cross-sectional area A_c shall not include this (these) part(s) of subpanel(s); also $A_{c,eff.loc}$ will be relative to the same resulting width (Figure 4.2).
- (7) Should shear lag effects be significant, then the cross-sectional A_c shall take account for shear lag effects and will then be the geometric area reduced by the reduction factor from shear lag. For the determination of $\beta_{A,c}$ according to equation (4.8) the reduction factor from shear lag has no effect as it is involved in both numerator and denominator

EN 1993-1-5
§4.5.2(1)

EN 1993-1-5
§4.5.1(4)

EN 1993-1-5
Fig. 4.4

EN 1993-1-5
§4.5.2(1)

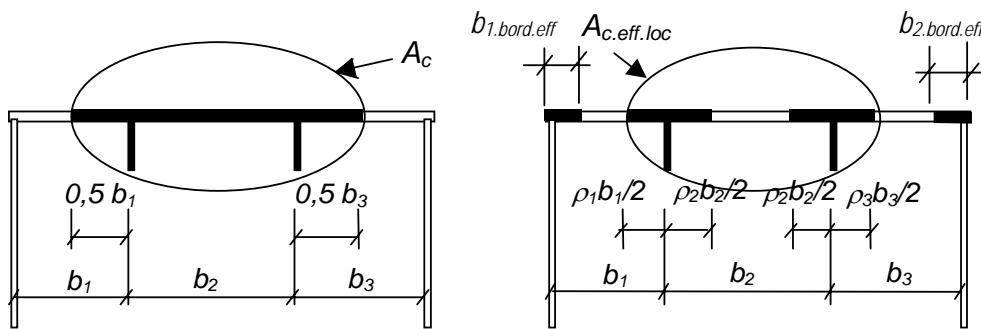


Figure 4.2: Definition of A_c and $A_{c,eff.loc}$ for a stiffened plate element (uniform compression)

- (8) The critical plate buckling stress $\sigma_{cr,p}$ of an unstiffened plate element or of a stiffened plate element writes:

$$\sigma_{cr,p} = k_\sigma \frac{\pi^2 E}{12(1-\nu^2)} \left(\frac{t}{b}\right)^2 = 190000 k_\sigma \left(\frac{t}{b}\right)^2 \tag{4.9}$$

- (9) For simply supported *unstiffened compression plate elements* – including wall elements of longitudinal stiffeners – subjected to *uniform compression*, the buckling coefficient k_σ is given as:

$$k_\sigma = \left(\frac{\alpha}{n} + \frac{n}{\alpha}\right)^2 \quad \text{with } \alpha = \frac{a}{b} \tag{4.10}$$

where a and b are the length (in the direction of the direct stresses) and the width of the unstiffened plate element in consideration, and n is an integer

EN 1993-1-5
§A.1(2)

⁸ The stiffness of the discrete longitudinal stiffeners is spreaded out across the breadth of the plate element

which represents the number of half sine waves in the direction of compression to be associated to the aspect ratio α . In practice, the above expression of k_{σ} is relevant only when $n=1$, which corresponds to $\alpha \leq \sqrt{2}$; indeed, larger values of n result in values of k_{σ} which are only slightly larger than 4. The value of 4 is a good approximation also in the range $1 \leq \alpha \leq \sqrt{2}$. Accordingly, for the so-called *long plates* ($\alpha \geq 1$), it is usual to adopt conservatively $k_{\sigma} = 4$.

For plate elements with one longitudinal edge simply supported and the other one free, $k_{\sigma}=0,43$ is taken regardless of the aspect ratio.

For short plates the actual value increases and an approximate expression for this increase can be found in Section 11.

- (10) For simply supported *unstiffened compression plate elements* – including wall elements of longitudinal stiffeners – subjected to a *linear stress distribution*, the buckling coefficient k_{σ} is given in Table 4.1 and Table 4.2 for long plates.

EN 1993-1-5
Table 4.1
Table 4.2

Table 4.1: Internal compression element

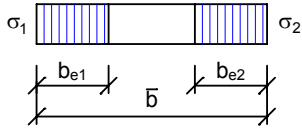
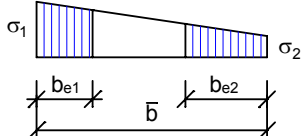
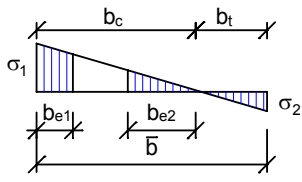
Stress distribution (compression positive)				Effective ^p width b_{eff}		
				$\underline{\psi = 1:}$ $b_{eff} = \rho \bar{b}$ $b_{e1} = 0,5 b_{eff} \qquad b_{e2} = 0,5 b_{eff}$		
				$\underline{1 > \psi \geq 0:}$ $b_{eff} = \rho \bar{b}$ $b_{e1} = \frac{2}{5 - \psi} b_{eff} \quad b_{e2} = b_{eff} - b_{e1}$		
				$\underline{\psi < 0:}$ $b_{eff} = \rho b_c = \rho \bar{b} / (1 - \psi)$ $b_{e1} = 0,4 b_{eff} \qquad b_{e2} = 0,6 b_{eff}$		
$\psi = \sigma_2 / \sigma_1$	1	$1 > \psi > 0$	0	$0 > \psi > -1$	-1	$-1 > \psi > -3$
Buckling factor k_{σ}	4,0	$8,2 / (1,05 + \psi)$	7,81	$7,81 - 6,29\psi + 9,78\psi^2$	23,9	$5,98 (1 - \psi)^2$

Table 4.2: Outstand compression elements

Stress distribution (compression positive)		Effective ^p width b_{eff}			
		$1 > \psi \geq 0:$ $b_{eff} = \rho c$			
		$\psi < 0:$ $b_{eff} = \rho b_c = \rho c / (1-\psi)$			
$\psi = \sigma_2/\sigma_1$	1	0	-1	$1 \geq \psi \geq -3$	
Buckling factor k_σ	0,43	0,57	0,85	$0,57 - 0,21\psi + 0,07\psi^2$	
		$1 > \psi \geq 0:$ $b_{eff} = \rho c$			
		$\psi < 0:$ $b_{eff} = \rho b_c = \rho c / (1-\psi)$			
$\psi = \sigma_2/\sigma_1$	1	$1 > \psi > 0$	0	$0 > \psi > -1$	-1
Buckling factor k_σ	0,43	$0,578 / (\psi + 0,34)$	1,70	$1,7 - 5\psi + 17,1\psi^2$	23,8

(11) Information on the determination of the critical plate buckling stress $\sigma_{cr,p}$ of stiffened plate elements is given in section 11.

4.3.3 Column behaviour

- (1) Because they account for a post-buckling strength reserve, the above expressions of ρ are representative of a plate behaviour. However, a column type behaviour with no such post-buckling reserve at all may be exhibited when small aspect ratio a/b (<1 for a non stiffened plating) and/or large plate orthotropy (if longitudinally stiffened plate element). Then a reduction factor χ_c relative to column buckling is required, that is more severe than ρ , applicable to typical plate buckling.
- (2) Modelling the column behaviour is simply achieved by removing the longitudinal supports of the plate element.

EN 1993-1-5 §4.5.3

EN 1993-1-5 §4.4(6)

(3) The elastic critical column buckling stress $\sigma_{cr,c}$ is computed as follows:

- For a plating (= unstiffened plate element):

$$\sigma_{cr,c} = \frac{\pi^2 E}{12(1-\nu^2)} \left(\frac{t}{a}\right)^2 \tag{4.11}$$

EN 1993-1-5
§4.5.3(2)

- For a stiffened plate element:

It is first referred to buckling stress $\sigma_{cr,sl}$ of a pin-ended axially loaded strut composed of : i) the stiffener that is located closest to the panel edge with the highest compressive stress, and ii) an adjacent contributive part of plating (Figure 4.3):

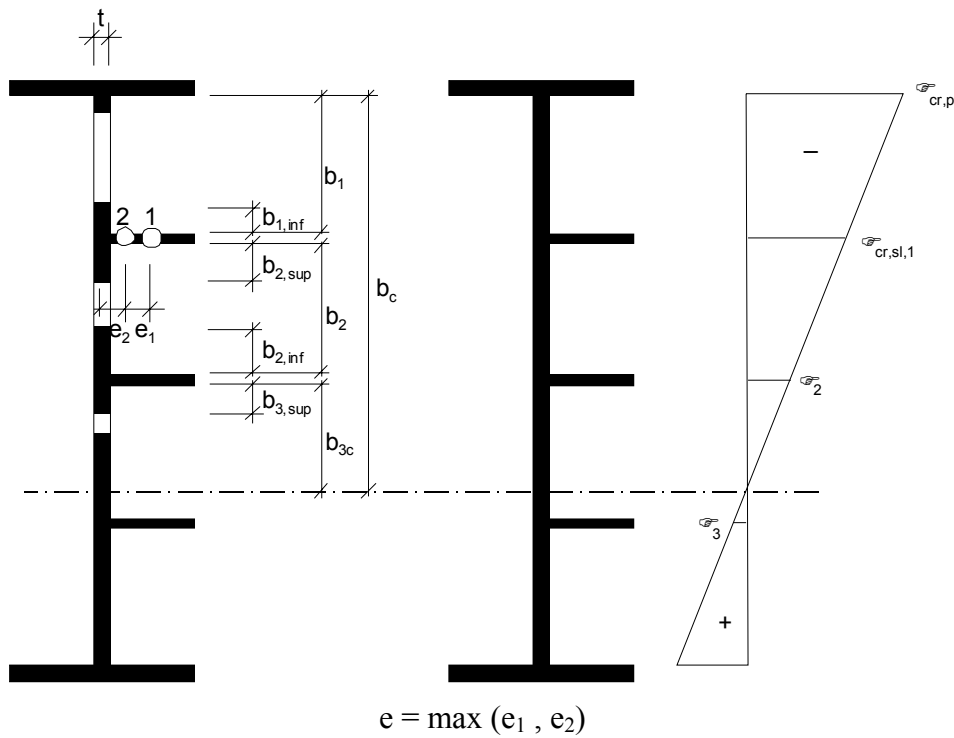
$$\sigma_{cr,sl} = \frac{\pi^2 E I_{sl,1}}{A_{sl,1} a^2} \tag{4.12}$$

EN 1993-1-5
§4.5.3(3)

where:

$I_{sl,1}$ Second moment of area for the gross cross section, relative to the out-of-plane bending of the stiffened plate element, of the above defined strut;

$A_{sl,1}$ Gross cross-sectional area of the above defined strut (see column “gross area” in Figure 4.3).



	width for gross area	width for effective area according to EN 1993-1-5, Table 4.1	condition for ψ_i
$b_{1,inf}$	$\frac{3 - \psi_1}{5 - \psi_1} b_1$	$\frac{3 - \psi_1}{5 - \psi_1} b_{1,eff}$	$\psi_1 = \frac{\sigma_{cr,sl,1}}{\sigma_{cr,p}} > 0$
$b_{2,sup}$	$\frac{2}{5 - \psi_2} b_2$	$\frac{2}{5 - \psi_2} b_{2,eff}$	$\psi_2 = \frac{\sigma_2}{\sigma_{cr,sl,1}} > 0$
$b_{2,inf}$	$\frac{3 - \psi_2}{5 - \psi_2} b_2$	$\frac{3 - \psi_2}{5 - \psi_2} b_{2,eff}$	$\psi_2 > 0$
$b_{3,sup}$	$0,4 b_{3c}$	$0,4 b_{3c,eff}$	$\psi_3 = \frac{\sigma_3}{\sigma_2} < 0$

Figure 4.3: Determination of the participating part of plating

EN 1993-1-5
Fig. A.1

Again, for consistency with $\sigma_{cr,p}$, which is relative to the edge with the highest compressive stress, the stress $\sigma_{cr,sl}$ shall be extrapolated up to the same edge according to:

$$\sigma_{cr,c} = \sigma_{cr,sl} \frac{b_c}{\bar{b}} \tag{4.13}$$

EN 1993-1-5
§4.5.3(3)

where b_c is the depth of the compression zone and \bar{b} the location of the stiffener measured from the fibre of zero direct stress.

(4) The relative column slenderness $\bar{\lambda}_c$ is given as the square root of the ratio between the squash load and the elastic critical column buckling load of :

- A plating strip of unit width when unstiffened plate element is concerned:

$$\bar{\lambda}_c = \sqrt{\frac{f_y}{\sigma_{cr,c}}} \quad (4.14)$$

- A strut composed of the stiffener and the adjacent part of plating:

$$\bar{\lambda}_c = \sqrt{\frac{A_{sl,1,eff,loc} f_y}{A_{sl,1} \sigma_{cr,c}}} = \sqrt{\frac{\beta_{A,c} f_y}{\sigma_{cr,c}}} \quad (4.15)$$

EN 1993-1-5
§4.5.3(4)

where :

$$\beta_{A,c} = \frac{A_{sl,1,eff,loc}}{A_{sl,1}} \quad (4.16)$$

EN 1993-1-5
§4.5.3(4)

The cross sectional area $A_{sl,1,eff}$ is the reduced section of the above strut when due attention is paid to local plate buckling in the plating and/or possibly in the wall elements of the stiffener (for the plating, see column “effective area” in Figure 4.3).

(5) The expression for the relevant reduction factor χ_c is the same as for usual column buckling:

$$\chi_c = \frac{1}{\phi + \sqrt{\phi^2 - \bar{\lambda}_c^2}} \quad (4.17)$$

where:

$$\phi = 0,5 \left[1 + \alpha_e (\bar{\lambda}_c - 0,2) + \bar{\lambda}_c^2 \right] \quad (4.18)$$

and α_e is a modified imperfection parameter which accounts for larger initial geometric imperfection (see (6) below).

(6) It is usual to stiffen a plating with one-sided longitudinal stiffeners, with the result that the middle plane of the plating is not the neutral plane of the stiffened plate element. The eccentricity of the stiffeners with respect to the plating (Figure 4.4) is accounted for by simply magnifying the value of the generalised imperfection parameter α governing the analytical expressions of the buckling curves:

$$\alpha_e = \alpha + \frac{0,09}{i/e} \quad (4.19)$$

EN 1993-1-5
§4.5.3(5)

where:

$$i = \sqrt{\frac{I_{sl,1}}{A_{sl,1}}} \quad (4.20)$$

and:

$I_{sl,1}$ Second moment of area, relative to the out-of-plane bending of the stiffened plate element, of the stiffener fitted with an adjacent contributive part of plating (Figure 4.4);

$A_{sl,1}$ Gross cross-sectional area of the stiffener fitted with an adjacent contributive part of plating (Figure 4.4);

$e = \max(e_1, e_2)$ The largest distance from the respective centroids of the plating and the one-sided stiffener (or of the centroids of either set of stiffeners when present on both sides of the plating) to the neutral axis of the stiffener including the contributive plating (Figure 4.4).

The use of closed section stiffeners results in a better stability and in less residual stresses (because of thin walls and one-sided fillet welds) justifies $\alpha = 0,34$; a larger value $\alpha = 0,49$ is required for open section stiffeners.

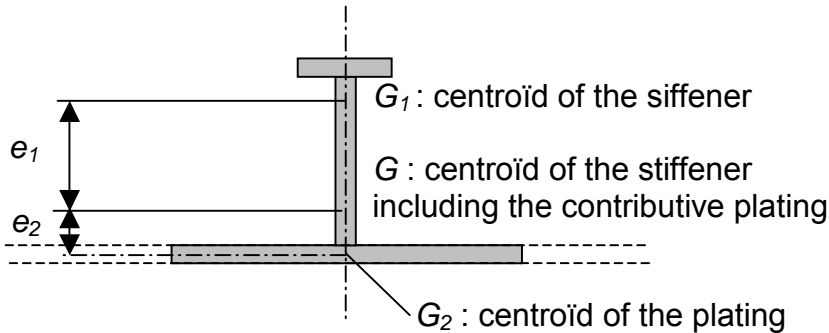


Figure 4.4: Eccentricities of the stiffeners

4.3.4 Interpolation between plate behaviour and column behaviour

- (1) First, the reduction factors are computed based respectively on a plate behaviour (reduction factor ρ) and on a column behaviour (reduction factor χ_c) as indicated in Sections 4.3.2 and 4.3.3.
- (2) The actual behaviour is often somewhere between these two extreme situations. Then, the resistance in the ULS of a longitudinally stiffened plate has to reflect this intermediate behaviour between plate behaviour and column behaviour by means of a resulting reduction factor ρ_c such that:

$$\chi_c \leq \rho_c \leq \rho \tag{4.21}$$

- (3) The reduction factor ρ_c is simply determined based on a simple interpolation formula; the latter is proposed to be [5]:

$$\rho_c = \xi(2 - \xi)(\rho - \chi_c) + \chi_c \tag{4.22}$$

where the parameter ξ is a kind of measure of the “distance” between the elastic critical plate and column buckling stresses according to:

$$\xi = \frac{\sigma_{cr,p}}{\sigma_{cr,c}} - 1 \text{ but } 0 \leq \xi \leq 1 \tag{4.23}$$

The limits assigned to the parameter ξ are physically justified as follows:

- Plate behaviour may never be more detrimental than column behaviour, so that $\sigma_{cr,p} \geq \sigma_{cr,c}$ with the result of an always positive value of ξ ;

EN 1993-1-5 §4.5.4

EN 1993-1-5 §4.5.4(1)

- It is agreed that column behaviour is irrelevant when $\sigma_{cr,p}$ is significantly larger than $\sigma_{cr,c}$, let us say $\sigma_{cr,p} \geq 2\sigma_{cr,c}$; then one needs $\rho_c = \rho$, so that $\xi \leq 1$.

- (4) This interpolation formula between column behaviour and plate behaviour is plotted in Figure 4.5.
- (5) Once the reduction factor ρ_c has been determined, the effective^p area of the compression zone of a stiffened plate is taken as (see Figure 11.2 and Section 4.3.2):

$$A_{c,eff} = \rho_c A_{c,eff,loc} + \Sigma b_{edge,eff} t \tag{4.24}$$

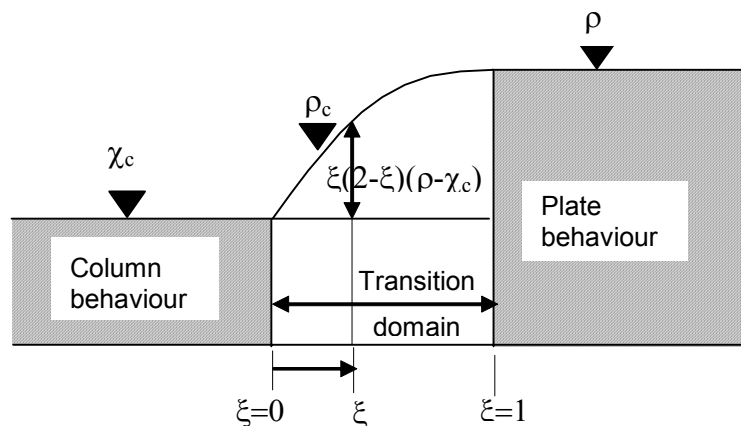


Figure 4.5: Interpolation between plate behaviour and column behaviour

4.3.5 Plate buckling check

- (1) The buckling check consists of verifying that the maximum compressive design stress σ_{xEd} does not exceed the yield stress:

$$\eta = \frac{\sigma_{xEd}}{f_y / \gamma_{M1}} \leq 1 \tag{4.25}$$

The stress σ_{xEd} is obtained by using the elementary theory of beams, as:

$$\sigma_{xEd} = \frac{M_{Ed}}{W_{eff}} \tag{4.26}$$

with :

M_{Ed} : design bending moment existing in the cross-section;

$W_{eff} = \frac{I_{eff}}{v}$: elastic section modulus of the cross-section;

I_{eff} : second moment of area of the cross-section about the relevant axis of bending;

EN 1993-1-5
§4.6

v : distance of the (extreme) fibre under consideration from the axis of bending.

For the determination of W_{eff} , I_{eff} and v , reference shall be made to a cross-section composed of plate elements, the compression zones of which are accounted for through their effective^p area only (see 4.3.4(5)). As a simplification, the reduction due to ρ_c may be taken as uniformly distributed over the relevant compressed area.

- (2) Further indications relative to the design of both longitudinal and transverse stiffeners are given in another chapter (see Chapter 9).

4.3.6 Validation of plate buckling check procedure

- (1) The rules applied to longitudinally stiffened panels have been validated by comparison with results of tests conducted on individual compression panels stiffened by multiple longitudinal stiffeners (Table 4.3). It is not possible to use all the available test results because some tests are not sufficiently documented while some other specimens exhibit an unduly large out-of-flatness, the magnitude of which exceeds substantially the fabrication tolerance that is implicitly covered by the design rules. The 25 specimens kept for the validation have stiffeners made with either flats, bulb flats or angles and the wall elements of some of these stiffeners did not comply with the b/t limits of Class 3 elements so that they are in principle not fully effective.
- (2) The recommended minimum value of the partial safety factor γ_M will be given in the application parts of the Eurocodes, e.g. in EN 1993-1-1 for buildings and EN 1993-2 for bridges. The value $\gamma_M = 1,10$ (it is now 1 in EN 1993-1-1) is on the safe side (see Figure 4.6).

EN 1993-1-1
EN 1993-2

Table 4.3: Tests used for calibration of the design rules

Test	Designation	Tests	Type of stiffener
Dorman & Dwight	Nr 3 (TPA3)	4	Bulb flat
	Nr 4 (TPA4)		
	Nr 7 (TPB3)		
	Nr 8 (TPB3)		
Scheer & Vayas	Nr 3 (TPA3)	3	Bulb flat
	Nr 4 (TPA4)		
	Nr 7 (TPB3)		
Fukumoto	B-1-1	6	Flat
	B-1-1r		
	B-2-1		
	B-3-1		
	C-1-4		
	C-2-1		
Lutteroth 1 Kretzschmar	All	12	9 tests with flats and 3 tests with flats and angles

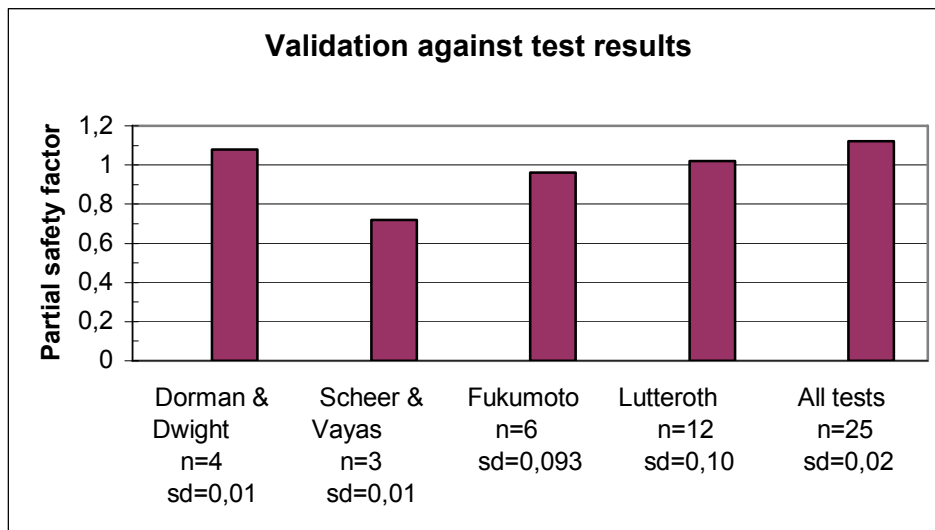


Figure 4.6: Longitudinally stiffened panels: Required partial factor on the resistance

4.4 References

[1] ECCS Technical Committee 8 – Structural Stability, Behaviour and Design of steel Plated Structures, edited by P. Dubas and E. Gehri, Publication n° 44, Applied Statics and Steel Structures, ETH Zurich, 1986.

- [2] Johansson B. and Veljkovic M., Steel Plated Structures, Progress in Structural Engineering and Materials, 3:1 2001, John Wiley & Sons Ltd.
- [3] Klöppel K. and Scheer J., Beulwerte ausgesteifter Rechteckplatten (Band I), W.Ernst & Sohn, Berlin, 1960.
- [4] Klöppel K. and Möller K.H., Beulwerte ausgesteifter Rechteckplatten (Band II), W.Ernst & Sohn, Berlin-München, 1968.
- [5] Johansson B., Maquoi R., Sedlacek G., Müller Ch. and Schneider R., Die Behandlung des Beulens bei dünnwandigen Stahlkonstruktionen in ENV 1993-Teil 1.5, Stahlbau, Heft 11, 1999, pp 857

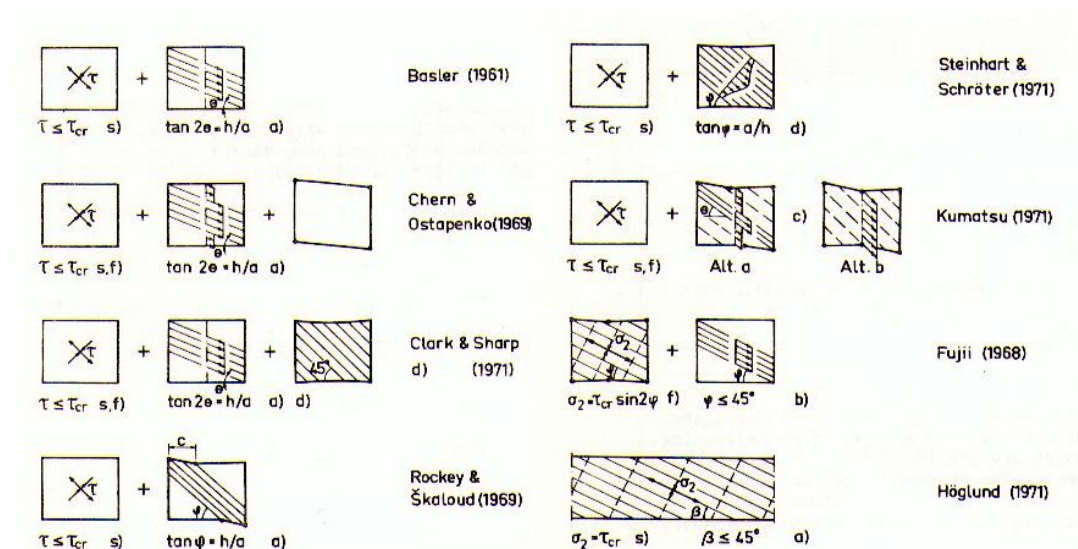
5 Resistance to shear

EN 1993-1-5, §5

Darko Beg, Faculty of Civil and Geodetic Engineering, University of Ljubljana

5.1 Introduction

Slender web panels in shear possess a significant post-buckling resistance, when a proper anchorage of tension membrane stresses that develop after buckling is assured. Many design methods based on tension field action have been developed so far. A good overview of tension field theories is given by Höglund [1] and Galambos [2] (see Figure 5.1 taken from Höglund [1]). These theories mainly assume superposition of buckling and post-buckling shear strength and differ regarding the definition of tension field action. EN 1993-1-5 implemented the method known as "rotated stress field" developed by Höglund [3,4]. This method was first developed for unstiffened webs with large aspect ratios (Höglund [3]), where other tension field methods give very conservative results. It was used in ENV 1993-1-5 for plated steel structures and in ENV 1999-1-1 for aluminium structures, but not in ENV 1993-1-1 where the so-called Cardiff-Prague tension field method was used and the simple post-critical method was added to overcome conservative results for large web panel aspect ratios. This simple post-critical method is very similar to the rotated stress field method for non-rigid end posts.



Notes

- | | | |
|------------------------------|------------------|-----------------------------------|
| Assumption for τ_{cr} : | Yield criterion: | Miscellaneous: |
| s) Simple support | a) von Mises | c) Two alternative tension fields |
| f) Fixed for rotation | b) Tresca | d) Aluminium |
| s, f) Elastic restraint | | |

Figure 5.1: Overview of tension field models (from Höglund [1])

The rotated stress field method is described in detail in Höglund [3,4]. Here only some basic ideas are given (Figure 5.2). The basic assumption is that there are no membrane stresses in the transverse direction of the web panel. This is true for webs of long girders without transverse stiffeners other than the ones at the supports. After buckling compressive membrane stresses σ_2 cannot increase any more, but tension membrane stresses σ_1 may still increase until the ultimate

resistance is reached. Under such conditions the equilibrium requires the rotation of the stress field (Figure 5.2(g)). When principal tension stresses increase the angle ϕ must decrease because of equilibrium reasons, see equations (5.1) and (5.2).

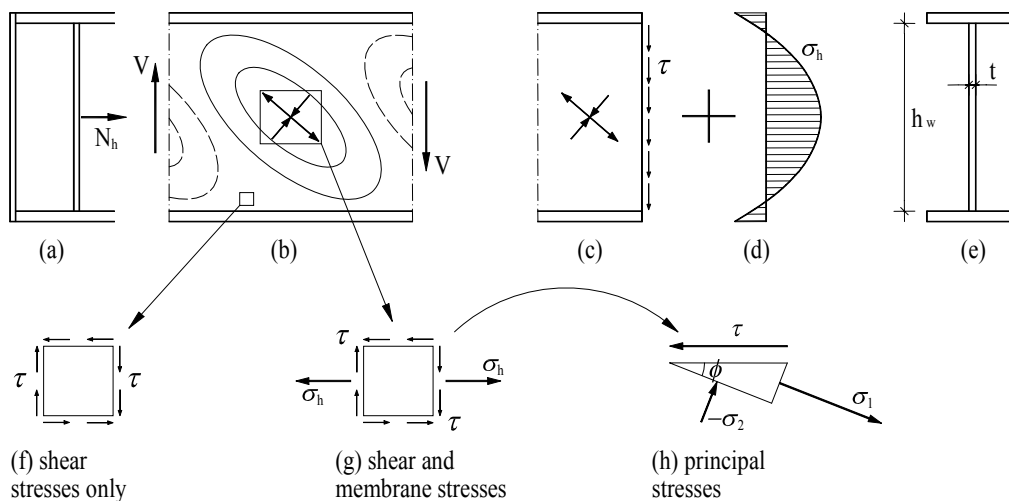


Figure 5.2: Mechanical model of the rotated stress field

N_h in Figure 5.2 is the total longitudinal force existing in the web at the post-critical stage to be anchored onto the end post, and σ_h is the corresponding normal stress in the longitudinal direction.

For the principal stresses the following relations are valid (Figure 5.2):

$$\sigma_1 = \frac{\tau}{\tan \phi} \tag{5.1}$$

$$\sigma_2 = -\tau \cdot \tan \phi \tag{5.2}$$

By limiting the compression membrane stress:

$$\sigma_2 = -\tau_{cr} \tag{5.3}$$

implementing the von Mises yield criterion:

$$\sigma_1^2 - \sigma_1 \sigma_2 + \sigma_2^2 = f_{yw}^2 \tag{5.4}$$

and eliminating σ_1 , σ_2 and $\tan \phi$ the following ultimate shear resistance τ_u – normalized with respect to the yield strength in shear $f_{yw} / \sqrt{3}$ - is obtained as a function of $\bar{\lambda}_w$:

$$\frac{\tau_u}{f_{yw} / \sqrt{3}} = \frac{1}{\bar{\lambda}_w^2} \sqrt{\sqrt{3\bar{\lambda}_w^4 - \frac{3}{4}} - \frac{1}{2}} \tag{5.5}$$

where $\bar{\lambda}_w$ is the shear panel slenderness:

$$\bar{\lambda}_w = \sqrt{\frac{f_{yw} / \sqrt{3}}{\tau_{cr}}} \tag{5.6}$$

τ_{cr} is the elastic shear buckling stress of a perfect shear panel:

$$\tau_{cr} = k_{\tau} \sigma_E = k_{\tau} \frac{\pi^2 E}{12(1-\nu^2)} \left(\frac{t}{h_w} \right)^2 \quad (5.7)$$

For large values of $\bar{\lambda}_w$ ($\bar{\lambda}_w > 2.5$) the normalized shear resistance reduces to:

$$\frac{\tau_u}{f_{yw}/\sqrt{3}} = \frac{1,32}{\bar{\lambda}_w} \quad (5.8)$$

The theoretical resistance is based on the presence of a rigid end post. Before being used in the code it has to be reduced for the scatter in the test results due to varying imperfections.

5.2 Design shear resistance according to EN 1993-1-5

EN 1993-1-5,
§5.2

5.2.1 General

Design shear resistance is taken as

$$V_{b,Rd} = V_{bw,Rd} + V_{bf,Rd} \leq \frac{\eta f_{yw} h_w t}{\sqrt{3} \gamma_{M1}} \quad (5.9)$$

EN 1993-1-5,
§5.2(1)

where

$$V_{bw,Rd} = \frac{\chi_w f_{yw} h_w t}{\sqrt{3} \gamma_{M1}} \text{ is the contribution from the web;} \quad (5.10)$$

$V_{bf,Rd}$ is the contribution from flanges;

χ_w is the reduction factor for the shear resistance of the sole web, depending on the web slenderness;

γ_{M1} is the partial factor for the resistance to instability;

η is the coefficient that includes the increase of shear resistance at smaller web slenderness;

NOTE 2 to 5.1 (2) of EN 1993-1-5 recommends the following values:

$\eta = 1,2$ for S235 to S460

$\eta = 1,0$ for steel grades over S460.

h_w, t are dimensions, see Figure 5.3.

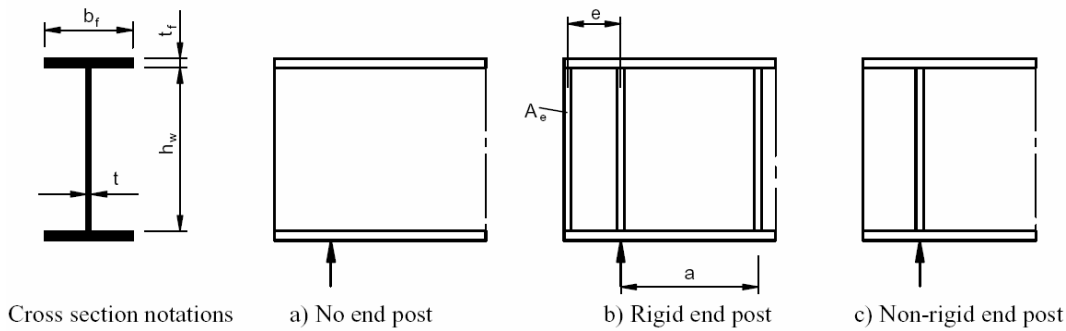


Figure 5.3: End-stiffeners

The reasons why η can be taken larger than 1 may be explained as follows. In the tests on beams with stocky webs the ultimate resistance in shear reaches 0,7 to 0,8 times the yield strength in tension. Such behaviour can be observed in Figure 5.4, where the shear stress to yield strength ratio is plotted against normalized shear strain $\gamma G/f_y$. One reason for this is strain hardening of steel, which can be utilized because it does not give excessive deformations. There is probably also a contribution from the flanges, but the respective contributions from strain hardening and flanges cannot easily be separated and also this effect has not been studied in detail. For this reason the increase in resistance is not allowed for the isolated shear panels that are not attached to flanges to form I-like cross sections. There are no test results available supporting this increase for higher steel grades than S460. In other cases such an increase up to at least 20% is possible.

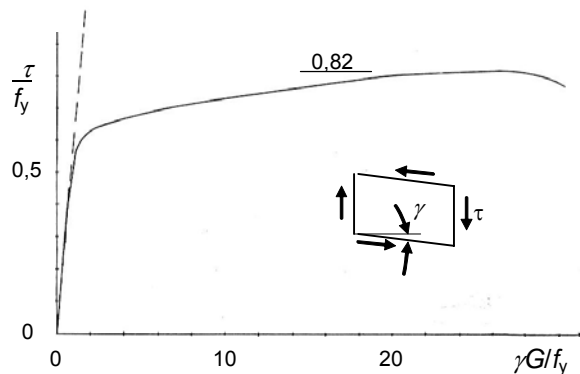


Figure 5.4: Average shear stress as function of average shear strain from test with HEA 240

For stocky webs with:

$$\frac{h_w}{t} \leq \frac{72}{\eta} \varepsilon \quad \text{for unstiffened webs or}$$

$$\frac{h_w}{t} \leq \frac{31}{\eta} \varepsilon \sqrt{k_\tau} \quad \text{for transversely stiffened webs} \quad (5.11)$$

there is no danger of shear buckling and χ_w can be taken as η . These requirements are in accordance with the plateau of the reduction factor χ_w for shear resistance (see Figure 5.5).

EN 1993-1-5,
§5.2(2)

It is worth mentioning that η larger than 1,0 means higher resistance, but also more stringent h_w/t limit ratio, because buckling has to be prevented at higher levels of stresses and strains.

Design resistance formula (5.9) can be used, when the following requirements are met:

- Panels are rectangular and flanges are parallel within an angle not greater than 10°;
- Webs may be stiffened in the longitudinal and/or transverse direction;
- Stiffeners should comply with the requirements in Section 9;
- All holes and cut outs in the webs are small; their diameter d should satisfy $d/h_w \leq 0,05$;
- Members are uniform;
- Panels that do satisfy the requirement (5.11) for unstiffened support should be checked for patch loading resistance according to section 6;
- Panels that do not satisfy requirements (5.11) should be fitted with transverse stiffeners at the supports.

When some of these requirements are not met, more rigorous analysis should be carried out or a safe-sided approach has to be applied (stiffeners placed around holes; equivalent rectangular panel used instead of a non-rectangular one with unfavourable largest dimensions of a panel taken to determine $\bar{\lambda}_w \dots$).

5.2.2 Contribution from the web

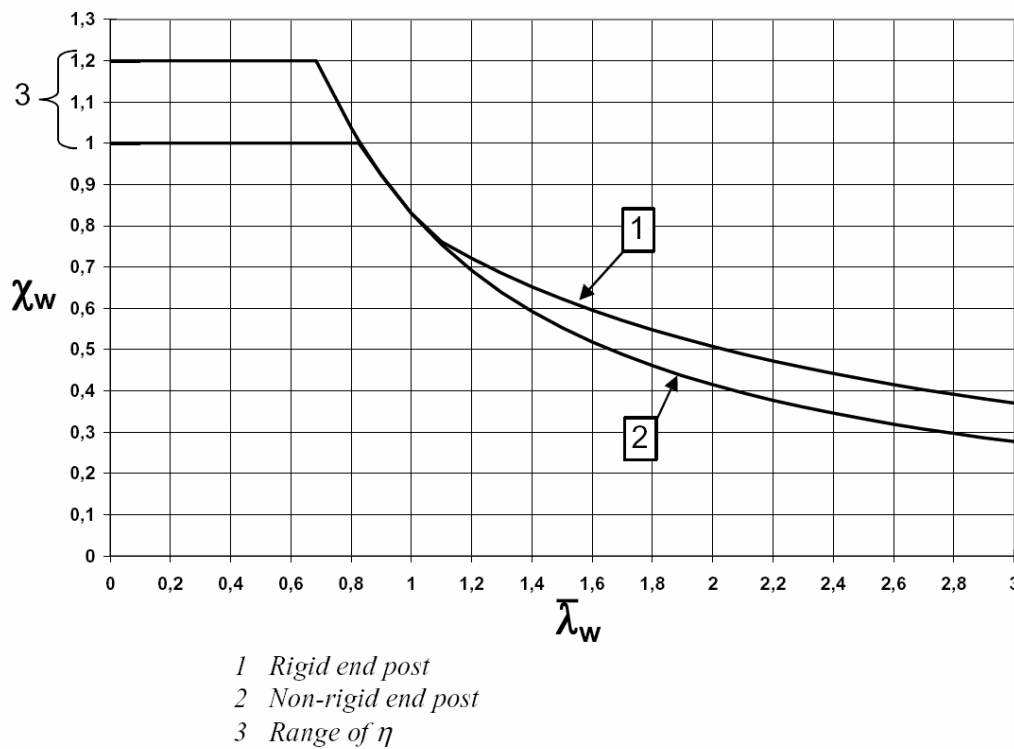
The factor χ_w for the contribution of the web to the shear resistance is given in Table 5.1 and plotted in Figure 5.5.

Table 5.1: Shear resistance function of the web

	Rigid end post	Non-rigid end post
$\bar{\lambda}_w < 0,83/\eta$	η	η
$0,83/\eta \leq \bar{\lambda}_w < 1,08$	$0,83/\bar{\lambda}_w$	$0,83/\bar{\lambda}_w$
$\bar{\lambda}_w \geq 1,08$	$1,37/(0,7 + \bar{\lambda}_w)$	$0,83/\bar{\lambda}_w$

EN 1993-1-5, §5.3

EN 1993-1-5, §5.3, Tab. 5.1



EN 1993-1-5,
§5.3, Fig. 5.2

Figure 5.5: Reduction factor for shear resistance of the web

χ_w is based on the rotated stress field method (Eq. (5.5) and (5.8)), but finally defined from test results to get a proper safety margin and to allow for rigid as well as non-rigid end posts. χ_w can be regarded as

$$\chi_w = \frac{\tau_u}{f_{yw} / \sqrt{3}} \quad (5.12)$$

For the slenderness parameter $\bar{\lambda}_w$ in Table 5.1 the standard definition applies:

$$\bar{\lambda}_w = \sqrt{\frac{f_{yw}}{\sqrt{3}\tau_{cr}}} = 0,76 \sqrt{\frac{f_{yw}}{\tau_{cr}}} \quad (5.13)$$

where

$$\tau_{cr} = k_\tau \frac{\pi^2 E}{12(1-\nu^2)} \frac{t^2}{h_w^2} \quad (5.14)$$

By putting (5.14) into (5.13), slenderness $\bar{\lambda}_w$ can be rewritten as:

$$\bar{\lambda}_w = \frac{h_w}{37,4t\varepsilon\sqrt{k_\tau}} \quad (5.15)$$

For unstiffened and longitudinally stiffened webs k_τ is given in 0.

EN 1993-1-5,
§5.3(3)

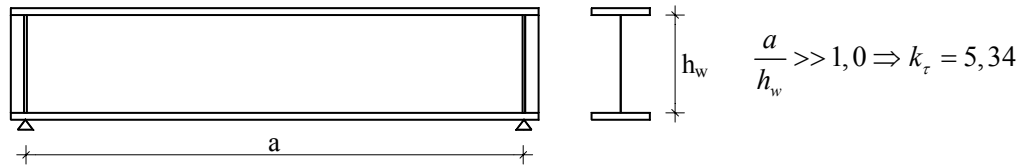


Figure 5.6: Unstiffened web panel

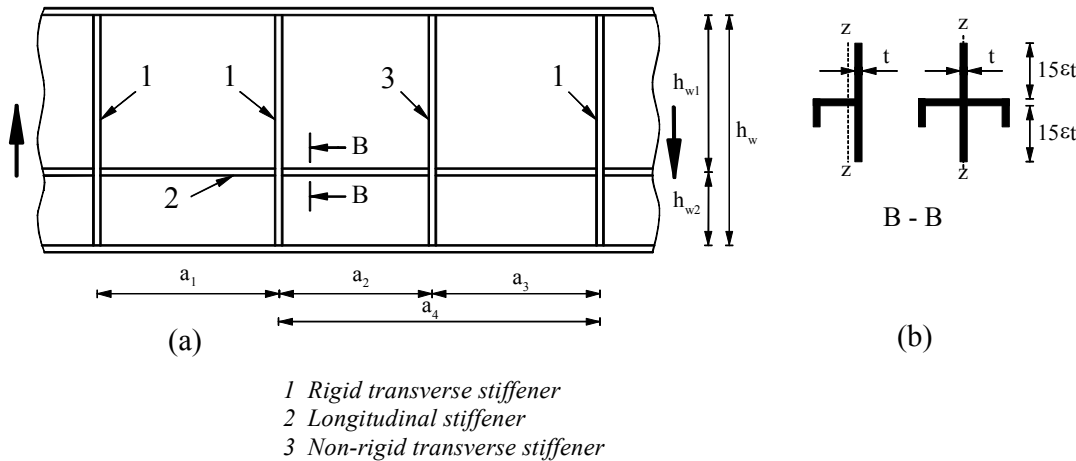


Figure 5.7: Web with transverse and longitudinal stiffeners

For webs with transverse stiffeners only at the supports (Figure 5.6), the aspect ratio a/h_w is large and k_τ approaches the value 5,34. In this case Eq. (5.15) becomes

$$\bar{\lambda}_w = \frac{h_w}{86,4t\epsilon} \tag{5.16}$$

For webs with transverse stiffeners at the supports and with intermediate transverse and/or longitudinal stiffeners Eq. (5.15) applies.

Both rigid and non-rigid stiffeners may be used. Stiffeners are rigid when they prevent transverse displacements of the web panels along the web-stiffener junction line and remain straight in the post-buckling stage. Non-rigid stiffeners increase both the strength and stiffness of web panels but they buckle together with the web plate. When a part of a web plate is surrounded by only rigid transverse and longitudinal stiffeners or flanges it can be treated simply as an isolated plate. When at least one of the stiffeners is non-rigid, larger panels containing non-rigid stiffeners should be checked too, as explained below.

The shear buckling coefficient k_τ is determined in the following ways:

- Only rigid transverse stiffeners are used (panel $a_1 \times h_w$ in Figure 5.7).

k_τ is determined from 0, where the contribution of longitudinal stiffeners is taken into account. Rigid boundaries may be assumed along the flanges and rigid transverse stiffeners, and the panel $a_1 \times h_w$ may be assumed as being an isolated panel.

EN 1993-1-5, §5.3, Fig. 5.3

EN 1993-1-5, §5.3(3)

- Non-rigid transverse stiffener is placed between rigid transverse stiffeners (panel $a_4 \times h_w$ in Figure 5.7). Individual panels between the adjacent transverse stiffeners ($a_2 \times h_w$ and $a_3 \times h_w$) and the whole panel between the adjacent rigid transverse stiffeners ($a_4 \times h_w$) should be checked for the smallest k_τ . For the panels $a_2 \times h_w$ and $a_3 \times h_w$, k_τ may be determined from 0. For the panel $a_4 \times h_w$ that contains an intermediate non-rigid transverse stiffener, k_τ may be determined from appropriate design charts or using an eigenvalue analysis of the panel (see section 12 and Annex C of EN 1993-1-5), because the formulae in 0 do not cover cases with intermediate non-rigid transverse stiffeners.
- For the webs with multiple non-rigid transverse stiffeners the following simplification in the calculation of k_τ may be used:
 - a) check two adjacent panels with one non-rigid transverse stiffener (panel $a_1 \times h_w$ in Figure 5.8);
 - b) check the adjacent panels with two non-rigid transverse stiffeners (panel $a_2 \times h_w$ in Figure 5.8);

and take the smallest of both values as k_τ , while in both cases the panels are regarded as rigidly supported along the outer edges.

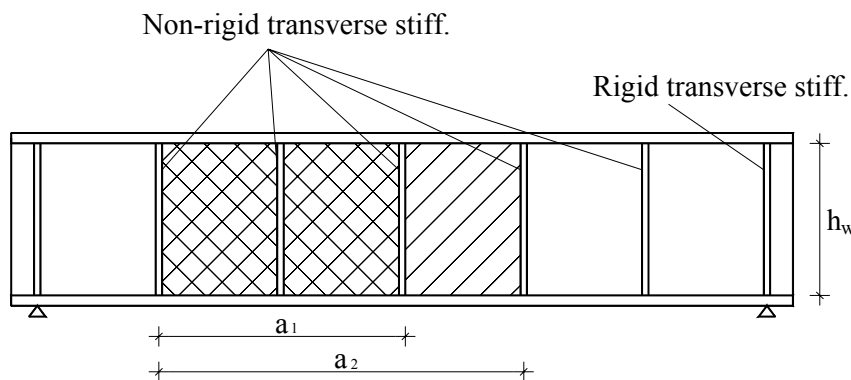


Figure 5.8: Web panel with multiple non-rigid transverse stiffeners

For web panels containing longitudinal stiffeners the slenderness parameter $\bar{\lambda}_w$ should not be taken less than the largest slenderness of all sub-panels:

$$\bar{\lambda}_w = \frac{h_{wi}}{37,4t\epsilon\sqrt{k_{\tau i}}} \tag{5.17}$$

EN 1993-1-5, §5.3(5)

where h_{wi} and $k_{\tau i}$ refer to the sub-panel with the largest slenderness parameter $\bar{\lambda}_w$ of all sub-panels within the web panel under consideration. For the panel $a_1 \times h_w$ (Figure 5.7) obviously the sub-panel $a_1 \times h_w$ is the decisive one.

Post-buckling behaviour is more pronounced in unstiffened webs than in longitudinally stiffened webs, because longitudinal stiffeners increase the overall strength, but temper the development of the tension field.

For this reason the influence of the longitudinal stiffeners, coming from the linear buckling through the calculation of k_τ and χ_w , is overestimated. To be allowed to use the same resistance function χ_w in both cases, the slenderness parameter $\bar{\lambda}_w$ should be increased accordingly. In EN 1993-1-5 this is done by reducing the

second moment of area of the longitudinal stiffeners to 1/3 of their actual value. This reduction was validated by experimental evidence (see 5.2.5 and Figure 5.12). Very few tests were related to the panels stiffened with closed longitudinal stiffeners and recent research results (Pavlovčič, Beg and Kuhlmann [5]) show that this reduction is not really necessary for closed stiffeners, because of their substantial torsional stiffness.

Shear buckling coefficients

EN 1993-1-5 gives the expressions of the shear buckling coefficient k_τ for the following two basic cases:

- plates with rigid transverse stiffeners;
- longitudinally stiffened plates between rigid transverse stiffeners.

No information is given for plates reinforced with non-rigid transverse stiffeners. In this case k_τ can be obtained from the appropriate design charts or eigenvalue analysis of the stiffened plate.

Plates with rigid transverse stiffeners

The standard solution for the plate between two rigid transverse stiffeners (simply supported edges are assumed, Figure 5.9(a)) is:

$$\begin{aligned}
 k_\tau &= 5,34 + \frac{4,00}{\alpha^2} && \text{when } \alpha \geq 1,0 \\
 k_\tau &= 4,00 + \frac{5,34}{\alpha^2} && \text{when } \alpha < 1,0
 \end{aligned}
 \tag{5.18}$$

where:

$$\alpha = a/h_w .$$

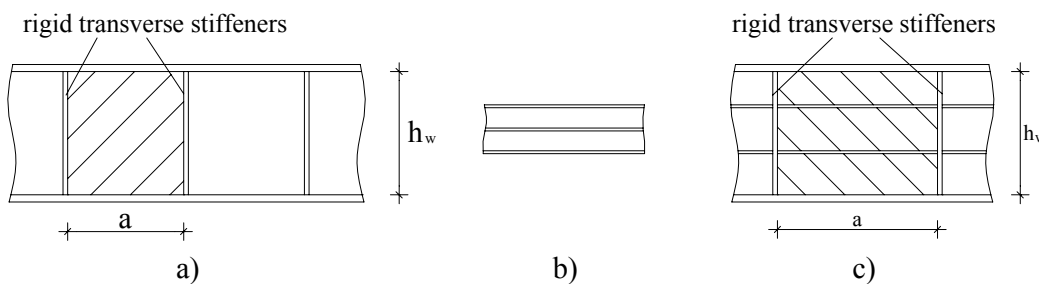


Figure 5.9: Different web panels for the calculation of k_τ

EN 1993-1-5, A.3

EN 1993-1-5, A.3(1)

Longitudinally stiffened plates

The theoretical solution for k_τ of a long longitudinally stiffened plate (Figure 5.9(b)) was obtained by Crate and Lo [6]. A good approximation is given by Eq. (5.19) (Höglund [4]):

$$k_\tau = 5,34 + 1,36\sqrt[3]{\gamma} \quad (5.19)$$

where:

$$\gamma = \frac{12(1-\nu^2)I_{sl}}{h_w t^3} = 10,92 \frac{I_{sl}}{h_w t^3} \quad (5.20)$$

is the relative flexural stiffness of the stiffener for bending out of the web plane.

By comparison to Klöppel and Scheer [7] charts it can be shown that for closely spaced transverse stiffeners (Figure 5.9(c)) the following approximations can be used:

$$k_\tau = 5,34 + \frac{4}{\alpha^2} + \frac{3,45\gamma^{3/4}}{\alpha^2} \quad (\text{Höglund [4]}) \quad (5.21)$$

$$k_\tau = 4,1 + \frac{6,3 + 0,05\gamma}{\alpha^2} + 1,44\sqrt[3]{\gamma} \quad (\text{Beg}) \quad (5.22)$$

Eq. (5.22) gives better results for only one and two longitudinal stiffeners and $\alpha < 3$. In other cases Eq. (5.21) shall be applied, but not less than k_τ from Eq. (5.19) (important at large values of α). Eq. (5.22) represents the best fit for an arbitrary position of one or two longitudinal stiffeners. Therefore the lack of complete compatibility with (5.21) at $\alpha = 3$.

As mentioned above, stiffened plates possess less post-buckling strength compared to unstiffened plates, and I_{sl} should be reduced accordingly. With this reduction to 1/3 and by accounting for expression (5.20), Eq. (5.19), (5.21) and (5.22) write according to the formulae given in Annex A.3 of EN 1993-1-5:

- For plates with rigid transverse stiffeners and with longitudinal stiffeners the shear buckling coefficient k_τ is:

$$\begin{aligned} k_\tau &= 5,34 + 4,00 \left(\frac{h_w}{a} \right)^2 + k_{\tau st} & \text{when } \frac{a}{h_w} &\geq 1,0 \\ k_\tau &= 4,00 + 5,34 \left(\frac{h_w}{a} \right)^2 + k_{\tau st} & \text{when } \frac{a}{h_w} &< 1,0 \end{aligned} \quad (5.23)$$

where:

$$k_{\tau st} = 9 \left(\frac{h_w}{a} \right)^2 \sqrt[4]{\left(\frac{I_{sl}}{t^3 h_w} \right)^3} \quad \text{but not less than} \quad \frac{2,1}{t} \sqrt[3]{\frac{I_{sl}}{h_w}}$$

a is the distance between rigid transverse stiffeners (see Figure 5.9)

I_{sl} is the actual second moment of area of the longitudinal stiffener with regard to the z-axis, see Figure 5.7(b). Reduction to 1/3 of its actual value is taken into account by appropriately changed values of constants (9 and 2,1). For webs with two or more longitudinal stiffeners, not

EN 1993-1-5,
A.3(2)

EN 1993-1-5,
A.3(1)

necessarily equally spaced, I_{sl} is the sum of the stiffness of individual stiffeners.

- When there are only one or two longitudinal stiffeners and $\alpha = \frac{a}{h_w} < 3$, the shear buckling coefficient should be taken from:

$$k_\tau = 4,1 + \frac{6,3 + 0,18 \frac{I_{sl}}{t^3 h_w}}{\alpha^2} + 2,2 \sqrt[3]{\frac{I_{sl}}{t^3 h_w}} \quad (5.24)$$

Also in Eq. (5.24) I_{sl} is the actual second moment of area. Reduction discussed above is taken into account by appropriately adapted constants in (5.24).

Eq. (5.23) may be used also for plates without longitudinal stiffeners by putting $k_{\tau st} = 0$.

EN 1993-1-5, A.3(2)

5.2.3 Contribution from the flanges

The tests on web panels subjected to shear show that at the ultimate state a kind of plastic mechanism is nearly formed in the flanges (plastic hinges E, H, G and K in Figure 5.10), caused by the tension field between the flanges. Under the assumption that this tension field does not influence the shear resistance of the web obtained on the basis of the rotated stress field theory (Figure 5.10a), the shear resistance coming from the flanges can be added to the contribution of the web.

EN 1993-1-5, §5.4

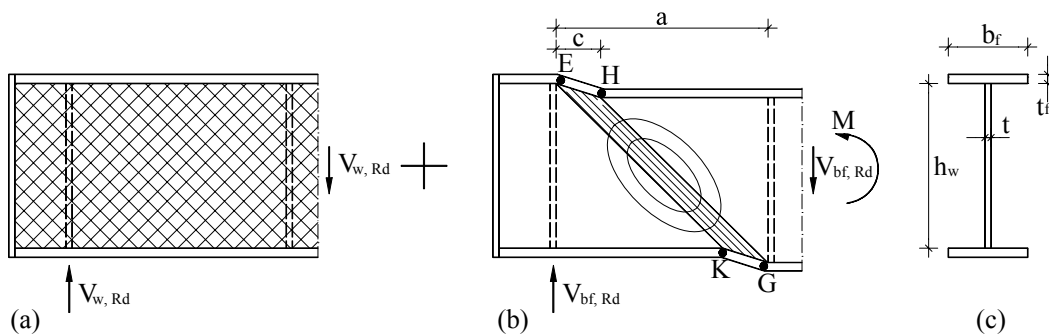


Figure 5.10: Tension field carried by bending resistance of flanges

Tests by Skaloud [8] and by Rockey and Skaloud [9] show that distance c between the hinges varies between 0,16 and 0,75 times the length a of the panel. According to Höglund [4] distance c for steel plate girders can be approximated in the following way:

$$c = a \left(0,25 + 1,6 \frac{M_{pl,f}}{M_{pl,w}} \right) = a \left(0,25 + \frac{1,6 \cdot b_f \cdot t_f^2 \cdot f_{yf}}{t \cdot h_w^2 \cdot f_{yw}} \right) \quad (5.25)$$

where $M_{pl,f}$ and $M_{pl,w}$ are the plastic moment resistances of flanges and web, respectively:

$$M_{pl,f} = \frac{b_f t_f^2 f_{yf}}{4}, \quad M_{pl,w} = \frac{t h_w^2 f_{yw}}{4} \quad (5.26)$$

EN 1993-1-5, §5.4(1)

and f_{yf} the yield strength of the flange material.

The value of c , calculated according to (5.25), is usually smaller than the values observed in the tests. This may be explained with the fact that in reality the plastic mechanism in the flanges (Figure 5.10) cannot develop freely because there is always some additional support from the web. Consequently, both contributions from the flanges and the web cannot be separated completely.

The shear resistance $V_{bf,Rd}$ provided by the flanges can be calculated based on the plastic mechanism in the flanges (see Figure 5.10b):

$$V_{bf,Rd} = \frac{4M_{pl,f,Rd}}{c} = \frac{b_f t_f^2 f_{yf}}{c \gamma_{M1}} \quad (5.27)$$

The contribution of flanges can be added to the shear resistance of web panels only when the flanges are not completely utilized in withstanding the bending moments:

$$M_{Ed} \leq M_{f,Rd} \quad (5.28)$$

where:

$$M_{f,Rd} = \frac{M_{f,k}}{\gamma_{M0}}$$

is the design moment resistance of the cross section consisting of the effective flanges only (Figure 5.11).

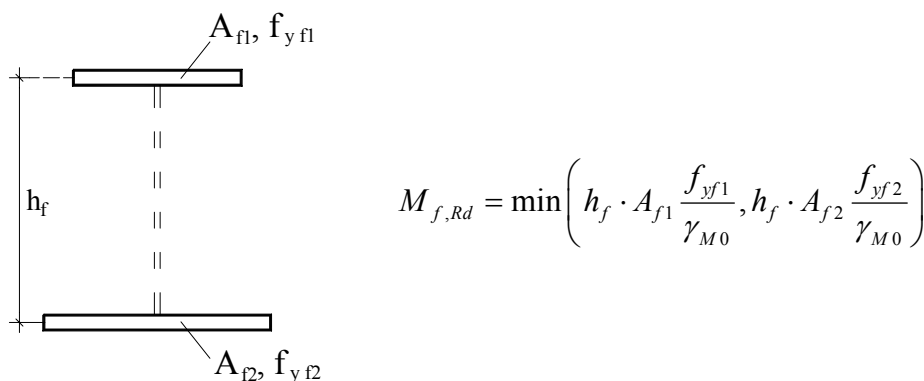


Figure 5.11: Definition of $M_{f,Rd}$

Under the assumption that bending moment M_{Ed} is only resisted by the flanges, the influence of the bending moment causing axial forces in flanges is taken into account by the reduction factor:

$$\left(1 - \left(\frac{M_{Ed}}{M_{f,Rd}} \right)^2 \right) \quad (5.29)$$

By combining (5.27) and reduction factor given by (5.29), the contribution $V_{bf,Rd}$ of the flanges is obtained as follows:

$$V_{bf,Rd} = \frac{b_f t_f^2 f_{yf}}{c \gamma_{M1}} \left(1 - \left(\frac{M_{Ed}}{M_{f,Rd}} \right)^2 \right) \quad (5.30)$$

EN 1993-1-5,
§5.4(1)

In the presence of an axial force N_{Ed} , which is again supposed to be carried only by the flanges, $M_{f,Rd}$ should be reduced accordingly by the factor:

$$\left(1 - \frac{N_{Ed}}{(A_{f1} + A_{f2}) f_{yf} / \gamma_{M0}} \right) \quad (5.31)$$

EN 1993-1-5,
§5.4(2)

Usually the contribution of flanges is small and can be neglected. This contribution is important only when strong flanges are used, which are not fully utilised from bending moments in the girder, which may be the case at the end supports.

5.2.4 Shear resistance check

EN 1993-1-5,
§5.5(1)

The verification of the shear resistance is performed according to the following expression:

$$\eta_3 = \frac{V_{Ed}}{V_{b,Rd}} \leq 1,0 \quad (5.32)$$

where V_{Ed} is the design shear force including any shear force due to possible torque.

5.2.5 Verification of the shear resistance formula

EN 1993-1-5,
§2.1(1)

The verification of the design shear resistance formula (5.9) against the test results shows that the design rules can accurately predict the shear resistance with a reasonably small scatter of results and consequently low γ_{M1} factors (Figure 5.12 and Figure 5.13). 366 tests on steel girders and 93 tests on aluminium girders were taken into account (Höglund [4], Background document to Eurocode 3 [10]).

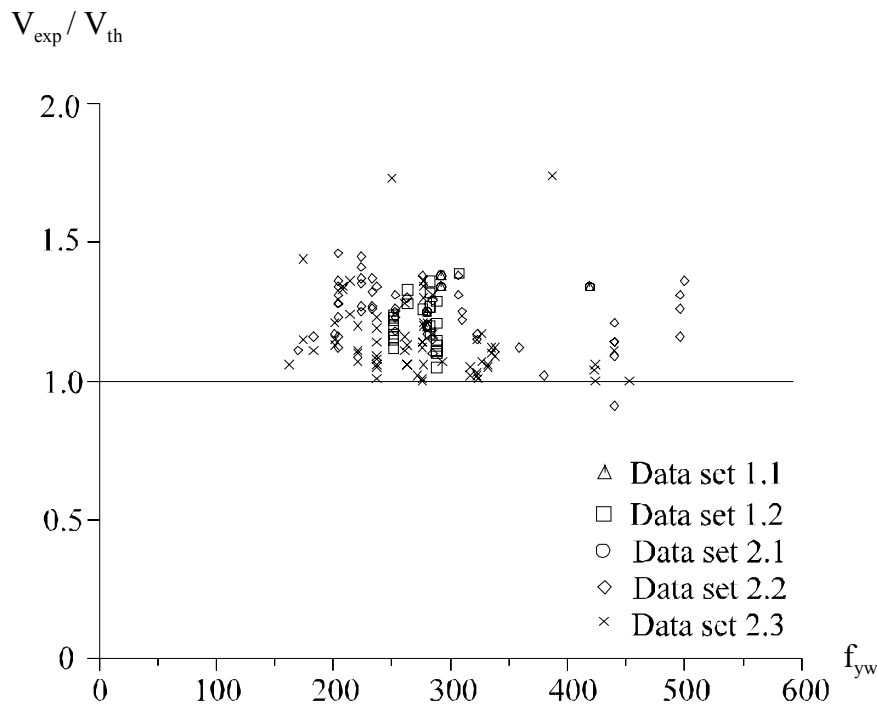


Figure 5.12: Comparison of experimental and theoretical values of shear resistance of plates

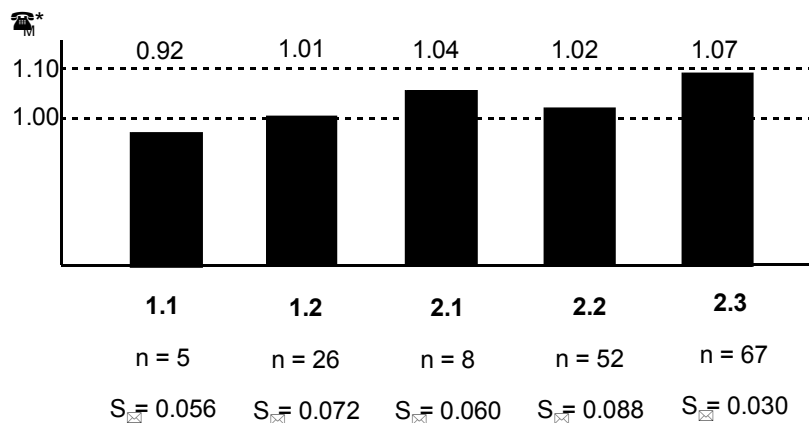


Figure 5.13: Partial factor γ_{M1} for shear resistance of plates

Data sets 1.1, 1.2, 2.1, 2.2 and 2.3 designate the groups of tests that were analysed separately in this verification (see Höglund [4]).

5.3 Conclusions

The main advantages and characteristics of the rotated stress field method are the following:

- The method is valid for small as well as large aspect ratios of shear panels, what is not the case for other tension field models that usually give good results for short panels and very conservative results for long ones.
- The method is simple to use as no calculation of tension field inclination and the stress in the tension field is required.

- The method is applicable not only to unstiffened, but also to transversally and/or longitudinally stiffened webs.
- Both full anchorage (rigid end post) and partial anchorage (non-rigid end post) of tension membrane stresses are considered.
- Besides the contribution from the web also the contribution from the flanges to the shear resistance is taken into account.
- It is important to note that the design of the relevant components (end posts, intermediate transverse stiffeners, see section 9) of plate girders is not performed strictly in accordance with the rotated stress field method. Simple safe-sided checks are introduced, see section 9.
- The method gives the best agreement with the full set of the available test results.
- The partial factor γ_{M1} may be chosen in the range $\gamma_{M1} = 1,0$ to $\gamma_{M1} = 1,10$.

5.4 References

- [1] T. Höglund, Design of thin plate I-girders in shear and bending with special reference to web buckling (in Swedish), Bulletin No.94 of the Division of Building Statics and Structural Engineering, The Royal Institute of Technology, Stockholm, Sweden, 1981.
- [2] T.V. Galambos (ed.), Guide to stability design criteria for metal structures, 5th edition, John Willey & Sons, 1998.
- [3] T. Höglund, Behaviour and strength of the web of thin plate I-girders (in Swedish), Bulletin No.93 of the Division of Building Statics and Structural Engineering, The Royal Institute of Technology, Stockholm, Sweden, 1971.
- [4] T. Höglund, Shear buckling resistance of steel and aluminium plate girders, Thin-Walled Structures, Vol. 29, Nos. 1-4, pp.13-30, 1997.
- [5] L. Pavlovčič, D. Beg, U. Kuhlmann, Longitudinally stiffened panels in shear, Eurosteel 2005 Conference, Volume A, pp. 1.4-128 – 1.4.136, Maastricht, 2005.
- [6] H. Crate, H. Lo, NACA Tech Note, No. 1589, June 1948.
- [7] K. Klöppel, J. Scheer, Beulwerte ausgesteifter Rechteckplatten, Wilhelm Ernst & Sohn, 1960.
- [8] M. Skaloud, Ultimate load and failure mechanism of webs in shear, IABSE Colloquium, Vol. II, pp.115-130, London, 1971.
- [9] K. Rockey, M. Skaloud, Influence of the flexural rigidity of flanges upon the load-carrying capacity and failure mechanism in shear, Acta Technica CSAV, 3, 1969.
- [10] Background document to Eurocode 3, Design of steel structures, Part 2 – Bridges, Document No. II.5.1: Evaluation of test results for the design rules of shear buckling resistance for stiffened and unstiffened webs, 1996.

6 Resistance to transverse loads

EN 1993-1-5,
§6

Bernt Johansson, Division of Steel Structures, Luleå University of Technology.

6.1 Background

Concentrated transverse forces on girders are commonly referred to as patch loads. Such loads occur in many applications and if the loads are moving as for a crane girder or a bridge girder during launching, the load has to be resisted by the web alone i. e. without assistance of vertical stiffeners. The design for such loads has traditionally comprised two independent checks, one for yielding and one for buckling. A short review is presented below.

6.1.1 Buckling

The question of predicting the resistance to buckling has a history of almost 100 years. In 1906 Sommerfeld solved the problem of buckling of a plate loaded by opposite concentrated loads at the long edges and in 1935 Girkmann solved the more complex problem with a load on one edge only. Later, when computers came into use, several authors have solved this buckling problem for realistic girders taking the flange and the patch length into account, which results in complicated solutions. These solutions concerned critical forces according to classical theory of stability and as in most other plate buckling problems the ultimate resistance is quite different. Strange enough, Basler whose work opened for using post buckling strength in girder design, stuck to critical forces for the resistance to patch loading. One of the first reasonable estimates of the actual resistance was developed by Carl-Adolf Granholm 1960 [1] at Chalmers University, Sweden. Granholm reported seven tests with concentrated loads on girders with slender webs. He ended up with a resistance to patch load according to the formula:

$$F_u = 0,85t_w^2 \text{ (Mp with the web thickness } t_w \text{ in mm)}$$

The format of the equation is not dimensionally consistent and with present knowledge it can be converted. Assuming that the girders (S275) that were tested had an average yield strength of 350 MPa the ultimate resistance can be rewritten to:

$$F_u = t_w^2 \sqrt{f_{yw} E} \quad (6.1)$$

This formula shows the influence of the most important parameters on the patch loading resistance. This is the same format as the resistance of a slender plate according to the von Karman's model and numerically it is about half the resistance of a uniformly compressed plate (actually 1/1,9).

Bergfelt and co-workers continued the tradition of studying patch loading at Chalmers University. He went on studying this problem for a long time and proposed step by step several empirical formulae for the patch loading resistance including more and more parameters. At the same time Rockey and Roberts were working with the same problem in Cardiff. Roberts presented a mechanical model based on a folding mechanism in the web to predict the buckling resistance [2], see Figure 6.1.

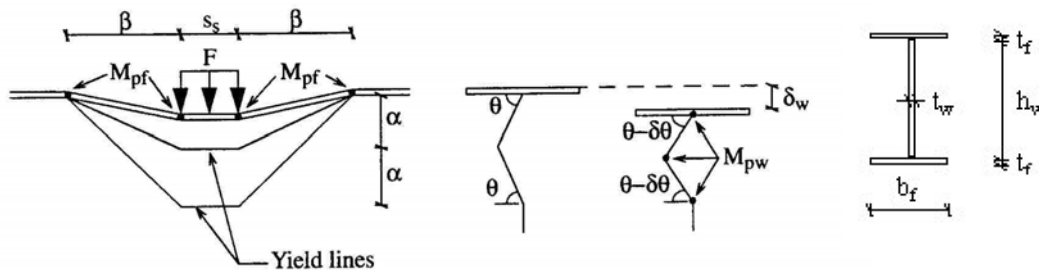


Figure 6.1: Mechanical model for patch loading resistance according to Roberts

A folding mechanism like that in Figure 6.1 gives a resistance that is decreasing with increasing deformation and in order to get a fixed value Roberts assumed that the deformation was given by the elastic bending deformation of the flange. This assumption is a bit arbitrary but was justified by tests results. This model was the basis for the formula in ENV 1993-1-1 in which the buckling resistance was given by:

$$F_{sRd} = 0,5t_w^2 \sqrt{E f_{yw}} \left[\sqrt{\frac{t_f}{t_w}} + 3 \frac{t_w s_s}{t_f h_w} \right] \frac{1}{\gamma_{M1}} \quad (6.2)$$

A limitation that s_s should not to be taken as more than $0,2h_w$ applies, which makes the contribution from the second term in the brackets quite small.

ECCS/TWG8.3 published recommendations for the design of plate girders in 1986 [3]. This included a formula for the buckling resistance derived from a von Karman approach, which means that the resistance was taken as the square root of the yield load times the critical load. It contains essentially the same parameters as (6.2) but differently arranged. This formula was further developed and improved by Duchêne and Maquoi [4]. This study included computer simulations considering geometrical imperfections and residual stresses and also a calibration against a large number of test results. The study shows that the influence of geometrical imperfections within common tolerances is small and that the influence of residual stresses is small for slender plates.

6.1.2 Yielding

The elastic stress distribution under a concentrated load is commonly estimated by the assumption of load spreading in 45° through the flange and other steel parts. This leads to an elastic resistance to patch load that is:

$$F_{Rel} = f_{yw} t_w (s_s + 2t_f) \quad (6.3)$$

The loaded length is defined in a similar way as shown in Figure 6.3. Equation (6.3) is based on first yielding and it is rarely used for design. The elastic stresses are however used for fatigue design. In special cases the stresses at some distance from the load introduction are needed. In 3.2.3 of EN 1993-1-5 an approximate formula for the maximum stress is given [5]. The stress distribution is valid for an infinite plate. For a girder web without stiffeners with infinite depth the maximum stress at a distance z below the patch load is shown in Figure 6.2.

EN 1993-1-5,
§3.2.3

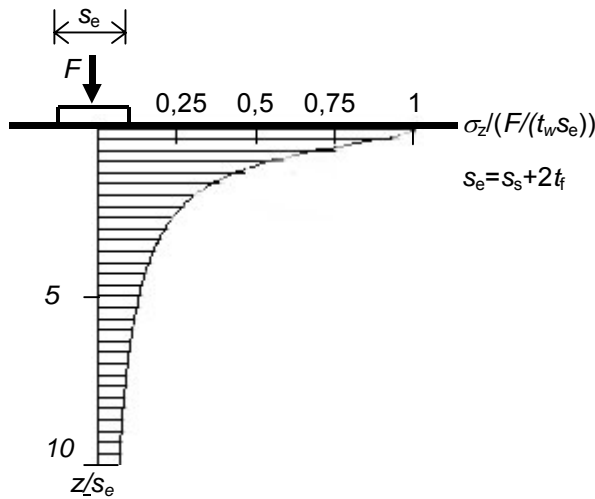


Figure 6.2: Normalised maximum stress under patch load on an unstiffened web

For a girder with limited depth h_w the stress distribution may be corrected by subtracting $\sigma_z = \sigma_{z,Ed} \left(z = h \right) \frac{z}{h_w}$ from formula (3.2) in EN 1993-1-5.

The plastic resistance sets a limit for the patch load if the web is stocky. As the yielding progresses the load is spread out on a larger length and the web material strain hardens. How far this redistribution can be pushed depends on how stocky the web is and the limit is given by buckling in the plastic range. This means that the plastic resistance is not well defined from a simple model as it is for axial force or bending moment. A realistic estimate of the plastic resistance was given by Zoetemeijer in 1980 [6]. For rolled beams the resistance was written as:

$$F_{pl} = f_{yw} t_w (s_s + 5(r + t_f)) \tag{6.4}$$

where r denotes the fillet radius. The original equation included the influence of coexisting bending stresses and shear stresses. Roberts developed a similar expression for welded plate girders [2]:

$$F_{pl} = f_{yw} t_w \left[s_s + 2t_f \sqrt{\frac{f_{yf} b_f}{f_{yw} t_w}} \right] \tag{6.5}$$

A limitation that b_f should not be taken larger than $25t_f$ applies. A comparison shows that (6.5) normally gives a higher resistance than (6.4) if applied to a plate girder. For rolled beams the opposite usually holds.

6.1.3 Combined models

The design models for other types of instability are using the yield resistance as a maximum and a reduced resistance depending on a slenderness parameter. The reduction factor is intended to give a gradual transition from the elasto-plastic buckling at small slenderness to – in this case – the post-critical resistance at large slenderness. A first attempt to develop such a representation for patch loading was suggested by Ungermann in his thesis [7]. Independently Lagerqvist and Johansson worked on the same idea. After some iteration the rules in

ENV 1993-1-5 (which were the same as in the present EN) were developed [8], [9]. The rules also merge the three separate verifications in ENV 1993-1-1 for crushing, crippling and buckling. The ENV rules were poorly harmonized and used different approaches. The new rules also cover a wider range of load applications and steel grades. The rules have been checked for steel grades up to S690.

In a recently published thesis Müller [10] made an attempt to develop a unified approach for all kinds of buckling problems including cases of coupled instability and complex load cases. The basic idea was to define the slenderness parameter λ from load multipliers for defining the plastic resistance and the critical load, respectively. The success of this method calls for general reduction factors. In a comparison between reduction factors for different cases of plate buckling it turns out that the patch loading sticks out by falling below the other reduction factors. In order to harmonize, the reduction factor for patch loading should be lifted and accordingly the plastic resistance be lowered. This could possibly be an improvement.

A study by Davaine, Raoul and Aribert [11] became available after the content of EN 1993-1-5 was settled. It is based on a large number of computer simulations of typical bridge girders with longitudinal stiffeners. It shows that the idea of reducing the plastic resistance and increasing the reduction factor works well for the data set studied. More specifically they put $m_2 = 0$ in (6.7) and used an alternative reduction factor according to Annex B of EN 1993-1-5 with $\alpha_p = 0,49$ and $\bar{\lambda}_{p0} = 0,7$. Applying the same idea to test data behind the model in EN 1993-1-5 shows that it works for slender webs but not for stocky for which the result is unconservative. The idea seems viable but it needs further development.

The conclusion is that the present model is not the final answer and there is still room for future improvements by continued research. Such research is going on in several places and preliminary results show that model may be in error but fortunately on the conservative side.

Similarly to the present design procedures for all other stability problems, the one for patch loading includes three parameters, which will be described in the following:

- the plastic resistance F_y ,
- the elastic buckling force F_{cr} , which defines a slenderness parameter

$$\bar{\lambda} = \sqrt{\frac{F_y}{F_{cr}}}$$

- a reduction factor $\chi = \chi(\bar{\lambda})$ which reduces the yield resistance for $\bar{\lambda}$ larger than a certain limiting value such that $F_R = F_y \chi$.

EN 1993-1-5,
§6.2(1)

6.2 Model for patch loading resistance

EN 1993-1-5,
§6.3 and 6.5

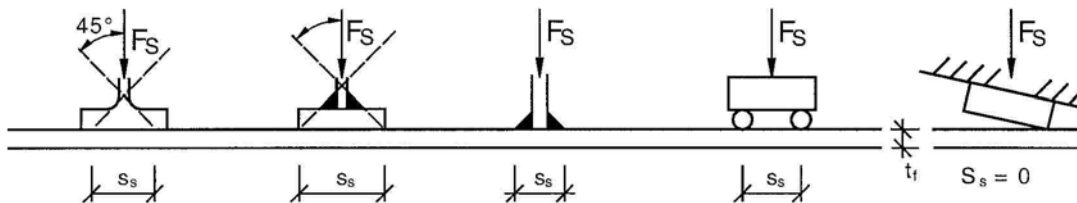
6.2.1 Plastic resistance

The plastic resistance can be written as:

$$F_y = f_{yw} t_w l_y \tag{6.6}$$

EN 1993-1-5,
§6.5

The crucial parameter is the length l_y over which the web is supposed to yield.



EN 1993-1-5,
§6.3, Fig. 6.2

Figure 6.3: Definition of stiff loaded length

The first step is to determine the loaded length on top of the flange. This is done according to Figure 6.3. It can be seen that it uses the assumption of load spread in 45°. For the case of load from two rollers the model requires two checks, one as shown in Figure 6.3 for the combined influence of the two loads with s_s as the distance between the loads and for the loads individually with $s_s = 0$.

The mechanical model according to Figure 6.4 is used for the plastic resistance when the load is far from the end of the girder. The mechanical model has four plastic hinges in the flange. It can be noted that the distance between the two central hinges is set to $s_s + 2t_f$, which reflects the fact that the hinges are not point-like but have a certain length. The plastic moment resistance of the hinges will depend on the flange and a possible contribution from the web that is connected with the flange. For the inner plastic hinges the resistance M_i is calculated under the assumption that the flange alone contributes to the resistance because the web is assumed to be stressed to yielding in the transverse direction. If it had contributed to the bending resistance of the flange it would have been stressed in tension in the longitudinal direction, which would have violated the von Mises yield criterion. For the outer plastic hinges, M_o , it is assumed that a part of the web contributes to the resistance. In those hinges the web is subject to biaxial compression and it can resist the yield strength in both directions at the same time. This assumption is based on the observations from the tests that the length of the deformed part of the web increased when the web depth increased. With a simplified expression for M_o , the effective loaded length l_y for the model in Figure 6.4 is given by :

$$l_y = s_s + 2t_f (1 + \sqrt{m_1 + m_2}) \tag{6.7}$$

EN 1993-1-5,
§6.5(2)

where

$$m_1 = \frac{f_{yf} b_f}{f_{yw} t_w} \tag{6.8}$$

EN 1993-1-5,
§6.5(1)

$$m_2 = 0,02 \left(\frac{h_w}{t_f} \right)^2 \tag{6.9}$$

The contribution from the web, reflected by m_2 , may in some cases be too high. It has been assessed empirically from tests and should be seen as a fictitious parameter relevant for slender webs. For cases not included in the test data base it may overestimate the resistance and for that reason m_2 should be taken as zero if the slenderness $\bar{\lambda} < 0,5$. The result will then be the same as equation (6.5). Unfortunately this creates a discontinuity in the resistance. Another limitation is that l_y should not be taken as larger than the distance between transverse stiffeners a . The model is obviously not applicable if the length l_y would include transverse stiffeners. They would have some positive effect, which has not been studied, and the limitation is clearly a conservative assumption.

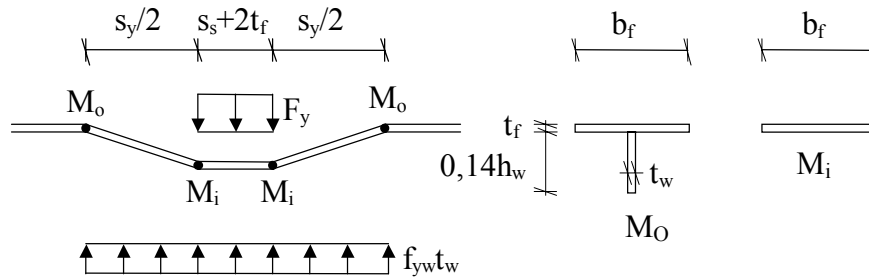


Figure 6.4: Mechanical model for the plastic resistance for patch loading

If the load is applied at an unstiffened end of a girder the plastic resistance may be governed by several different failure modes, see Figure 6.5. The most common case of end patch loading is a support reaction acting at the end of the girder and therefore the load is shown acting on the bottom flange in Figure 6.5. The support is assumed to be prevented from rotation and because of the slope of the girder it will sit on a corner of the support for failure mode 1. This failure mode occurs if the load is close to the end of the girder and there is only one plastic hinge in the flange. If the load is moved farther from the end another plastic hinge may form at the load as shown by failure mode 2. A further shift of load away from the end may result in failure mode 3, which includes two hinges at the load. The load is assumed to be concentrated to one corner of the support and the distance between the hinges is given by the physical extension of the hinges. Finally, at large distance from end the failure mode 4 occurs and it is the same as the one in Figure 6.4 with $s_s = 0$. Depending on the circumstances any of the failure modes may govern. It would be possible to give criteria for the applicability of each mode but it would include as much calculations as checking all of them and to use the lowest value. The failure mode 3 has for simplicity been omitted and l_y is taken as the smallest of (6.7), (6.10) and (6.11). When using (6.7) $s_s = 0$ should be used unless the concentrated force is introduced in such a way that the loading device follows the slope of the girder end.

$$l_y = l_e + t_f \sqrt{\frac{m_1}{2} + \left(\frac{l_e}{t_f}\right)^2} + m_2 \quad (\text{mode 1}) \quad (6.10)$$

$$l_y = l_e + t_f \sqrt{m_1 + m_2} \quad (\text{mode 2}) \quad (6.11)$$

where:

EN 1993-1-5,
§6.5(3)

$$l_e = \frac{k_F E t_w^2}{2 f_{yw} h_w} \text{ but not exceeding } s_s + c \tag{6.12}$$

k_F = buckling coefficient for concentrated load.

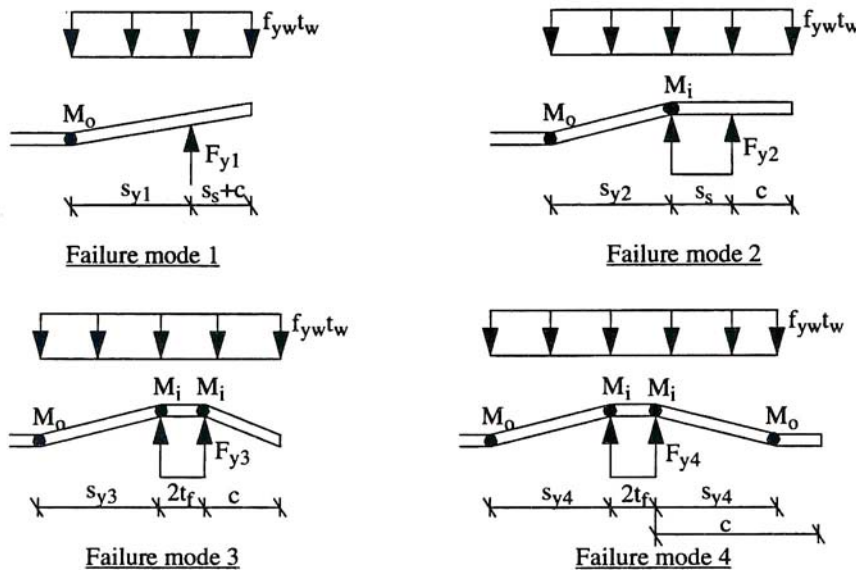


Figure 6.5: Failure modes for plastic resistance for end patch loading

The notation l_e stands for a reduced yielded length based on the buckling force. This reduction has been deemed necessary in order to use the same reduction factor for all loading cases.

6.2.2 Critical force

The design rules in EN 1993-1-5 cover three different cases of patch loading shown in Figure 6.6. Type a is referred to as patch loading, type b opposite patch loading and type c end patch loading. The critical force can be represented in the form:

$$F_{cr} = k_F \frac{\pi^2 E}{12(1-\nu^2)} \frac{t_w^3}{h_w} \approx 0,9 k_F \frac{E t_w^3}{h_w} \tag{6.13}$$

where the coefficient k_F depends on the type of loading and the geometry. As mentioned in the background there are many solutions for the critical force but the number of influencing parameters makes it unmanageable to use exact solutions in a code. Simplified expressions were derived in [8] based on computer simulations. These expressions were further simplified in EN 1993-1-5 to the ones given in Figure 6.6. The more detailed expressions will be shown below. The buckling coefficients were derived assuming that the rotation of the flange was prevented at the point of load application. This is the case in many practical applications. The buckling coefficient without rotational restraint is sometimes significantly lower but fortunately the ultimate resistance is not influenced so much. Therefore, the buckling coefficients can be used for practical girders with normal flanges. They are however not valid for a plate without a flange.

EN 1993-1-5, §6.1 and 6.2

EN 1993-1-5, §6.4(1)

For patch loading type a the full expression is

$$k_F = \left[5,3 + 1,9 \left(\frac{h_w}{a} \right)^2 + 0,44 \sqrt{\frac{b_f t_f^3}{h_w t_w^3}} \right] \left[1 + \frac{s_s}{2h_w} \right] \quad (6.14)$$

This gives approximately the influence of all essential parameters. This kind of expression was deemed too complicated to put into a code and it was simplified to the expression given in Figure 6.6. For most practical cases the simplified expression is conservative. For opposite patch loading, type b, the full expression is:

$$k_F = \left[3,4 + 1,8 \left(\frac{h_w}{a} \right)^2 + 0,14 \sqrt{\frac{b_f t_f^3}{h_w t_w^3}} \right] \left[1 + \frac{s_s}{2h_w} \right] \quad (6.15)$$

and for end patch loading:

$$k_F = \left[1,6 + 0,34 \sqrt{\frac{b_f t_f^3}{h_w t_w^3}} \right] \left[1 + 3 \frac{s_s + c}{h_w} \right] \quad (6.16)$$

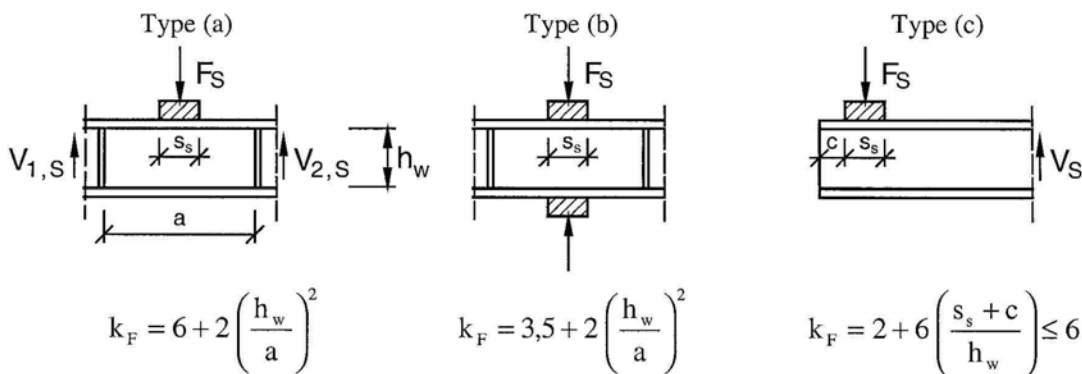


Figure 6.6: Different types of patch loading and approximate buckling coefficients

EN 1993-1-5, §6.1(4)

6.2.3 Reduction factor

EN 1993-1-5, §6.4

The reduction factor χ described in 6.1.3 has been derived by curve fitting to test results. The original proposal in [8] was:

$$\chi(\bar{\lambda}) = 0,06 + \frac{0,47}{\bar{\lambda}} \leq 1 \quad (6.17)$$

where:

$$\bar{\lambda} = \sqrt{\frac{F_y}{F_{cr}}} \quad (6.18)$$

During the drafting of ENV1993-1-5 there were concerns over the large increase of the resistance compared to the rules in ENV 1993-1-1. The result of the discussions was that (6.17) was changed to

$$\chi(\bar{\lambda}) = \frac{0,5}{\bar{\lambda}} \leq 1 \quad (6.19)$$

EN 1993-1-5, §6.4(1)

which is always lower than (6.17). This equation is shown in Figure 6.7 together with test results with patch loading type a and bending moment less than 0,4 times the bending resistance. The tests included have been selected as in [8]. For larger bending moment an interaction is expected, see Section 7.2. It should be noted that the evaluation has been done with the approximate values of k_F in Figure 6.6 and the more accurate values cannot necessarily be used together with this reduction factor.

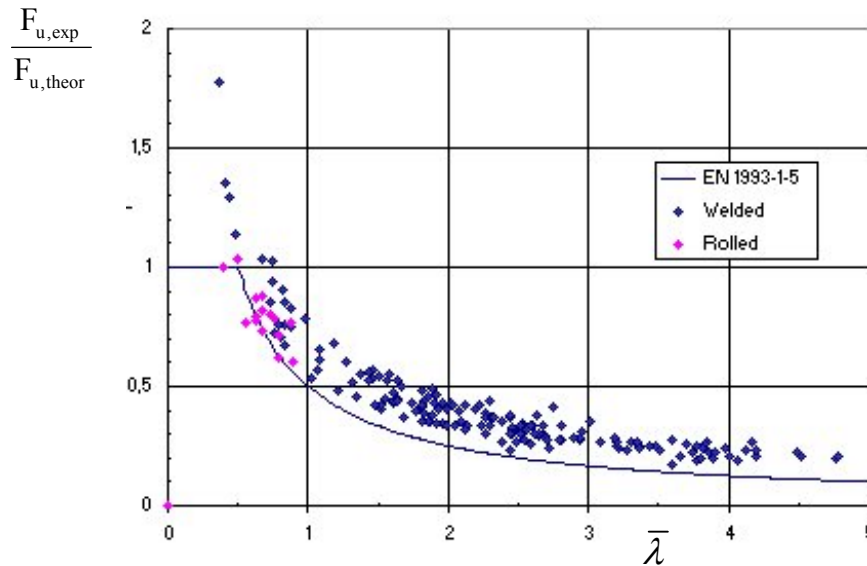


Figure 6.7: Equation (6.19) together with results from patch loading tests with small bending moment

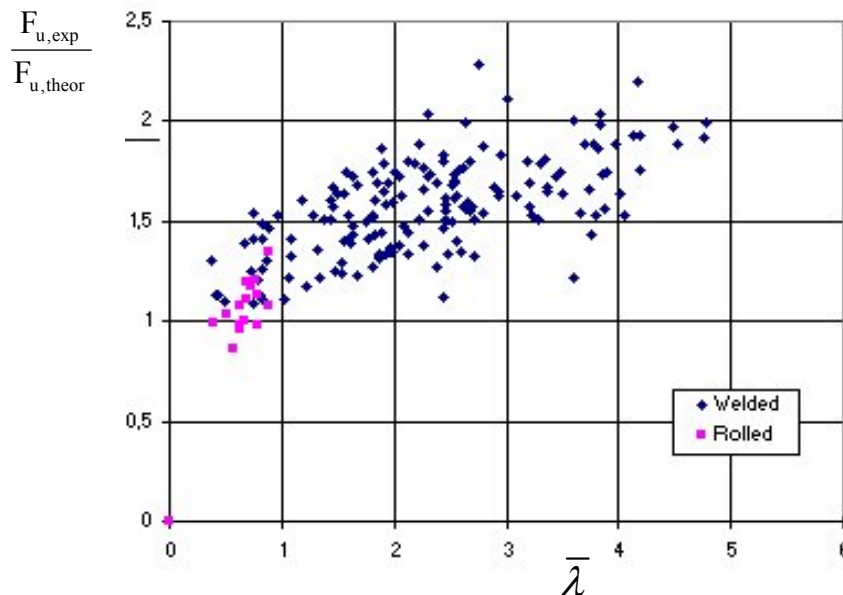


Figure 6.8: Test results over prediction with χ according to (6.19) as function of slenderness $\bar{\lambda}$ for tests with small bending moment

The fit in Figure 6.7 may seem fairly good but actually there is a quite substantial difference between (6.17) and (6.19) for large slenderness. A representation of test result F_u over prediction:

$$F_R = F_y \chi \tag{6.20}$$

shown in Figure 6.8 reveals that there is a bias for underprediction with increasing slenderness. Using (6.17) this bias would not occur and the trend line would have been more horizontal.

For opposite patch loading type b and end patch loading type c the test databases are more limited than for patch loading. The available results are shown in Figure 6.9 and Figure 6.10 together with equation (6.17). The diagrams have been taken from [8], which is the reason for comparing with (6.17) instead of (6.19). It can be seen that most tests are on rolled beams with fairly stocky webs. The tests denoted Weldox 700 are welded girders made of S690.

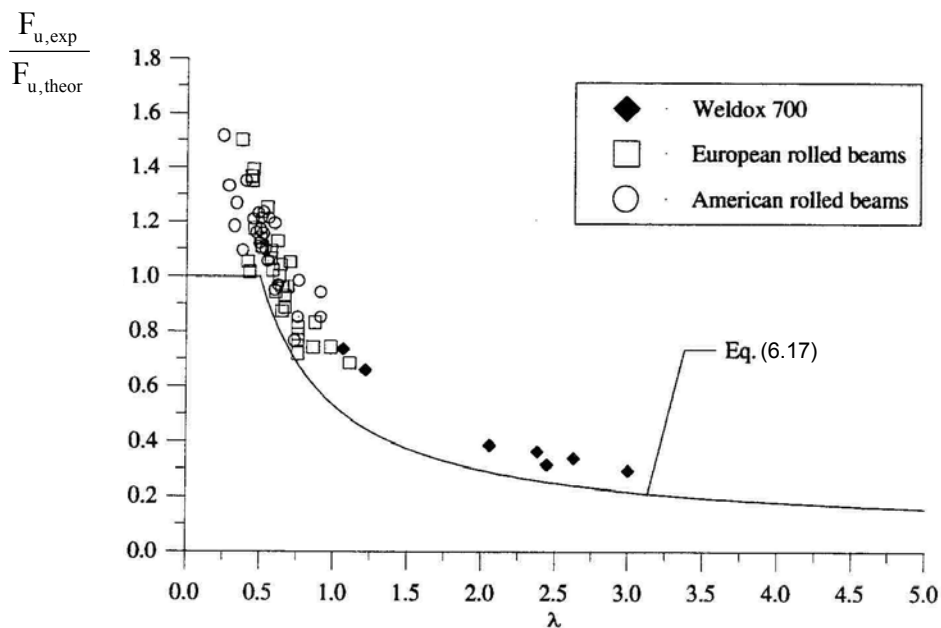


Figure 6.9: Test results over prediction with χ according to (6.19) as function of slenderness $\bar{\lambda}$ for tests with small bending moment

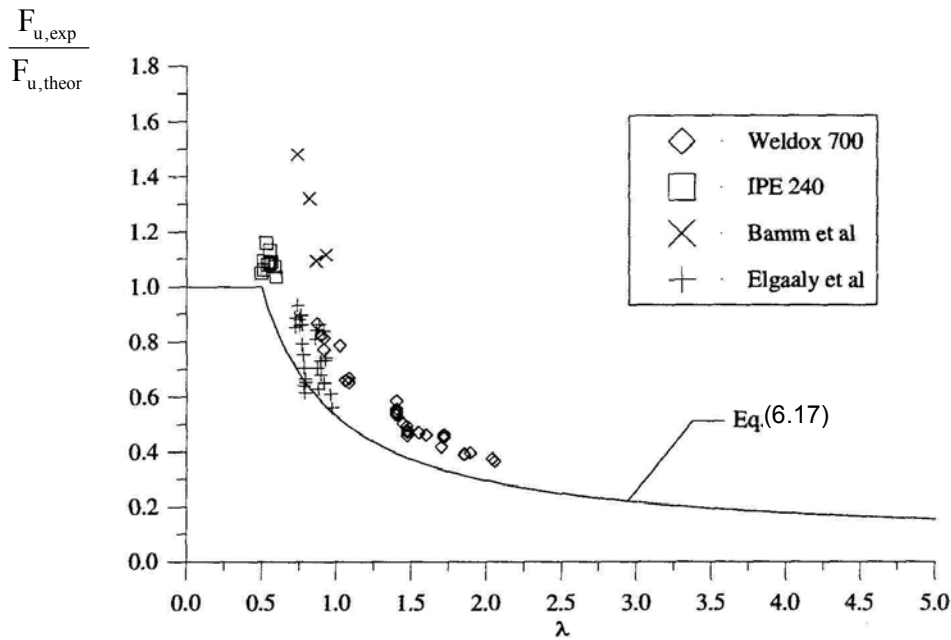


Figure 6.10: Equation (6.17) together with results from 68 tests with end patch loading

As the derivation of the reduction factor is empirical it is important to check if the essential parameters are represented correctly. Several such checks were done in [8] and the checks showed no significant bias. One important difference between the rules in ENV 1993-1-1 eq. (6.2) and in EN 1993-1-5 is the influence of the patch length s_s . The former had a limitation that s_s/h_w should not be taken as larger than 0,2 and the latter rules have the limitation 1. This is important for launching of bridges because the simplest way of increasing the resistance is to increase the length of the launching device. The influence of the patch length in relation to the panel length is shown in Figure 6.11 and in relation to the web depth in Figure 6.12. As there are only a small number of tests with long patch loads, tests by Bossert and Ostapenko [12] have been included in the database. These ten tests had a loaded length equal to a full panel length, 0,7 to 1,5 m. They were not included in the evaluation in [8] because it was considered to be too favourable with load on the full panel length. In one of the tests a wooden board was used to distribute the load and that has not been included in this evaluation. Further it should be noted that five of these tests had $M_E/M_R > 0,4$, which means that they are in the interaction area where the bending moment is supposed to reduce the patch resistance. No correction has been done for the interaction so the results may actually underestimate the patch resistance.

Looking at Figure 6.11 it can be seen that these tests ($s_s/a = 1,0$) are in the high end of the scatter compared to the rest of the tests. It may also be noted that the tests with $s_s/a = 1,0$ were made at girders with very slender webs $h_w/t_w = 300$ so the results show that there is a substantial post-critical resistance in this case as well. In Figure 6.12 the results cover a range of s_s/h_w up to 1,6 but with only a few results. The results do not seem to support the restriction in EN 1993-1-5 that s_s/h_w should not be taken larger than 1,0. This restriction can be seen as a precaution to avoid column like behaviour, which can be expected if the loaded length is increased. The limitation is most likely conservative but the problem has not been studied in detail.

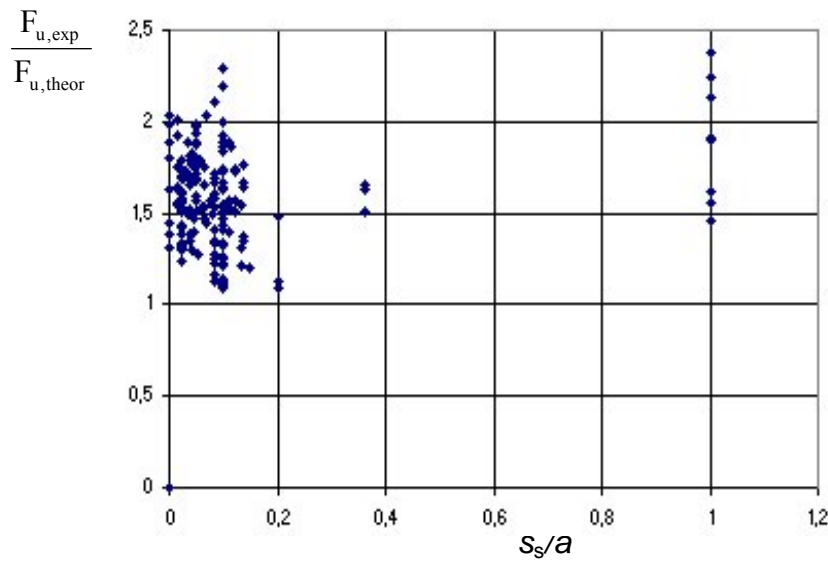


Figure 6.11: Test results over prediction as function of patch length over panel length

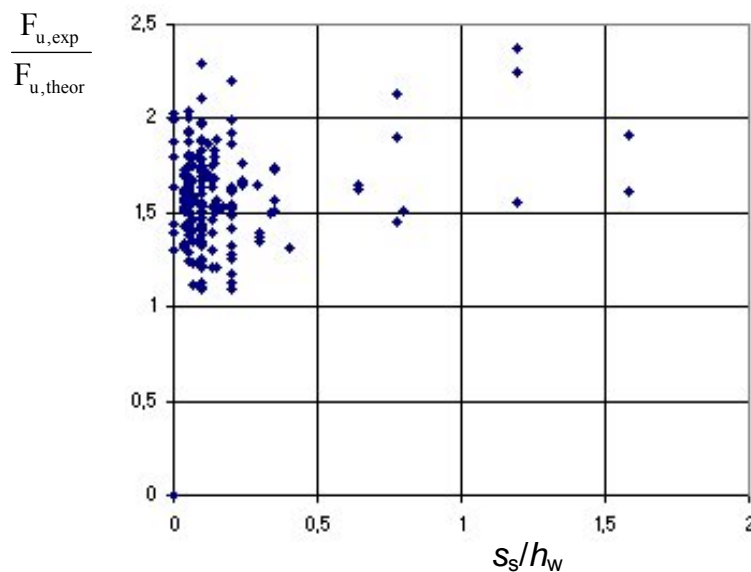


Figure 6.12: Test results over prediction as function of patch length over web depth

6.2.4 Influence of longitudinal stiffeners

Longitudinal stiffeners should increase the resistance to patch loading but the influence will depend on several parameters like the position of the stiffener, its bending stiffness and also its torsional stiffness. Figure 6.13 illustrates the effect on the buckling mode of a longitudinal stiffener. If the bending stiffness is large enough the case (a) in Figure 6.13 will occur. The stiffener forms a nodal line and the web deforms in a S-shape. Note that the stiffener undergoes twisting. If the stiffness is small (b) or (c) is relevant where the buckling involves deformation of

EN 1993-1-5, §6.4(2)

the stiffener. In this case the stiffener will increase the buckling load by restraining the out-of-plane deformations.

Several researchers have studied the effect of longitudinal stiffeners on the patch loading resistance, which is not necessarily the same as the effect on the critical load. It has been noted that the effect of the stiffener is small if the loaded panel has a slenderness b_1/t_w larger than 40 but there are also some tests showing a noticeable increase for higher slenderness. The problem is obviously not only a matter of the slenderness of the loaded panel. The BS 5400 [13] uses a simple correction of the resistance of an unstiffened web according to (6.2). The correction is the factor derived by Markovic and Haijdin [14] and reads

$$f_s = 1,28 - 0,7 \frac{b_1}{h_w} > 1,0 \text{ for } 0,1 < b_1/h_w < 0,4 \tag{6.21}$$

No requirement on the stiffness of the stiffener is associated with the formula.

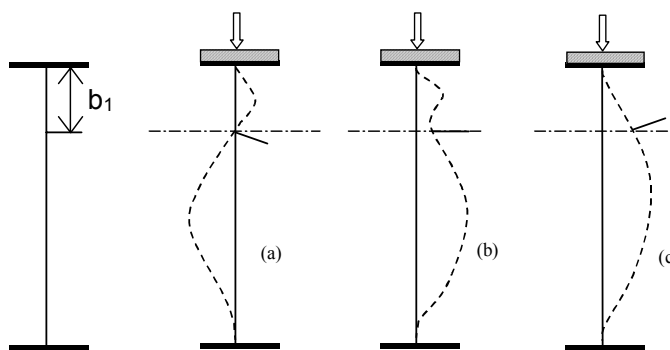


Figure 6.13: Buckling modes for girder with patch load on a longitudinally stiffened web

A summary of the state of art 2002 can be found in the thesis of Graciano [15]. He collected a database of 130 tests and studied several models for predicting the resistance. One of these models was to use the one described above for webs without longitudinal stiffeners but with the critical force considering the stiffener. This was introduced in EN 1993-1-5 because it required only an addition of k_F -values for a stiffened web. The method may not be ideal but it gives in some cases a useful increase of the resistance.

The bending stiffness of the longitudinal stiffener is represented by the parameter

$$\gamma_s = \frac{12(1-\nu^2)I_{sl}}{h_w t_w^3} = 10,9 \frac{I_{sl}}{h_w t_w^3} \tag{6.22}$$

I_{sl} is the second moment of area of the stiffener including contributing parts of the web taken as $15\epsilon t_w$ on each side of the stiffener. In [15] also the influence of the torsional stiffness was studied, which is of importance for closed stiffeners. This was for simplicity not included in EN 1993-1-5. An example of buckling coefficients is shown in Figure 6.14. For increasing relative stiffness of the stiffener the buckling coefficient first increases and at a certain relative stiffness a plateau is reached. This reflects the change of buckling mode according to Figure 6.13. The curves do not become completely horizontal, which depends on the influence of the torsional rigidity. The effect of the longitudinal stiffener is approximated by an addition to the buckling coefficient without longitudinal stiffener according to the formula:

$$k_F = 6 + 2 \left(\frac{h_w}{a} \right)^2 + \left(5,44 \frac{b_1}{a} - 0,21 \right) \sqrt{\gamma_s} \quad \text{for the range } 0,05 \leq \frac{b_1}{h_w} \leq 0,3 \quad (6.23)$$

EN 1993-1-5,
§6.4(2)

The plateau is represented by the rule that γ_s should not be introduced in (6.23) with a higher value than:

$$\gamma_s \leq \gamma_s^* = 13 \left(\frac{a}{h_w} \right)^3 + 210 \left(0,3 - \frac{b_1}{a} \right) \quad \text{for } \frac{b_1}{a} \leq 0,3 \quad (6.24)$$

For $\gamma_s \geq \gamma_s^*$ the buckling mode is according to (a) in Figure 6.13 and for smaller γ_s the modes (b) or (c) occurs.

Compared to the original proposal in [15] some coefficients have been rounded off. Another change is the range of applicability, which was originally given as a limitation of only b_1/a and here a restriction of b_1/h_w has been added. The reason is a suspicion that stiffeners placed far away from the loaded flange might be attributed a positive effect that does not exist.

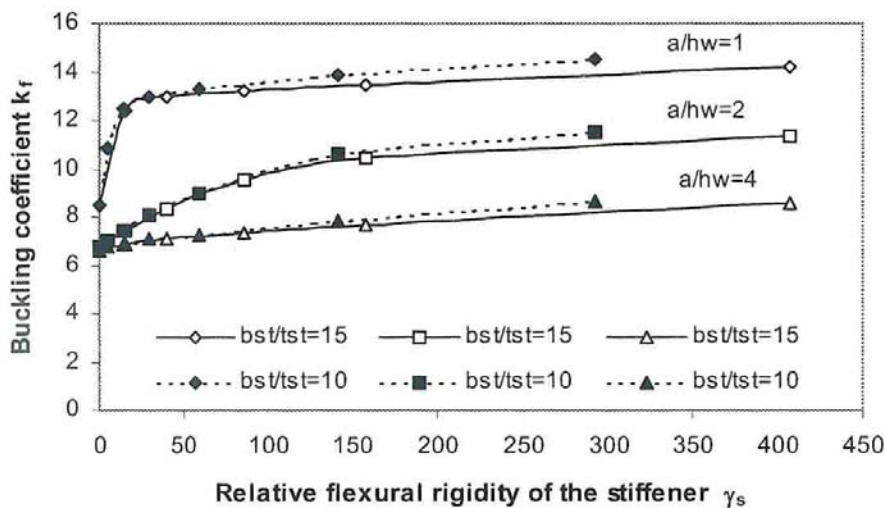


Figure 6.14: Buckling coefficients for web with stiffener at $b_1 = 0,2h_w$

The predictions of the resistance compared with results from 130 tests is shown in Figure 6.15. It can be seen that the scatter is slightly larger than in Figure 6.7 for webs without longitudinal stiffeners.

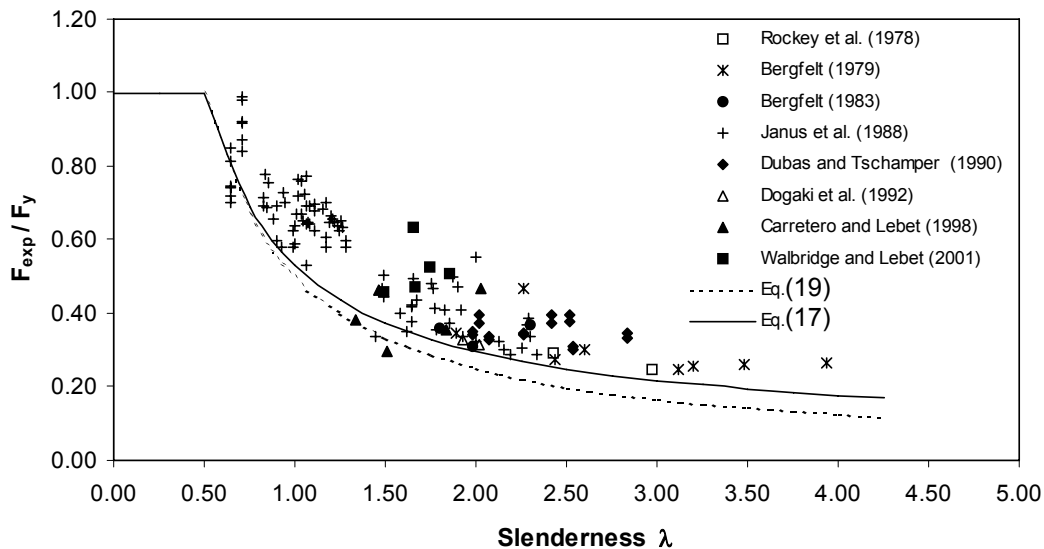


Figure 6.15: Results from 130 tests with longitudinally stiffened webs subject to patch loading

6.3 Calibration of design rules versus test results

The statistical evaluation for the design model of patch loading for webs without longitudinal stiffeners has been published in [16]. It was carried out with the method described in Section 1 with test results from [8]. The data bank contained test results for welded and rolled I-girders, which were loaded by patch loading, end patch loading or opposite patch loading, see Figure 6.6. The calibration was done with the rules given in EN 1993-1-5 and it turned out that a γ_m around 1,1 was required. However, on second thoughts it seems that this calibration was too conservative. If the original reduction factor (6.17) is used instead of (6.19) the bias seen in Figure 6.8 is eliminated and the coefficient of variation of F_u/F_R is reduced. As the evaluation procedure works this seems to lead to an overestimate of the required γ_m . This is an imperfection of the method, which takes deliberate deviations as random. A recalibration has therefore been done using (6.17). As (6.19) always is lower than (6.17) the γ_m derived with (6.17) must be sufficient if (6.19) is used.

The plot of test results r_e as function of prediction $r_t = F_R$ according to (6.20) is shown in Figure 6.16. The mean value correction factor and coefficient of variation become:

$$b=1,159$$

$$v_\delta = 0,130$$

The result of the calibration is that :

$$\gamma_{M1} = 1,02$$

should be applied to the resistance (6.20) using nominal values of the basic variables. This is close enough to 1,0, which is the recommended value.

EN 1993-1-5,
§6.2(1)

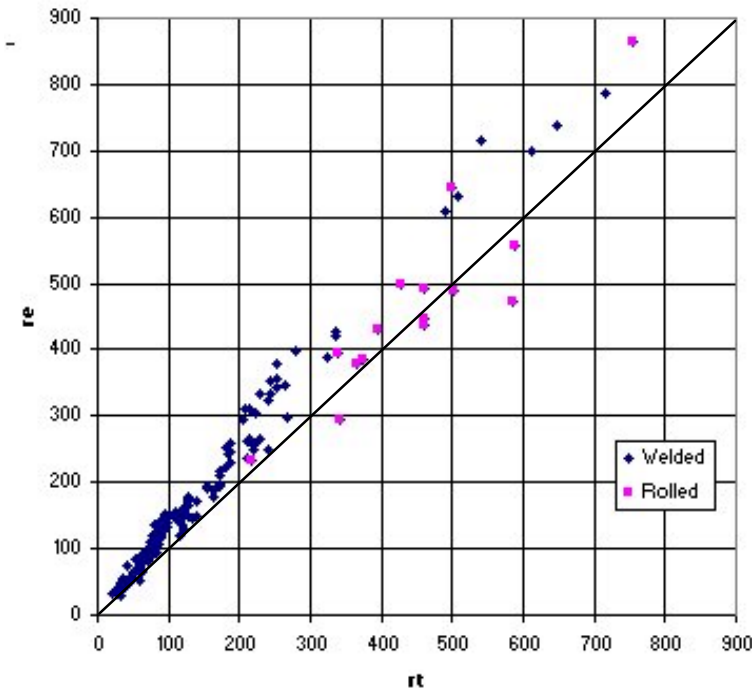


Figure 6.16: Plot of test results r_e as function of prediction r_t

The rules for patch loading on webs with longitudinal stiffeners were calibrated in [15]. The method and assumptions are the same as described in Section 1. The calibration was done for each set of tests and for all tests together as shown in Figure 6.17. Some of the calibrations of the individual test sets are not very reliable as the number of tests is too small. Looking at the calibration of all tests it would be justified to use $\gamma_{M1} = 1,0$.

Figure 6.18 shows the sensitivity plot for webs with longitudinal stiffeners. The scatter is quite large but there is no apparent bias.

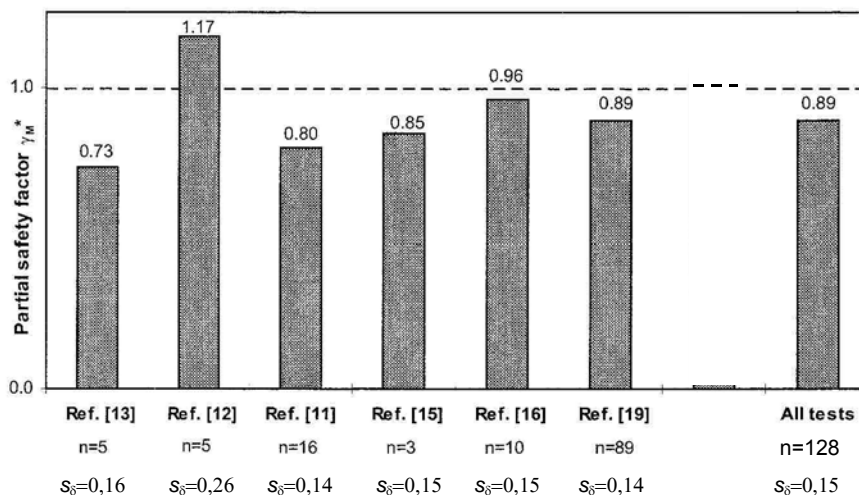


Figure 6.17: γ_M^* -values for the design model of patch loading for webs with longitudinal stiffeners; for references see [15]

EN 1993-1-5,
§2.1(1)

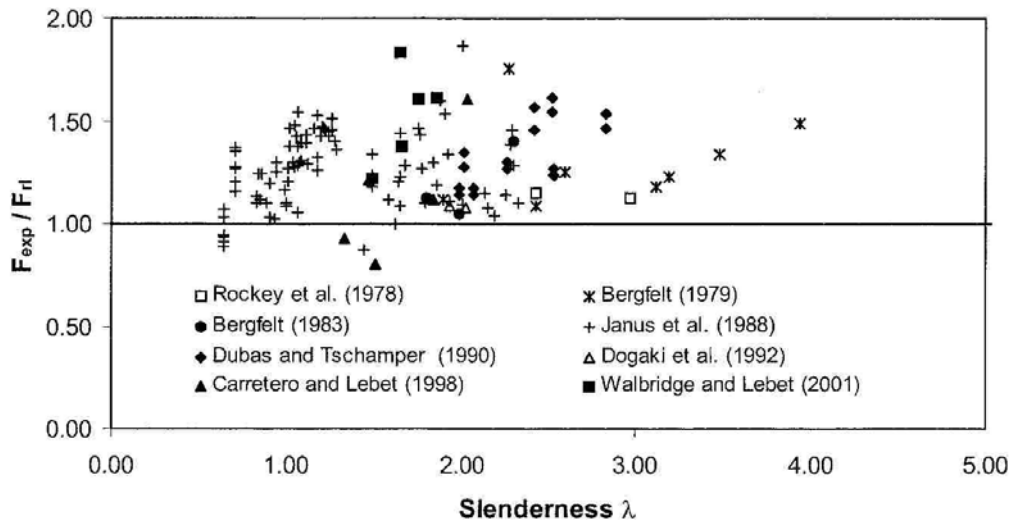


Figure 6.18: Sensitivity plot for webs with longitudinal stiffeners with respect to the slenderness λ

6.4 Outlook

In a recently finished research project, Combri, sponsored by RFCS further studies of patch loading problem have been carried out by the Universities of Stuttgart and Luleå and by SETRA. The studies showed that the design rules of EN 1993-1-5 were always safe but sometimes too much on the safe side. The project resulted in several improvements of the design rules for patch loading, which will be proposed for the next edition of EN 1993-1-5.

It was noted in [10] that the design rules for patch loading deviated notably from other plate buckling rules. The yield resistance was comparably high and the reduction function was on the other hand low. This has been corrected in the new proposed rules in the following way.

The yield resistance is lowered by setting m_2 in formula (6.6) to zero, which results in

$$l_y = s_s + 2t_f \left[1 + \sqrt{\frac{f_{yf} b_f}{f_{yw} t_w}} \right] \tag{6.25}$$

The reduction factor has to be increased and the starting point for this was the format given in Annex B in EN 1993-1-5 and formula (6.19) should be replaced by

$$\chi = \frac{1}{\varphi_F + \sqrt{\varphi_F^2 - \bar{\lambda}}} \leq 1,2 \tag{6.26}$$

where

$$\varphi_F = \frac{1}{2} (1 + 0,5(\bar{\lambda} - 0,6) + \bar{\lambda}) \tag{6.27}$$

The imperfection factor and the plateau length have been calibrated to fit the test results in the best possible way and the fit is better than to rules in EN 1993-1-5. At the same time it brings the plate buckling rules for different cases a step closer to each other. This makes the application of Section 10 of EN 1993-1-5 less problematic when patch loading is included.

In the Combri project longitudinally stiffened webs were also studied and design rules based on the model given above were developed. The model works if the critical force is taken as the smallest of the critical load according to 6.4(2) of EN 1993-1-5 and the critical load of the directly loaded panel, which can be calculated with formula (6.13) with h_w substituted by b_1 and k_F according to

$$k_F = \left(\frac{0,8s_s + 1,6t_f}{a} + 0,6 \right) \left(\frac{a}{b_1} \right)^{\left(\frac{0,6s_s + 1,2t_f}{a} + 0,5 \right)} \quad (6.28)$$

6.5 References

- [1] Granholm C-A, Proving av balkar med extremt tunt liv (Testing of girders with extremely thin webs), Rapport 202, Inst. för Byggnadsteknik, CTH, 1960.
- [2] Roberts, T. M.; Slender plate girders subject to edge loading, Proceedings of the Institution of Civil Engineers, Part 2 Vol. 71 September 1981, pp805-819.
- [3] Dubas, P., Gehri, E. (editors) Behaviour and design of steel plated structures, ECCS Publication No. 44, Brussels 1986.
- [4] Duchêne, Y., Maquoi, R., Contribution, par voie numérique, à l'étude de la résistance des âmes aux charges transversales, Construction Métallique No 2 1994, pp 43-73.
- [5] Stein, P., Beitrag zur Berechnung von orthogonal anisotropen Scheiben, Stahlbau und Baustatik, edited by H. Grengg, W. Pelikan and F. Reinitzhuber, Springer Verlag, Wien, New York 1965.
- [6] Zoetemeijer P., The influence of normal, bending and shear stresses on the ultimate compression force exerted laterally to European rolled sections, Report 6-80-5, Faculty of Civil Engineering, Technical University of Delft, 1980.
- [7] Ungermann D., Bemessungsverfahren für Vollwand- und Kastenträger unter besonderer Berücksichtigung des Stegverhaltens, Heft 17, Stahlbau, RWTH Aachen 1990.
- [8] Lagerqvist, O. Patch loading, Resistance of steel girders subjected to concentrated forces, Doctoral Thesis 1994:159 D, Department of Civil and Mining Engineering, Division of Steel structures Luleå University of Technology.
- [9] Lagerqvist O., Johansson B. Resistance of I-girders to concentrated loads, Journal of Constructional Steel Research Vol. 39, No. 2, pp 87-119, 1996.
- [10] Müller C., Zum Nachweis ebener Tragwerke aus Stahl gegen seitliches Ausweichen, Dissertation D82, RWTH Aachen, 2003.

- [11] Davaine, L., Raoul, J., Aribert J.M., Patch loading resistance of longitudinally stiffened bridge girders, Proceedings of the conference Steel bridge 2004, Millau 2004.
- [12] Bossert, T. W., Ostapenko, A., Buckling and ultimate loads for plate girder web plates under edge loading, Report No. 319.1, Fritz engineering laboratory, Department of Civil Engineering, Lehigh University, Bethlehem, Pa, June 1967.
- [13] BS 5400-3:2000 Steel, concrete and composite bridges: Code of practice for design of steel bridges, May 2001.
- [14] Marković, N.; Hajdin, N. A Contribution to the Analysis of the Behaviour of Plate girders Subjected to Patch Loading, JCSR, Vol. 21, 1992, pp. 163-173.
- [15] Graciano, C. Patch loading resistance of longitudinally stiffened girder webs, Doctoral Thesis 2002:18D, Division of Steel structures, Luleå University of Technology
- [16] Johansson B., Maquoi R., Sedlacek G., Müller C., Schneider R., Die Behandlung des Beulens bei dünnwandigen Stahlkonstruktionen in ENV 1993-Teil 1.5 (Eurocode 3-1-5), Stahlbau 11 1999, page 857-879.
- [17] COMBRI Competitive Steel and Composite Bridges by Improved Steel Plated Structures, RFCS Contract N°: RFS-CR-03018, Final report (to be published).

7 Interaction

EN 1993-1-5, §7

Bernt Johansson, Division of Steel Structures, Luleå University of Technology

7.1 Interaction between shear force, bending moment and axial force

EN 1993-1-5, §7.1

The design rules for interaction between shear force and bending moment in Eurocode 3 are found in EN 1993-1-1 for Class 1 and 2 sections and in EN 1993-1-5 for class 3 and 4 sections. The rules in EN 1993-1-1 given in 6.2.8 are based on the plastic shear resistance and if shear buckling reduces the resistance they refer to EN 1993-1-5. The slenderness limit for which shear buckling starts to reduce the resistance in an unstiffened plate girder is $h_w/t_w = 72 \varepsilon/\eta$ and that limit is normally somewhere between the limits for Class 2 and 3. The rules are stated differently because different models for the interaction are used. This commentary deals with both models for the sake of completeness and clarifies their relation. The derivations and the discussions concerns characteristic resistance and for design purpose relevant partial safety factors should be introduced, which are γ_{M0} for the plastic resistance and γ_{M1} for the buckling resistance.

7.1.1 Plastic resistance

The lower bound theorem of plastic theory can be used for deriving a theoretical interaction formula. Two possible states of stress are shown in Figure 7.1, both compatible with von Mises yield criterion. The stress distributions are valid for class 1 or 2 cross sections.

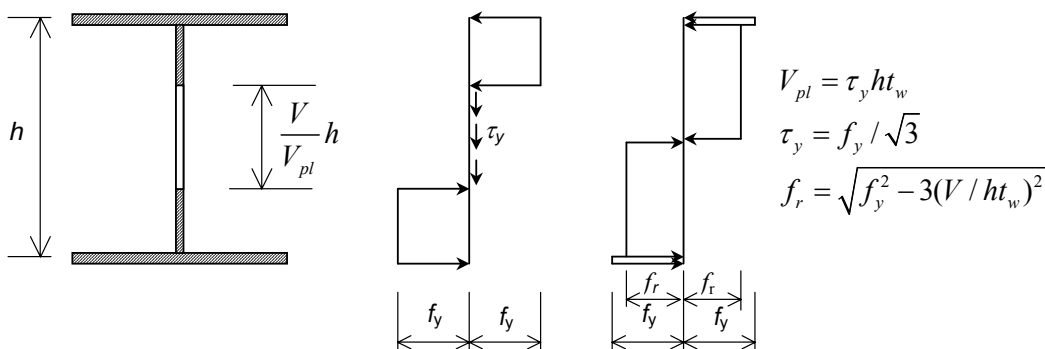


Figure 7.1: I-section of class 1 or 2 subject to combined bending and shear and two possible stress distributions compatible with the von Mises yield criterion

With the simplification that the flange thickness is small compared to the beam depth the left hand stress distribution results in a bending moment:

$$M = M_{pl} - \frac{f_y t_w}{4} \left(\frac{V}{V_{pl}} h \right)^2 \tag{7.1}$$

After rearrangement and introduction of the notation $M_f = f_y h A_f$ for the bending moment that the flanges can carry alone equation (7.1) becomes:

$$\frac{M}{M_{pl}} + \left(1 - \frac{M_f}{M_{pl}}\right) \left(\frac{V}{V_{pl}}\right)^2 = 1 \quad \text{if } M > M_f \quad (7.2)$$

If the bending moment is smaller than M_f , a statically admissible direct stress distribution in the flanges only can carry the bending moment and the web can be fully mobilised for resisting shear, and there is no interaction. The formula (7.2) should be understood such that it gives a set of M and V representing the limit of the resistance of the cross section. For design purpose the equal sign is changed to “smaller than”.

The stress distribution to the right in Figure 7.1 was used by Horne in a study of the influence of shear on the bending resistance [1]. It gives the following interaction formula:

$$\frac{M}{M_{pl}} + \left(1 - \frac{M_f}{M_{pl}}\right) \left(1 - \sqrt{1 - \left(\frac{V}{V_{pl}}\right)^2}\right) = 1 \quad \text{if } M > M_f \quad (7.3)$$

Equations (7.2) and (7.3) are shown in Figure 7.2 for a girder with $M_f/M_{pl}=0,7$. It can be seen that (7.3) is always higher than (7.2), which means that (7.3) is the best estimate of the plastic resistance in accordance with the static theorem of the theory of plasticity.

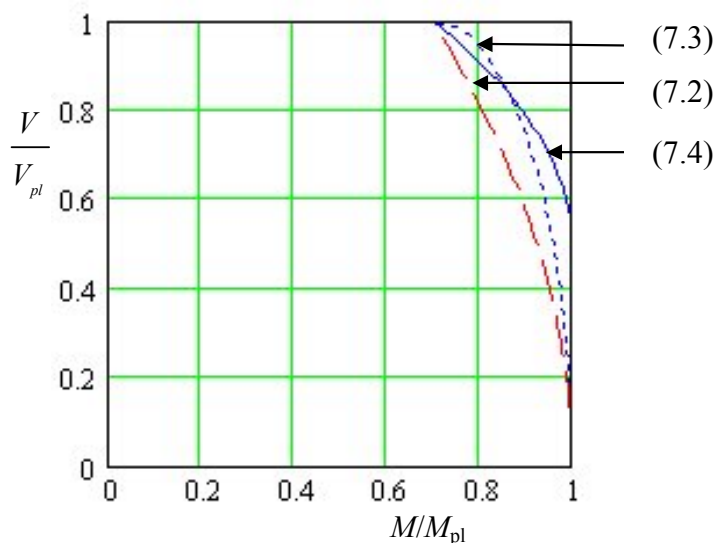


Figure 7.2: Interaction curves (7.2), (7.3) and (7.4) for shear and bending for a beam in class 1 or 2 with $M_f/M_{pl}=0,7$

The interaction formula (6.30) in EN 1993-1-1 is similar to (7.2) but starts the reduction of bending resistance when $V > 0,5V_{pl}$. Omitting the partial safety factor it can be rewritten as:

$$\frac{M}{M_{pl}} + \left(1 - \frac{M_f}{M_{pl}}\right) \left(\frac{2V}{V_{pl}} - 1\right)^2 = 1 \quad \text{if } V > 0,5V_{pl} \quad (7.4)$$

This formula is shown in Figure 7.2. It can be seen that this interaction formula is more favourable in part of the range than the theoretically determined formulae. The justification for this is empirical. There are test results available on rolled sections showing no interaction at all. This is even true if the increased plastic

EN 1993-1-5,
§7.1(1)

shear resistance $\eta f_y A_w$ is used, which can be resisted at the same time as the full plastic bending moment. The reason for this is mainly strain hardening of the material and it has been documented for steel grades up to S355. In this case the strain hardening can be utilised without excessive deformations. The reason is that the presence of high shear leads to a steep moment gradient, which in turn means that the plastic deformations are localised to a small part of the beam. Formula (7.4) can be seen as a cautious step in direction to utilise this fact. The cautiousness can be justified by lack of evidence for higher steel grades and because of the relatively lower strain hardening for higher grades it can be expected that such steel would show a less favourable behaviour.

7.1.2 Buckling resistance

When it comes to slender webs for which buckling influences the resistance there are no useful theories for describing the interaction. An empirical model based on observations from tests was developed by Basler [2]. The model is similar to the lower bound theorem of plastic theory but it is here applied to a problem where instability governs, which is outside the scope of the lower bound theorem. The model is shown in Figure 7.3 and it can be seen that the assumed state of stress is very similar to the left one in Figure 7.1. The only difference is that the strength in shear is not the yield strength but the reduced value $\chi_w \tau_y$. Actually, Basler of course used his own model for the shear resistance, which does not coincide with the one in EN 1993-1-5.

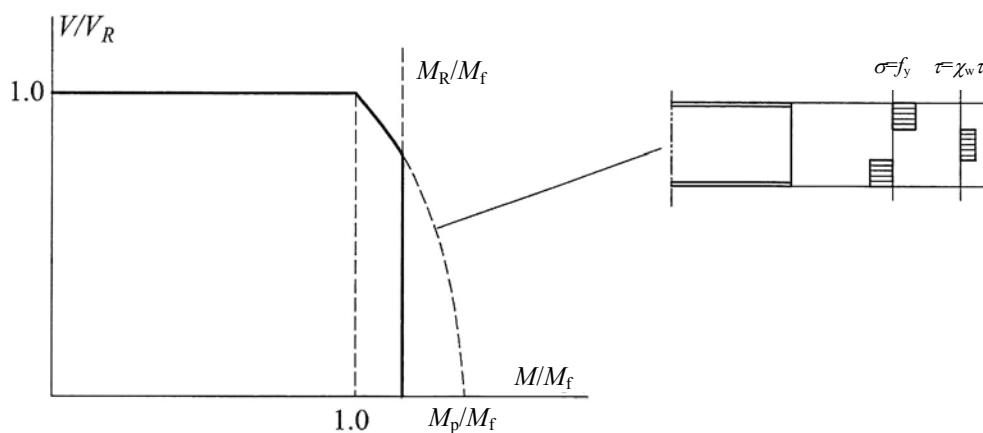


Figure 7.3: Interaction between bending moment and shear according to Basler

As in the case of plastic resistance there is no interaction if the moment is smaller than M_f and for larger values the interaction curve is a parabola. In this case the cross section is in class 3 or 4 and the bending resistance M_R is smaller than plastic resistance. This is represented by a cut-off in Figure 7.3 with a vertical line at M_R/M_f .

The interaction formula used in EN 1993-1-5 is a modification of Basler’s model as the reduction starts at $V/V_{wb,R} = 0,5$:

$$\frac{M}{M_{pl}} + \left(1 - \frac{M_f}{M_{pl}}\right) \left(\frac{2V}{V_{bw,R}} - 1\right)^2 = 1 \text{ if } V > 0,5V_{bw,R} \tag{7.5}$$

The difference compared with (7.4) is that $V_{bw,R}$ is the resistance to shear buckling of the web according to Section 5. Equation (7.5) goes continuously over in (7.4) when the web slenderness is decreasing. M_{pl} is used also for Class 4 sections. It means that the formula has to be supplemented with a condition that:

$$M \leq M_{R,eff} \tag{7.6}$$

where $M_{R,eff}$ is the resistance calculated with effective cross section.

Formula (7.5) is shown in Figure 7.4 for different geometries of test girders and the corresponding test results [3]. The girders were simply supported and tested in three point bending and fitted with vertical stiffeners at supports and under the load. The webs were mainly in Class 4 and some of the webs were more slender than the limit for flange induced buckling in Section 8. The interaction formula (7.5) depends on the geometry of the girder and Figure 7.4 shows the extreme cases. The curves above $V/V_{bw,R} = 1$ are examples of the contribution from flanges, which may be added if M is smaller than M_f .

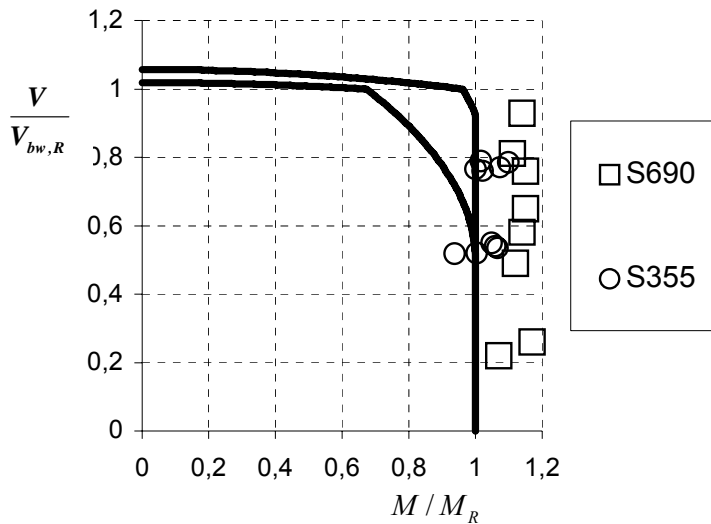


Figure 7.4: Interaction diagrams according to (7.5) for some girders with different geometries and test results [3]

The plot in Figure 7.4 shows very little of interaction, if any. This has been shown also in other tests as well as with computer simulations. The difference between S355 and S690 is noticeable and it reflects the smaller influence of imperfections for higher grades of steel. The resistance is governed by local buckling and the effect of a geometrical imperfection of a certain size is smaller for high strength than for low strength. Also the residual stresses are smaller compared with the yield strength for a high strength, which contributes to the relative difference.

An example of results from computer simulations is shown in Figure 7.5 [4]. The simulations were realistic non-linear FE-simulations of typical Swiss composite bridges and the numbers in the legends refer to the span of the girder in meters. The solid symbols refer to simulations of the steel girder alone and the open symbols to simulations including the effect of the concrete slab. In the notation LiR, the “i” denotes the span in meters. The reference resistance to bending and shear acting alone, respectively, are from the computer simulations, not from a design code. It is interesting to note that the bending resistance increases slightly when a small shear force is added. The reference bending resistance comes from

simulations with uniform bending and the increase is attributed to the moment gradient. Similar results have been obtained in [3]. The diagrams show that there is a small interaction for shear forces exceeding 0,8 times the shear resistance. These results show clearly that there is no need to consider interaction for small values of the shear force. The results can not be used for a direct evaluation of the design rules of EN 1993-1-5 as the reference resistances were taken from the computer simulations. However, a separate study in [4] compared the predictions of the rules in EN 1993-1-5 and ENV 1994-1-1 with test results for composite girders. The comparison showed that the rules were conservative both for bending and for shear. The results in Figure 7.5 can anyway be taken as a confirmation that there is no need for considering interaction for smaller shear forces than half the shear resistance.

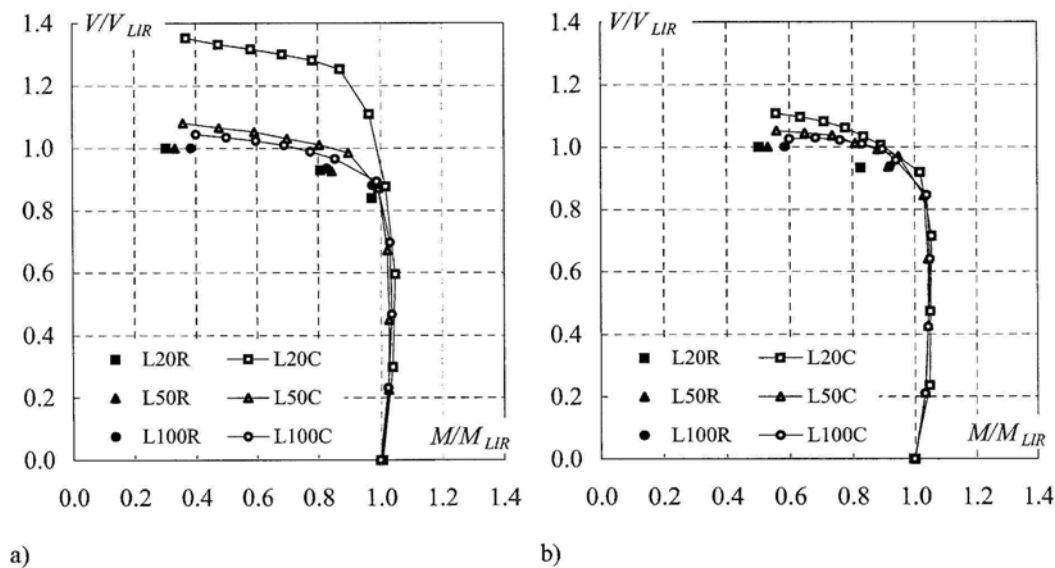


Figure 7.5: Interaction curves from computer simulations of bridge girders [4]. a) panel length over web depth = 1 and b) = 2

A rule given in 7.1(2) of EN 1993-1-5 states that the interaction need not be checked in cross-sections closer to an intermediate support than half the web depth. This rule reduces the effect of interaction and it is based on engineering judgement. The reasoning is that the buckles of the web have an extension along the girder and that the state of stress close to a vertical stiffener is not relevant for a buckling check. However, the resistance without reduction for buckling should not be exceeded at the support. For girders with longitudinal stiffeners the rule in 7.1(2) may be a bit optimistic. Nothing is stated in the standard about how to interpret the rule. It is here suggested that the rule is interpreted such that the cross section for verifying the interaction is taken as that at a distance of half the depth of the largest subpanel as that is governing the size of the buckles.

The presence of an axial force causes further interaction effects. It is taken into account by reducing M_f and M_{pl} for the presence of the axial force.

7.2 Interaction between transverse force, bending moment and axial force

EN 1993-1-5, §7.2

The patch loading resistance will be reduced if there are simultaneous bending moment or axial force. There are two reasons for this interaction. One is that the longitudinal stresses in the web interact with the vertical stresses due to the patch load and the resistance of the flange to bending is reduced by the longitudinal stresses from global bending. Another is that the curvature of the girder due to bending induces vertical compression in the web, see Section 8, that add to the stresses from the patch load. This problem has not been analysed in detail and there are no theoretical models available. The influences have so far not been separated and the interaction is accounted for by an empirical condition (7.7). It follows that when the ratio $M/M_R \leq 0,5$, the bending moment has no influence on the patch load resistance, see Figure 7.6.

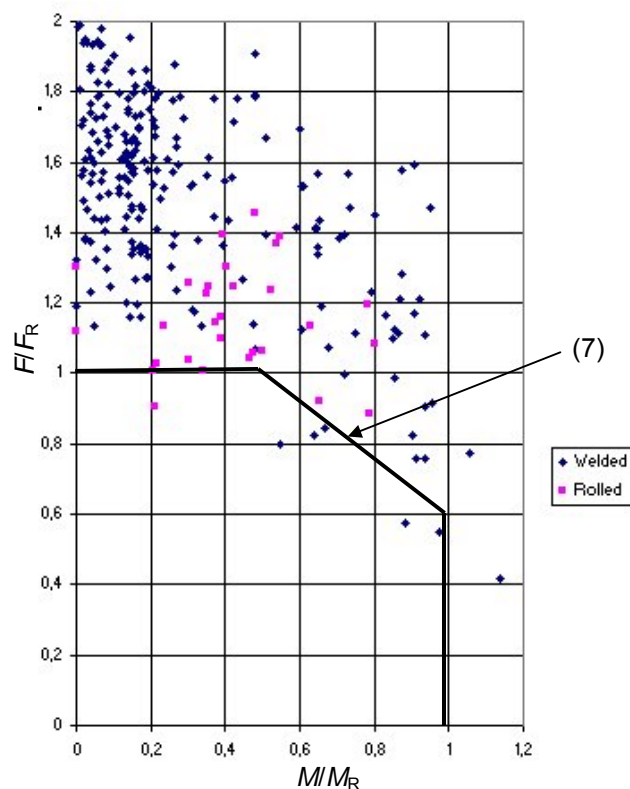


Figure 7.6: Interaction between patch load and bending moment with 254 test results

$$\frac{F}{F_R} + 0,8 \frac{M}{M_R} \leq 1,4 \tag{7.7}$$

EN 1993-1-5, §7.2(1)

M_R is the applicable resistance to bending, which means the plastic resistance for class 1 and 2, the elastic resistance for class 3 and the resistance of the effective cross-section for class 4 sections. F_R is the patch loading resistance according to Section 6. In addition to (7.7) the individual actions should not exceed M_R and F_R , respectively.

Figure 7.6 shows also test results with different combinations of utilisation. The test results are taken from [5]. The evaluation of them is new and it considers the differences between the proposal in [5] and the final rules of EN 1993-1-5, see

Section 6. It is a quite a large scatter, which mainly can be blamed on the estimate of the resistance to patch load. There are several other proposals for this interaction but the problem with the large scatter is not solved by any of them.

The presence of an axial force causes an additional interaction effect. As the criterion is written in eq. (7.2) of EN 1993-1-5 in the second term η_1 includes the direct effect of the axial force. This rule is mainly based on judgement, as the problem has not been investigated for girders.

The interaction with shear has been dealt with in some studies. It is usually argued that all tests include at least a shear force equal to half the patch load. Accordingly, the effect of that shear force is already included in the test result. A few tests referred in [5] have been performed with high shear forces but they do not show a significant influence. The conclusion in [5] was that the interaction could be ignored. A recent study [6] on patch loading of girders with longitudinal stiffeners reports one test with high shear. It shows a reduction of the resistance to patch load of 20% compared to a corresponding girder with small shear. Although the reduction is significant, the test result is still way above the prediction of EN 1993-1-5. The problem has also been studied by computer simulations for instance in [7]. The study indicates that there is an influence of the shear force as well as the bending moment. Interaction formulae were proposed but they used different reference resistances than EN 1993-1-5.

As indicated in Section 6, there is a need for improvement of the rules for patch load resistance. This is also relevant for the question of interaction and further studies are needed in order to separate different influences. However, according to present results the rules of EN 1993-1-5 are safe and in some cases unduly safe.

7.3 References

- [1] Horne, M. R., The Plastic Theory of Bending of Mild Steel Beams with Particular Reference to the Effect of Shear Forces, Proceedings of the Royal Society A, vol 207, 1951.
- [2] Basler, K., Strength of plate girders under combined bending and shear, Journal of the Structural Division ASCE, Vol 87, No ST 7 1961, pp 181-197.
- [3] Veljkovic, M., Johansson, B., Design for buckling of plates due to direct stress. Proceedings of the Nordic Steel Construction Conference Helsinki, 2001
- [4] Lääne, A., Post-critical behaviour of composite bridges under negative moment and shear, Thesis No 2889 (2003), EPFL, Lausanne, 2003.
- [5] Lagerqvist, O. Patch loading, Resistance of steel girders subjected to concentrated forces, Doctoral Thesis 1994:159 D, Department of Civil and Mining Engineering, Division of Steel structures Luleå University of Technology.
- [6] Kuhlmann, U., Seitz, M., Longitudinally stiffened girder webs subjected to patch loading, Proceedings of the conference Steel bridge 2004, Millau 2004.
- [7] Roberts, T. M., Shahabian, F., Ultimate resistance of slender web panels to combined bending shear and patch loading, Journal of Constructional Steel Research, Volume 57, Issue 7, Pages 779-790, July 2001.

8 Flange induced buckling

EN 1993-1-5,
§8

René Maquoi, Department M&S, Université de Liège

- (1) When an initially straight girder is bent, the curvature is the cause of transverse compression forces, which are likely to produce web buckling; after failure, the compression flange looks as having buckled into the web, therefore the terminology of “flange induced buckling”.
- (2) The criterion aimed at preventing flange induced buckling is established based on the model of a symmetrical uniform I-section girder subjected to pure bending, so that the loading results in a constant curvature. Because this loading condition is the worst, the rules derived from this model are conservative.
- (3) The curvature of the bent girder is governed by the variation $\Delta\varepsilon_f$ in the strain occurring in the mid-plane of both flanges; it is measured by the radius $R = 0,5h_w / \Delta\varepsilon_f$ (Figure 8.1). This expression is based on the simplification that the flange thickness is disregarded with respect to the web depth; thus the latter is taken as the distance between the centroids of the flanges
- (4) The limit state of the flanges is reached when the stress σ_f in both flanges is equal to the material yield strength f_{yf} in all their fibres.
- (5) A same residual strain pattern is assumed in both flanges, with a peak tensile residual strain $\varepsilon_f = 0.5\varepsilon_y$ in the region adjacent to the web-to-flange junction and lower compressive residual strains (in absolute value) elsewhere.

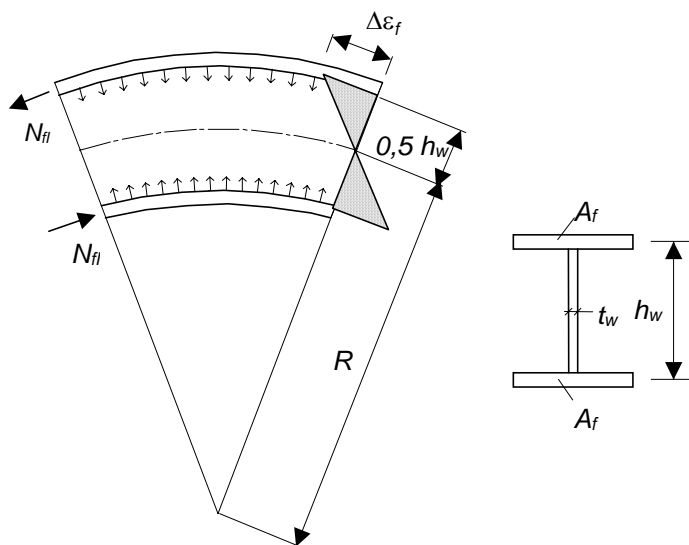


Figure 8.1: Transverse compression in a deflected girder subjected to pure bending

- (6) The strain variation $\Delta\varepsilon_f$ is the one required to get a complete yielding of the compression flange, i.e. to reach there the yield strain in compression at the vicinity of the web-to-flange junction. With due account of the residual strain pattern, the required strain variation amounts $\Delta\varepsilon_f = \varepsilon_y + 0.5\varepsilon_y = 1.5f_{yf} / E$. Due to the symmetry supposed for the girder, the same strain variation occurs in the tension flange and superimposes the residual strain. That results in a fully yielded tension flange too; the maximum resultant tensile strain is reached at the web-to-flange junction, where it amounts to $2f_{yf} / E$, which is a still acceptable strain magnitude.
- (7) With reference to the deflected shape of the flanges, equilibrium of the latter - considered as separate elements - requires that radial uniformly distributed forces $\sigma_v t_w = f_{yf} A_{fc} / R$ per unit length are applied by the web onto the flanges of cross-sectional area A_{fc} ; with due account taken of the above expressions of R and $\Delta\varepsilon_f$, one get:

$$\sigma_v = 3 \frac{A_{fc}}{A_w} \frac{f_{yf}^2}{E} \tag{8.1}$$

where $A_w = h_w t_w$ is the cross-sectional area of the web.

- (8) Uniform transverse compression in the web is induced by the reciprocal transverse forces ($-\sigma_v t_w$); web buckling is prevented by simply requiring that the magnitude of the corresponding stress σ_v does not exceed the elastic critical buckling stress, i.e.:

$$\sigma_v \leq \frac{\pi^2 E}{12(1 - \nu^2)} \left(\frac{t_w}{h_w} \right)^2 \tag{8.2}$$

- (9) Above condition of buckling prevention leads to :

$$\frac{h_w}{t_w} \leq 0,55 \frac{E}{f_{yf}} \sqrt{\frac{A_w}{A_{fc}}} = k \frac{E}{f_{yf}} \sqrt{\frac{A_w}{A_{fc}}} \tag{8.3}$$

where:

$A_w = h_w t_w$ Cross-sectional area of the web;

A_{fc} Cross-sectional area of the compression flange, used as reference flange;

f_{yf} Yield strength of the compression flange material;

k Factor amounting 0,55 (other values apply when substantially larger strains are required in the flange: 0,40 corresponding to $\Delta\varepsilon_f = 2,8f_y/E$ when plastic moment resistance is utilised and 0,30 corresponding to $\Delta\varepsilon_f = 5f_y/E$ when plastic rotation is required).

EN 1993-1-5,
§8(1)

- (10) When the girder is initially curved in elevation with a constant radius r in the non loaded configuration, above expression is modified according to:

EN 1993-1-5, §8(2)

$$\frac{h}{t_w} \leq K \frac{\frac{E}{f_{yf}} \sqrt{\frac{A_w}{A_{fc}}}}{\sqrt{1 + \frac{h}{3rf_{yf}} \frac{E}{t_w}}} \quad (8.4)$$

with :

r Radius of curvature of the compression flange in the web plane ($r = \infty$ for an initially straight flange);

Above limitation does not account for the influence of longitudinal stiffeners, so that it is especially conservative when such stiffeners are located in the close vicinity of the compression flange.

- (11) In case of a composite compression flange it may have a substantial area and also a substantial bending stiffness that prevents a very localized buckling. In this case the transverse compression in the web will be governed by the tensile force in the tension flange.

The derivation shown above will still be valid but with A_{fc} taken as the tension flange area.

This interpretation has been introduced in EN 1994-2 and is deemed to be conservative.

The web may very well buckle from the transverse compression, but as soon as the buckle grows the curvature of the bottom flange will reduce and the transverse compression will decrease. It will be a self-stabilizing system that is not likely to lead to collapse.

9 Stiffeners and detailing

Darko Beg, Faculty of Civil and Geodetic Engineering, University of Ljubljana

EN 1993-1-5, §9

9.1 Introduction

EN 1993-1-5, §9.1

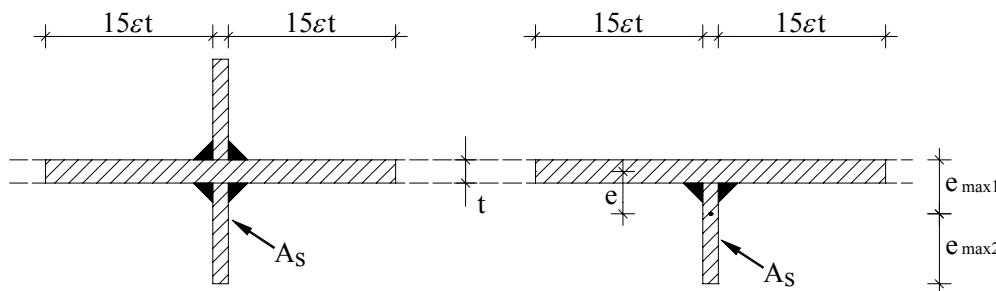
In addition to the plate buckling rules given in Sections 4 to 7, longitudinal and transverse stiffeners should fulfil the rules given in this Section.

Requirements are given in the following order:

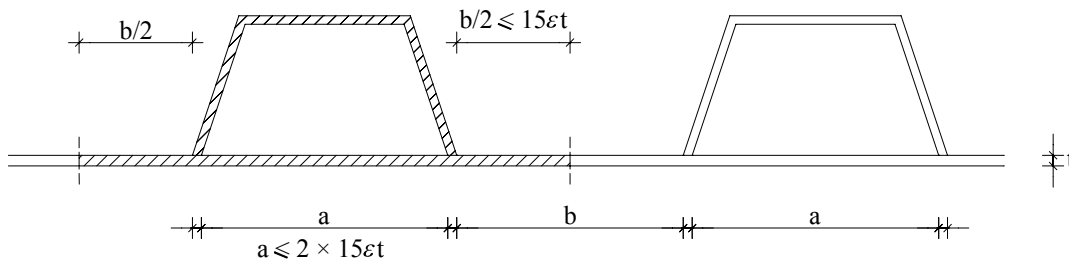
- transverse and longitudinal stiffeners under the influence of direct stresses from bending moments and axial forces in the plate girder;
- transverse and longitudinal stiffeners under the influence of shear forces in the plate girder;
- transverse stiffeners under the influence of the transverse loading on the plate girder.

To check specific requirements for stiffeners an equivalent cross-section consisting of the gross cross-section of the stiffeners plus a contributing width of the plate equal to $15\varepsilon t$ on each side of the stiffener may be used (Figure 9.1), where t is the plate thickness and $\varepsilon = \sqrt{235/f_y}$ (f_y in MPa). Contributing width of plating $15\varepsilon t$ should be within the actual dimensions available and overlapping is not permitted.

EN 1993-1-5, §9.3



a) No overlapping in contributing plating



b) Overlapping of contributing plating

Figure 9.1: Effective cross-sections of stiffeners

It is important to note that the contributing width of $15\epsilon t$ is used only for the additional rules given in Section 9. When stiffeners are directly involved in the plate buckling checks (Sections 4 to 7) effective widths for the adjacent plating apply.

9.2 Direct stresses

EN 1993-1-5, §9.2

9.2.1 Minimum requirements for transverse stiffeners

EN 1993-1-5, §9.2.1

Transverse stiffeners should preferably provide a rigid support up to the ultimate limit state for a plate with or without longitudinal stiffeners. They should be able to carry deviation forces from the adjacent compressed panels and be designed for both appropriate strength and stiffness.

In principle, based on the second order elastic analysis, the following criteria should be satisfied:

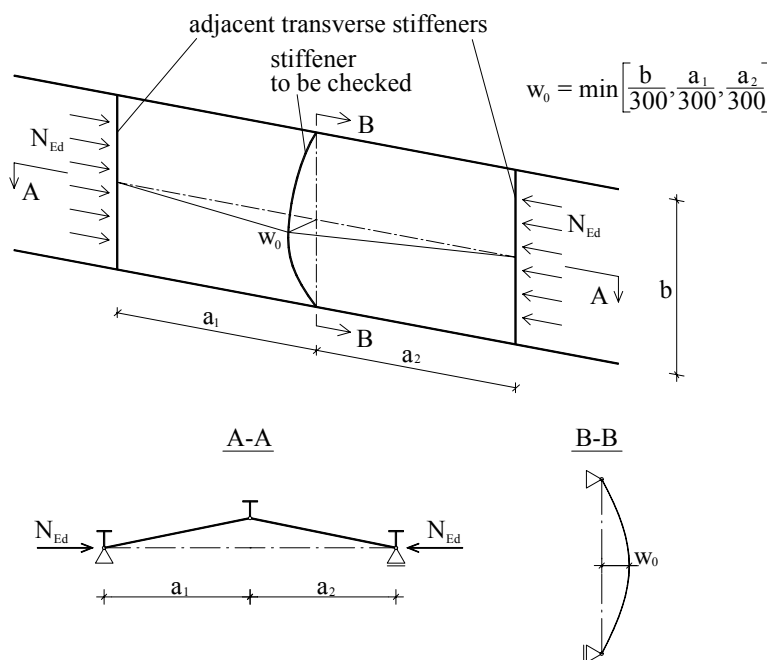
- the maximum stress in the stiffener under design load should not exceed f_y/γ_{M1} ;
- the additional deflection should not exceed $b/300$, therefore:

$$\sigma_{\max} \leq \frac{f_y}{\gamma_{M1}}, \quad w \leq \frac{b}{300}, \quad (9.1)$$

EN 1993-1-5, §9.2.1(4)

where b is the plate width (see Figure 9.2).

Any other relevant load acting on the stiffener (axial force in the stiffener – e.g. due to directly applied external force – or possible horizontal transverse loading on the stiffener – e.g. due to in-plane curvature of the girder) should be included. Also eccentricities of a stiffener should be accounted for in the presence of axial forces in a stiffener.



EN 1993-1-5, §9.2.1, Fig. 9.2

Figure 9.2: Static scheme for transverse stiffener

The static scheme that should be used to check each individual transverse stiffener is given in Figure 9.2. The transverse stiffener under consideration should be treated as a simply supported beam fitted with an initial sinusoidal imperfection of amplitude w_0 (Figure 9.2). The adjacent compressed panels and the longitudinal stiffeners, if any, are considered to be simply supported at the transverse stiffener and both adjacent transverse stiffeners are supposed to be straight and rigid.

In the most general case (Figure 9.3) a transverse stiffener may be loaded with:

- a transverse deviation force q_{dev} , originated from longitudinal compressive force of the adjacent panels N_{Ed} ,
- an external transverse loading q_{Ed} in the horizontal direction;
- an axial force in the transverse stiffener $N_{st,Ed}$, coming from vertical transverse loading on the girder ;
- an axial force $N_{st,ten}$, originated from diagonal tension field, developed in shear (see Eq. (9.48) and Figure 9.17).

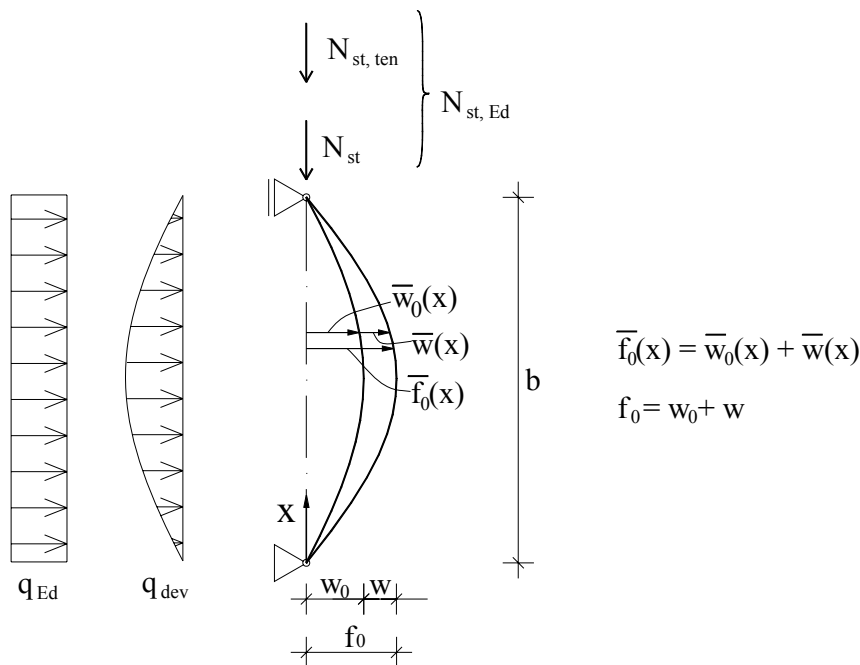


Figure 9.3: General loading conditions for the transverse stiffener

To make the design of transverse stiffeners easier for typical cases the requirements (9.1) can be transformed into a more suitable and explicit form. The most unfavourable uniform distribution of the longitudinal compressive force N_{Ed} over the depth of the web will be considered and other distributions will be discussed later.

The deviation force q_{dev} can be expressed as:

$$q_{dev}(x) = \bar{f}_0(x) \frac{N_{Ed}}{b} \left(\frac{1}{a_1} + \frac{1}{a_2} \right) \frac{\sigma_{cr,c}}{\sigma_{cr,p}} = (\bar{w}_0(x) + \bar{w}(x)) \sigma_m \tag{9.2}$$

where:

EN 1993-1-5,
§9.2.1(7)

$$\sigma_m = \frac{\sigma_{cr,c}}{\sigma_{cr,p}} \frac{N_{Ed}}{b} \left(\frac{1}{a_1} + \frac{1}{a_2} \right)$$

$$\bar{w}_0(x) = w_0 \sin\left(\frac{\pi x}{b}\right),$$

EN 1993-1-5,
§9.2.1(5)

where $\sigma_{cr,c}$ and $\sigma_{cr,p}$ are respectively the elastic critical column-like buckling stress and the elastic critical plate-like buckling stress of the adjacent panels (see 4.3.1(5)). The ratio $\sigma_{cr,c}/\sigma_{cr,p}$ is introduced into q_{dev} to account for the influence of plate type behaviour of the adjacent panels that reduce deviation forces. According to 4.5.4(1) of EN 1993-1-5 the relevant values of the ratio $\sigma_{cr,c}/\sigma_{cr,p}$ are between 0,5 and 1,0. It is to be understood that the same limits apply to the expression (9.2) although this is not explicitly said in the code. For panels with large aspect ratios the ratio $\sigma_{cr,c}/\sigma_{cr,p}$ can be very small, but the values below 0,5 are not reasonable because they lead to unacceptable reduction of the deviation force q_{dev} . As a conservative solution $\sigma_{cr,c}/\sigma_{cr,p}$ may be taken as its maximum value, i.e. 1,0.

When the compressive force N_{Ed} is not constant over the depth of the panel, as it is usually the case in plate girders, the resultant axial force relative to the part of the panel in compression is relevant but it is taken as uniformly distributed over the height of the panel (for the sake of simplicity and on the safe side). In order to maintain the importance of requirements (9.1) for transverse stiffeners the compressive force N_{Ed} should not be taken less than the largest compressive stress times half the effective^p compression area of the panel including longitudinal stiffeners. This limitation may be decisive for instance for symmetric plate girders in pure bending. When the axial forces in adjacent panels differ, the larger of the two is taken into consideration.

For the following three cases direct requirement will be derived from requirements (9.1):

- stiffened panels loaded by longitudinal compression forces N_{Ed} only;
- stiffened panels loaded by longitudinal compression forces N_{Ed} and axial forces in the transverse stiffener ($N_{st,Ed}$ and/or $N_{st,ten}$);
- general case.

Stiffened panels loaded by longitudinal compression forces N_{Ed} only

When the transverse stiffener is loaded only by the deviation forces coming from longitudinal compression force in the panels N_{Ed} , the requirements (9.1) are presumably satisfied by providing the transverse stiffener with a minimum second moment of inertia I_{st} .

With N_{Ed} uniformly distributed over the width of the panel and $\bar{w}_0(x)$ taken as sine function from Eq. (9.2), both the additional deflection $\bar{w}(x)$ and the deviation force $q_{dev}(x)$ have a sinusoidal shape too. By taking this into consideration, the maximum stress σ_{max} and the maximum additional deflection w can be calculated as:

$$\sigma_{\max} = \frac{M_{\max} e_{\max}}{I_{st}} = \frac{q_{dev,0} b^2 e_{\max}}{\pi^2 I_{st}} = \frac{(w_0 + w) \sigma_m b^2 e_{\max}}{\pi^2 I_{st}} \quad (9.3)$$

$$w = \frac{q_{dev,0} b^4}{\pi^2 E I_{st}} = \frac{(w_0 + w) \sigma_m b^4}{\pi^2 E I_{st}} = \frac{\sigma_{\max} b^2}{\pi^2 E e_{\max}} \quad (9.4)$$

where:

M_{\max} is maximum value of the bending moment in the stiffener caused by the deviation force;

e_{\max} is the distance from the extreme fibre of the stiffener to the centroid of the stiffener;

$q_{dev,0} = (w_0 + w) \sigma_m$ is the amplitude of the deviation force $q_{dev}(x)$.

Introducing (9.4) into (9.3) results in a relation between I_{st} and σ_{\max} :

$$I_{st} = \frac{\sigma_m}{E} \left(\frac{b}{\pi} \right)^4 \left(1 + w_0 \frac{\pi^2 E e_{\max}}{b^2 \sigma_{\max}} \right) \quad (9.5)$$

With due account taken of (9.4), I_{st} can be expressed in terms of w :

$$I_{st} = \frac{\sigma_m}{E} \left(\frac{b}{\pi} \right)^4 \left(1 + \frac{w_0}{w} \right) \quad (9.6)$$

To get minimum allowable values for I_{st} , maximum allowable values of $\sigma_{\max} = f_y / \gamma_{M1}$ and $w = b/300$ are introduced in (9.5) and (9.6), respectively. Because of (9.4) expressions (9.5) and (9.6) can be then merged into:

$$I_{st} \geq \frac{\sigma_m}{E} \left(\frac{b}{\pi} \right)^4 \left(1 + w_0 \frac{300}{b} u \right) \quad (9.7)$$

where:

$$u = \frac{\pi^2 E e_{\max} \gamma_{M1}}{b 300 f_y} \geq 1.$$

When u is less than 1,0 a displacement check is decisive and u is taken as 1,0 in (9.7), otherwise a strength check is governing.

Stiffened panels loaded by longitudinal compression forces N_{Ed} and axial forces in the transverse stiffener $N_{st,Ed}$ (N_{st} and/or $N_{st,tension}$)

When in addition to the deviation forces the transverse stiffener is loaded by an external axial force, then the deviation force is transformed into an additional axial force $\Delta N_{st,Ed}$ in the stiffener:

$$\Delta N_{st,Ed} = \frac{\sigma_m b^2}{\pi^2} \quad (9.8)$$

EN 1993-1-5,
§9.2.1(5)

EN 1993-1-5,
§9.2.1(6)

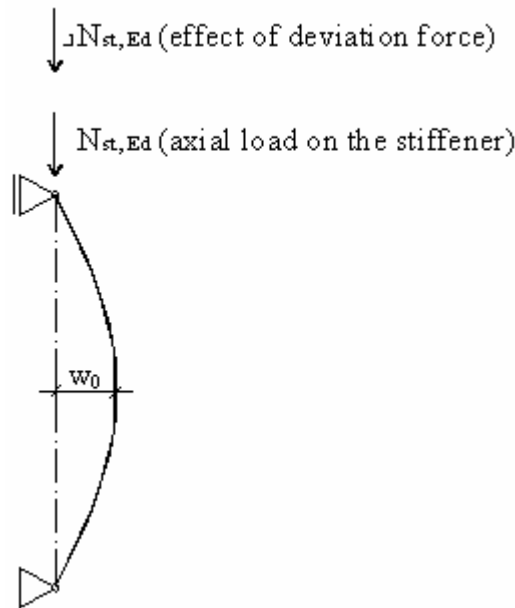


Figure 9.4: Simplified analysis of the axially loaded transverse stiffener

For this case the mechanical model is shown in Figure 9.3 (excluding q_{Ed}). The stiffener is loaded with a deviation force originated from longitudinal compression in the panels (N_{Ed}) and axial force $N_{st,Ed}$ in the stiffener, resulting from the tension field action ($N_{st,ten}$ – see 9.3.3) and/or from the external loading. The force $N_{st,Ed}$ is in most cases not constant and it is a conservative assumption to regard it as constant. For a concentrated force F introduced at one flange only the resulting axial force $N_{st,Ed}$ may be taken as an equivalent constant axial force of a reduced magnitude $0,6F$.

Equilibrium differential equation of the stiffener can be written for $N_{st,Ed}$ being a constant or an equivalent constant as:

$$EI_{st} \bar{w}_{,xxxx} + N_{st,Ed} (\bar{w}_{0,xx} + \bar{w}_{,xx}) = q_{dev}(x) = \sigma_m (\bar{w}_0 + \bar{w}) \tag{9.9}$$

or:

$$\bar{w}_{,xxxx} + \omega^2 \bar{w}_{,xx} - \alpha^2 \bar{w} = \alpha^2 \bar{w}_0 - \omega^2 \bar{w}_{0,xx}, \quad \omega^2 = \frac{N_{st,Ed}}{EI_{st}}, \quad \alpha^2 = \frac{\sigma_m}{EI_{st}} \tag{9.10}$$

The sine function:

$$\bar{w} = w \sin \frac{\pi x}{b} \tag{9.11}$$

automatically fulfils all static and kinematic boundary conditions and can be taken as a suitable solution of (9.10). A free constant w is easily obtained from (9.10):

$$w = \frac{\omega^2 \frac{\pi^2}{b^2} + \alpha^2}{\frac{\pi^4}{b^4} - \omega^2 \frac{\pi^2}{b^2} - \alpha^2} w_0 = K w_0 \tag{9.12}$$

Constant K can be rewritten as follows:

$$K = \frac{\beta^2}{\frac{\pi^4}{b^4} - \beta^2} \quad (9.13)$$

where:

$$\beta^2 = \frac{\pi^2}{EI_{st}b^2} (N_{st,Ed} + \Delta N_{st,Ed}) \quad \text{and} \quad \Delta N_{st,Ed} = \frac{\sigma_m b^2}{\pi^2} \quad (9.14)$$

By introducing:

$$\Sigma N_{st,Ed} = N_{st,Ed} + \Delta N_{st,Ed} \quad (9.15)$$

and the Euler buckling load of a stiffener:

$$N_{cr,st} = \frac{\pi^2 EI_{st}}{b^2} \quad (9.16)$$

the amplitudes of both the additional deflection w and the total deflection f are:

$$w = w_o \frac{1}{\frac{N_{cr,st}}{\Sigma N_{st,Ed}} - 1} \quad (9.17)$$

$$f = w_o + w = w_o \frac{1}{1 - \frac{\Sigma N_{st,Ed}}{N_{cr,st}}} \quad (9.18)$$

Comparing (9.17) and (9.18) to the standard solution for the compressed imperfect bar, it is evident that the deviation force q_{dev} coming from longitudinal compression in the web panels (N_{Ed}) can be replaced by the additional axial force $\Delta N_{st,Ed} = \sigma_m b^2 / \pi^2$ in the stiffener. $\Delta N_{st,Ed}$ is a small fraction of a longitudinal compression force N_{Ed} in the plate panels. This solution is very simple and easy to apply. When the distribution of the longitudinal compression stresses is not constant (i.e. web panel of a girder under bending moment), the results are on the safe side.

Both stiffness and strength requirements (see (9.1)) may be checked according to the following procedure that takes second order effects into account:

$$w = w_o \frac{1}{\frac{N_{cr,st}}{\Sigma N_{st,Ed}} - 1} \leq \frac{b}{300} \quad (9.19)$$

$$\sigma_{\max} = \frac{N_{st,Ed}}{A_{st}} + \frac{\Sigma N_{st,Ed} e_{\max}}{I_{st}} f = \frac{N_{st,Ed}}{A_{st}} + \frac{\Sigma N_{st,Ed} e_{\max}}{I_{st}} w_o \frac{1}{1 - \frac{\Sigma N_{st,Ed}}{N_{cr,st}}} \leq \frac{f_y}{\gamma_{M1}} \quad (9.20)$$

Note that only the axial force $N_{st,Ed}$ needs to be considered in the first term of (9.20). Rather than being a real axial force, $\Delta N_{st,Ed}$ is simply equivalent (for what regards its effects) to the deviation force q_{dev} . For the case $N_{st,Ed} = 0$, expressions (9.19) and (9.20) reduce to (9.7). Requirements (9.19) and (9.20) are valid only for double sided stiffeners.

For single sided transverse stiffeners the mechanical model is shown in Figure 9.5. The equilibrium equation (9.10) is still valid; only the boundary conditions change due to end moments $M_{EN} = N_{st,Ed} e_o$, where e_o is the eccentricity of the centroid of single sided stiffener relative to the mid-plane of the web. With new boundary conditions the solution of (9.10) becomes much more complicated than the solution given by (9.17) and is not suitable for practical use. To overcome this problem, a simplified approach may be used, based on the expression for maximum displacements and stresses at mid height of double sided stiffeners (9.19) and (9.20).

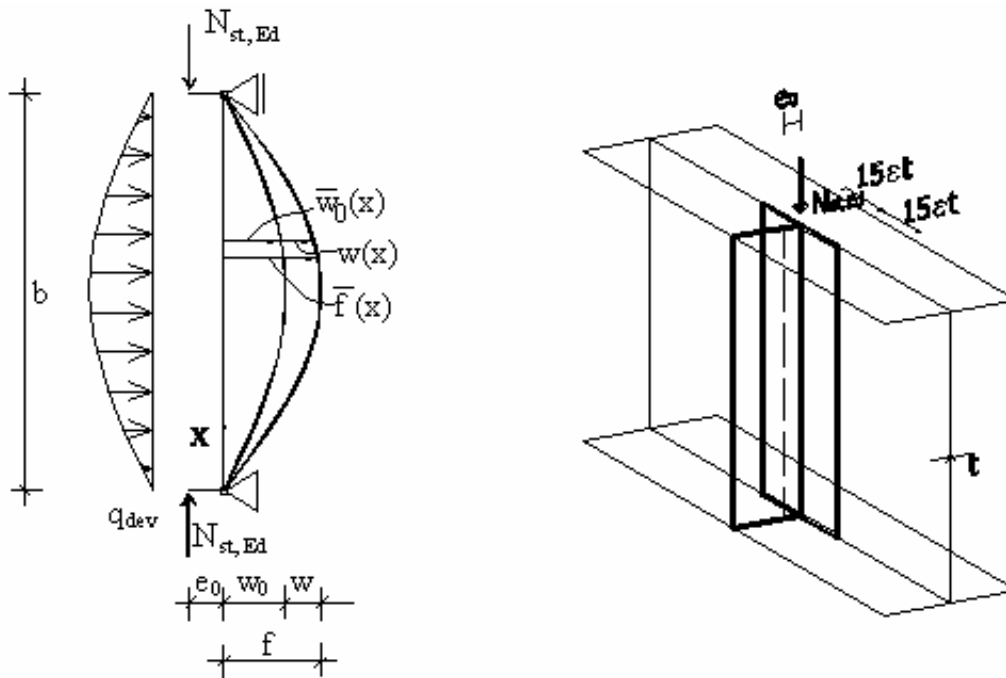


Figure 9.5: The mechanical model of a single sided stiffener

It is considered that $N_{st,Ed}$ is related to the maximum eccentricity $e_o + w_o$ and $\Delta N_{st,Ed}$ from deviation force only to w_o . In this case expression (9.20) rewrites as follows:

$$\sigma_{max} = \frac{N_{st,Ed}}{A_{st}} + \frac{e_{max}}{I_{st}} \left(\sum N_{st,Ed} w_o \cdot \frac{1}{1 - \frac{\sum N_{st,Ed}}{N_{cr,st}}} + N_{st,Ed} e_o \cdot \frac{1}{1 - \frac{\sum N_{st,Ed}}{N_{cr,st}}} \right) \quad (9.21)$$

and after rearranging:

$$\sigma_{max} = \frac{N_{st,Ed}}{A_{st}} + \frac{\sum N_{st,Ed} e_{max} w_o}{I_{st}} \cdot \frac{1}{1 - \frac{\sum N_{st,Ed}}{N_{cr,st}}} (1 + q_m) \leq \frac{f_y}{\gamma_{M1}} \quad (9.22)$$

where:

$$q_m = \frac{N_{st,Ed} e_o}{\sum N_{st,Ed} w_o}$$

If the same amplification factor $(1+q_m)$ is applied to the displacements, equation (9.19) rewrites as follows:

$$w = w_0 \frac{1}{\frac{N_{cr,st}}{\Sigma N_{st,Ed}} - 1} (1 + q_m) \leq \frac{b}{300} \quad (9.23)$$

Expressions (9.21) and (9.22) were tested against the solution of the equilibrium equation (9.10). Based on an extensive parametric study it was found (Beg and Dujc [1]), that safe and very accurate results are obtained, when q_m is multiplied by a factor 1,11 in (9.22) and by a factor 1,25 in (9.23). This means that single sided transverse stiffeners may be checked to fulfil the requirements (9.1) with the following simplified expressions:

$$\sigma_{max} = \frac{N_{st,Ed}}{A_{st}} + \frac{\Sigma N_{st,Ed} e_{max} w_0}{I_{st}} \cdot \frac{1}{1 - \frac{\Sigma N_{st,Ed}}{N_{cr,st}}} (1 + 1,11 q_m) \leq \frac{f_y}{\gamma_{M1}} \quad (9.24)$$

$$w = w_0 \frac{1}{\frac{N_{cr,st}}{\Sigma N_{st,Ed}} - 1} (1 + 1,25 q_m) \leq \frac{b}{300} \quad (9.25)$$

For single sided stiffeners e_{max} has to be understood as the distance from the web surface (opposite to the stiffener) to the stiffener centroid, if this distance is smaller than e_{max} . This is due to the fact that the most unfavourable situation is present when the initial bow imperfection w_0 extends to the stiffener side of the web. In this case compression stresses from the axial force and from bending sum up at the web side of the stiffener.

General case

In the most general case, where besides deviation forces q_{dev} also transverse loading q_{Ed} and axial force $N_{st,Ed}$ act on the stiffener, the deviation force q_{dev} shall be calculated explicitly and then used in the analysis of the stiffener. The numerical models for double and single sided stiffeners are shown in Figure 9.6a and b, respectively. The deviation force q_{dev} depends on the additional deflection $w(x)$ that itself depends on the loads N_{Ed} , $N_{st,Ed}$, q_{Ed} acting on the stiffener. For this reason an iterative procedure is required to calculate q_{dev} .

Due to the sinusoidal shape of the initial imperfections and assuming similarly a sinusoidal shape for the transverse loading q_{Ed} (for the sake of simplicity), the deviation force q_{dev} writes:

$$q_{dev}(x) = \sigma_m (w_0 + w) \sin\left(\frac{\pi x}{b}\right) \quad (9.26)$$

where w is the additional deflection due to a deviation force that needs to be determined iteratively (effects of the second order theory) or conservatively be taken as the maximum additional deflection $w = b/300$. With this simplification, the iterative procedure is avoided, but certainly a displacement check has to be

performed to make certain that $w(q_{dev}, q_{Ed}, N_{st,Ed}) \leq b/300$. In most cases this simplification does not result in a significant increase in the stiffener cross-sectional size.

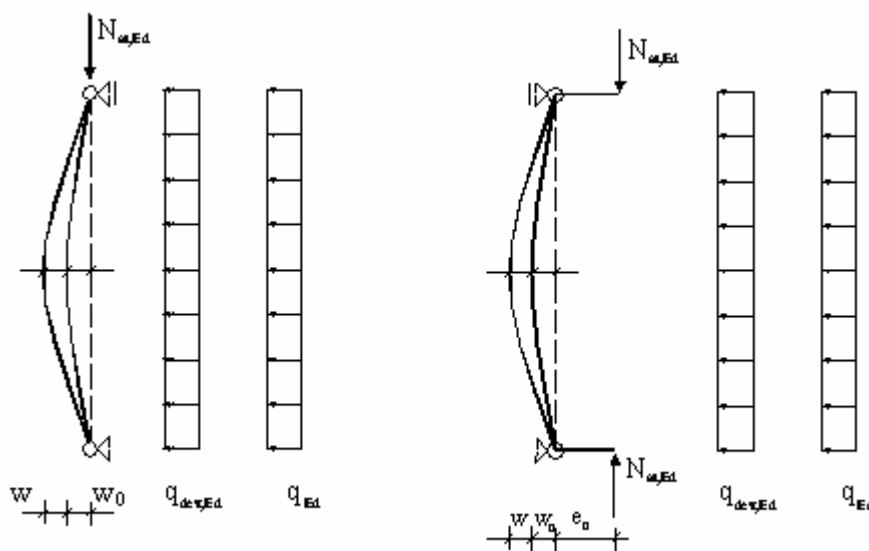
Instead of the sinusoidal deviation force, EN 1993-1-5 proposes an equivalent uniformly distributed deviation force that causes the same maximum bending moment in the stiffener:

$$q_{dev,eq} = \frac{\pi}{4} \sigma_m (w_0 + w) \tag{9.27}$$

EN 1993-1-5, §9.2.1(7)

Actually, theoretically correct transformation parameter is $8/\pi^2$ instead of $\pi/4$, but the difference is only 3%.

In the presence of axial force $N_{st,Ed}$ the second order analysis should be performed even if w is taken as $b/300$.



a) Double sided stiffener

b) Single sided stiffener

Figure 9.6: Transverse stiffener under general loading conditions

This general approach is easily applicable to the first two cases where only longitudinal axial force in the adjacent panels (first case) and in addition axial force in the stiffeners (second case) are present. For the first case for instance $q_{dev,eq}$ may be calculated from (9.22) by taking $w = b/300$. From the corresponding bending moments and deflections requirements (9.1) may be checked.

Torsional buckling of stiffeners

When loaded axially, the torsional buckling of transverse stiffeners shall be avoided. Unless more sophisticated analysis is carried out, the following criteria should be satisfied:

$$\sigma_{cr} \geq \theta f_y \tag{9.28}$$

EN 1993-1-5, §9.2.1(9)

where:

σ_{cr} is the elastic critical stress for torsional buckling;

θ is a parameter to ensure class 3 behaviour.

For open cross-section stiffeners having a small warping resistance (e.g. flat or bulb stiffeners) $\theta = 2$ is adopted and (9.28) can be rewritten using standard solution for σ_{cr} :

$$\sigma_{cr} = G \frac{I_t}{I_p} = \frac{E}{2(1+\nu)} \frac{I_t}{I_p} \geq 2f_y \tag{9.29}$$

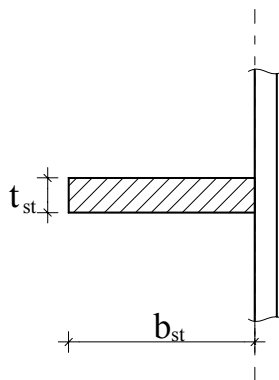
$$\frac{I_t}{I_p} \geq 5,2 \frac{f_y}{E} \tag{9.30}$$

EN 1993-1-5,
§9.2.1(8)

In EN 1993-1-5, condition (9.28) is presented in the form of (9.30) with the constant 5,3 instead of 5,2, where:

I_p is the polar second moment of area of the stiffener alone around the edge fixed to the plate (see Figure 9.7);

I_t is the St. Venant torsional constant of the stiffener alone.



$$I_p = \frac{b_{st}^3 t_{st}}{3} + \frac{t_{st}^3 b_{st}}{12} \approx \frac{b_{st}^3 t_{st}}{3}$$

$$I_t = \frac{b_{st} t_{st}^3}{3}$$

$$\frac{I_t}{I_p} = \left(\frac{t_{st}}{b_{st}} \right)^2 \geq \frac{5,3 f_y}{E}$$

$$\frac{b_{st}}{t_{st}} \leq \sqrt{\frac{E}{5,3 f_y}} = \begin{cases} 13,0 & (S235) \\ 10,5 & (S355) \end{cases}$$

Figure 9.7: Preventing torsional buckling of flat stiffeners

Stiffeners exhibiting a significant warping stiffness (e.g. T, L sections and especially closed section stiffeners) should either fulfil the conservative requirement (9.30) or the basic requirement (9.28) where $\theta = 6$ is recommended. The critical stress for the torsional buckling does not include rotational restraint provided by the plating, but includes the warping stiffness of the stiffener.

$\theta = 2$ corresponds to the plateau of the buckling reduction function up to the relative slenderness 0,7. For flat stiffeners this long plateau, typical for local buckling, can be justified by the fact that torsional buckling of flat stiffeners is very similar to its local buckling. It gives similar criteria as for Class 3 cross sections. $\theta = 6$ corresponds to the plateau length of 0,4, similar to that of lateral-torsional buckling of members (in buildings) with end restraints the influence of which is not explicitly accounted for in the determination of the elastic critical moment.. For the open cross sections with significant warping resistance it is very unlikely that the requirement (9.30) will be fulfilled, unless the cross section is very stocky (b/t of single plate elements less than 9 in the most favourable case) and Saint-Venant torsion becomes important.

σ_{cr} of open cross-sections with warping resistance may be calculated with the well known expression:

$$\sigma_{cr} = \frac{1}{I_p} \left(\frac{\pi^2 EI_w}{l^2} + GI_t \right) \tag{9.31}$$

EN 1993-1-5,
§9.2.1(9)

For rather long stiffeners σ_{cr} calculated according to equation (9.31) also does not guarantee fulfilment of the requirement (9.30), because the contribution from the warping stiffness becomes very small and the contribution of Saint Venant torsion is anyway small.

The possible solution would be to include the plating as a continuous torsional elastic support and treat the stiffener as a compression element attached to this continuous elastic support characterized by the rotational stiffness c_θ (see Figure 9.8). A similar approach has been used for the determination of the critical buckling stress of plates stiffened by one or two stiffeners (EN 1993-1-5, A.2.2).

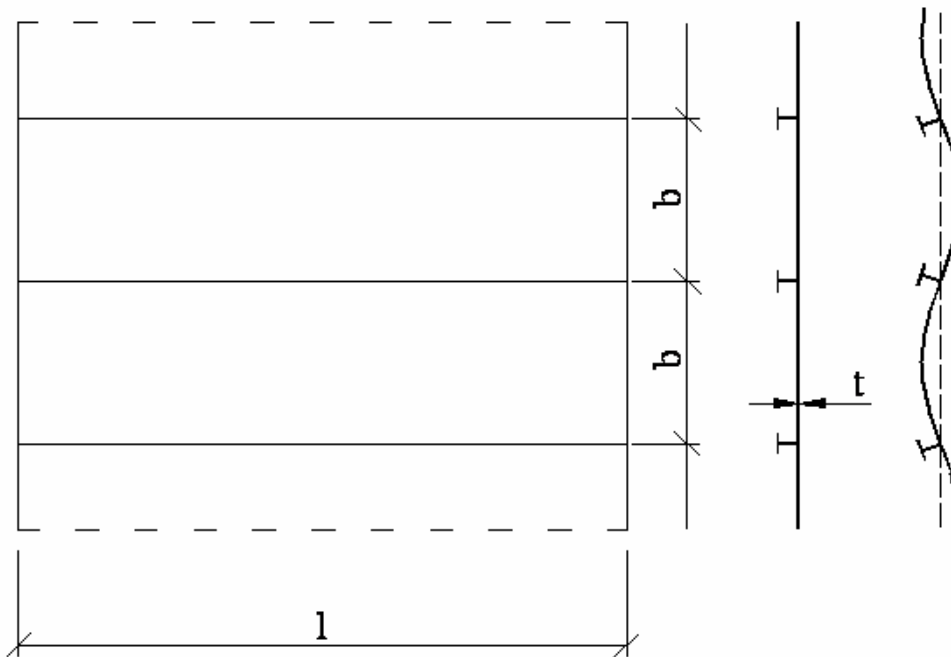


Figure 9.8: Stiffener and plating

An equilibrium differential equation for one of such stiffeners can be written as follows (for elastic material and perfect geometry):

$$EI_w \theta^{IV} + (Ni_p^2 - GI_t) \theta'' = m_\theta = -c_\theta \theta \tag{9.32}$$

or:

$$\theta^{IV} + \omega^2 \theta'' + \alpha^2 \theta = 0 \tag{9.33}$$

where:

- θ torsional rotation;
- I_w warping cross-section constant;
- N compression axial force in the stiffener;
- i_p polar radius of gyration;

$$\omega^2 = \frac{Ni_p^2 - GI_t}{EI_w}$$

c_θ elastic restraint constant.

$$\alpha^2 = \frac{c_\theta}{EI_w}$$

The equation (9.33) can be easily solved by choosing the following expression for the torsional rotation is chosen:

$$\theta = A \sin \frac{m\pi x}{l} \tag{9.34}$$

where m is an arbitrary integer and x is a longitudinal coordinate of the stiffener. Then the critical compression stress $\sigma_{cr} = N_{cr}/A_{st}$ is obtained in the following form:

$$\sigma_{cr} = \frac{1}{I_p} \left(EI_w \frac{m^2 \pi^2}{l^2} + \frac{c_\theta l^2}{m^2 \pi^2} + GI_t \right) \tag{9.35}$$

EN 1993-1-5,
§9.2.1(9)

From the first derivative of σ_{cr} (in respect to m) set to zero, a condition for the minimum value of σ_{cr} is derived:

$$\frac{m^2 \pi^2}{l^2} = \sqrt{\frac{c_\theta}{EI_w}} \tag{9.36}$$

By inserting (9.36) into (9.35) a minimum value of σ_{cr} is obtained:

$$\sigma_{cr-MIN} = \frac{1}{I_p} (2\sqrt{c_\theta EI_w} + GI_t) \tag{9.37}$$

that is valid for long stiffeners, where $m \geq 2$. From (9.36) with $m = 1$ l_{cr} writes:

$$l_{cr} = \pi \sqrt[4]{\frac{EI_w}{c_\theta}} \tag{9.38}$$

For stiffeners longer than l_{cr} equation (9.37) applies and for shorter ones equation (9.35) with $m = 1$ does.

As expected the expression (9.37) is not more dependant on the length of the stiffener l and gives more favourable results than the solution without continuous restraint (expression (9.31)).

For the stiffened plate on Figure 9.8 the elastic restraint constant c_θ is given as:

$$c_\theta = \frac{4EI_{pl}}{b} = \frac{Et^3}{3b} \tag{9.39}$$

For longitudinal stiffeners the effects of the plating can be affected by longitudinal compression stresses in the plate and the elastic restraint constant c_θ should then be reduced accordingly. A reduction by a factor 3 seems to be adequate.

9.2.2 Minimum requirements for longitudinal stiffeners

EN 1993-1-5,
§9.2.2

No additional strength checks are needed because the strength checks of longitudinal stiffeners under direct stresses are included in the design rules for stiffened plates (EN 1993-1-5, Sections 4.5.3 to 4.6).

Requirement (9.28) for preventing torsional buckling also applies to longitudinal stiffeners.

The following limitations should be considered when discontinuous stiffeners do not pass through openings made in transverse stiffeners or are not connected to both sides of the transverse stiffeners:

- to be used only for webs (i.e. not allowed in flanges);
- to be neglected in global analysis;
- to be neglected in the calculation of stresses,
- to be considered in the calculation of the effective^p widths of sub-panels;
- to be considered in the calculation of the critical stresses.

In other words, discontinuous stiffeners should be taken into account only to increase bending stiffness of the stiffened plates and in the calculation of effective widths of sub-panels, but should be excluded from transferring forces from one stiffened panel to another.

It is important that discontinuous stiffeners terminate sufficiently close to the transverse stiffeners to avoid undesirable local failure modes in the plating (Figure 9.9).

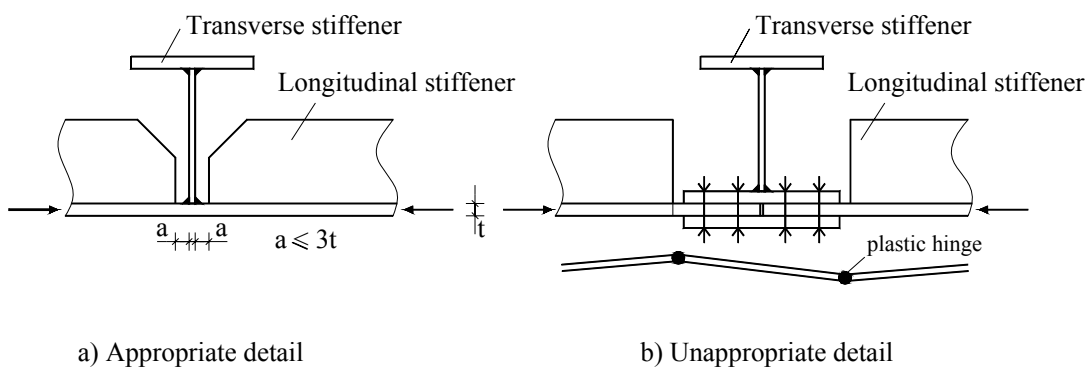


Figure 9.9: Discontinuity of longitudinal stiffener

9.2.3 Splices of plates

When due to design considerations the plate thickness is changed, the transverse welded splice should be sufficiently close to the transverse stiffener so that the effects of eccentricity and welding deformations may be disregarded in the analysis. Therefore the distance *a* of the weld splice from a transverse stiffener should fulfil the requirement given in Figure 9.10. If this condition is not satisfied, detailed account of eccentricity should be taken in the design.

EN 1993-1-5,
§9.2.3

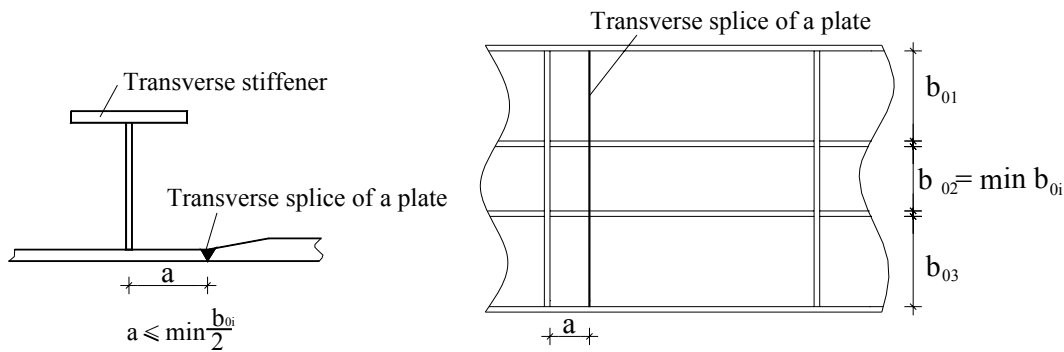


Figure 9.10: Splice of plates

9.2.4 Cut-outs in stiffeners

Cut-outs should be limited in length and depth to prevent plate buckling (Figure 9.11) and to control the net section resistance. In 1971 the well known Koblenz bridge collapsed during the construction due to a very long cut out in the longitudinal stiffeners of the bottom flange of the box girder.

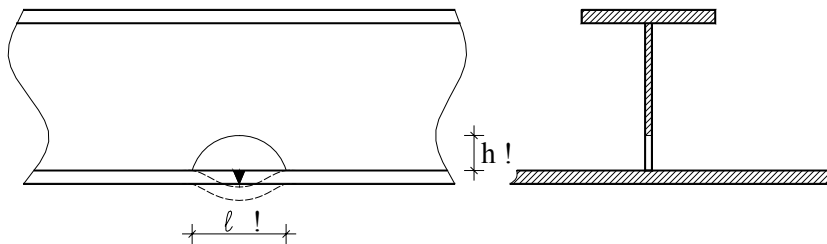


Figure 9.11: Plate buckling at too large cut-out

Detailed rules are given in EN 1993-1-5, Section 9.2.4.

9.3 Shear stresses

9.3.1 Rigid end post

Besides acting as a bearing stiffener resisting the reaction force at the support, a rigid end post should be able to provide adequate anchorage for the longitudinal component of the membrane tension stresses in the web. Anchorage may be provided in different ways, as shown in Figure 9.12. A short I-beam can be formed at the end of the plate girder by providing two double-sided stiffeners or by inserting a hot-rolled section. This short beam resists longitudinal membrane stresses by its bending strength (Figure 9.12a). The other possibility is to limit the length g of the last panel, so that the panel resists shear loading for the non-rigid end post conditions (Figure 9.12b).

EN 1993-1-5, §9.2.4

EN 1993-1-5, §9.3

EN 1993-1-5, §9.3.1

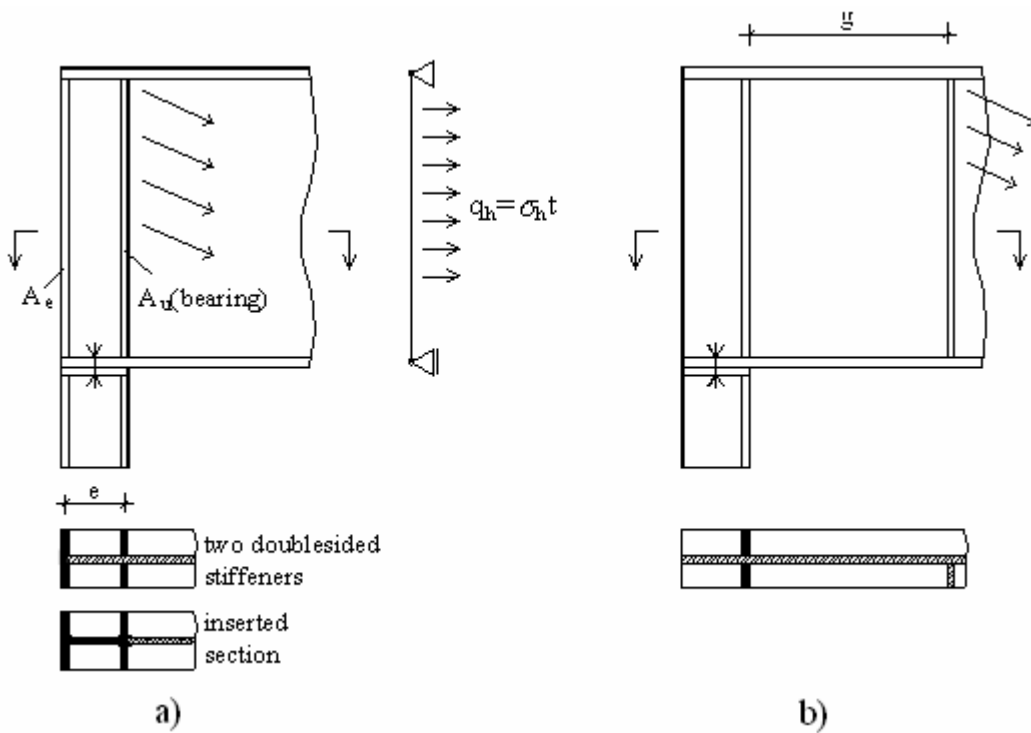


Figure 9.12: End post details

To assure adequate stiffness the centre to centre distance between the stiffeners should be:

$$e > 0,1 \cdot h_w \tag{9.40}$$

The required cross-section A_e of one flange of the short beam is determined from bending demands. Höglund (see 5.4 [3]) showed that the horizontal component of the tension membrane stresses σ_h in the web (see Figure 9.12) for larger slenderness parameters $\bar{\lambda}_w$ (i.e. the range where post buckling behaviour is important) can be approximated as:

$$\frac{\sigma_h}{f_y} = \frac{0,43}{\bar{\lambda}_w} \tag{9.41}$$

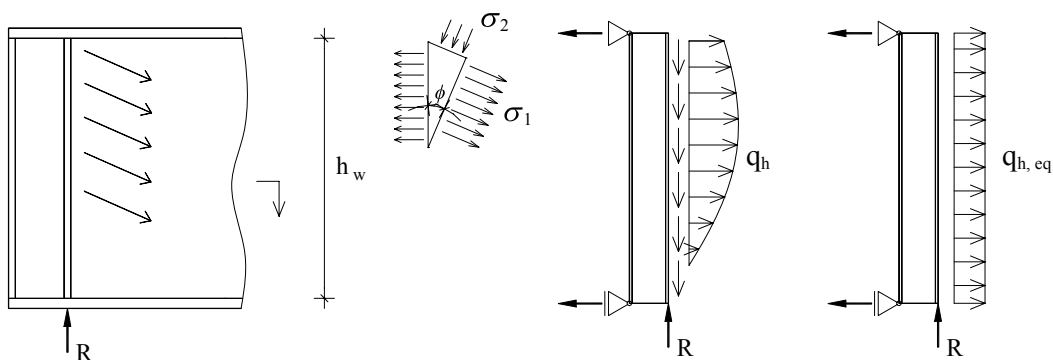


Figure 9.13: Loads on the end post

By inserting (5.15) into (9.41), the upper bound of the horizontal load $q_h = \sigma_h t$ acting on the short beam is obtained as:

$$q_h = 16,1 \frac{f_y t^2 \varepsilon \sqrt{k_\tau}}{h_w} \leq 49 \frac{t^2 f_y}{h_w} \quad (k_{\tau MAX} \approx 9,34, \varepsilon = 1,0) \quad (9.42)$$

Because in reality q_h varies along the depth of the girder and because the theoretical value of σ_h (see (9.41)) is somewhat larger than characteristic values used for design purposes, a smaller equivalent uniformly distributed load $q_{h.eq}$ is chosen in EN 1993-1-5:

$$q_{h.eq} = 32 \frac{t^2 f_y}{h_w} \quad (9.43)$$

With:

$$M_{MAX} = \frac{q_{h.eq} h_w^2}{8}, \quad W = A_e e \quad (9.44)$$

and:

$$\sigma_{MAX} = \frac{M_{MAX}}{W} = \frac{4t^2 f_y h_w^2}{h_w A_e e} \leq f_y \quad (9.45)$$

a requirement for A_e is reached:

$$A_e \geq \frac{4h_w t^2}{e} \quad (9.46)$$

EN 1993-1-5, §9.3.1(3)

The other flange of a short beam with a cross-section A_u should be checked also as a bearing stiffener to carry reaction force R .

9.3.2 Non-rigid end post

EN 1993-1-5, §9.3.2

When design criteria presented in Section 9.3.1 are not fulfilled, the end posts shall be considered as non-rigid. The reduced shear resistance of the end panels shall be calculated accordingly.

Examples of non-rigid end posts are shown in Figure 9.14.

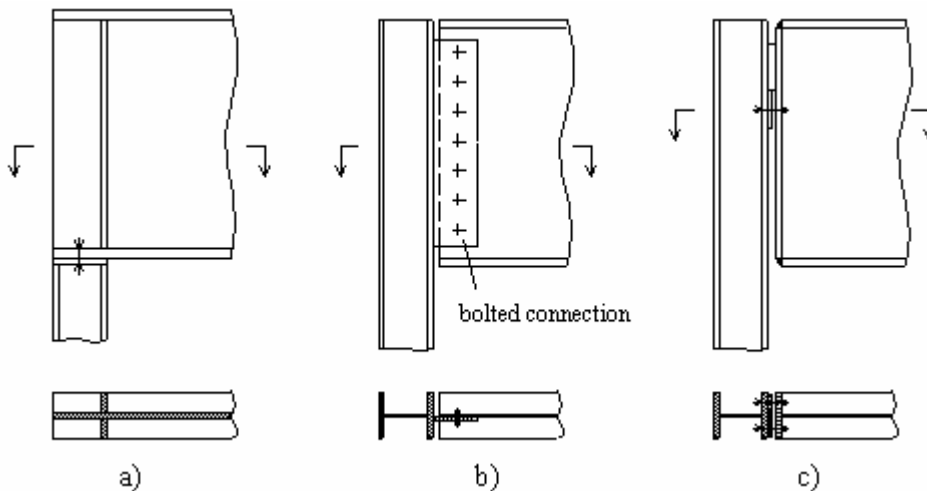


Figure 9.14: Non-rigid end posts

In case a) in Figure 9.14 the stiffener – that should be double-sided – acts as a bearing stiffener.

9.3.3 Intermediate transverse stiffeners

Intermediate transverse stiffeners that act as a rigid support at the boundary of inner web panels shall be checked for strength and stiffness. If the relevant requirements are not met, transverse stiffeners are considered flexible. Their actual stiffness may be considered in the calculation of the shear buckling coefficient k_τ . Annex A.3 of EN 1993-1-5 does not give information for such cases and appropriate design charts or FE eigenvalue analysis has to be used.

Adequate stiffness for an intermediate transverse stiffener being considered rigid is:

$$\begin{aligned}
 I_{st} &\geq 1,5h_w^3 t^3/a^2 & \text{for} & \quad a/h_w < \sqrt{2} \\
 I_{st} &\geq 0,75h_w t^3 & \text{for} & \quad a/h_w \geq \sqrt{2}
 \end{aligned}
 \tag{9.47}$$

Requirements (9.47) assure that at the ultimate shear resistance the lateral deflection of intermediate stiffeners remains small compared with that of the web. They were derived from linear elastic buckling theory but the minimum stiffness was increased from 3 (for long panels) to 10 times (for short panels) to take account of post-buckling behaviour [2]. These requirements are relatively easy to meet and do not impose very strong stiffeners.

The strength is checked for the axial force $N_{st,ten}$ coming from the tension field action in the two adjacent panels (Figure 9.15).

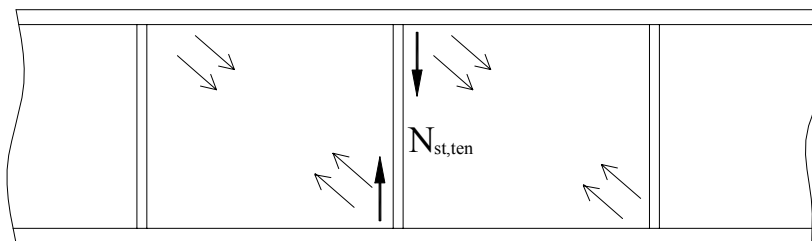


Figure 9.15: Axial force in the intermediate transverse stiffeners

A simplified procedure for the determination of $N_{st,ten}$ is implemented into EN 1993-1-5, Section 9.3.3. The axial force in the stiffener $N_{st,ten}$ is taken as the difference between the shear force V_{Ed} in the panels and the elastic critical shear force carried by the tension field action.

$$N_{st,ten} = V_{Ed} - \frac{1}{\lambda_w^2} \cdot t \cdot h_w \frac{f_{yw}}{\sqrt{3}}
 \tag{9.48}$$

EN 1993-1-5, §9.3.3

EN 1993-1-5, §9.3.3(3)

EN 1993-1-5, §9.3.3(3)

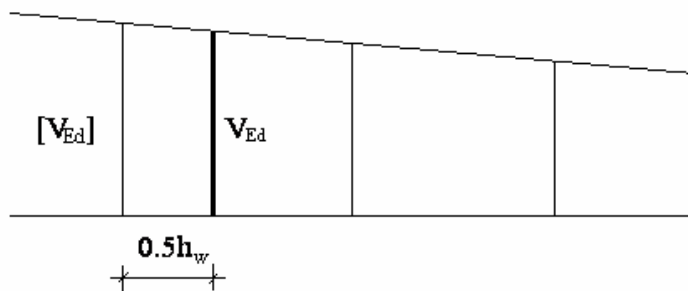


Figure 9.16: Shear force V_{Ed} (intermediate transverse stiffener)

It was shown [3, 4] that axial force $N_{st,ten}$ calculated from equation (9.48) is larger than the actual force induced in the transverse stiffeners, measured in the tests or calculated in numerical simulations. A reduced (“average”) shear force V_{Ed} may be taken at the distance $0,5h_w$ from the edge of the panel with the largest shear force (see Figure 9.16).

If $N_{s,ten}$ is negative, it is taken as 0. $N_{st,ten}$ should be accounted for when satisfying the minimum requirements (9.1) for transverse stiffeners.

Intermediate stiffeners should be checked against buckling in the same way as bearing stiffeners (see Section 9.4 in EN 1993-1-5). If necessary, the axial force $N_{st,ten}$ should be considered when checking transverse stiffeners to resist the deviation forces due to compression in the web (see 9.2.1).

9.3.4 Longitudinal stiffeners

EN 1993-1-5, §9.3.4

No direct strength check is required for the longitudinal stiffeners located in the panels loaded in shear. Their stiffness is taken into consideration in the calculation of k_τ and results in a higher shear resistance. When longitudinal stiffeners are also under the influence of direct stresses, all the necessary checks should be performed (see 9.2). When the web panel is loaded in shear, the influence of longitudinal stiffeners on the design of transverse stiffeners is small and is not included in the design rules for transverse stiffeners given in 9.3.1 to 9.3.3.

9.3.5 Welds

EN 1993-1-5, §9.3.5

Web to flange welds should normally be designed for the average shear flow $v_{Ed} = V_{Ed}/h_w$. When the contribution of flanges to the shear resistance is present, welds should be stronger (full shear plastic strength of the web):

$$\begin{aligned}
 v_{Ed} &= \frac{V_{Ed}}{h_w} && \text{when} && V_{Ed} \leq \chi_w h_w t \frac{f_{yw}}{\sqrt{3}\gamma_{M1}} \\
 v_{Ed} &= \eta \cdot t \frac{f_{yw}}{\sqrt{3}\gamma_{M1}} && \text{when} && V_{Ed} > \chi_w h_w t \frac{f_{yw}}{\sqrt{3}\gamma_{M1}}
 \end{aligned}
 \tag{9.49}$$

EN 1993-1-5, §9.3.5(1)

The second requirement of (9.49) can be relaxed when the state of stress is investigated in detail.

9.4 Transverse loads

When concentrated loads act on one flange of a girder the resistance to patch loading shall be verified (see Section 6). A transverse stiffener shall be provided at the location of concentrated loads if patch loading resistance is exceeded. The out-of-plane buckling resistance of such stiffeners should be checked as shown in Figure 9.17. Due to non-uniform distribution of the axial force along the stiffener, the equivalent buckling length may be taken as $0,75h_w$ if the axial force is considered constant at its maximum value.

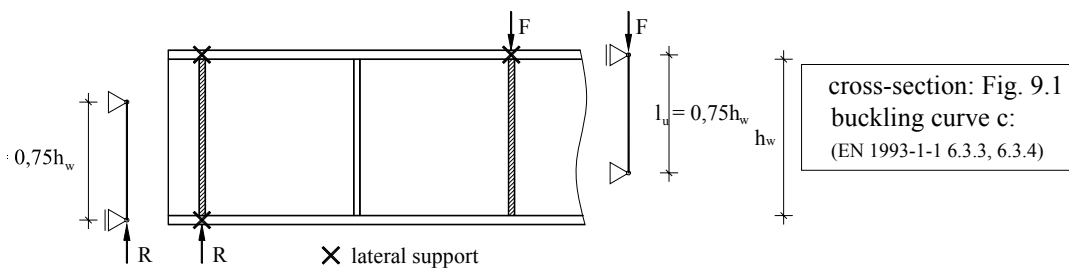


Figure 9.17: Buckling check of transverse stiffener under transverse loading

A longer buckling length l_u should be used for conditions that provide less restraint, i.e. a girder end with an unbraced top flange, top flange braced laterally at some distance from stiffener location or a concentrated load acting at both ends of a stiffener. If stiffeners have cut-outs at the loaded end, their cross-sectional resistance should be checked at that end.

Any eccentricity coming either from one-sided stiffener or from asymmetric stiffener should be accounted for in accordance with 6.3.3 and 6.3.4 of EN 1993-1-1.

9.5 References

- [1] D. Beg, J. Dujc, Eccentric loading on single sided transverse stiffeners, background document DB-C008 to EN 1993-1-5, 2005.
- [2] Kerensky O. A., Flint A. R. & Brown W. C., The basis for design of beams and plate girders in the revised British Standard 153, Proceedings of the Institution of Civil Engineers, August, 1956.
- [3] Private communications with T. Höglund, 2005.
- [4] M. Xie, J.C. Chapman, Design of web stiffeners: axial forces, Journal of Constructional Steel Research, Vol 59, pp.1035-1056, 2003.

10 The reduced stress method

Gerhard Sedlacek, Christian Müller, Lehrstuhl für Stahlbau und Leichtmetallbau, RWTH Aachen

EN 1993-1-5,
§10,
Annex B

10.1 Basic procedure

- (1) The basis of the reduced stress method is the design load F_{Ed} , for which the amplification factor α_u is needed to reach the characteristic value of the ultimate resistance F_{Rk} .
- (2) This amplification factor is obtained from:

$$\alpha_u = \rho \alpha_{ult,k} \quad (10.1)$$

where $\alpha_{ult,k}$ is the minimum load amplifier to reach the characteristic value of resistance without taking into account the out-of-plane instability;

ρ is the plate buckling reduction factor depending on the plate slenderness $\bar{\lambda}$ to take account of out-of-plane buckling.

- (3) The verification reads:

$$\frac{F_{Ed}}{F_{Rd}} = \frac{F_{Ed}}{\rho \frac{\alpha_{ult,k} F_{Ed}}{\gamma_{M1}}} \leq 1 \quad (10.2)$$

or:

$$\frac{\rho \alpha_{ult,k}}{\gamma_{M1}} \geq 1 \quad (10.3)$$

- (4) The plate buckling reduction factor is obtained in the following way:

a) From $\alpha_{ult,k}$, which may be obtained from the Mises criterion:

$$\frac{1}{\alpha_{ult,k}^2} = \left(\frac{\sigma_{x,Ed}}{f_y} \right)^2 + \left(\frac{\sigma_{z,Ed}}{f_y} \right)^2 - \left(\frac{\sigma_{x,Ed}}{f_y} \right) \left(\frac{\sigma_{z,Ed}}{f_y} \right) + 3 \left(\frac{\tau_{Ed}}{f_y} \right)^2 \quad (10.4)$$

and from α_{crit} , which is the minimum amplifier for the design loads to reach the elastic critical load F_{crit} of the plate, the slenderness rate:

$$\bar{\lambda} = \sqrt{\frac{F_{Rk}}{F_{crit}}} = \sqrt{\frac{\alpha_{ult,k}}{\alpha_{crit}}} \quad (10.5)$$

is determined.

b) The relevant plate buckling reduction factor ρ may be obtained as:

- either ρ_{\min} as the the minimum of ρ_{cx} , ρ_{cz} or χ_v

where ρ_{cx} is the plate buckling factor for $\bar{\lambda}$ taking account of the interaction between plate like behaviour and column like behaviour in the direction of σ_x ;

ρ_{cz} is the plate buckling factor for $\bar{\lambda}$ taking account of the interaction between plate like behaviour and column like behaviour in the direction of σ_z ;

χ_v is the plate buckling factor for $\bar{\lambda}$ for shear stresses.

Where the Mises criterion is used for $\alpha_{ult,k}$, this procedure would lead to the verification formula:

$$\left(\frac{\sigma_{x,Ed}}{f_y/\gamma_{M1}}\right)^2 + \left(\frac{\sigma_{z,Ed}}{f_y/\gamma_{M1}}\right)^2 - \left(\frac{\sigma_{x,Ed}}{f_y/\gamma_{M1}}\right)\left(\frac{\sigma_{z,Ed}}{f_y/\gamma_{M1}}\right) + 3\left(\frac{\tau_{Ed}}{f_y/\gamma_{M1}}\right)^2 \leq \rho_{\min}^2 \quad (10.6)$$

- or by an appropriate interpolation between ρ_{cx} , ρ_{cz} and χ_v .

Where the Mises criterion is used for the interpolation, this would lead to:

$$\left(\frac{\sigma_{x,Ed}}{\rho_{cx} f_y/\gamma_{M1}}\right)^2 + \left(\frac{\sigma_{z,Ed}}{\rho_{cz} f_y/\gamma_{M1}}\right)^2 - \left(\frac{\sigma_{x,Ed}}{\rho_{cx} f_y/\gamma_{M1}}\right)\left(\frac{\sigma_{z,Ed}}{\rho_{cz} f_y/\gamma_{M1}}\right) + 3\left(\frac{\tau_{Ed}}{\chi_v f_y/\gamma_{M1}}\right)^2 \leq 1 \quad (10.7)$$

(5) The interaction between plate like behaviour and column like behaviour can be performed for both the directions x and z in the following way:

$$\rho_{cx} = (\rho_p - \chi_{cx}) \xi_x (2 - \xi_x) + \chi_{cx} \quad (10.8)$$

$$\rho_{cz} = (\rho_p - \chi_{cz}) \xi_z (2 - \xi_z) + \chi_{cz} \quad (10.9)$$

where $\xi_x = \frac{\alpha_{crit}}{\alpha_{c,crit,x}} - 1$ but $0 \leq \xi_x \leq 1$

$\xi_z = \frac{\alpha_{crit}}{\alpha_{c,crit,z}} - 1$ but $0 \leq \xi_z \leq 1$

$\alpha_{c,crit,x}$ is the amplifier for column like buckling of the plate in direction x;

$\alpha_{c,crit,z}$ is the amplifier for column like buckling of the plate in direction z.

(6) The values $\alpha_{c,crit}$ can be determined for the design load F_{Ed} by using a plate model with free edges along the directions x and z. In case of multiple plate fields continuous over transverse stiffeners point supports at the edges can be provided where transverse stiffeners are connected.

(7) Figure 10.1 shows the interaction between plate-like and column-like behaviour.

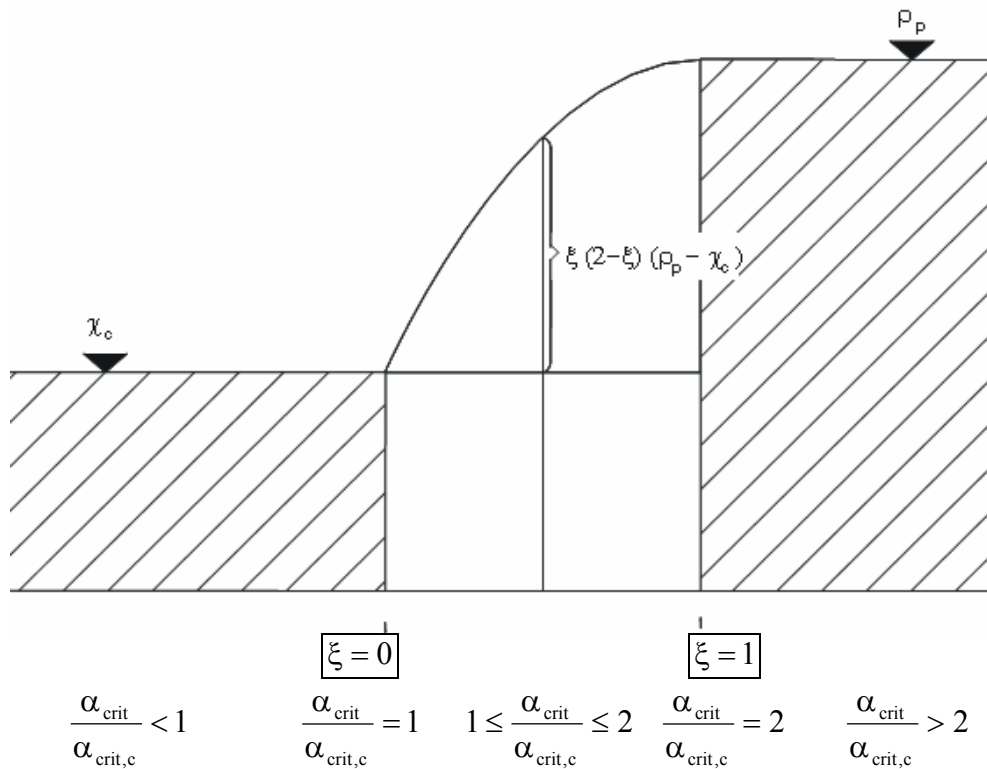


Figure 10.1: Interaction between plate like and column like behaviour

10.2 Modification of plate buckling curves

- (1) In order to simplify the choice of the relevant plate buckling curve ρ_p or χ_v the various analytical expressions given in EN 1993-1-5, see Table 10.1, can be harmonised.

Table 10.1: Plate buckling curves acc. to EN 1993-1-5

Plate buckling for σ_{Ed}		
$\rho = \frac{\bar{\lambda} - 0,055(3 + \psi)}{\bar{\lambda}^2}$		$\rho = \frac{\bar{\lambda} - 0,188}{\bar{\lambda}^2}$
Shear buckling for τ_{Ed}		
	stiff end stiffeners	flexible end stiffeners
$\bar{\lambda} < 0,83/\eta$	$\chi_w = \eta$	$\chi_w = \eta$
$0,83/\eta \leq \bar{\lambda} < 1,08$	$\chi_w = 0,83/\bar{\lambda}$	$\chi_w = 0,83/\bar{\lambda}$
$\bar{\lambda} \geq 1,08$	$\chi_w = 1,37 / (0,7 + \bar{\lambda})$	$\chi_w = 0,83/\bar{\lambda}$
$1,0 \leq \eta \leq 1,2$		

- (2) This harmonisation follows the way how the column buckling curves have been derived, see Table 10.2.

Table 10.2: Derivation of plate buckling curve acc. to EN 1993-1-5, Annex B

	Column buckling curve	Plate buckling curve
Ayrton-Perry approach	$(1 - \chi_c)(1 - \chi_c \bar{\lambda}_c^2) = \alpha_c (\bar{\lambda}_c - \bar{\lambda}_{c0}) \chi_c$	$(1 - \rho_p)(1 - \rho_p \bar{\lambda}_p) = \alpha_p (\bar{\lambda}_p - \bar{\lambda}_{p0}) \rho_p$
Reduction factor	$\chi_c = \frac{1}{\Phi_c + \sqrt{\Phi_c^2 - \bar{\lambda}_c^2}}$ with $\Phi_c = \frac{1}{2} (1 + \alpha_c (\bar{\lambda}_c - \bar{\lambda}_{c0}) + \bar{\lambda}_c^2)$	$\rho_p = \frac{1}{\Phi_p + \sqrt{\Phi_p^2 - \bar{\lambda}_p}}$ with $\Phi_p = \frac{1}{2} (1 + \alpha_p (\bar{\lambda}_p - \bar{\lambda}_{p0}) + \bar{\lambda}_p)$

(3) The values for α_p and $\bar{\lambda}_{p0}$ proposed in EN 1993-1-5, Annex B are given in Table 10.3.

Table 10.3: α_p and $\bar{\lambda}_{p0}$ for plate buckling curve acc. to EN 1993-1-5, Annex B

Product	predominant buckling mode	α_p	$\bar{\lambda}_{p0}$
hot rolled	direct stress for $\psi \geq 0$	0,13 (curve a ₀)	0,70
	direct stress for $\psi < 0$		0,80
	shear transverse stress		
welded and cold formed	direct stress for $\psi \geq 0$	0,34 (curve b)	0,70
	direct stress for $\psi < 0$		0,80
	shear transverse stress		

- (4) Best fit for plate buckling for $E_d(\sigma_x, \sigma_z, \tau)$ is reached for plated girders that are welded, where $\alpha_p = 0,34$ and $\bar{\lambda}_{p0} = 0,8$ (curve b).
- (5) In the following justifications for using this modified unique plate buckling curve are presented.

10.3 Justification of the procedure

10.3.1 Stiffened panels with a stress field $\sigma_{x,Ed}$

- (1) For a panel with longitudinal stiffeners and a stress field $E_d = \sigma_{x,Ed}$ as given in Figure 10.2 a comparison between the plate buckling curve and test results shows the conservatism of the procedure.

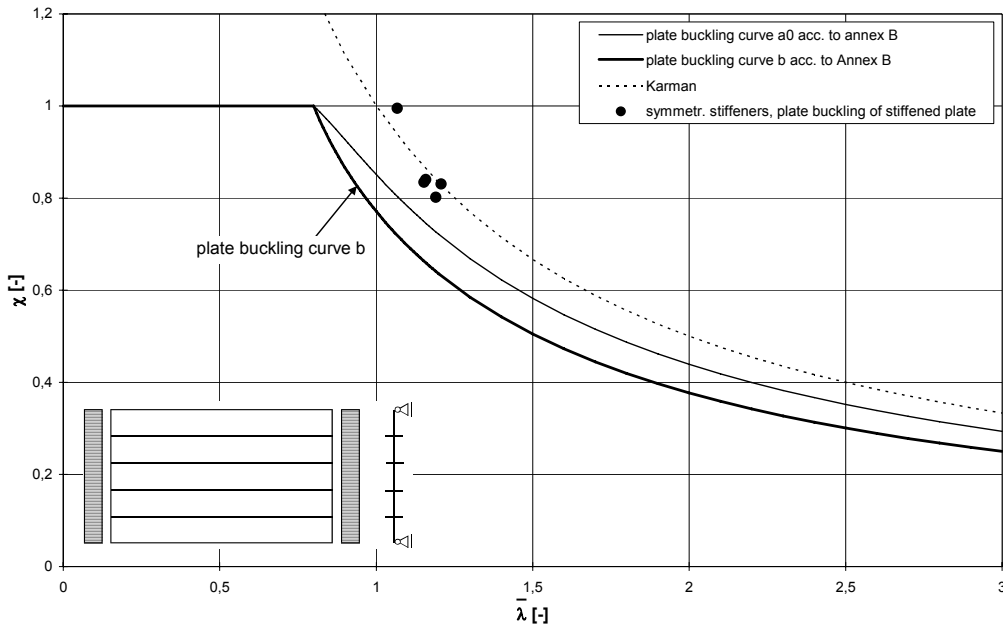
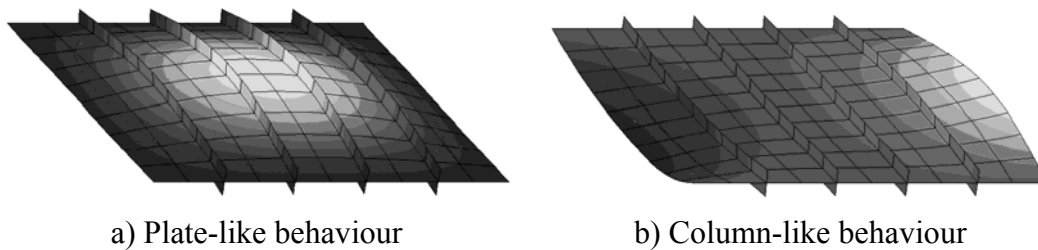


Figure 10.2: Panel with longitudinal stiffeners

- (2) For that case the different eigenmodes for α_{crit} (plate-like behaviour) and $\alpha_{crit,c}$ (column-like behaviour) may be taken from Figure 10.3.



a) Plate-like behaviour

b) Column-like behaviour

Figure 10.3: Plate like and column like behaviour

10.3.2 Unstiffened and stiffened panels with stress fields $\sigma_{x,Ed}$, $\sigma_{z,Ed}$ and τ_{Ed}

- (1) For test beams as shown in Figure 10.4 various test results are compared with the plate buckling curves.

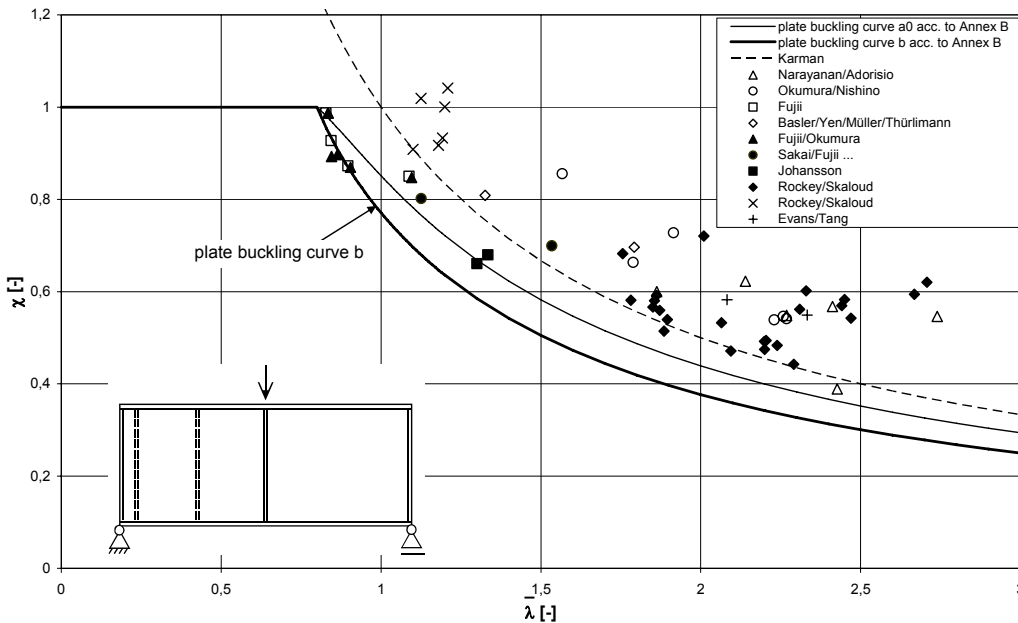


Figure 10.4: Plate buckling under shear stresses and longitudinal stresses

- (2) The eigenmodes for stiff end stiffeners, stiff end stiffeners together with transverse stiffeners and flexible end stiffeners are given Figure 10.5.

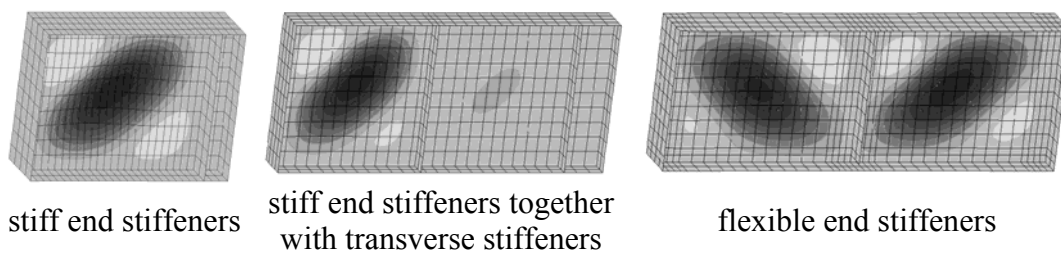


Figure 10.5: Eigenmodes under shear stresses and longitudinal stresses

(3) Table 10.4 gives the γ_M -values determined from the test evaluation.

Table 10.4: Safety evaluation for buckling under shear stresses and longitudinal stresses

Input data					
$v_{rt} = 0,08$ (geometry and yield strength)					
$v_{fy} = 0,07$ (yield strength)					
Results					
Standardnormal distribution			log-normal distribution		
$\bar{b} = 1,141$		$s_\delta = 0,088$	$\bar{b} = 1,154$		$s_\delta = 0,101$
$v_\delta = 0,0769$ (model)		$v_R = 0,1110$ (total)		$v_\delta = 0,0875$ (model)	
$\gamma_M = 1,234$	$\Delta k = 0,918$	$\gamma_M^* = 1,133$		$\gamma_M = 1,180$	$\Delta k = 0,918$
			$\gamma_M^* = 1,084$		

10.3.3 Unstiffened panels with stress fields from patch loading

(1) For patch loading situations as given in Figure 10.6 the comparison between the plate buckling curve and test results may be taken from Figure 10.7.

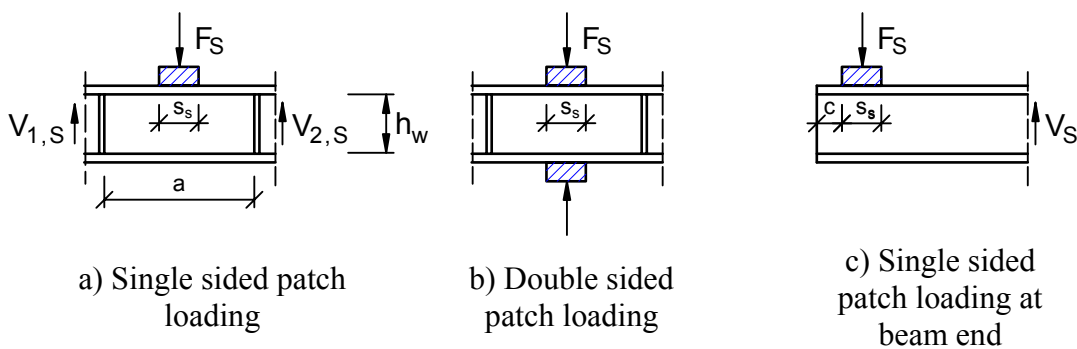


Figure 10.6: Patch loading for different loading situations

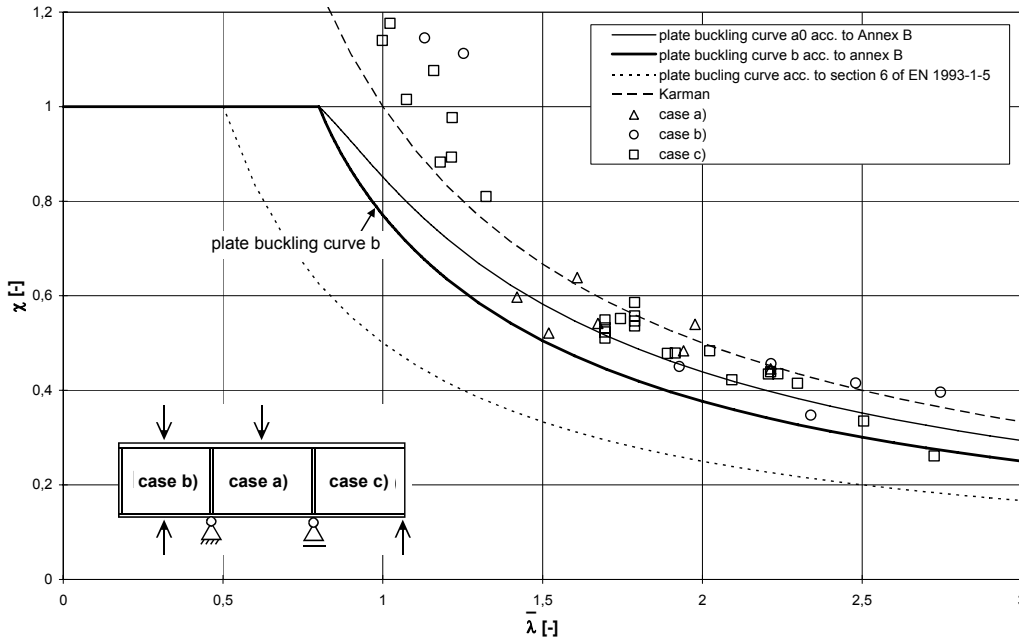


Figure 10.7: Plate buckling under patch loading for cases a), b) and c) of Figure 10.6

(2) γ_M -factors for these cases are given in Table 10.5.

Table 10.5: Safety evaluation for buckling under patch loading

Input values			
$v_{rt} = 0,08$ (geometry und yield strength)			
$v_{fy} = 0,07$ (yield strength)			
Results			
Standardnormal distribution		log-normal distribution	
Common evaluation of the tests for three type of patch loading			
$\bar{b} = 1,298$	$s_\delta = 0,157$	$\bar{b} = 1,305$	$s_\delta = 0,168$
$v_\delta = 0,1201$ (model)	$v_R = 0,1451$ (total)	$v_\delta = 0,1291$ (model)	$v_R = 0,1519$ (total)
$\gamma_M = 1,363$	$\Delta k = 0,856$	$\gamma_M^* = 1,167$	$\gamma_M^* = 1,064$

(3) To check the situation for slender beams with great depths not included in the tests Figure 10.8 gives a comparison between the results of a FEM-

analysis using geometrical and material non linearities and imperfections and the use of the reduced stress method.

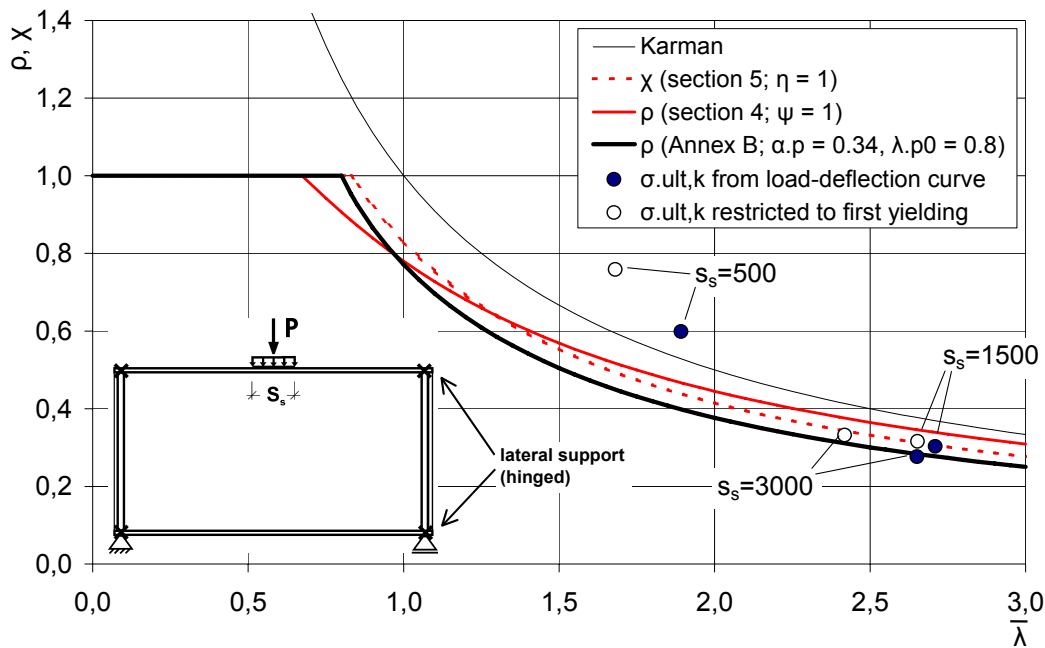


Figure 10.8: Patch loading of slender webs

10.3.4 Stiffened panels with stress field from patch loading

- (1) For the situation given in Figure 10.9 a comparison between the results from a FEM-analysis using geometrical and material non linearities and imperfections and the use of the reduced stress method are shown in Figure 10.10.

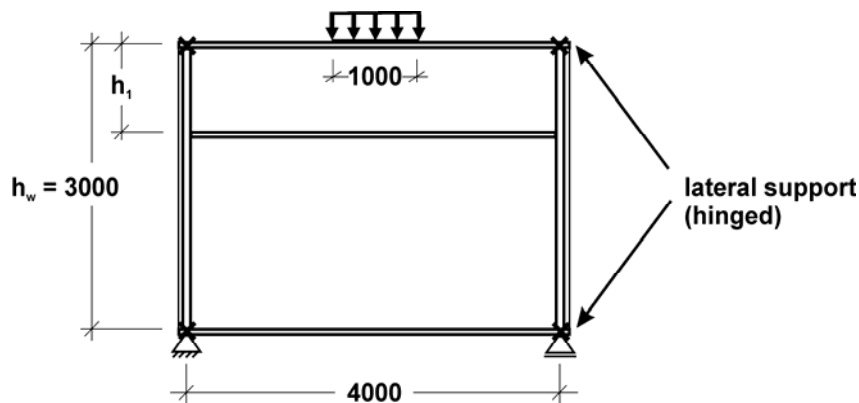


Figure 10.9: Patch loading situation of a stiffened plate

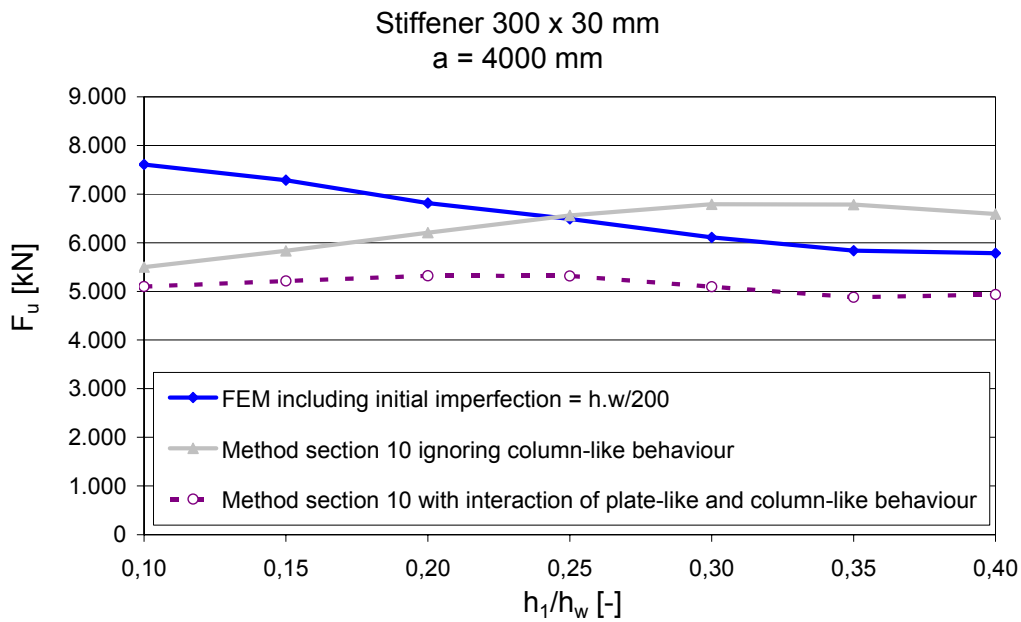


Figure 10.10: Patch loading of a stiffened plate

10.3.5 Unstiffened panels with stress field for patch loading, bending and shear

(1) For beams given in Figure 10.11 which were subjected to combined patch loading, bending and shear the plate buckling modes are given in Figure 10.12 and the γ_M -values in Table 10.6. α_u has been derived by Finite Element analysis and the plastic resistance for patch loading is different from the plastic resistance according to EN 1993-1-5, section 6.

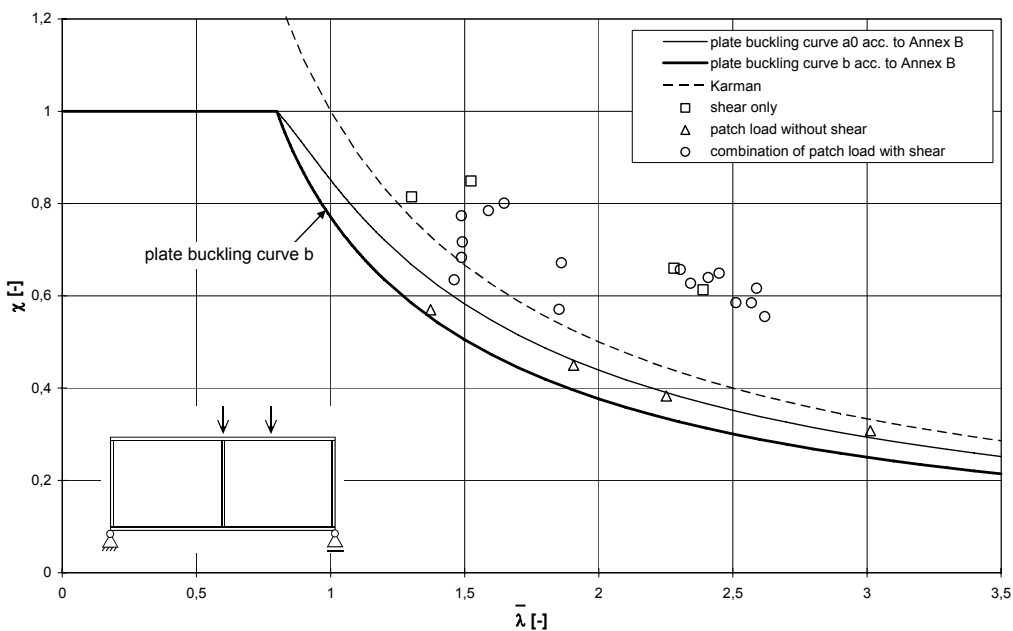


Figure 10.11: Patch loading, bending and shear

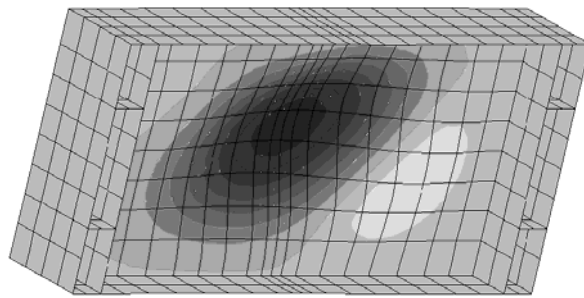


Figure 10.12: Plate buckling mode under combined patch loading, bending and shear

Table 10.6: Safety evaluation for buckling combined patch loading, bending and shear

Input data					
$v_{rt} = 0,08$ (geometry und yield strength)					
$v_{fy} = 0,07$ (yield strength)					
Results					
Standardnormal distribution			log-normal distribution		
1. Evaluation for N = 24					
$\bar{b} = 1,445$		$s_{\delta} = 0,235$		$\bar{b} = 1,522$	
$v_{\delta} = 0,1629$ (model)		$v_R = 0,1815$ (total)		$v_{\delta} = 0,2105$ (model)	
$\gamma_M = 1,623$		$\Delta k = 0,827$		$\gamma_M^* = 1,343$	
$\gamma_M = 1,387$		$\Delta k = 0,848$		$\gamma_M^* = 1,176$	
2. Evaluation for N > 30					
$\gamma_M = 1,567$		$\Delta k = 0,822$		$\gamma_M^* = 1,288$	
$\gamma_M = 1,365$		$\Delta k = 0,841$		$\gamma_M^* = 1,148$	

10.3.6 Concluding comparison of test and calculation results

- (1) The ratios r_e/r_t of test results and calculation results versus the slenderness rate $\bar{\lambda}$ are given in Figure 10.13.

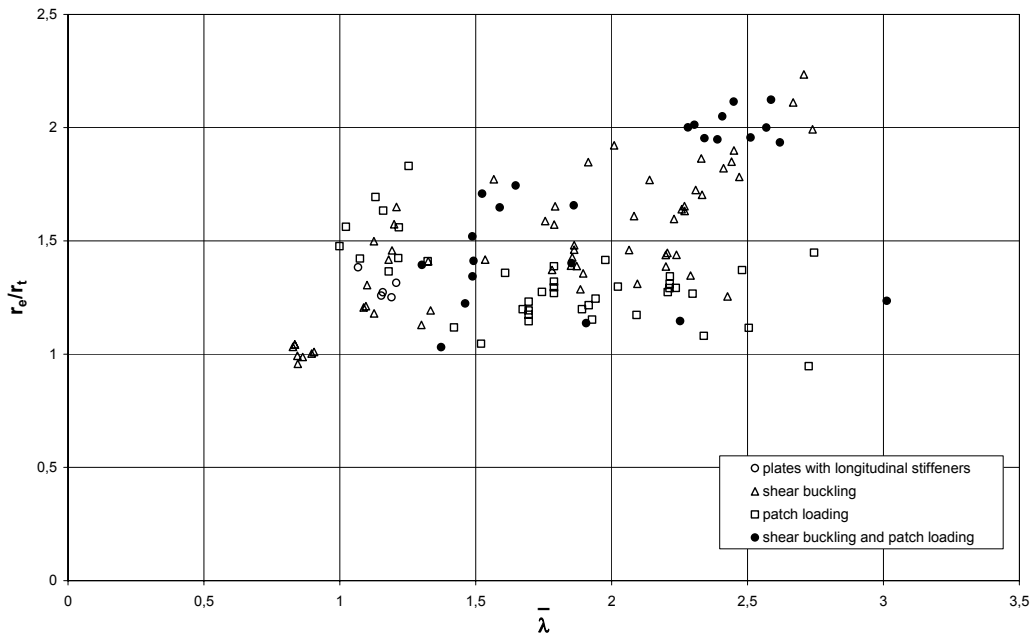


Figure 10.13: Sensivity diagram for all tests on plated structures examined

(2) Table 10.7 shows the γ_M -value from the evaluation of all tests on plated structures examined.

Table 10.7: Safety evaluation for all tests on plated structures examined

Input data					
$v_{rt} = 0,08$ (geometry und yield strength)					
$v_{fy} = 0,07$ (yield strength)					
Results					
Standardnormal distribution			log-normal distribution		
$\bar{b} = 1,195$		$s_\delta = 0,106$		$\bar{b} = 1,221$	
$v_\delta = 0,0888$ (model)		$v_R = 0,1196$ (total)		$v_\delta = 0,1065$ (model)	
$v_R = 0,1332$ (total)		$\gamma_M = 1,263$		$\Delta k = 0,890$	
$\gamma_M^* = 1,123$		$\gamma_M = 1,204$		$\Delta k = 0,890$	
$\gamma_M^* = 1,123$		$\gamma_M = 1,204$		$\gamma_M^* = 1,072$	

11 Annex A to EN 1993-1-5 – Calculation of critical stresses for stiffened plates

René Maquoi, Department M&S, Université de Liège

11.1 Case of multiple stiffeners

- (1) The determination of the buckling coefficient k_{σ} for longitudinally stiffened plate elements is quite complex. Indeed k_{σ} depends not only on the aspect ratio and the support conditions but also on many other parameters, such as the extensional, flexural and torsional relative cross-sectional properties of the stiffeners (so-called relative because compared to the similar properties of the sole plating) and the location of these stiffeners. Conservatively, the supported edges of plate elements should be supposed to be *simply supported*; only such support conditions are indeed susceptible of enabling the amount of post-critical strength which is implicitly exploited by the design rules of EN 1993-1-5.

EN 1993-1-5, A.1(2)

The calculation of k_{σ} may be conducted in several ways:

- From charts or tables;
- From simplified expressions;
- By using appropriate software or numerical techniques.

Whatever the way, it shall be reminded, as said above, that the equivalent orthotropic plate element with smeared stiffeners is explicitly exploited by the design rules of EN 1993-1-5.

- (2) The so-called buckling charts due to *Klöppel et al* ([3], [4] in section 4.4) are surely the best known and the most widely spread amongst the practitioners. Unfortunately, they contain only a small number of charts established for smeared stiffeners. Moreover, the limits of the graphs make them unpracticable in many situations encountered in practice. Last, the torsional relative rigidity of the stiffeners is disregarded in the *Klöppel* charts.
- (3) For rectangular stiffened plate elements of length a and width b , such that $\alpha = a/b \geq 0,5$, with at least three equally spaced longitudinal stiffeners, the plate buckling coefficient k_{σ} for global buckling of the equivalent orthotropic plate may be approximated from the following expressions deduced from the theory of orthotropic plates:

EN 1993-1-5, A.1(2)

$$k_{\sigma,p} = \frac{2\left((1+\alpha^2)^2 + \gamma - 1\right)}{\alpha^2(\psi + 1)(1 + \delta)} \quad \text{if} \quad \alpha \leq \sqrt[4]{\gamma} \quad (11.1)$$

$$k_{\sigma,p} = \frac{4(1 + \sqrt{\gamma})}{(\psi + 1)(1 + \delta)} \quad \text{if} \quad \alpha > \sqrt[4]{\gamma} \quad (11.2)$$

with:

$$\psi = \frac{\sigma_2}{\sigma_1} \geq 0,5 \quad \text{Extreme stress ratio across the width } b;$$

$\gamma = \frac{\sum I_{sl}}{I_p}$ Relative flexural rigidity of the stiffeners;

$\delta = \frac{\sum A_{sl}}{A_p}$ Extensional relative rigidity of the stiffeners;

σ_1 Larger edge stress;

σ_2 Smaller edge stress;

$\sum I_{sl}$ Sum of the second moment of area of the whole stiffened plate;

I_p Second moment of area of the sole plating for bending out-of-plane
($= bt^3/12(1-\nu^2) = bt^3/10,92$);

$\sum A_{sl}$ Sum of the gross cross-sectional areas of the individual longitudinal stiffeners (without adjacent parts of plating);

A_p Gross area of the plating ($= bt$).

It shall be noticed that this expression reduces to the exact one $k_\sigma = (\alpha + 1/\alpha)^2$ when the plate is not longitudinally stiffened ($A_{sl} = 0$ and $\gamma=1$) and is subjected to uniform compression ($\psi = 1$).

NOTE A quite useful software, designated EBPlate, has been developed by CTICM in the frame of a RFCS research contract, in which several of the authors of the present document have been involved. This software provides critical buckling stresses of rectangular plates with various boundary conditions. It is designed such, that it is possible to suppress local plate buckling; it deals not only with open section stiffeners but also with closed section stiffeners. It will be soon available free of charge on the web site of CTICM (www.cticim.com).

11.2 Case of one or two stiffeners

- (1) The elastic critical plate buckling stress $\sigma_{cr,p}$ may be computed based on the column buckling stress $\sigma_{cr,sl}$ of a stiffener strut on an elastic foundation.
- (2) The *gross* cross-sectional area of this strut is composed of:
 - The gross cross-sectional area $A_{sl,l}$ of the stiffener;
 - The cross-sectional area of adjacent parts of contributive plating
- (3) The adjacent parts of the contributive plating are as follows (Figure 11.1):
 - A proportion $(3-\psi)/(5-\psi)$ of the subpanel width b_1 - where ψ is the extreme stress ratio relative to the plating subpanel in consideration - when the latter is fully in compression;
 - A proportion $0,4$ of the depth \bar{b}_c of the compression zone of the plating subpanel when the direct stress in the latter changes from compression to tension.

EN 1993-1-5,
A.2

EN 1993-1-5,
A.2.1(2)

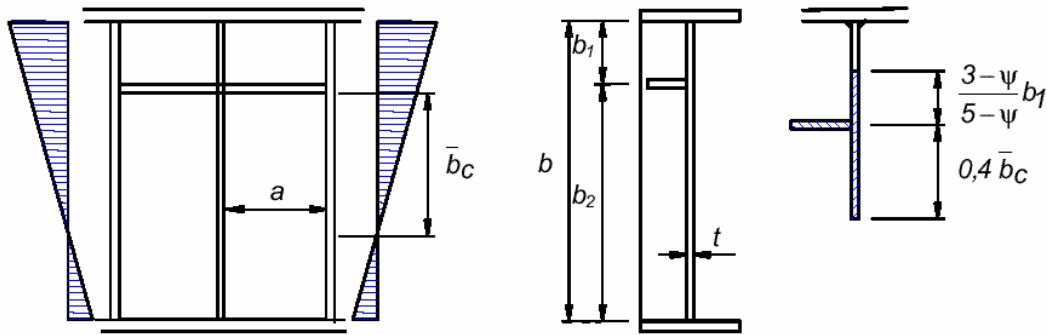


Figure 11.1: Model when a single longitudinal stiffener in the compression zone

- (4) The equilibrium differential equation of a pin-ended strut having a length a , a flexural rigidity $EI_{sl,1}$ and a cross sectional area $A_{sl,1}$, lying on an elastic foundation of rigidity k_f and subjected to an axial force N writes:

$$EI_{sl,1} \frac{d^4 v}{dx^4} + N \frac{d^2 v}{dx^2} + k_f v = 0 \tag{11.3}$$

where N is the axial compression force and v is the buckling deflection. Choosing the latter as composed of m half sine waves of length a/m (Figure 11.2), where m is an integer:

$$v = A \sin(m\pi x / a) \tag{11.4}$$

so as to fulfil the end support conditions, leads to:

$$N_{cr} = \frac{\pi^2 EI_{st}}{a^2} \left(m^2 + \frac{k_f a^4}{m^2 \pi^4 EI_{st}} \right) \tag{11.5}$$

This equation gives the critical load as a function of m , which depends on the properties of both the stiffener and the elastic foundation.

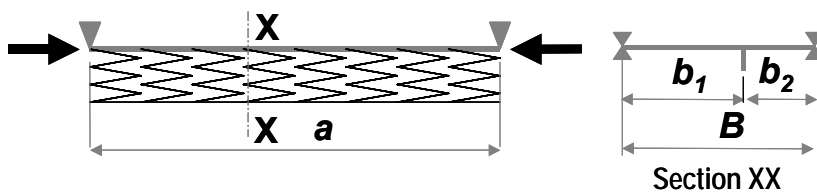


Figure 11.2: Compressed strut supported by an elastic foundation

The rigidity k_f of the elastic foundation provided by the transverse bending of the plating is given as the reciprocal of the transverse displacement of a plating strip of thickness t , unit width and span $(b_1 + b_2)$ subjected to a unit transverse line load considered as the reaction of the stiffener on the plating. It amounts to:

$$k_f = \left[\frac{b_1^2 b_2^2}{3(b_1 + b_2)EI_{plating}} \right]^{-1} = \frac{(b_1 + b_2)Et^3}{3,64 b_1^2 b_2^2} \quad (11.6)$$

When there is no foundation or when the rigidity k_f of the foundation is small, m must be taken equal to 1. This means that the elastic foundation is still sufficiently flexible to enable buckling without an intermediate inflexion point. The critical load is:

$$N_{cr} = \frac{\pi^2 EI_{st}}{a^2} + \frac{Et^3(b_1 + b_2)a^2}{35,92 b_1^2 b_2^2} \quad (11.7)$$

By gradually increasing k_f , one reaches a condition where N becomes smaller for $m = 2$ than for $m = 1$; then the buckled stiffener has an inflection point at the middle. Increasing k_f furthermore leads to more half waves ($m = 3, 4, \dots$) and $(m-1)$ intermediate inflexion points. Then, k_f being given, there is a length \bar{a} which, for each value of the integer m larger than 1, minimises the value of N ; it is drawn from the condition $\partial N/\partial m=0$. The latter gives:

$$\bar{a} = m\pi \sqrt[4]{\frac{EI_{sl,1}}{k_f}} \quad (11.8)$$

Replacing \bar{a} by above expression in the expression of N leads to:

$$N_{cr,min} = 2\sqrt{k_f EI_{sl,1}} = \frac{1,05}{b_1 b_2} E \sqrt{I_{sl,1} t^3 (b_1 + b_2)} \quad (11.9)$$

This minimum value is clearly a constant that is independent of m . It is taken conservatively as the critical load when $m>1$, i.e when $a > a_c$, where a_c is the value of \bar{a} for $m=1$:

$$a_c = 4,33 \sqrt[4]{\frac{I_{sl,1} b_1^2 b_2^2}{(b_1 + b_2)t^3}} \quad (11.10)$$

As a conclusion, it shall be distinguished between two cases: $a_c < a$, where there are indeed several half sine waves ($m>1$) along the length a , and $a_c > a$, where the buckling length is forced to be equal to the length a and $m = 1$. In terms of critical stresses, one has:

$$\text{If } a > a_c \quad \sigma_{cr,sl} = \frac{1,05}{A_{st} b_1 b_2} E \sqrt{I_{sl,1} t^3 (b_1 + b_2)} \quad (11.11)$$

$$\text{If } a < a_c \quad \sigma_{cr,sl} = \frac{\pi^2 EI_{sl,1}}{A_{sl,1} a^2} + \frac{Et^3 (b_1 + b_2)a^2}{35,92 A_{sl,1} b_1^2 b_2^2} \quad (11.12)$$

- (5) The above procedure, fully described for a single stiffener, can be extended to the case of two longitudinal stiffeners in the compression zone as follows (Figure 11.3). Each of these two stiffeners, considered separately, is supposed to buckle while the other one is assumed to be a rigid support; the procedure for one stiffener in the compression zone is thus applied twice

EN 1993-1-5,
A.2.2(1)

EN 1993-1-5,
A.2.2(1)

EN 1993-1-5,
A.2.2(2)

with appropriate values of section properties and distances b_1 and b_2 , designated here b_1^* and b_2^* ; this results in two values of the elastic critical buckling stress designated respectively $\sigma_{cr,sl,I}$ and $\sigma_{cr,sl,II}$.

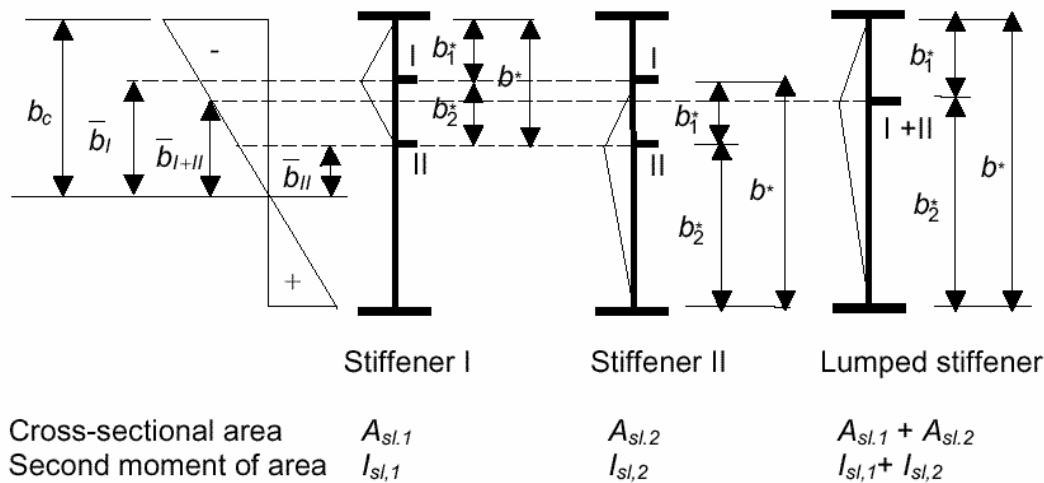


Figure 11.3: Model with two longitudinal stiffeners in the compression zone

Then, as a conservative approach, a fictitious lumped stiffener is substituted for the two individual stiffeners. It is such that:

- Its section properties (cross-sectional area and second moment of area) are the sum of the properties of the individual stiffeners;
- Its location is the point of application of the stress resultant of the respective forces in the individual stiffeners;

That results in a third value of the elastic critical buckling stress, designated $\sigma_{cr,sl,I+II}$.

The use of lumped stiffeners frequently gives over-conservative results (see for instance the worked example in section 17 of the present document). The use of appropriate software, such as EBPlate (see section 11.1), can be used to overcome the problem.

- (6) For consistency with the fibre used as reference for $\sigma_{cr,p}$, which is the edge with the highest compressive stress, the stress $\sigma_{cr,sl}$, which refers to the location of the stiffener in consideration, needs to be extrapolated up to the same edge according to:

$$\sigma_{cr,p} = \sigma_{cr,sl} \frac{b_c}{\bar{b}} \tag{11.13}$$

where b_c is the depth of the compression zone and \bar{b} the location of the above stiffener measured from the fibre where the direct stress vanishes. This fibre is the neutral axis when the girder is subjected to bending only.

- (7) In the case of a single longitudinal stiffener in the compression zone, this formula applies directly with $\bar{b} = \bar{b}_c$ (see Figure 11.1). In the case of two longitudinal stiffeners in this zone, three values $\sigma_{cr,sl,i}$ ($i = I, II, I+II$) are

EN 1993-1-5,
§4.5.3(3)

calculated based on the following pairs of values: $\sigma_{cr,sl,I}$ and $\bar{b} = \bar{b}_I$, $\sigma_{cr,sl,II}$ and $\bar{b} = \bar{b}_{II}$, $\sigma_{cr,sl,I+II}$ and $\bar{b} = \bar{b}_{I+II}$ (see Figure 11.3); the lowest one is kept.

12 Annex C to EN 1993-1-5 – Finite Element Methods of analysis (FEM)

Bernt Johansson, Division of Steel Structures, Luleå University of Technology

Christian Müller, Gerhard Sedlacek, Lehrstuhl für Stahlbau und Leichtmetallbau, RWTH Aachen

12.1 Introduction

The Finite Element Method (FEM) is widely used in design of structures. FEM can be used with different degrees of sophistication for different purposes as indicated in Table 12.1 (Table C.1 of EN 1993-1-5). Most common is linear elastic analysis (1 in Table 12.1) and also geometrically non-linear elastic analysis (4 in Table 12.1) of frames. Such analyses give load effects and together with limiting criteria from codes it forms a design method for structures. These methods are well established for frames using beam elements. The imperfections needed for a non-linear analysis are bow and sway imperfections, which are given in EN 1993-1-1.

EN 1993-1-5,
C.1

Table 12.1: Assumption for FE-methods

No	Material behaviour	Geometric behaviour	Imperfections, see EN 1993-1-5, C.5	Example of use
1	linear	linear	no	elastic shear lag effect, elastic resistance
2	non linear	linear	no	plastic resistance in ULS
3	linear	non linear	no	critical plate buckling load
4	linear	non linear	yes	elastic plate buckling resistance
5	non linear	non linear	yes	elastic-plastic resistance in ULS

In order to deal with plate buckling problems the structure has to be modelled with shell elements or solid elements, which gives models with many more degrees of freedom (DOF) than using beam elements. Non-linear FE simulations (number 5 in Table 12.1) are usually needed in order to describe the behaviour at ULS. Such methods are today used mainly as a research tool. It is fairly time consuming to create a proper model and in cases where instability governs the results may be quite sensitive to the assumed imperfections. Also, the computer power needed for solving large problems used to be a limitation. With modern computers this restriction seems to be disappearing and it is today possible to solve most problems on a PC. Another breakthrough which facilitates use of FEA is object oriented pre-processing and efficient coupling between CAD programs with a pre-processor of computational software. Furthermore, new versions of computational software are more user friendly, with icon based options and very powerful documentation. For this reason it is to be expected that non-linear FE simulations will become a design tool in the near future.

The methods 2 and 3 in Table 12.1 may be used for generating input to the design method described in Annex B. Method 3 is also used to calculate critical stresses of plate element for determining the slenderness parameter used in the conventional design rules.

The rules in EN 1993-1-5 should be seen as a first attempt to codify the use of non linear FEM for design purpose. The rules aim at making design using FEM comparable with the conventional design by formulae concerning reliability. Although some of the content is normative much of text is at the level of guidance. The rules are not as far developed as the rules in the main text of the standard. It is therefore important that the rules are supplemented by the experience and good judgement of the designer.

12.2 Modelling for FE-calculations

As already stated the size of the model (DOF) is frequently a problem and it is of interest to limit its size. One way out is to model only a part of the structure. This requires some care in order to get the boundary conditions correct. If the expected behaviour is symmetric this can be used to model only half the structure and using symmetry boundary conditions. If individual plates forming part of a member are analysed separately the common assumption is hinged support along the edges connected to other plates, which is compatible with conventional design. This assumption requires that the supporting plate does not deform significantly in its plane. For instance, a small edge stiffener of a plate can usually not be modelled as a support but it has to be included in the model as it really is.

At the member level it is usually conservative to neglect continuity and assume hinged ends at supports as far as the resistance is governed by instability. This is also valid in case of interaction between local and global instability.

Another question that is essential for the size of the model is the meshing. A too coarse mesh may lead to unconservative results when local buckling governs. The common way of checking, if experience of similar structures is not available, is to successively refine the mesh until stable results are achieved. However, a too fine mesh increases the numerical errors so there is a limit for how fine the mesh can be made. A rule of thumb for shell elements is that there should be at least six elements in the expected half wavelength of a buckle.

Shell elements are commonly used for modelling plated structures. They usually give accurate enough results if the structure is properly modelled. An example is where essential stresses and gradients occur over the thickness of plate like a concentrated load on a flange. For such a case solid elements may have to be used, at least three over the thickness.

12.3 Choice of software and documentation

A host of software is available on the market and the suitability for different tasks varies. In order to solve non-linear problems properly the following features are of importance:

- Robust solver for solving a system of non-linear equations, for example Riks method (arch-length method);
- A simple way to define initial imperfections (geometrical and structural).

EN 1993-1-5,
C.3

EN 1993-1-5,
C.2

It is essential that the simulations are properly documented. In principle all information necessary for reproducing the simulation should be available in the documentation. It is also important that the results are reviewed by an experienced designer who should check that they are reasonable. A good advice is to compare results with approximate analytical methods that create upper and lower bounds of a solution.

12.4 Use of imperfections

12.4.1 Geometrical imperfections

The model has to include imperfections corresponding to the most likely instability modes. For plated structures the imperfections can be either local or global. Local imperfections are buckles in a plate or twist of a flange or stiffener. Global imperfections or bow imperfections consist of a bow deformation of a stiffener or the whole member. The imperfections guide the subsequent deformation and they should be directed such that the worst case is achieved. This means that it is sometimes necessary to check different directions of imperfections for unsymmetric plates.

Usually the imperfections are introduced as eigenmodes that are scaled to a proper magnitude. The critical mode is easily obtained for simple cases. Figure 12.1 shows the case of an I-girder loaded in three point bending; there the web buckling dominates. If the magnitude of the largest web buckle is set to a prescribed design value the whole deformation pattern is defined. Assuming that it is not clear if buckling of the web or the flange is governing, it may be necessary to increase the flange buckle to its design value. This can be done by superposing another eigenmode where the flange buckling dominates. However, this will also change the deformation pattern of the web. An alternative method is rotating the flange without considering the compatibility with the web.

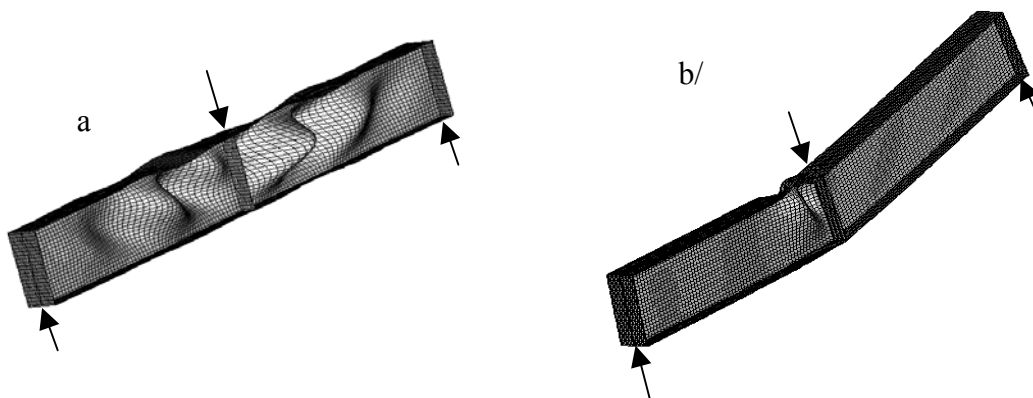


Figure 12.1: a/ Initial deformation of a beam loaded in three point bending, b/ failure mode

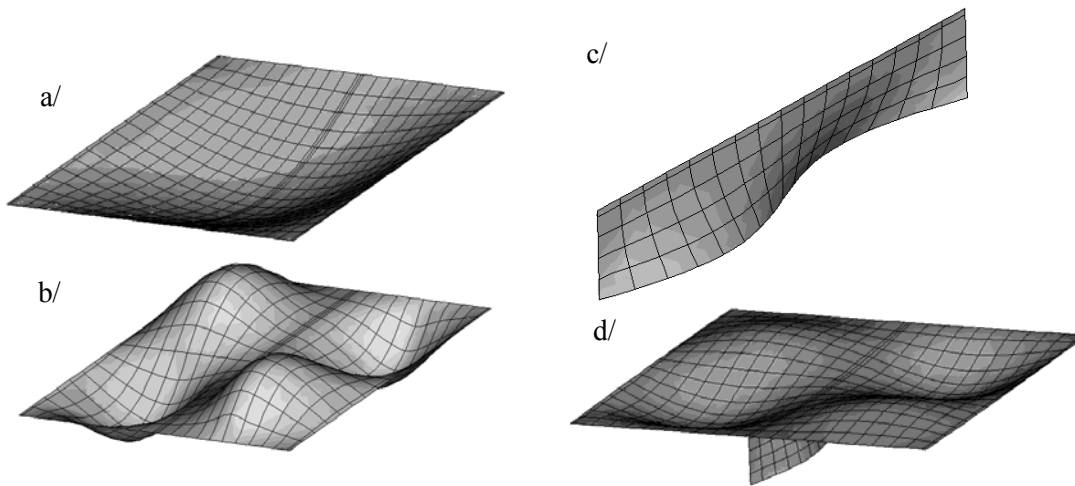
If there are many elements in the structure that may suffer instability, this method becomes inconvenient. It may very well happen that some relevant eigenmode will have a very high modal number and will be hard to find. It may be simpler to use the pre-knowledge of what are the possible instability modes and to use a sine function shape of initial deformation. This approach makes it possible to choose the amplitude of the deformation of each plate element individually.

EN 1993-1-5,
C.5

An example of a longitudinally stiffened plate is shown in Figure 12.2. It includes three components of imperfections. Figure 12.2a shows the global bow imperfection of the stiffener and the plate deformation that is a consequence of the stiffeners deformation. Figure 12.2b shows the local plate deformation, which in this case is two half waves in the longitudinal direction and a nodal line along the stiffener. The number in the longitudinal direction should be chosen to fit the length of the plate. Figure 12.2c shows the initial local deformation of the stiffener. It is shown as compatible with the plate deformation but it may also be chosen independently. Figure 12.2d shows all the initial deformations added together.

The global imperfection of longitudinal stiffeners require some care. If the distance between transverse stiffeners is long and the plate is narrow it is possible that the global buckling of the stiffener will take place in two or more half-waves. The assumed imperfection should have the correct number of half-waves. This may be found by analysis of eigenmodes and the one giving the lowest critical load is the most likely one. The amplitude should be a fraction of the length of the half-wave rather than the total length.

The magnitude of the initial deformations is often taken as the tolerance limits for fabrication. This may seem rational but it is not necessarily the right choice in the context of a probabilistic safety concept. The characteristic resistance is intended to be a 5% fractile taking all the scatter of the influencing parameters into account. Assuming that the statistical distribution of the initial deformations were known it would be possible to calculate a design value to be used. Systematic measurements of initial deformations are however rarely published so there is a lack of reliable data. The suggested level of imperfections equal to 0,8 times the tolerance limit is based on engineering judgement. Some justification can be found in a study there the resistance of uniformly compressed plates supported along all edges according to the Winter formula has been compared with computer simulations [1]. It showed that computer simulations taking geometrical imperfections equal to the tolerance $b/250$ and residual compressive stresses $0,2f_y$ in compression into account gave a resistance more than 15% smaller than the Winter formula. In order to get the same resistance as the Winter formula the imperfections had to be reduced considerably. One set of such imperfections was no residual stresses the geometrical imperfection $b/420$; another one is residual stresses in compression $0,1f_y$ and $b/500$. These are more favourable assumptions than the recommendations in EN 1993-1-5. On the other hand the study concerned only a simple case and the recommendations are intended to be general. It is however likely that further studies will lead to improved recommendations.



- a/ global initial deformation of the stiffener
 b/ local initial deformation of the plate.
 c/ local imperfection of the stiffener.
 d/ total initial deformation.

Figure 12.2: Initial deformations of a longitudinally stiffened plate

12.4.2 Residual stresses

Residual stresses are present in most plated structures. They are mainly caused by the welding and it is in most cases impractical to anneal the structure. The magnitude of the residual stresses varies systematically and also randomly. The known systematic variation depends on the heat input or the weld size and has been investigated, see e. g. [2]. There is a substantial scatter in residual stresses from fabrication and this has to be considered when choosing the design values in the same way as discussed in the previous paragraph. The proposal to use mean values is deemed to be reasonable in that context.

Residual stresses are sometimes taken into account by fictitious additional initial deformations as those suggested in Table C.2 of EN 1993-1-5. This does work reasonably well for flexural buckling of a column. For plate buckling it may lead to over-conservative results. The levels of equivalent imperfections given in the code have been chosen to cover the worst case of plate buckling. It is however possible to include the residual stresses in the model with modern FE codes. This is the most adequate way to get their influence correct and in some cases this influence is negligible for slender plates.

EN 1993-1-5,
C.5(2)

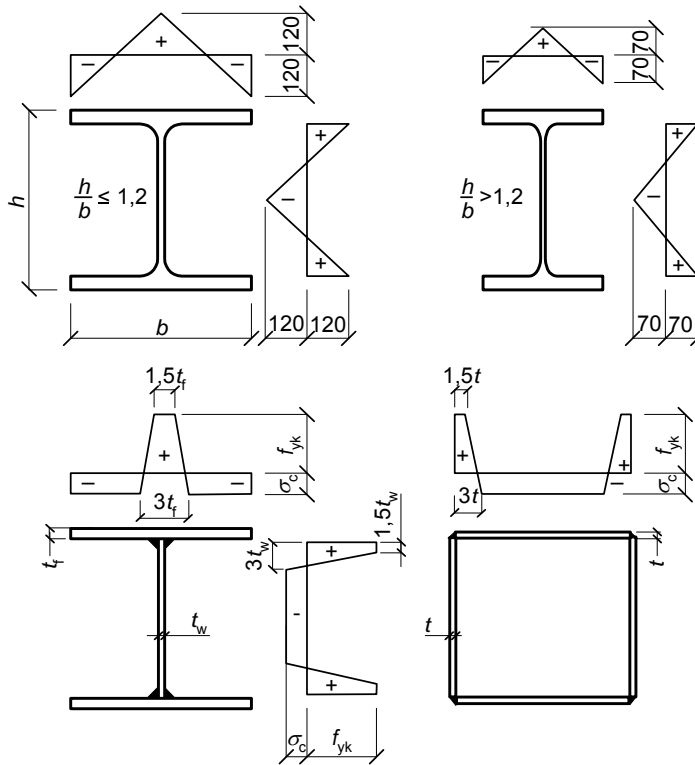


Figure 12.3: Distributions of residual stresses from Swedish design code BSK [3]

Figure 12.3 shows residual stress patterns from [3] for rolled sections and welded sections. For the welded sections the compressive stress σ_c should be determined such that equilibrium with the tensile stresses is achieved for each part of the cross section. Some recent studies have shown that the assumption that the tensile stress is equal to the yield strength tends to overestimate the residual stresses, see summary in [4]. No firm conclusion has been drawn but as a temporary recommendation it is suggested to use 500 MPa as an upper limit even if the actual yield strength is higher.

12.4.3 Combination of imperfections

As mentioned in 12.4.1 taking the magnitude of imperfections equal to the tolerances leads to a too low characteristic resistance. This is even more pronounced in case where several imperfections interact. The combination should be done in a probabilistic manner and the method suggested in EN 1993-1-5 is a first attempt to apply the same method as for load combination. The rule states that one leading imperfection should be taken with full magnitude and the others may be taken as 70% of the full value. The rule should be applied such that one imperfection a time is tried as leading, which means that several combinations have to be investigated.

An application of the rule on simulation of the patch loading resistance of a girder with a longitudinally stiffened web that had been tested has been published in [5]. The elementary imperfections are shown in Figure 12.4 and their magnitudes were chosen according to Table C.2 of EN 1993-1-5. They were realised by loading the panels with a lateral pressure where p_1 was applied to the smaller upper panel, p_2 to lower panel and p_3 as a line load along the stiffener. Table 12.2 shows results

EN 1993-1-5,
C.5(5)

from the simulations and also a comparison with the test result. It is interesting to note that the worst combination almost coincides with the test result and that other combinations show a varying degree of overprediction of the resistance.

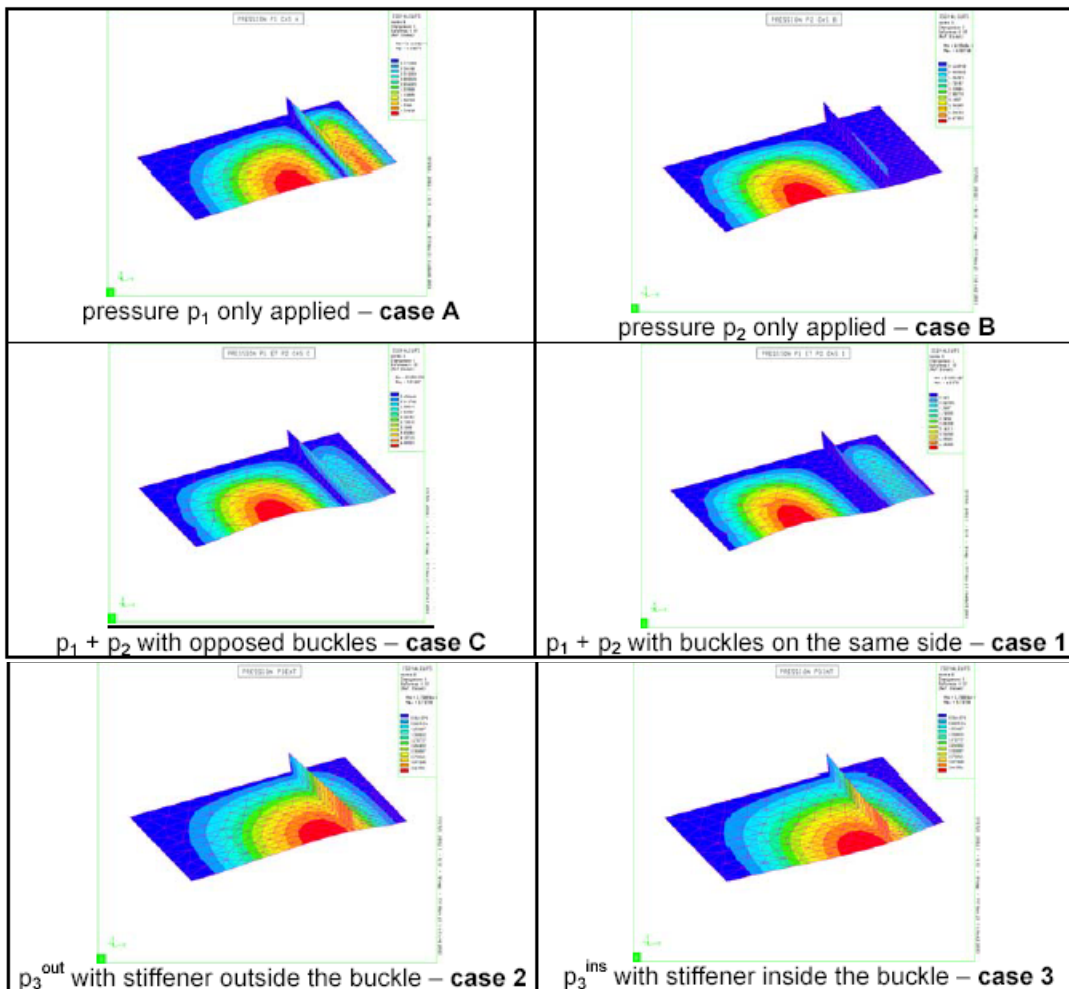


Figure 12.4: Elementary imperfections from study in [5]

Table 12.2: Result of FE-simulations with different combinations of geometric imperfections compared to test result [5]

Case	Description	F_u^{FEM} [kN]	Diff. [%]
0	No geometric imperfection	811.9	+ 12.8
A	p_1 only – upper sub panel – buckle opposed to stiffener	718.6	- 0.2
B	p_2 only – lower sub panel – buckle opposed to stiffener	796.7	+ 10.7
C	$p_1 + p_2$ – initial deformation similar to future collapse	725.8	+ 0.8
D	like case C but initial deformation opposed to the future collapse	738.4	+ 2.6
2	p_3^{out} only - stiffener outside buckle	813.0	+ 12.9
3	p_3^{ins} only – stiffener inside buckle	811.5	+ 12.7
4 (with C)	$(p_1 + p_2) + 0,7 \cdot p_3^{out}$ = case C + 0,7 . case 2	731.2	+ 1.6
5 (with C)	$(p_1 + p_2) + 0,7 \cdot p_3^{ins}$ = case C + 0,7 . case 3	721.0	+ 0.1
6 (with C)	$p_3^{out} + 0,7 \cdot (p_1 + p_2)$ = case 2 + 0,7 . case C	753.0	+ 4.6
7 (with C)	$p_3^{ins} + 0,7 \cdot (p_1 + p_2)$ = case 3 + 0,7 . case C	738.1	+ 2.5
1	$p_1 + p_2$ – upper and lower buckles on the same side of the web	716.9	- 0.4
4 (with 1)	$(p_1 + p_2) + 0,7 \cdot p_3^{out}$ = case 1 + 0,7 . case 2	703.3	- 2.3
5 (with 1)	$(p_1 + p_2) + 0,7 \cdot p_3^{ins}$ = case 1 + 0,7 . case 3	722.4	+ 0.3
6 (with 1)	$p_3^{out} + 0,7 \cdot (p_1 + p_2)$ = case 2 + 0,7 . case 1	892.5	+ 24.0
7 (with 1)	$p_3^{ins} + 0,7 \cdot (p_1 + p_2)$ = case 3 + 0,7 . case 1	746.5	+ 3.7
first mode	first buckling mode	768.5	+ 6.7
exp.	experimental result	720.0	/

12.5 Material properties

EN 1993-1-5,
C.6

First it is worth considering the fact that, in most structural elements with compressive stresses, local buckling will occur, either above or below the yield strength. If it appears after that the yield strength is reached over the whole panel, the strength increase above the plastic is usually small but the local buckling will still limit the deformation capacity. In order to get a model that can manage both stocky and slender plates, the material properties have to be modelled reasonably well. The most commonly used model is based on an incremental theory of plasticity and isotropic hardening. The only input that is needed concerning the material is a uniaxial stress-strain relation.

In Figure C.2 of EN 1993-1-5 some examples of uniaxial stress-strain curves are shown. The alternative a) is the elastic-perfect plastic relation that is frequently used in theoretical studies of steel structures. It can be used in cases like column buckling where the primary stresses and the secondary stresses due to instability have the same direction and the strains at failure are small. The horizontal plateau may cause numerical problems when used in FE-simulations. The alternative b) with nominal slope of the plateau can be used to solve such problems.

In model a) and b) the yield plateau is modelled with continuous strains. The actual material behaviour is however discontinuous and the plateau is caused by narrow Lüders-bands propagating through the material. The material is accordingly in either an elastic state or a strain hardening state. This does not matter when the secondary stresses due to buckling have the same direction as the primary stresses but for plate buckling it may have implications. In plate buckling the secondary stresses caused by buckling include bending stresses in both directions of the plate and shear stresses. The state of stress is biaxial and the Lüders-strains occur mainly in the direction of the primary strains. The consequence of modelling the yield plateau as continuous is that a plate loses too much of its bending stiffness as soon as yielding from the primary stresses starts. This will result in a prediction of local buckling occurring too early. As there are no material models available that take the discontinuous yielding into account some trick is required. One such trick is to neglect the yield plateau completely as in model c) in Figure C.2. This helps to get the correct resistance but it means also that some deformation capacity is neglected. If redistribution of moments to other parts of the structure is of importance it may be necessary to add some artificial deformation capacity. However, there is no established method of doing this. If this problem is neglected there is no danger, the results will be conservative. The slope of the strain hardening part of the curve, $E/100$, is reasonable for all steel grades and moderate strains, say smaller than 5%. In most cases this is sufficient for reaching the maximum load when buckling is governing. A precaution to avoid unconservative results could be to apply the suggested limitation of tensile stresses to 5%, see 12.7, also for compression. Another solution is to use the full true stress-strain curve according to alternative d) in Figure C.2.

The assumption of isotropic hardening may in special cases cause problems. It is known that this assumption is wrong as it neglects the Bauschinger effect, which is of importance if large enough strain reversals occur. There are several proposals for material models that more correctly describe the material response. Most of those have the drawback that they contain a lot of parameters that have to be determined by testing. A reasonably correct material model containing only a few

parameters is described in [6]. This model has also been implemented and tested in some FE codes. If this problem is neglected, the results may be unconservative. It is most likely to occur for material that is cold worked through stretching and the conservative solution is to use strength values from compression tests in the predominant stress direction.

12.6 Loads

Several different situations may occur depending on the purpose of the FE-simulation. In case that a separate component is studied it is common to run the simulation in displacement mode and record the whole load-displacement curve. In such a case the load effects have to be obtained by analysis of the whole structure and compared with the response.

If the simulation concerns a whole or part of a structure it should be loaded by the design loads including relevant load factors and load combination factors. This set of loads is then increased by a load multiplier α in steps until failure. The use of a single load multiplier is a simplification. The different loads have different probabilities of occurrence with high values, which would call for different load multipliers. Methods for taking this into account are however not available. The use of a single load multiplier is consistent with the normal design procedure.

12.7 Limit state criteria

The ultimate limit state criteria should be used as follows:

1. for structures susceptible to buckling:
attainment of the maximum load of the load deformation curve;
2. for regions subjected to tensile stresses:
attainment of a limiting value of the principal membrane strain, for which a value of 5% is recommended.

12.8 Partial factors

The load magnification factor α_{Rd} in the ultimate limit state should be sufficient to achieve the required reliability. The partial factor γ_{M1} should consist of two factors as follows:

1. γ_C to cover the model uncertainty of the FE-modelling used for calculating $\alpha_{ult,k}$ and α_{crit} . It should be obtained from evaluations of test calculations, see Annex D to EN 1990. Where the FE-model proves to be sufficient from bench mark tests γ_C may be taken as 1,00.
2. γ_R to cover the scatter of the resistance model when this is compared with test results.

The partial factor reads as follows:

$$\gamma_{M1} = \gamma_C \gamma_R \tag{12.1}$$

For the rules given in EN 1993-1-5 and $\gamma_C = 1,00$, γ_{M1} takes values between 1,00 and 1,10 where instability governs.

EN 1993-1-5,
C.7

EN 1993-1-5,
C.8

EN 1993-1-5,
C.9

Where FE calculations are used to determine the limit state for structural components in tension associated with fracture, then γ_{M1} should be substituted by γ_{M2} .

12.9 References

- [1] Rusch, A., Lindner, J., Tragfähigkeit von beulgefährdeten Querschnittselementen unter Berücksichtigung von Imperfektionen, Stahlbau 70 (2001) Heft 10, p 765-774.
- [2] Merrison A. W., Inquiry into the basis of design and method of construction of steel box girder bridges, HMSO 1971, Interim report
- [3] BSK 99, Swedish design rules for steel structures, Boverket 1999.
- [4] Clarin, M., High strength steel. Local Buckling and Residual Stresses, Licentiate Thesis 2004:54, Luleå University of Technology, 2004
- [5] Davaine, L., Raoul, J., Aribert J.M., Patch loading resistance of longitudinally stiffened bridge girders, Proceedings of the conference Steel bridge 2004, Millau 2004.
- [6] Granlund, J., Structural Steel Plasticity – Experimental study and theoretical modelling, Doctoral Thesis 1997: 24, Division of Steel Structures, Lulea University of Technology, August 1997.

13 Annex D to EN 1993-1-5 – Plate girders with corrugated webs

Bernt Johansson, Division of Steel Structures, Luleå University of Technology

13.1 Background

This section will give background and justification of the design rules for girders with corrugated webs. The rules have been developed during the drafting of EN 1993-1-5 and the background has not been published. For this reason this section will be quite detailed giving the reasoning behind the choice of design rules for shear resistance.

Girders with corrugated webs are marketed as a product from specialised fabricators or as one-off structures. One example of the former is Ranabalken, which has been on the Swedish market for about 40 years [1]. Its main use is as roof girder. It has a web geometry that is fixed because of the production restraints. A vertical section through the web is shown in Figure 13.1. The thickness of the web is minimum 2 mm, which is governed by the welding procedure. The welding is single sided, which is important for the competitiveness. The maximum depth is 3 m.

In Austria the company Zeman & Co is producing similar beams named Sin-beam but with sinusoidally corrugated webs with the web geometry also shown in Figure 13.1. The web depth is limited to 1500 mm and the web thickness is from 2 to 3 mm. The web has single sided welds.

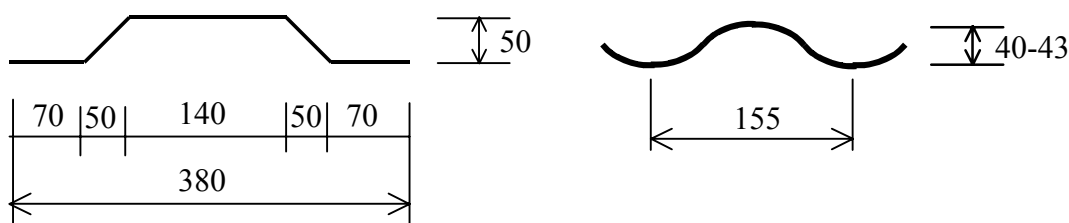


Figure 13.1: Geometry of web plate of Ranabalken, Sweden and Sin-beam, Austria

Corrugated webs have been used for bridges in several countries, including France, Germany and Japan. In France at least three composite bridges have been built of which one was doubly composite with box section. The corrugated steel web was provided with very small flanges, just enough for fixing the shear connectors. The concrete slabs were post-tensioned and when it is important that the steel flanges do not offer too much resistance to the imposed strains. A similar but larger bridge has been built at Altwipfergrund in Germany. It is a three span bridge built by cantilevering with a central span of 115 m and the depth varies from 2,8 m in the span to 6 m at the intermediate supports. The use of single sided welds is not recommended for bridges as it would cause problems with the corrosion protection and the fatigue resistance is not documented.

13.2 Bending moment resistance

EN 1993-1-5,
D.2.1

As the web is corrugated it has no ability to sustain longitudinal stresses. The conventional assumption is to ignore its contribution to the bending moment resistance. This is the basis for the rules in D.2.1. For a simply supported girder supporting a uniformly distributed load the bending resistance is simply the smallest axial resistances of the flanges times the distance between the centroids of the flanges. This axial resistance may be influenced by lateral torsional buckling if the compression flange is not braced closely enough. Reference is given to the rules in 6.3 of EN 1993-1-1. There may be a positive influence of the corrugated web on the lateral buckling resistance compared to a flat web as the corrugation gives the web a substantial transverse bending stiffness. This should reduce the influence of cross sectional distortion but this influence has not been studied in detail and there is no basis for giving rules. There is also an increase in warping stiffness that may be utilized.

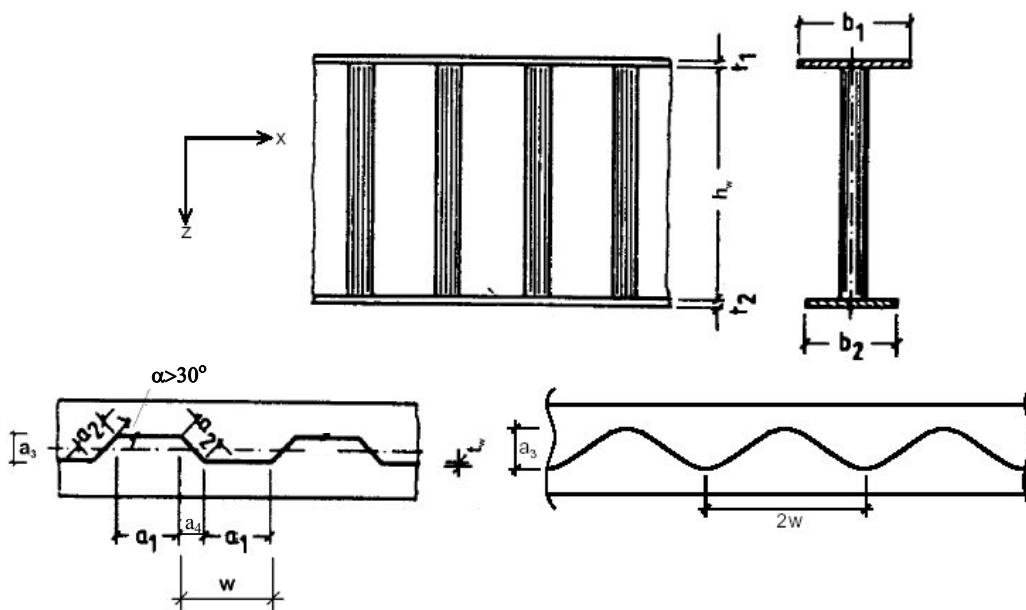
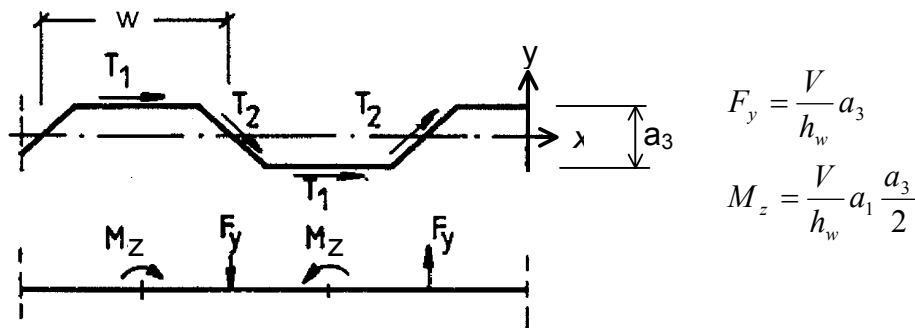


Figure 13.2: Geometry and notations for girders with corrugated webs

If there is a substantial shear force in the cross section of maximum bending moment there may be an influence of the flange axial resistance from lateral bending. Rules for this have been included in the German design rules [2]. A model for calculating these secondary bending moments is shown in Figure 13.3. The shear flow in the web will be constant V/h_w and its effect can be modelled as shown in the lower part of Figure 13.3. The maximum transverse bending moment $M_{z,max}$ occurs where the inclined part of the web intersects the centreline of the flange. It becomes:

$$M_{z,max} = \frac{Va_3}{4h_w}(2a_1 + a_4) \tag{13.1}$$

where V is the coexisting shear force and other notations are according to Figure 13.2.



$$F_y = \frac{V}{h_w} a_3$$

$$M_z = \frac{V}{h_w} a_1 \frac{a_3}{2}$$

Figure 13.3: Action model for calculating secondary lateral bending moments in a flange caused by a corrugated web

In [2] the reduction of the bending resistance is expressed by the factor:

$$f_T = 1 - 0,4 \sqrt{\frac{6M_{z,max} \gamma_{M0}}{f_{yf} b_f^2 t_f}} \tag{13.2}$$

This reduction is not large and actually it has not been considered in the Austrian and Swedish design rules. From a theoretical point of view these bending moments are required for reasons of equilibrium. However, it is questionable how important they actually are in real life. They have been included just as a precaution but for sinusoidally corrugated webs the factor is put to 1,0.

In case yielding of the flange governs the bending resistance becomes:

$$M_{Rd} = \frac{f_{yf} f_T b_f t_f}{\gamma_{M0}} \left(h_w + \frac{t_1 + t_2}{2} \right) \tag{13.3}$$

where $b_f t_f$ should be taken as the smaller of $b_1 t_1$ and $b_2 t_2$.

Local flange buckling is of importance for the bending resistance. It will obviously be influenced by the geometry of the web. The question is to define the flange outstand c to be used for calculating the slenderness. There is little information on this question in the literature. One of few published studies is by Johnson & Cafolla [3] who suggested that the average outstand could be used if:

$$\frac{(a_1 + a_4) a_3}{(a_1 + 2a_4) b_1} < 0,14 \tag{13.4}$$

where b_1 is the width of the compression flange and other notations are according to Figure 13.2. It is not stated what to do if this criterion is not fulfilled but presumably the idea is to use the larger outstand. The average outstand was defined as the average of the smaller and the larger outstand each calculated from free edge to the toe of the weld.

EN 1993-1-5,
D.2.1(2)

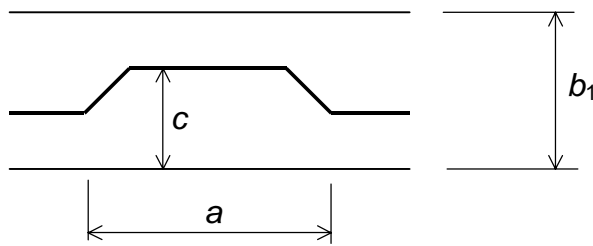


Figure 13.4: Notations for flange geometry

The design rules for Ranabalken states that the outstand should be taken as half the flange width minus 30 mm. This is actually smaller than the smallest outstand, which seems quite optimistic. The corresponding rule for the Sin-beam is half the flange width minus 11 mm.

The flange buckling may in general take place in two different modes. One possibility is a plate type buckling of the larger outstand and another is a torsional buckling where the flange rotates around the centreline of the web. General rules without restrictions on the geometry have to consider both possibilities. The first mode may be relevant for a long corrugation in combination with a narrow flange for which the larger outstand will govern the buckling. However, the flange will be supported by the inclined parts of the web. Assuming an equivalent rectangular plate supported along three edges a safe approximation of the relevant length should be $a = a_1 + 2a_4$, see Figure 13.2 and Figure 13.4. The buckling coefficient of such a plate assuming conservatively a hinged support along the web is approximately [4]:

$$k_{\sigma} = 0,43 + (c/a)^2 \tag{13.5}$$

with:

c = largest outstand from weld to free edge

$$a = a_1 + 2a_4$$

For a geometry with small corrugations compared to the flange width the flange will buckle in a mode of rotation around the centreline of the web. Then c is taken to $0,5b$. A corrugated web will however give a stronger restraint than a flat web. The buckling coefficient ranges from 0,43 for simple support to 1,3 for fixed. A solution for elastic rotational restraint is given in [4] but it is not easy to use. A simplification in form of a reasonably conservative value is instead suggested, which is also used in [2]:

$$k_{\sigma} = 0,60 \tag{13.6}$$

The rules for flange buckling in 4.4 (1) and (2) of EN 1993-1-5 are used with the buckling coefficients given above together with the relevant outstand c . In general, both (13.5) and (13.6) have to be checked and the most unfavourable case governs.

13.3 Shear resistance

EN 1993-1-5,
D.2.2

13.3.1 Introduction

The shear resistance of corrugated webs has attracted interest from many researcher. Accordingly, there are several proposals for the shear resistance e. g. Leiva [5], Lindner [6], Höglund [7] and Johnson & Cafolla [8]. These will be compared with 70 test results presented in Table 13.1. The formulae for the shear resistance actually used in EN 1993-1-5 were developed during the evaluation. This work was done in close co-operation with Professor Torsten Höglund of the Royal Institute of Technology, Stockholm. He was in charge of the corresponding rules in EN 1999-1-1, which are now harmonized with EN 1993-1-5.

Notations for the corrugated web are shown in Figure 13.2. For the sinusoidally corrugated web the measures a_3 and $2w$ are relevant and the developed length of one full wave is denoted $2s$. For the trapezoidal web the following relations and definitions apply.

$$a_2 = a_3/\sin\alpha$$

$$a_4 = a_3\cot\alpha$$

$$w = a_1 + a_4$$

$$s = a_1 + a_2$$

t_w = thickness of web

h_w = depth of web

$$a_{\max} = \max(a_1, a_2)$$

There are two shear buckling modes; one local governed by the largest flat panel and one global involving one or more corrugations. The critical stress for local buckling is taken as that for a long plate, which can be written as:

$$\tau_{cr,\ell} = 4,83 E \left[\frac{t_w}{a_{\max}} \right]^2 \tag{13.7}$$

For a sinusoidally corrugated web the local buckling is less likely to occur. A formula for critical shear stress for local buckling of webs with dimension as given in Figure 13.1 can be found in [19] and reads:

$$\tau_{cr,l} = \left(5,34 + \frac{a_3 s}{h_w t_w} \right) \frac{\pi^2 E}{12(1-\nu^2)} \left(\frac{t_w}{s} \right)^2 \tag{13.8}$$

This formula was developed for the type of corrugation used in an Austrian girder but it has turned out that the formula is not general enough and the formula may give large errors if the dimensions are different to those given in Figure 13.1. For this reason sinusoidally corrugated webs have to be designed by testing with regard to local shear buckling where dimensions other than those given in Figure 13.1 are used. There is also a possibility to calculate the critical shear stresses for local buckling with FEM and to use it in the design rules given here.

The critical stress for global buckling is given by [9]:

$$\tau_{cr,g} = \frac{32,4}{t_w h_w^2} \sqrt[4]{D_x D_z^3} \tag{13.9}$$

where:

$$D_x = \frac{Et_w^3}{12(1-\nu^2)} \frac{w}{s} = \frac{Et_w^3}{12(1-\nu^2)} \frac{a_1 + a_4}{a_1 + a_2} \tag{13.10}$$

$$D_z = \frac{EI_z}{w} = \frac{Et_w a_3^2}{12} \frac{3a_1 + a_2}{a_1 + a_4} \tag{13.11}$$

The first versions of the formulae (13.10) and (13.11) are relevant for sinusoidally corrugated webs where I_z is the second moment of area of one half wave. The second versions are relevant for trapezoidally corrugated webs.

Both critical stresses are valid for simply supported long plates. The global buckling stress is derived from orthotropic plate theory, see e. g. [9]. Some authors have defined D_x without the factor $(1-\nu^2)$ in the denominator. It is theoretically more correct to include it as in (13.10). In [9] there is also a solution for restrained rotation along the edge. For fully clamped edges the coefficient 32,4 in (13.9) increases to 60,4. This has been used for evaluating tests e. g. in [5] but it is hard to believe that this corresponds to the actual conditions at tests. The flanges are not likely to be rigid enough to provide a rotational restraint for such a stiff plate as a corrugated web. In this evaluation (13.9) will be used throughout.

Table 13.1: Data for test girders and test results (The shading shows the governing model and V_{R1} and V_{R2} are according to the EN 1993-1-5 as described in 13.3.6)

No	Test	original	ref ⁹	h_w mm	t_w mm	f_{yw} MPa	α	a_1 mm	a_3 mm	V_u kN	χ_u	λ_1	λ_2	V_u/V_{R1}	V_u/V_{R2}
0	L1A	5	994	1,94	292	45	140	48	280	0,860	0,931	0,558	1,370	0,860	
1	L1B	5	994	2,59	335	45	140	48	502	1,007	0,747	0,556	1,442	1,007	
2	L2A	5	1445	1,94	282	45	140	50	337	0,737	0,915	0,774	1,164	0,737	
3	L2B	5	1445	2,54	317	45	140	50	564	0,839	0,741	0,768	1,197	0,839	
4	L3A	5	2005	2,01	280	45	140	48	450	0,690	0,880	1,092	1,068	0,778	
5	L3B	5	2005	2,53	300	45	140	48	775	0,881	0,724	1,067	1,244	0,962	
6	B1	10	600	2,1	341	45	140	50	208	0,837	0,929	0,347	1,332	0,837	
7	B2	10	600	2,62	315	45	140	50	273	0,954	0,716	0,315	1,340	0,954	
8	B3	10	600	2,62	317	45	140	50	246	0,854	0,718	0,316	1,202	0,854	
9	B4b	10	600	2,11	364	45	140	50	217	0,815	0,956	0,358	1,315	0,815	
10	M101	10	600	0,99	189	45	70	15	53	0,817	0,734	0,750	1,160	0,817	
11	M102	10	800	0,99	190	45	70	15	79	0,908	0,736	1,003	1,292	0,912	
12	M103	10	1000	0,95	213	45	70	15	84	0,718	0,812	1,342	1,069	1,101	
13	M104	10	1200	0,99	189	45	70	15	101	0,778	0,734	1,501	1,106	1,428	
14	L1	11	1000	2,1	410	30	106	50	380	0,764	0,772	0,616	1,110	0,764	
15	L1	11	1000	3	450	30	106	50	610	0,782	0,566	0,590	0,996	0,782	
16	L2	11	1498	2	376	30	106	50	600	0,921	0,776	0,894	1,343	0,921	
17	L2	11	1498	3	402	30	106	50	905	0,867	0,535	0,836	1,081	0,867	
18	1	12	850	2	355	33	102	56	275	0,788	0,731	0,459	1,118	0,788	
19	2	12	850	2	349	38	91	56	265	0,773	0,642	0,466	1,036	0,773	

⁹ ref = bibliographical reference where the test results can be found

No	Test		h_w mm	t_w mm	f_{yw} MPa	α	a_1 mm	a_3 mm	V_u kN	χ_u	λ_1	λ_2	V_u/V_{R1}	V_u/V_{R2}
	original	ref ^o												
20	V1/1	13	298	2,05	298	45	144	102	68	0,646	0,917	0,099	1,021	0,646
21	V1/2	13	298	2,1	283	45	144	102	70	0,684	0,872	0,096	1,054	0,684
22	V1/3	13	298	2	298	45	144	102	81	0,789	0,940	0,100	1,262	0,789
23	V2/3	13	600	3	279	45	144	102	235	0,810	0,606	0,175	1,060	0,810
24	CW3	8	440	3,26	284	45	250	45	171	0,726	0,976	0,218	1,184	0,726
25	CW4	8	440	2,97	222	45	250	45	154	0,918	0,947	0,198	1,475	0,918
26	CW5	8	440	2,97	222	45	250	63	141	0,841	0,947	0,156	1,350	0,841
27	I/5	14	1270	2	331	62	171	24	260	0,535	1,223	1,483	0,987	0,963
28	II/11	14	1270	2	225	62	171	24	220	0,666	0,974	1,267	1,085	0,935
29	121216A	15	305	0,64	676	45	38	25	50	0,656	1,165	0,583	1,177	0,656
30	121221A	15	305	0,63	665	55	42	33	46	0,623	1,298	0,501	1,190	0,623
31	121221B	15	305	0,78	665	55	42	33	73	0,798	1,048	0,475	1,352	0,798
32	121232A	15	305	0,64	665	63	50	51	41	0,546	1,741	0,391	1,255	0,546
33	121232B	15	305	0,78	641	63	50	51	61	0,692	1,403	0,365	1,386	0,692
34	121809A	15	305	0,71	572	50	20	14	63	0,880	0,509	0,829	1,078	0,880
35	121809C	15	305	0,63	669	50	20	14	55	0,740	0,620	0,924	0,978	0,740
36	121832B	15	305	0,92	562	63	50	51	53	0,581	1,113	0,328	1,018	0,581
37	122409A	15	305	0,71	586	50	20	14	58	0,791	0,515	0,839	0,973	0,791
38	122409C	15	305	0,66	621	50	20	14	58	0,803	0,570	0,880	1,026	0,803
39	122421A	15	305	0,68	621	55	42	33	43	0,578	1,162	0,475	1,036	0,578
40	122421B	15	305	0,78	638	55	42	33	61	0,695	1,027	0,466	1,165	0,695
41	122432B	15	305	0,78	634	63	50	51	49	0,562	1,395	0,363	1,122	0,562
42	181209A	15	457	0,56	689	50	20	14	81	0,795	0,708	1,446	1,111	1,373
43	181209C	15	457	0,61	592	50	20	14	89	0,933	0,602	1,312	1,219	1,382
44	181216C	15	457	0,76	679	45	38	25	119	0,873	0,984	0,839	1,430	0,873
45	181221A	15	457	0,61	578	55	42	33	62	0,666	1,250	0,706	1,244	0,666
46	181221B	15	457	0,76	606	55	42	33	98	0,806	1,027	0,684	1,350	0,806
47	181232A	15	457	0,6	552	63	50	51	52	0,594	1,692	0,542	1,340	0,594
48	181232B	15	457	0,75	602	63	50	51	80	0,671	1,414	0,535	1,349	0,671
49	181809A	15	457	0,61	618	50	20	14	82	0,823	0,615	1,341	1,085	1,262
50	181809C	15	457	0,62	559	50	20	14	78	0,852	0,576	1,270	1,093	1,200
51	181816A	15	457	0,63	592	45	38	25	75	0,761	1,108	0,821	1,329	0,761
52	181816C	15	457	0,74	614	45	38	25	96	0,800	0,961	0,803	1,294	0,800
53	181821A	15	457	0,63	552	55	42	33	56	0,610	1,182	0,684	1,104	0,610
54	181821B	15	457	0,74	596	55	42	33	93	0,798	1,046	0,683	1,351	0,798
55	181832A	15	457	0,61	689	63	50	51	53	0,477	1,859	0,603	1,145	0,477
56	181832B	15	457	0,75	580	63	50	51	79	0,687	1,388	0,525	1,368	0,687
57	241209A	15	610	0,62	606	50	20	14	71	0,536	0,599	1,765	0,699	1,292
58	241209C	15	610	0,63	621	50	20	14	79	0,573	0,597	1,780	0,746	1,400
59	241216A	15	610	0,63	592	45	38	25	76	0,578	1,108	1,096	1,009	0,656
60	241216B	15	610	0,79	587	45	38	25	133	0,813	0,880	1,032	1,259	0,848
61	241221A	15	610	0,61	610	55	42	33	77	0,587	1,284	0,968	1,114	0,587
62	241221B	15	610	0,76	639	55	42	33	127	0,742	1,055	0,938	1,261	0,742
63	241232A	15	610	0,62	673	63	50	51	69	0,469	1,808	0,792	1,104	0,469
64	241232B	15	610	0,76	584	63	50	51	101	0,645	1,374	0,701	1,276	0,645

Test	h_w	t_w	f_{yw}	α	a_1	a_3	V_u	χ_u	λ_1	λ_2	V_u/V_{R1}	V_u/V_{R2}
No original ref ^o	mm	mm	MPa		mm	mm	kN					
65 Gauche	16	460	2	254	30,5	0	126 139	1,029	1,494	0,121	2,142	1,029
66 Droit	16	550	2	254	30,5	0	126 109	0,675	1,494	0,145	1,405	0,675
67 Sin 1	17	1502	2,1	225	2w=155	40	370	0,902	0,433	1,108	1,046	1,038
68 Sin 2	17	1501	2,1	225	2w=155	40	365	0,890	0,433	1,108	1,032	1,025
69 Sin 3	17	1505	2,1	225	2w=155	40	353	0,859	0,433	1,108	0,996	0,989

Slenderness parameters are defined by:

$$\lambda_i = \sqrt{\frac{f_{yw}}{\tau_{cri} \sqrt{3}}} \tag{13.12}$$

for $i = 1,2,3$ there 1 and 2 refers to equations (13.8) and (13.9) and 3 to equation (13.14) below.

Values for the slenderness parameters λ_1 and λ_2 for the test girders are given in Table 13.1. The characteristic shear resistance is represented by:

$$V_R = \chi \frac{f_{yw}}{\sqrt{3}} h_w t_w \tag{13.13}$$

where χ is the minimum of the reduction values χ_i determined for λ_1 and λ_2 .

The ultimate shear resistance V_u in the tests can be transformed to the non-dimensional parameter χ_u by equation (13.13) and it is also given in Table 13.1.

The parameters defined above are general and will be used throughout the analysis. The features of the different models will now be described briefly and evaluated.

13.3.2 Model according to Leiva [5]

Leiva does not fully develop a design model but his main concern is the interaction between local and global buckling, which is based on observations from tests. His idea is to consider this interaction by defining a combined critical stress τ_{cr3} as:

$$\frac{1}{\tau_{cr3}^n} = \frac{1}{\tau_{cr1}^n} + \frac{1}{\tau_{cr2}^n} \tag{13.14}$$

Leiva discussed only in case $n=1$ but the equation has been written more general for later use. He also considered yielding as a limit for the component critical stresses in an attempt to make a design formula. The idea of Leiva will not be evaluated but it will form the basis for a model that will be presented later called "Combined model".

13.3.3 Model according to Lindner [6]

Lindner made an evaluation of test results 0 to 23 in Table 13.1. He discussed different options for taking the interaction between local and global buckling into account, including using (13.14) with $n=2$. His conclusions were however that the

interaction could be taken into account implicitly by correcting λ_2 . Lindner's model has been introduced in German recommendations [2]. The reduction factor for the resistance:

$$\chi_{i,L} = \frac{0.588}{\lambda_i} \tag{13.15}$$

is used for both local and global buckling. λ_1 is as defined in (13.12) but λ_2 is changed according to:

$$\lambda_2 = \sqrt{\frac{2f_y}{\tau_{cr2}\sqrt{3}}} \text{ if } 0.5 < \tau_{cr1}/\tau_{cr2} < 2 \tag{13.16}$$

The model has been evaluated with results shown in Figure 13.5 and in Table 13.2 where χ_L is the smallest of χ_{1L} and χ_{2L} according to (13.15). The right hand diagram in Figure 13.5 shows that the model has a slight bias with respect to λ_2 . It is an under-prediction of the resistance that increases with the slenderness for global buckling. Further the model includes discontinuities in the prediction because of the stepwise correction in (13.15).

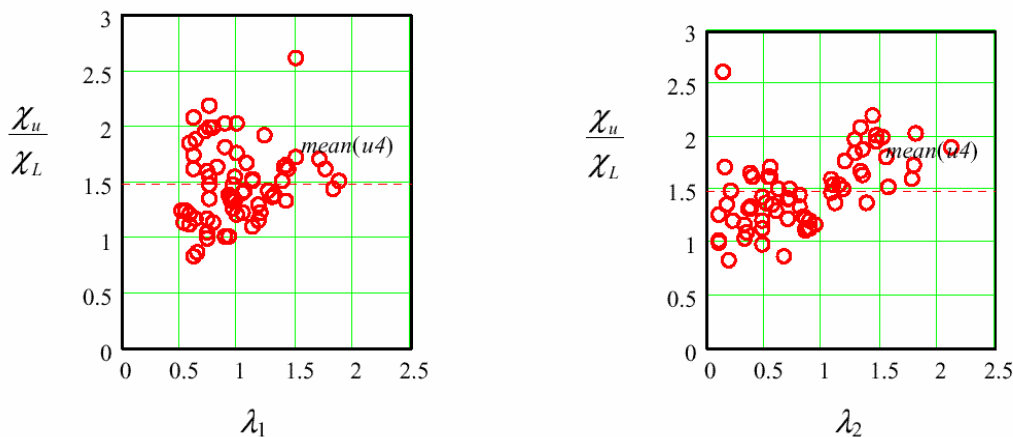


Figure 13.5: Test over prediction as function of λ_1 and λ_2 according to Lindner's model

13.3.4 Model according to Johnson [8]

The model according to Johnson involves three separate checks; one for local buckling, one for global buckling and one for combined local and global buckling. The check for local buckling is done with the post-buckling resistance predicted by:

$$\chi_{1,J} = \frac{0,84}{\lambda_1} < 1,0 \tag{13.17}$$

For the global buckling the critical stress (13.9) is used but with a coefficient 36 instead of 32,4 and without $(1-\nu^2)$ in the denominator of D_x which gives more or less the same results. The design strength is taken as 0,5 times the critical stress, which includes a partial safety factor of 1,1. Considering theses differences the characteristic reduction factor becomes:

$$\chi_{2J} = \frac{0,61}{\lambda_2^2} \tag{13.18}$$

if λ_2 is defined by (13.12) and (13.9).

Finally, the interaction between local and global buckling is considered with the critical stress τ_{cr3} according to (13.14) with $n=1$. The resistance is taken as the critical stress with a reduction factor $0,67 \times 1,1$, which leads to the reduction factor:

$$\chi_{3J} = \frac{0,74}{\lambda_3^2} \tag{13.19}$$

where λ_3 is defined by (13.12) and (13.14) with $n=1$.

The evaluation is shown in Figure 13.6 and Table 13.2. χ_J is taken as the lowest value from the three separate checks. The right hand diagram depicting the combined check shows a clear bias for under-prediction for high slenderness values, which is caused by the use of reduced critical stresses as design strength. The scatter in the quotient test over prediction shown in Table 13.2 is also fairly high.

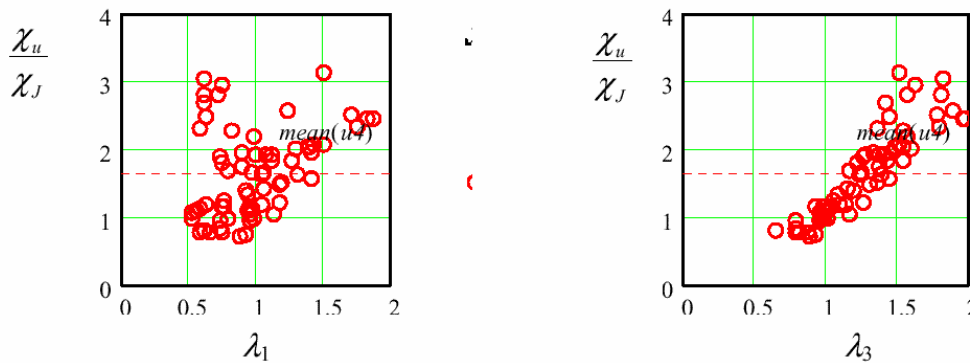


Figure 13.6: Test over prediction as function of λ_1 and λ_3 according to Johnson’s model

13.3.5 Combined model

The basic idea of this model was to define the resistance by a single reduction factor. A reduced critical stress will be defined by (13.14) in order to take the interaction between local and global buckling into account. This critical stress is used to calculate the slenderness parameter λ_3 from (13.12). It is used in combination with the strength function:

$$\chi_c = \frac{1,2}{0,9 + \lambda_3} < 1,0 \tag{13.20}$$

The results for $n=2$ are shown in Table 13.2 and in Figure 13.7. Also $n=4$ has been checked and the result is quite similar considering the statistical parameters. Both alternatives represent a quite weak interaction and the interaction becomes weaker the higher value of n is used. It can be seen that this model improves the prediction. However, the model is symmetrical in the influence of local and global buckling. It could be expected on theoretical grounds that the post-critical resistance is more pronounced for local buckling than for global. In the latter case

it is questionable if there is any at all. On the other hand the influence of imperfections in the range of medium slenderness can be expected to be smaller than for local buckling. This became clear when the tests with sinusoidally corrugated webs were included in the comparisons, which was done quite late in the work. This reasoning led to the model described in the next section.

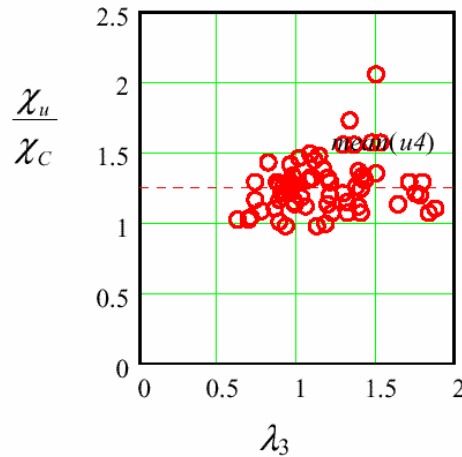


Figure 13.7: Test over prediction as function of λ_3 according to model Combined check, $n=2$

13.3.6 Model according to EN 1993-1-5

The model is based on the one proposed by Höglund [7]. It has two separate checks, one for local and one for global buckling. It has been modified in [18] and further modification has been done here as will be discussed below. The reduction factors for local and global buckling, respectively, is given by:

$$\chi_{1,EN} = \frac{1.15}{0.9 + \lambda_1} < 1.0 \tag{13.21}$$

$$\chi_{2,EN} = \frac{1.5}{0.5 + \lambda_2^2} \leq 1.0 \tag{13.22}$$

The reasoning behind the two checks is that the local buckling is expected to show a post-critical strength, which should not be present in the global buckling. This is reflected by λ_1 appearing linear and λ_2 is squared in the reduction factor. In [18] the reduction factor for local buckling has no plateau but the global buckling has the same reduction factor as (13.17). There is however one more difference. The restraint from the flanges to the global buckling is included in [18] and an increase of the buckling coefficient to 40 is suggested if a certain stiffness criterion is met. The predictions were compared with the test results in Table 13.1 and also with some tests on aluminium girders. The prediction is marginally better than the one using (13.21) and (13.22). The idea of increasing the global buckling coefficient has also been discussed by Leiva and it may very well be true. It has however not been included in the model in EN 1993-1-5 for simplicity and as an additional safety measure. The reduction factors (13.21) and (13.22) are shown in Figure 13.9 together with the Euler curve and the von Karman curve.

There are no test results that make it possible to evaluate the length of the plateau length for local buckling. Equation (13.21) has a plateau until $\lambda_1 = 0.25$, which is

very small compared to other buckling problems. For instance the design rules for flat webs give $\lambda = 0.83$ for the plateau length with $\eta = 1$. This question will remain unsettled until further experiments are available. It is believed that (13.21) is conservative enough.

The evaluation results are found in Figure 13.8 and Table 13.2. The notation χ_{EN} is the minimum of (13.21) and (13.22). The prediction is quite good with all the results between 1 and 1,5, except for test 65, which stick out in all the evaluations.

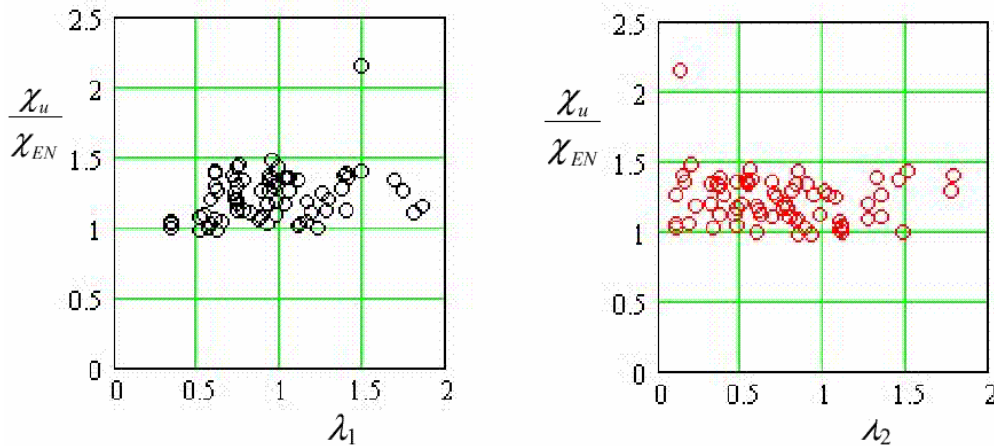


Figure 13.8: Test over prediction according to the model in EN 1993-1-5

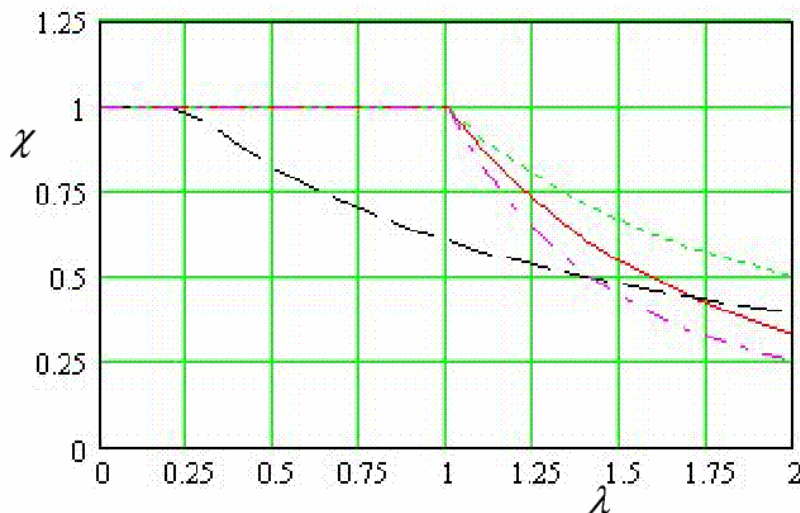


Figure 13.9: Reduction factors according to EN 1993-1-5; global buckling solid and local buckling dashed. As reference the Euler curve $1/\lambda^2$ is shown as dash-dots and the von Karman curve $1/\lambda$ as dots

Figure 13.10 shows the test results for which local buckling is supposed to govern and Figure 13.11 there global buckling is supposed to govern. The predictions gives almost the same statistical characteristics, mean 1,22 and 1,23 with coefficient of variation 0,15 and 0,14 for local and global buckling, respectively.

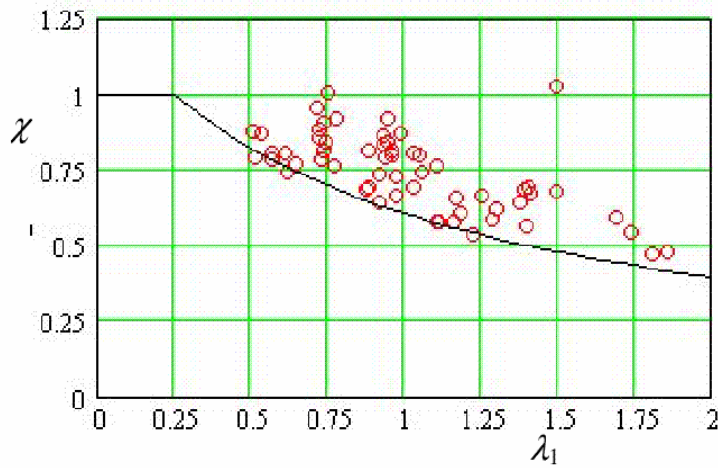


Figure 13.10: Reduction factor for local buckling together with 59 test results where local buckling is supposed to govern

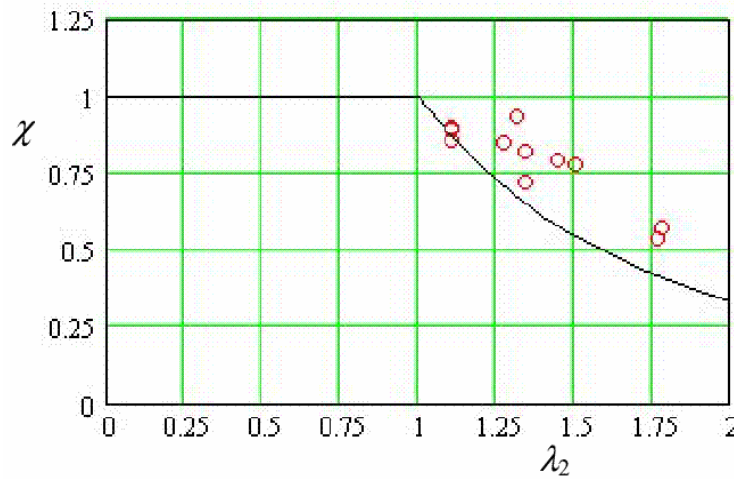


Figure 13.11: Reduction factor for global buckling together with 11 test result where global buckling is supposed to govern

Table 13.2: Evaluation of design models showing mean value, standard deviation and coefficient of variation of the quotient

$$\chi_u / \chi_{prediction}$$

Model	Lindner	Johnson	Combined n=2	EN1993-1-5
Mean	1.48	1.62	1.26	1.22
Stand dev	0.34	0.65	0.19	0.18
Coeff of var	0.23	0.39	0.15	0.15

13.3.7 Discussion

The test data base is quite large and covers a range of parameters for instance:

$$190 < f_y < 690 \text{ Mpa}$$

$$140 < h_w/t_w < 1200$$

$$30^\circ < \alpha < 63^\circ$$

Most of the tests are normal I-girders tested in three or four point bending. The exceptions are test 27 and 28, which were racking tests on container walls with an unsymmetrical corrugation. The report included one more shear test that has been discarded because the web was not continuously welded. Test 65 and 66 had a triangular corrugation (a_1 in Figure 13.2 equal to zero) and the girder had flanges of cold-formed channels. Test 65 showed a very high resistance compared to prediction, which to some extent may have been influenced by the flanges carrying some shear. However, it is not the whole truth as test 66 does not stick out. The tests by Hamilton [15] included four more tests with the remark “support induced failure”, which are not included in Table 13.1.

The normal procedure for dealing with buckling problems is to use the critical stress for defining a slenderness parameter as in (13.12) and to find a reduction factor that depends on this slenderness parameter. In all the models studied here a post critical strength is recognized for the local buckling. It is however less pronounced than for a flat web. This is likely to be so because the folds of the web are less efficient in supporting tension fields than the flanges of a girder with a flat web. One question is how small the angle α between adjacent panels can be made before the fold becomes insufficient as a support for the panels. The smallest angle in the tests is 30° . This has been taken as lower limit until further evidence is available.

The next question is interaction between the two buckling modes. This has been considered by most of the authors except Höglund. His reasoning is that the interaction, if any, is so weak that two separate checks are sufficient. The evaluation in Table 13.2 supports this opinion as the EN 1993-1-5 model based on Höglund's ideas, shows the lowest scatter. The suggestion of Lindner to increase the slenderness parameter for global buckling if the critical stresses for local and global buckling are close to each other is hard to justify and it creates an unnatural discontinuity. Using (13.14) for defining a reduced critical stress would give a continuous procedure that gives the highest interaction when the two critical stresses are equal. This seems intuitively reasonable. It will however be symmetrical in τ_{cr1} and τ_{cr2} , which is not likely to be true as indicated in the discussion in 13.3.5. Because of this theoretical objection and that the prediction of the test results is as good with the separate checks this was chosen.

For some low value of the slenderness the shear yield resistance of the web should be reached. The test results do not indicate at which slenderness this will be safely met. From Figure 13.10 it can be seen that the lowest slenderness there local failure was governing is $\lambda_1=0.5$. Judging from experiences of other plate buckling phenomena (13.21) will be very safe with $\lambda_1 = 0.25$ for reaching the yield resistance as discussed in 13.3.6.

The design model presented in EN 1993-1-5 has been shown to be a step forward compared to other existing or possible design models. It is certainly not the final

answer to the question of shear resistance of corrugated webs and future research will hopefully improve the model.

13.4 Patch loading

No rules for patch loading resistance are given in EN 1993-1-5. The rules for flat webs may be used but this is in most cases quite conservative, especially if the loaded length is larger than one half corrugation w . The patch loading resistance has been studied by several authors [10], [20], [21]. The results have however not been collated and merged into a design model. In [1] the design rule for patch loading includes only a check of the yield resistance. For sinusoidally corrugated webs for the patch loading resistance has been studied in [22] and [23].

13.5 References

- [1] Ranabalk. Produktbeskrivning och dimensioneringsregler (Specification and design rules for Rana girder), Ranaverken AB, 2000
- [2] DASt Richtlinien 015, Träger mit schlanken Stege, Stahlbau-Verlag, Köln, 1990
- [3] Johnson, R., Cafolla, J., Local flange buckling in plate girders with corrugated webs, Proceedings of the Institution of Civil Engineers Structures & Buildings May 1997 pp 148-156.
- [4] Timoshenko, S. P., Gere, J. M., Theory of elastic stability, Mc Graw-Hill, Second edition New York 1961.
- [5] Leiva, L., Skjuvbuckling av plåtbalkar med trapetsprofilerat liv. Delrapport 1. (Shear buckling of trapezoidally corrugated girder webs. Report Part 1.), Chalmers Univ. of Technology, Div. of Steel and Timber Structures Publ. S 83:3, Göteborg 1983 (In Swedish)
- [6] Lindner, J., Grenzscherbtragfähigkeit von I-Trägern mit trapezförmig profilierten Steg, Stahlbau 57 (1988) Heft 12 pp 377-380.
- [7] Höglund, T., Shear Buckling Resistance of Steel and Aluminium Plate Girders, Thin-walled Structures Vol. 29, Nos. 1-4, pp 13-30, 1997
- [8] Johnson, R., Cafolla, J., Corrugated webs in plate girders for bridges, Proceedings of the Institution of Civil Engineers Structures & Buildings May 1997 pp 157-164.
- [9] Peterson, J. M., Card, M. F., Investigation of the Buckling Strength of Corrugated Webs in Shear, NASA Technical Note D-424, Washington 1960 (referred in [5])
- [10] Bergfelt, A. , Edlund, B. & Leiva, L. , Trapezoidally corrugated girder webs. Ing. et Architects Suisses, No.1-2, Januar 1985 pp 65-69
- [11] Report No. RAT 3846 Technical Research Centre of Finland, Espoo 1983
- [12] Kähönen, A., About the calculation procedure of steel I-beam with corrugated webs. Master Thesis Lappeenranta University of Technology, 1983 (In Finnish)

- [13] Scheer, J., Versuche an Trägern mit Trapezblechstegen, Bericht Nr. 8127, Technische Univ. Braunschweig, Inst. für Stahlbau, Dezember 1984
- [14] Leiva-Aravena, L., Trapezoidal corrugated panels, Chalmers Univ. of Technology, Div. of Steel and Timber Structures Publ. S 87:1, Göteborg 1987
- [15] Elgaaly, M., Hamilton, R., Seshadri, A., Shear strength of beams with corrugated webs, Journal of the Structural Division, ASCE, 1996 122(4), 390-398
- [16] Frey, F., Essai d'une poutre a ame plisse, Rapport interne No 64, Nov 1975, Laboratoire de Mechanique des Materiaux et Statique de Constructions, Université de Liège
- [17] Pasternak, H., Branka, P., Zum Tragverhalten von Wellstegträgern, Bauingenieur 73 (1988) Nr. 10, pp 437-444
- [18] Ullman, R., Shear Buckling of Aluminium Girders with Corrugated Webs, Royal Inst of Technology, Structural Engineering, TRITA-BKN Bulletin, 2002
- [19] Pasternak H., Hannebauer D.: Träger mit profilierten Stegen, Stahlbaukalender 2004, Berlin, Verlag Ernst & Sohn
- [20] Leiva-Aravena, L., Edlund, B., Buckling of Trapezoidally Corrugated Webs, ECCS Colloquium on Stability of Plate and Shell Structures , Ghent University, 1987.
- [21] Elgaaly, M., Seshadri, A., Depicting the behaviour of girders with corrugated webs up to failure using non-linear finite element analysis, Advances in Engineering Software, Vol 29, No. 3-6, pp 195-208, 1998.
- [22] Pasternak H., Branka P.: Zum Tragverhalten von Wellstegträgern unter lokaler Lasteinleitung, Bauingenieur 74(1999) 219-224
- [23] Novák, R., Macháček, J., Design Resistance of Undulating Webs under Patch loading, Proceedings of the third International Conference Coupled Instability in Metal Structures CIMS'2000, Lisbon, Imperial College Press, pp 371-378.

14 Annex E to EN 1993-1-5 – Refined methods for determining effective cross sections

Bernt Johansson, Division of Steel Structures, Luleå University of Technology

14.1 Effective areas for stress levels below the yield strength

The modified Winter formulae in 4.4 of EN 1993-1-5 have been developed in order to describe the ultimate limit state where the stresses at the supported edges are at the level of the yield strength. At lower stress levels the effective width gets larger. Partially this effect is considered in 4.4(4) of EN 1993-1-5 by the use of the reduced slenderness parameter, which can be written

$$\bar{\lambda}_{p,red} = \bar{\lambda}_p \sqrt{\frac{\sigma_{com,Ed}}{f_y / \gamma_{M0}}} = \sqrt{\frac{\sigma_{com,Ed} \gamma_{M0}}{\sigma_{cr}}} \quad (14.1)$$

The reduced slenderness parameter takes into account that the stress level is smaller than the yield strength. However, the Winter formula gives the minimum effective width corresponding to the highest stress and strain. The strain at the edge of the plate does vary along the plate in such way that it is largest at the crest of the buckles and smallest at the nodal lines between the buckles, which is illustrated in Figure 14.1.

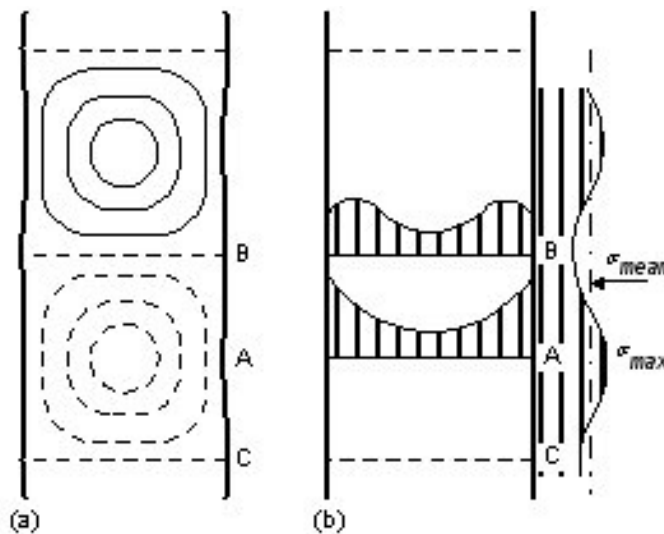


Figure 14.1: Stress distribution in a longitudinally compressed slender plate

Where deformations are of concern the average strain along one buckle is relevant. The average strain is always smaller than the strain calculated with the Winter formula, also when the maximum stress is equal to the yield strength. An example where both strength and stiffness are of importance is coupled global and local instability. This is illustrated in Figure 14.2 showing results from tests on studs with thin-walled C-section under compression together with calculated results using different expressions for the effective width [1]. In the left hand diagram, showing load versus deflection, it is shown that the Winter formula (14.3) gives too large deflections and too low resistance. The calculated curve labelled [1] is based on expressions developed in [1] and forming the basis for the

EN 1993-1-5,
E.1

formulae in Annex E. The right hand diagram shows the strains at mid span (compression positive) and calculated values with the two different effective widths described above. It can be seen that (14.3) gives an overestimate of the stresses. This is a combined effect of that the effective width is underestimated for stresses lower than the yield strength and that the average stiffness is underestimated, which causes larger deflections. This in turn increases the bending stresses due to axial force times deflection.

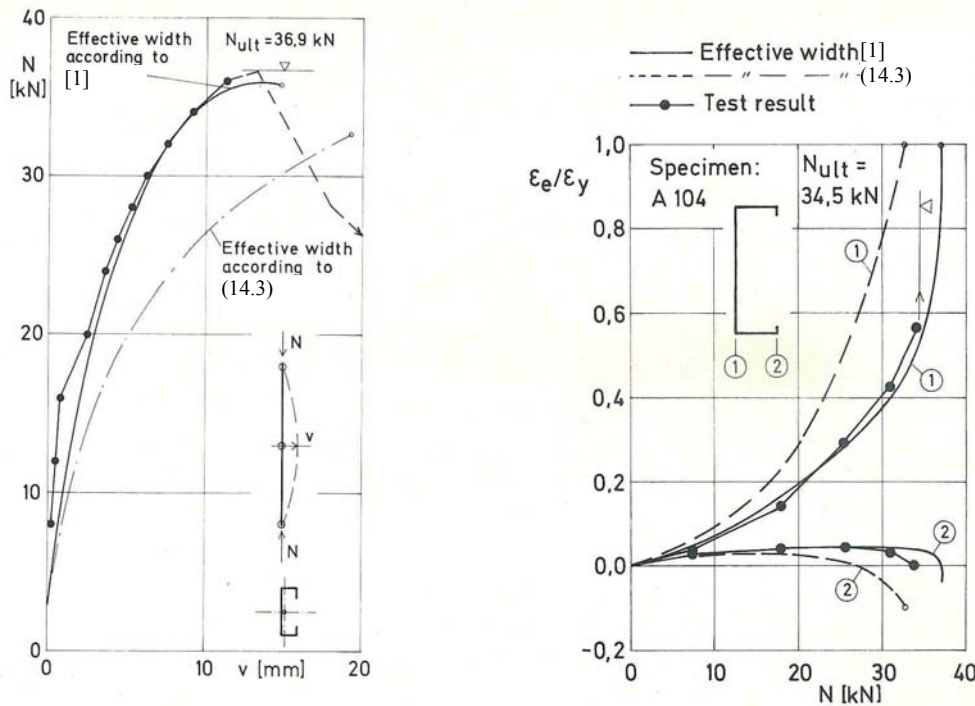


Figure 14.2: Results from tests on studs with thin-walled C-section under compression together with calculated values with two different estimates of the effective width [1]

The formulae (E.1) and (E.2) of EN 1993-1-5 were developed during the drafting of ENV 1993-1-3 based on the proposal in [1]. The original formulae were thought to be too complicated to introduce in a code. It takes about a page to present them so the reader is referred to [1]. A comparison is shown in Figure 14.2 for the case of a uniformly compressed plate supported at all edges. For this case (E.1) becomes:

$$\rho = \frac{1 - 0,22/\bar{\lambda}_{p,red}}{\bar{\lambda}_{p,red}} + 0,18 \frac{(\bar{\lambda}_p - \bar{\lambda}_{p,red})}{(\bar{\lambda}_p - 0,6)} \tag{14.2}$$

Figure 14.2 also shows as reference the Winter formula:

$$\rho = \frac{1 - 0,22/\bar{\lambda}_{p,red}}{\bar{\lambda}_{p,red}} \tag{14.3}$$

The Figure 14.3 shows three examples of different slenderness $\bar{\lambda}_p = 1, 2$ and 3 . It can be seen that (14.2) is a good approximation of the original formulae for $\bar{\lambda}_{p,red} > 0,7\bar{\lambda}_p$. Translated to stress level this means that the approximation is good down to stresses larger than half the yield strength.

It should be noted that the effective width according (14.2) depends on the actual stress in the plate, which in turn depends of the effective width. This means that the calculation becomes iterative but the convergence is quite rapid. The procedure in E.2 described below is an alternative that can be used for a direct calculation.

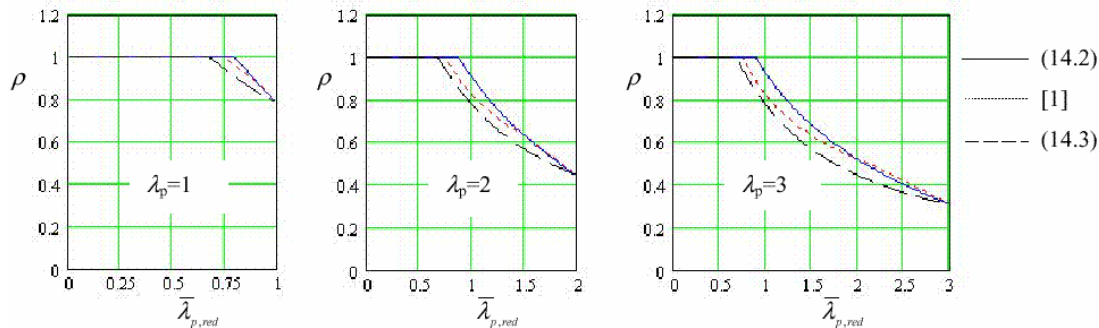


Figure 14.3: Comparison between the effective width formulae developed in [1] with the approximation in Annex E and with the Winter formula for stresses below the yield strength

14.2 Effective areas for stiffness

EN 1993-1-5, E.2

For common plated structures like bridge girders it is praxis in many countries to ignore the loss of stiffness due plate buckling. The justification is that for economical reasons the flanges are designed to be fully effective or with only a small reduction for local buckling. For webs it may be economical to accept a larger reduction because the web contributes relatively little to the bending stiffness. As EN 1993-1-5 is not only written for bridge girders there was a need to formalise some kind of rule that limits this praxis. The rule in 2.2(5) of EN 1993-1-5 states (accepting the recommendation in Note 1) that the loss of stiffness may be ignored if the effective area at ULS is not less than half the gross area of an element in compression. For a web where the stresses change sign the rule should be applied to the compression zone.

If the limit in 2.2(5) is not met or for some other reason a more accurate analysis is required the rules in E.2 may be used. This is a simple idea based on engineering judgement that was first introduced in the Swedish bridge code [2] for stress calculation. Here it is used for a wider purpose including global analysis and calculation of deflections.

The formula is a simple interpolation according to:

$$I_{eff} = I_{gr} - \frac{\sigma_{gr}}{\sigma_{com,Ed,ser}} (I_{gr} - I_{eff}(\sigma_{com,Ed,ser})) \tag{14.4}$$

The idea is that the formula should be used without iterations such that $I_{eff}(\sigma_{com,Ed,ser})$ should be calculated assuming a stress level that is not smaller than $\sigma_{com,Ed,ser}$. As a safe guess the yield stress can be used and it gives a too low second moment of area.

14.3 References

- [1] Thomasson, P-O, Thin-walled C-shaped Panels in Axial Compression, Swedish Council for Building Research, Document D1:1978, ISBN 91-540-2810-5.
- [2] Bro 88 (Swedish Bridge Code 1988), Swedish National Road Administration

15 Worked example – Launching of a box girder

Bernt Johansson, Division of Steel Structures, Luleå University of Technology

The bridge has been built at Vallsundet in central Sweden. It has dual carriageways and is designed as composite. It was erected by incremental launching schematically shown in Figure 15.1. The verification for patch loading and bending at support 2 will be shown in this example.

Just before the launching nose reaches support 3 the load effects including load factor at pier 2 are:

$$M = 80,5 \text{ MNm}$$

$$R = 4,0 \text{ MN}$$

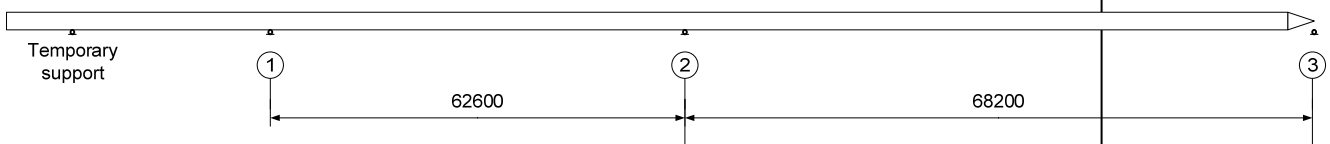


Figure 15.1: Schematic view of bridge during launching

The cross section is a box with dimensions shown in Figure 15.2 for the section that will be at pier 2 during launching. All measures refer to the centre lines of the plates. During launching the top flanges are connected by a trapezoidally corrugated sheet acting as a tie and diaphragm. It is also used as lost formwork for casting the concrete at a later stage. Note that the girder is slightly hybrid with top flanges in S460 and the rest in S420.

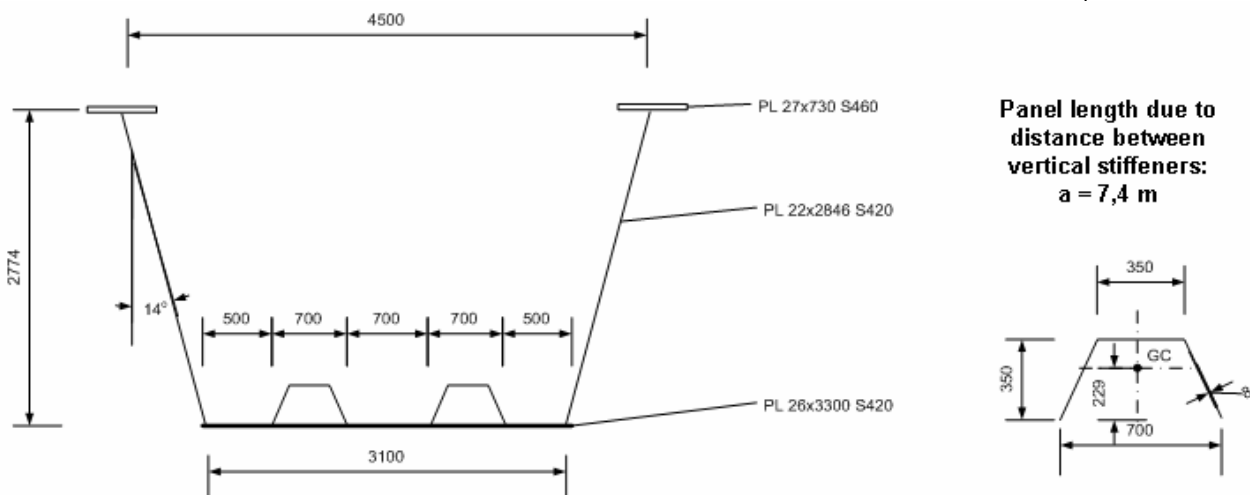


Figure 15.2: Cross section at pier 2 when the nose reaches pier 3

15.1 Patch loading

The support reaction is carried by both webs and the component in the plane of the web becomes:

$$F_{Ed} = \frac{4,0}{2 \cos 14} = 2,06 \text{ MN}$$

There is also a horizontal component of the support reaction, which acts as a patch load on the bottom flange:

$$F_{hEd} = \frac{4,0 \tan 14}{2} = 0,50 \text{ MN}$$

The launching shoe is assumed to have a length:

$$s_s = 0,5 \text{ m}$$

From Figure 6.1 of EN 1993-1-5 and the inclined width of the web according to Figure 15.2 we get:

$$k_F = 6 + 2 \left[\frac{2,846}{7,4} \right]^2 = 6,30$$

Formula (6.5) gives:

$$F_{cr} = 0,9 \cdot 6,3 \cdot 210000 \frac{0,022^3}{2,846} = 4,45 \text{ MN}$$

Paragraph 6.5(1) gives a limitation of the width of the flange to be taken into account to:

$$15 \varepsilon t_f = 15 \sqrt{\frac{235}{420}} \cdot 0,026 = 0,292 \text{ m}$$

on each side of the web. On the outside where is only 100 mm so the width becomes:

$$b_f = 0,292 + 0,1 = 0,392 \text{ m.}$$

$$m_1 = \frac{0,392}{0,022} = 17,8$$

$$m_2 = 0,02 \left[\frac{2,846}{0,026} \right]^2 = 240$$

The effective loaded length is given by formula (6.10):

$$l_y = 0,5 + 2 \cdot 0,026 (1 + \sqrt{17,8 + 240}) = 1,38 \text{ m}$$

The slenderness parameter is given by (6.4):

$$\lambda_F = \sqrt{\frac{1,38 \cdot 0,022 \cdot 420}{4,45}} = 1,69$$

Here it is noted that λ_F is larger than 0,5, which is a condition for the formula used for m_2 .

The reduction factor for the effective length is given in (6.3):

$$\chi_F = \frac{0,5}{1,69} = 0,296$$

Finally, the patch loading resistance is given by (6.1):

$$F_{Rd} = \frac{420 \cdot 0,296 \cdot 1,38 \cdot 0,022}{1,1} = 3,43 \text{ MN}$$

$$\eta_2 = \frac{2,06}{3,43} = 0,60 < 1,0$$

The resistance is clearly larger than the load effect and the first verification is OK.

The horizontal components of the patch loads produce an opposite patch loading and can obviously be resisted according to the model above as the bottom flange is thicker than the web and is stiffened by longitudinal stiffeners. However, there is a significant compression in the bottom flange from global bending, which will be calculated later. The transverse compression spreads quite rapidly and it is deemed sufficient to check for local yielding at the junction with the web:

$$\sigma_{Edx} = -360 \text{ MPa (from second last paragraph of this worked example)}$$

$$\sigma_{Edy} = -\frac{0,50}{0,5 \cdot 0,026} = -38 \text{ MPa}$$

$$\sigma_{Ed,eff} = \sqrt{360^2 + 38^2} - 360 \cdot 38 = 343 < 420 \text{ MPa.}$$

15.2 Bending

The gross section properties of the cross section in Figure 15.2 are:

$$A_{gr} = 0,2686 \text{ m}^2$$

$$I_{gr} = 0,315 \text{ m}^4$$

$$W_{gr,top} = 0,185 \text{ m}^3$$

$$W_{gr,bottom} = 0,294 \text{ m}^3$$

The effective section is calculated according to 4.5 starting with the effective section of the bottom flange, which is assumed to be loaded in uniform compression.

Bottom flange, panel width $b = 700 \text{ mm}$.

$$\varepsilon = \sqrt{\frac{235}{420}} = 0,748$$

$$\bar{\lambda}_p = \frac{0,7 / 0,026}{28,4 \cdot 0,748 \sqrt{4}} = 0,63 < 0,67 \rightarrow \rho_{loc} = 1$$

It is clear that also the 500 mm wide panels are fully effective for local buckling and hence the whole bottom flange. For the stiffeners we get for the top:

$$\bar{\lambda}_p = \frac{0,35/0,008}{28,4 \cdot 0,748 \cdot 2} = 1,03$$

$$\rho_{loc} = \frac{1,03 - 0,22}{1,03^2} = 0,763$$

$$b_{eff} = 0,763 \cdot 0,35 = 0,268 \text{ m}$$

The inclined web has a width of 391 mm and for simplicity it is considered to be uniformly compressed:

$$\bar{\lambda}_p = \frac{0,391/0,008}{28,4 \cdot 0,748 \cdot 2} = 1,15$$

$$\rho_{loc} = \frac{1,15 - 0,22}{1,15^2} = 0,703$$

$$b_{eff} = 0,703 \cdot 0,391 = 0,274 \text{ m}$$

The edge strips of the bottom flange that need not be reduced for stiffener buckling are with reference to Figure 4.4 and formula (4.5) of EN 1993-1-5:

$$\sum b_{edge,eff} t = (0,1 + 0,25) \cdot 2 \cdot 0,026 = 0,0182 \text{ m}^2$$

The central area of the bottom flange is depicted in Figure 15.3 and its effective area is:

$$A_{c,eff,loc} = 0,0806 \text{ m}^2$$

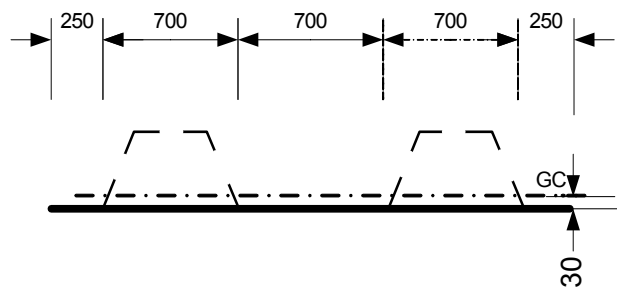


Figure 15.3: Effective cross section of central part of the bottom flange with respect to local buckling

For calculation of critical stresses the gross properties are needed. The cross section in Figure 15.3 but with fully effective stiffeners has the following data:

$$A_{sl} = 0,0858 \text{ m}^2$$

$$e = 0,051 \text{ m}$$

$$I_{sl} = 1,08 \cdot 10^{-3} \text{ m}^4$$

$$i = \sqrt{1,08/85,8} = 0,112 \text{ m}$$

The critical column buckling stress is calculated with formula (4.8):

$$\sigma_{cr,sl} = \frac{\pi^2 210000 \cdot 1,08 \cdot 10^{-3}}{0,0858 \cdot 7,4^2} = 475 \text{ MPa}$$

The critical plate buckling stress can be calculated with formula (A.2). The formula gives a critical stress lower than that for column buckling. The formula (A.2) is a too crude approximation for this case. A better estimate can be found with the theory of buckling of bars on elastic foundation, see 11.2. The method described in A.2.2 is based on this theory but the formulae are not suitable for the present application. Instead the basic theory will be used with a model according to Figure 15.4.

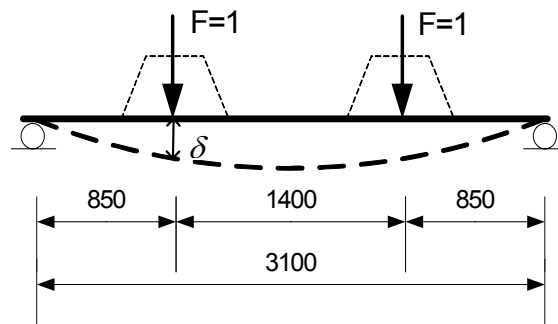


Figure 15.4: Model for deriving the spring stiffness $k = 1/\delta$

The two stiffeners are assumed to buckle simultaneously and the stiffeners are concentrated to their centres of gravity as shown in Figure 15.4. The bending stiffness of a 1 m wide strip of the bottom flange is:

$$D = \frac{210000 \cdot 0,026^3}{10,92} = 0,338 \text{ MNm}$$

The deflection of two unit loads (1 MN/m) becomes:

$$\delta = \frac{1 \cdot 0,85^2}{2 \cdot 0,338} \left[3,1 - \frac{4 \cdot 0,85}{3} \right] = 2,10 \text{ m}^2/\text{MN}$$

The spring stiffness becomes:

$$k = \frac{1}{\delta} = 0,476 \text{ MN/m}^2$$

For buckling in one half-wave the critical axial force becomes, noting that each stiffener has an area and second moment of area equal to half the values calculated for the overall plate:

$$EI = 210000 \cdot 0,0054 = 113 \text{ MNm}^2$$

$$N_{cr1} = \frac{\pi^2 113}{7,4^2} \left(1 + \frac{0,476 \cdot 7,4^4}{\pi^4 \cdot 113} \right) = 23,0 \text{ MN}$$

For two half-waves it becomes:

$$N_{cr,2} = \frac{\pi^2 113}{7,4^2} \left(4 + \frac{0,476 \cdot 7,4^4}{4\pi^4 \cdot 113} \right) = 82,1 \text{ MN}$$

The stiffeners buckles in one half-wave and the critical plate buckling stress becomes:

$$\sigma_{cr,p} = \frac{23,0}{0,0429} = 536 \text{ MPa}$$

The reduction factor for plate buckling ρ can now be calculated according to 4.5.2:

$$\beta_{A,c} = \frac{80,6}{85,8} = 0,939$$

$$\lambda_p = \sqrt{\frac{0,939 \cdot 420}{536}} = 0,857$$

$$\rho = \frac{0,857 - 0,22}{0,857^2} = 0,868$$

The reduction factor χ_c for column type buckling is calculated according to 4.5.3:

$$\bar{\lambda}_c = \sqrt{\frac{0,939 \cdot 420}{475}} = 0,911$$

$e = 0,191 \text{ m}$ (between GC of stiffener and GC of stiffened plate)

$i = 0,112 \text{ m}$

$\alpha = 0,34$ (closed stiffener)

$$\alpha_e = 0,34 + \frac{0,09}{0,112/0,191} = 0,49$$

$\chi_c = 0,594$ (from EN 1993-1-1 6.3.1.2)

The reduction factor ρ_c with respect to interaction between plate and column buckling is calculated from 4.5.4:

$$\xi = \frac{536}{475} - 1 = 0,128$$

$$\rho_c = (0,868 - 0,594) \cdot 0,128 \cdot (2 - 0,128) + 0,594 = 0,660$$

The effective area should also be reduced for shear lag effects, if any. In 3.1(1) a criterion is given:

$$L_e = 2 \cdot 68,2 = 136,4 \text{ m}$$

$$L_e / 50 = 2,73 \text{ m}$$

$b_e = 3,1/2 = 1,55 < 2,73 \text{ m}$, no reduction for shear lag.

The effective area of the compression flange is given by formula (4.5). Its two parts will for practical reasons be kept separate as they have different distances to

the centre of gravity. The reduction of area by ρ_c is thought of as uniform reduction such that its centre of gravity is maintained, see Figure 15.3.

Central part: $A_{eff} = 0,660 \cdot 0,0806 = 0,0532 \text{ m}^2$, $e = 30 \text{ mm}$ from centre of bottom flange.

Edge parts: $A_{eff} = 2 \cdot 0,026 \cdot (0,1 + 0,25) = 0,0182 \text{ m}^2$, $e=0$.

The rest of the cross section is so far the gross section shown in Figure 15.2 and the properties of the effective area is shown in Figure 15.5. Next step is to determine the effective area of the webs. This is done according to 4.4 assuming that the yield strength is reached:

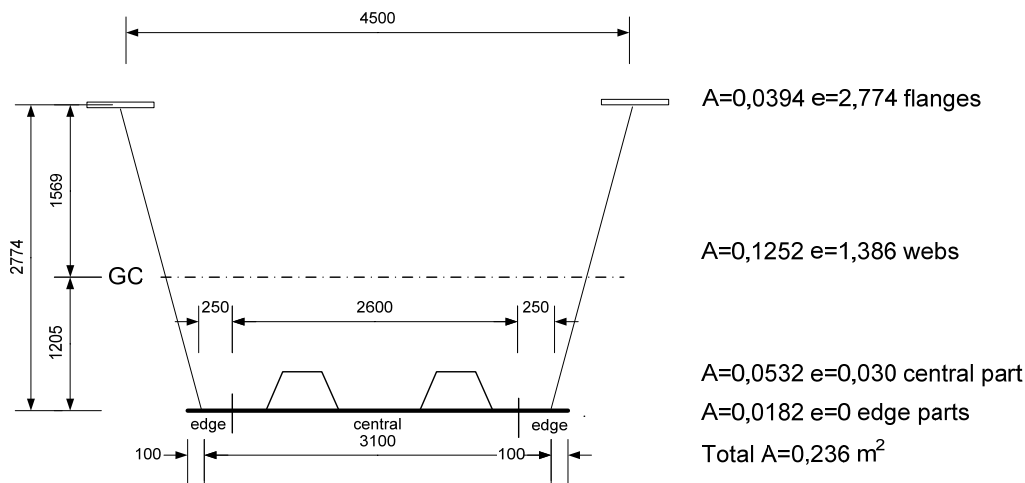


Figure 15.5: Effective cross section after reduction of the bottom flange

$$\psi = -\frac{1,569 - 0,0135}{1,205 - 0,013} = -1,30$$

$$k_\sigma = 7,81 + 6,29 \cdot 1,30 + 9,78 \cdot 1,30^2 = 32,5$$

$$\varepsilon = \sqrt{\frac{235}{420}} = 0,748$$

$$\bar{\lambda}_p = \frac{2,846}{0,022} \frac{1}{28,4 \cdot 0,748 \cdot \sqrt{32,5}} = 1,07$$

$$\rho = \frac{1,07 - 0,055(3 - 1,30)}{1,07^2} = 0,853$$

Inclined depth of the compression zone $(1,205 - 0,013) / \cos(14) = 1,229 \text{ m}$

$$b_{eff} = 0,853 \cdot 1,229 = 1,048 \text{ m}$$

This leaves a hole of $1,229 - 1,048 = 0,181 \text{ m}$ in the webs located with its centre at distance from centre of the bottom flange of

$$e_h = 0,013 + (0,4 \cdot 1,048 + 0,181 / 2) \cos 14 = 0,507 \text{ m}$$

The reduction of the web areas becomes

$$\Delta A = 2 \cdot 0,022 \cdot 0,181 = 0,00796 \text{ m}^2$$

The effective area of the cross section now becomes

$$A_{eff} = 0,236 - 0,00796 = 0,228 \text{ m}^2$$

and the GC shifts to

$$e = \frac{1}{0,228} (0,236 \cdot 1,205 - 0,00796 \cdot 0,507) = 1,229 \text{ m}$$

The second moment of area and section moduli calculated with respect to the centroid of the respective flanges for the final effective section becomes:

$$I_{eff} = 0,275 \text{ m}^4$$

$$W_{eff,top} = \frac{0,275}{(2,774 - 1,229)} = 0,178 \text{ m}^3$$

$$W_{eff,bottom} = \frac{0,275}{1,229} = 0,224 \text{ m}^3$$

The bending resistance will be the lowest of:

$$M_{Rd,top} = 460 \cdot 0,178 = 81,9 \text{ MNm}$$

$$M_{Rd,bottom} = 420 \cdot 0,224 = 94,0 \text{ MNm}$$

According to this calculation the top flange governs the bending resistance. However, the girder is hybrid with webs and lower flange in S420 and there will be partial yielding in the webs before the flange stress reaches 460 MPa. This is allowed according to 4.3(6) of EN 1993-1-5 but the bending resistance has to be corrected for yielding in the webs. When the stress is 460 MPa in the centre of the top flange the stress at the top of the web should be 456 MPa but it can only be 420 MPa. This means that $456 - 420 = 36$ MPa is “missing”. The depth of the yielded zone is 126 mm and the missing force is:

$$\Delta F = \frac{1}{2} \cdot 2 \cdot 36 \cdot 0,022 \cdot 0,126 = 0,10 \text{ MN}$$

As this is a small correction the shift of the neutral axis is neglected and the corrected bending resistance becomes:

$$M_{Rd} = 81,9 - 0,10 \cdot (1,545 - 0,027/2 - 0,126/3) = 81,75 \text{ MNm.}$$

The actual design bending moment is 80,5 MNm and:

$$\eta_1 = \frac{80,5}{81,75} = 0,985$$

From the check of patch loading resistance we have:

$$\eta_2 = 0,60$$

The final verification is for interaction according to 7.2:

$$0,60 + 0,8 \cdot 0,985 = 1,39 < 1,4 \text{ OK}$$

The actual stress in the bottom flange is:

$$\sigma_b = \frac{80,5 \cdot 1,229}{0,275} = 360 \text{ MPa}$$

instead of 420, which was assumed calculating the effective cross section. A recalculation using the actual stress would give a higher bending resistance.

The design criterion for interaction is empirical and it has been developed from tests on doubly symmetric I-beams. As it was applied above, the bending resistance was determined by yielding in the unloaded tension flange. Using that bending resistance in the interaction formula is most likely conservative because the interaction must be caused by the state of stress in the neighbourhood of the patch load where the bending stresses are lower.

16 Worked example – Orthotropic plate with trapezoid stiffeners

Darko Beg, P. Skuber, L. Pavlovic, P. Moze, Faculty of Civil and Geodetic Engineering, University of Ljubljana

16.1 Data

The orthotropic plate is a part of a bottom flange of a two span continuous box girder at the interior support. The height of the girder is equal to $h_w = 3,8$ m. Each of the adjacent spans L are 91 m long. The plate is loaded at the edges with compression stresses σ_{Ed} from bending moments and shear stresses τ_{Ed}^t from torque all related to the gross cross-section. Shear stresses τ_{Ed}^v from shear forces in the webs are shown for equilibrium reasons and are not relevant for the design of the orthotropic plate for global buckling but for checking the subpanels, see 7.1(5) of EN 1993-1-5.

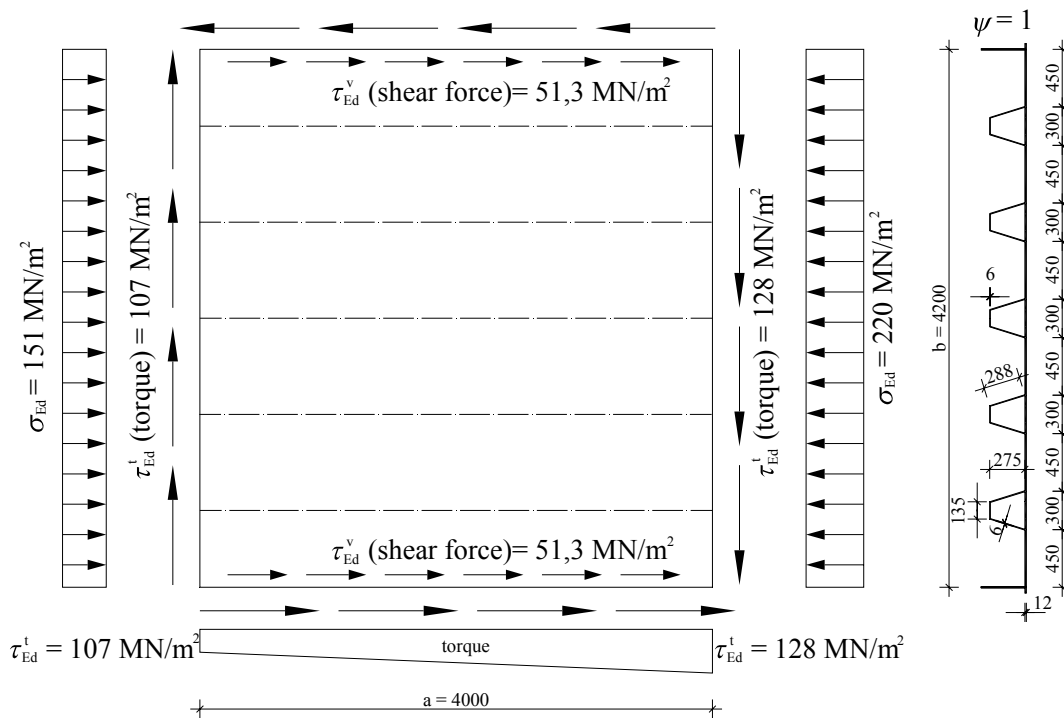


Figure 16.1: System and loading

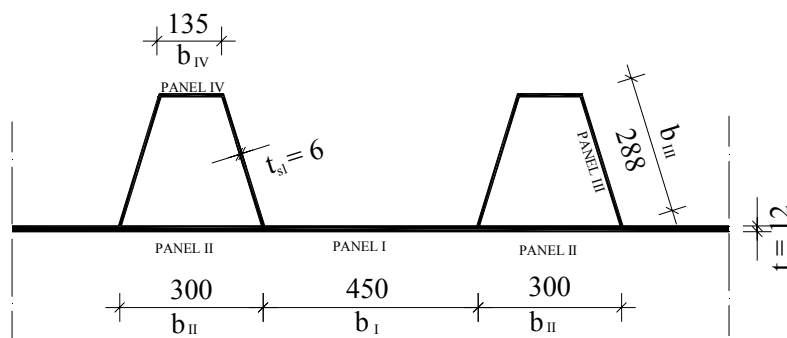


Figure 16.2: Stiffener

$$\text{Material S355} \quad f_y = 355 \text{ N/mm}^2 = 355 \cdot 10^6 \text{ N/m}^2 \quad \varepsilon = \sqrt{\frac{235}{355}} = 0,814$$

$$\gamma_{M0} = 1,00; \quad \gamma_{M1} = 1,10.$$

Geometric characteristics of sections were calculated by the use of AutoCAD 2000.

16.2 Direct stresses

16.2.1 Subpanels – calculation of effective^p areas of subpanels

Panel I (plate between two longitudinal stiffeners): $b_I = 450 \text{ mm} = 450 \cdot 10^{-3} \text{ m}$

$$\bar{\lambda}_{p,I} = \frac{b_I/t}{28,4\varepsilon\sqrt{k_\sigma}} = \frac{(450 \cdot 10^{-3})/(12 \cdot 10^{-3})}{28,4 \cdot 0,814 \cdot \sqrt{4}} = 0,811$$

$$\rho_I = \frac{\bar{\lambda}_{p,I} - 0,055(3 + \psi)}{\bar{\lambda}_{p,I}^2} = \frac{0,811 - 0,055(3 + 1)}{0,811^2} = 0,899$$

$$b_{\text{eff},I} = \rho_I b_I = 0,899 \cdot 450 \cdot 10^{-3} = 405 \cdot 10^{-3} \text{ m}$$

$$A_{\text{eff},I} = \rho_I A_I = 0,899 \cdot 450 \cdot 10^{-3} \cdot 12 \cdot 10^{-3} = 4,855 \cdot 10^{-3} \text{ m}^2$$

Panel II (plate between one longitudinal stiffener): $b_{II} = 300 \text{ mm}$

$$\bar{\lambda}_{p,II} = \frac{b_{II}/t}{28,4\varepsilon\sqrt{k_\sigma}} = \frac{(300 \cdot 10^{-3})/(12 \cdot 10^{-3})}{28,4 \cdot 0,814 \cdot \sqrt{4}} = 0,541 < 0,673 \Rightarrow \rho_{II} = 1,0 \Rightarrow$$

$$A_{\text{eff},II} = A_{II}, \quad b_{\text{eff},II} = b_{II}$$

No reduction for local buckling.

Panel III (stiffener – inclined web): $b_{III} = 288 \text{ mm} = 288 \cdot 10^{-3} \text{ m}$

$$\bar{\lambda}_{p,III} = \frac{b_{III}/t_{sl}}{28,4\varepsilon\sqrt{k_\sigma}} = \frac{(288 \cdot 10^{-3})/(6 \cdot 10^{-3})}{28,4 \cdot 0,814 \cdot \sqrt{4}} = 1,038$$

$$\rho_{III} = \frac{\bar{\lambda}_{p,III} - 0,055(3 + \psi)}{\bar{\lambda}_{p,III}^2} = \frac{1,038 - 0,055(3 + 1)}{1,038^2} = 0,759$$

$$b_{\text{eff},III} = \rho_{III} b_{III} = 0,759 \cdot 288 \cdot 10^{-3} = 219 \cdot 10^{-3} \text{ m}$$

$$A_{\text{eff},III} = \rho_{III} A_{III} = 0,759 \cdot 288 \cdot 10^{-3} \cdot 6 \cdot 10^{-3} = 1,312 \cdot 10^{-3} \text{ m}^2$$

Panel IV (stiffener – part parallel to plate): $b_{IV} = 135 \text{ mm} = 135 \cdot 10^{-3} \text{ m}$

$$\bar{\lambda}_{p,IV} = \frac{b_{IV} / t_{sl}}{28,4 \varepsilon \sqrt{k_{\sigma}}} = \frac{(135 \cdot 10^{-3}) / (6 \cdot 10^{-3})}{28,4 \cdot 0,814 \cdot \sqrt{4}} = 0,487 < 0,673 \Rightarrow$$

$$A_{\text{eff},IV} = A_{IV}, \quad b_{\text{eff},IV} = b_{IV}$$

No reduction for local buckling.

16.2.2 Stiffened plate

Relevant cross section

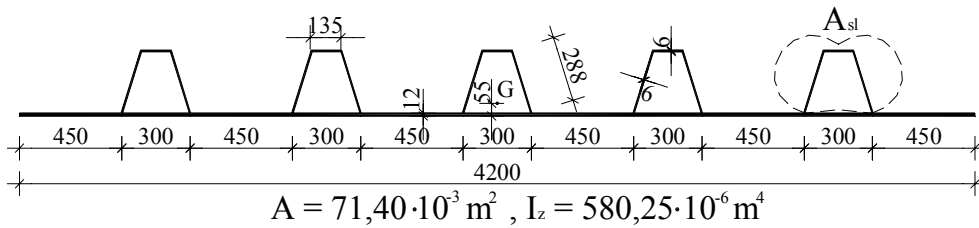


Figure 16.3: Gross cross section

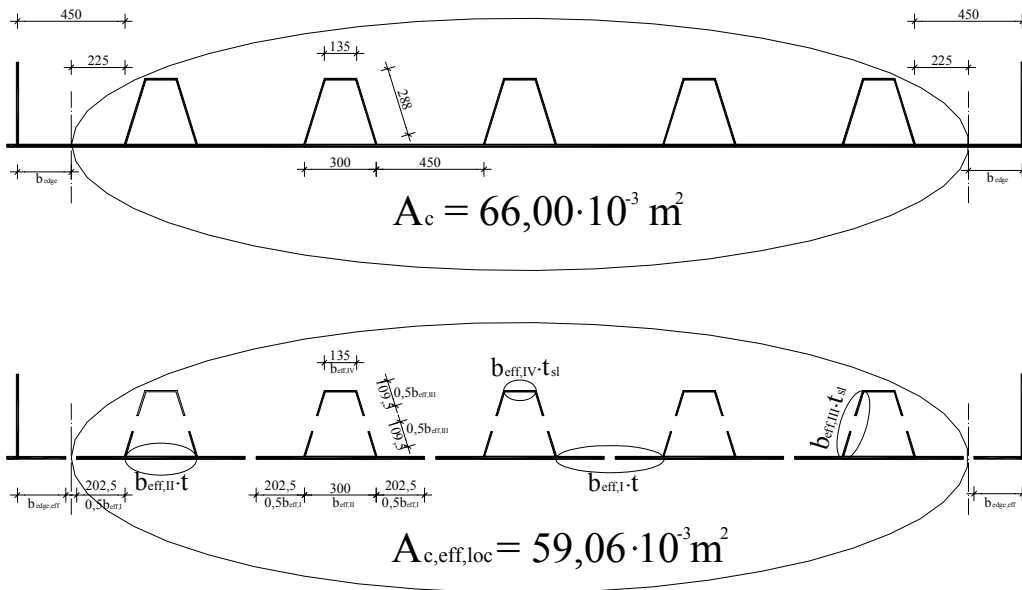


Figure 16.4: Cross section considered and $A_{c,eff,loc}$

A_c is the gross area of the compression zone of the stiffened plate except the parts of subpanels supported by an adjacent plate, see Figure 16.4

\sum_c applies to the part of the stiffened panel width that is in compression except the parts $b_{\text{edge,eff}}$, see Figure 16.4

$A_{c,eff,loc}$ is the effective^p section areas of all the stiffeners and subpanels that are fully or partially in the compression zone except the effective parts

supported by an adjacent plate element with the width $b_{edge,eff}$, see Figure 16.4.

$A_{sl,eff}$ is the sum of the effective^p section according to EN 1993-1-5, 4.4 of all longitudinal stiffeners with gross area A_{sl} located in the compression zone (see Figure 16.4)

$b_{c,loc}$ is the width of the compressed part of each subpanel

ρ_{loc} is the reduction factor from 16.2.1 for each subpanel.

$$A = 71,4 \cdot 10^{-3} \text{ m}^2, \quad I_z = 580,25 \cdot 10^{-6} \text{ m}^4$$

$$A_c = 71,4 \cdot 10^{-3} - 450 \cdot 10^{-3} \cdot 12 \cdot 10^{-3} = 66,0 \cdot 10^{-3} \text{ m}^2$$

$$A_{c,eff,loc} = A_{sl,eff} + \sum_c \rho_{loc} b_{c,loc} t = (5b_{eff,IV} t_{sl} + 10b_{eff,III} t_{sl}) + 5(b_{eff,I} t + b_{eff,II} t)$$

$$A_{c,eff,loc} = 59,06 \cdot 10^{-3} \text{ m}^2$$

Plate type buckling behaviour

Calculation of k_σ

$\sum I_{sl}$ is the sum of the second moment of area of the whole stiffened plate;

I_p is the second moment of area for bending of the plate

$$= \frac{bt^3}{12(1-\nu^2)} = \frac{bt^3}{10,92}$$

$\sum A_{sl}$ is the sum of the gross area of the individual longitudinal stiffeners;

A_p is the gross area of the plate = bt ;

$$\gamma = \frac{\sum I_{sl}}{I_p} = \frac{10,92 I_z}{bt^3} = \frac{10,92 \cdot 580,25 \cdot 10^{-6}}{4,2 \cdot (12 \cdot 10^{-3})^3} = 873,1$$

$$\delta = \frac{\sum A_{sl}}{A_p} = \frac{5 \cdot 4,2 \cdot 10^{-3}}{4,2 \cdot 12 \cdot 10^{-3}} = 0,417$$

$$\alpha = \frac{a}{b} = \frac{4}{4,2} = 0,952 \geq 0,5$$

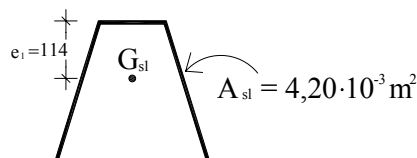


Figure 16.5: Cross section of single stiffener

$\alpha = 0,952 \leq \sqrt[4]{\gamma} = 5,44 \Rightarrow$ (using equation (A.2) of EN 1993-1-5)

$$\Rightarrow k_{\sigma,p} = \frac{2\left((1+\alpha^2)^2 + \gamma - 1\right)}{\alpha^2(\psi+1)(1+\delta)} = \frac{2\left((1+0,952^2)^2 + 873,1 - 1\right)}{0,952^2(1+1)(1+0,417)} = 681,9$$

$k_{\sigma,p}$ was calculated using the Equation A.2 from EN 1993-1-5. $k_{\sigma,p}$ may be determined in several ways: by simplified analytical expressions (e.g. Eq. A.2), by using suitable charts (e.g. Kloppel charts) or by FE analysis. The results can be substantially different depending on the accuracy of the tool used and on the accuracy of the boundary conditions taken into account.

Calculation of elastic critical plate buckling stress

$$\sigma_E = \frac{\pi^2 E t^2}{12(1-\nu^2)b^2} = \frac{\pi^2 \cdot 210 \cdot 10^9 \cdot (12 \cdot 10^{-3})^2}{12(1-0,3^2) \cdot 4,2^2} = 1,55 \cdot 10^6 \text{ N/m}^2$$

$$\sigma_{cr,p} = k_{\sigma,p} \sigma_E = 681,9 \cdot 1,55 \cdot 10^6 = 1,057 \cdot 10^9 \text{ N/m}^2$$

Slenderness of stiffened plate

$$\beta_{A,c} = \frac{A_{c,eff,loc}}{A_c} = \frac{59,06 \cdot 10^{-3}}{66,0 \cdot 10^{-3}} = 0,895$$

$$\bar{\lambda}_p = \sqrt{\frac{\beta_{A,c} f_y}{\sigma_{cr,p}}} = \sqrt{\frac{0,895 \cdot 355 \cdot 10^6}{1,057 \cdot 10^9}} = 0,548 \leq 0,673 \Rightarrow \rho = 1$$

No reduction for buckling of a stiffened plate.

Column type buckling behaviour

Critical stress of a stiffener

$A_{sl,1}$ is the gross cross-sectional area of the stiffener and the adjacent parts of the plate according to Figure 16.6

$I_{sl,1}$ is the second moment of area of the stiffener, relative to the out-of-plane bending of the plate according to Figure 16.6

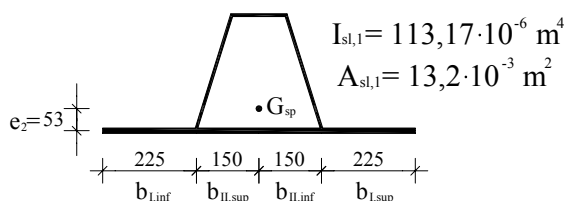


Figure 16.6: Cross section of single stiffener and adjacent parts

$$b_{l,inf} = \frac{3-\psi}{5-\psi} b_1 = 0,5b_1$$

$$b_{l,sup} = \frac{2}{5-\psi} b_1 = 0,5b_1$$

$$b_{II,inf} = \frac{3-\psi}{5-\psi} b_{II} = 0,5b_{II} \qquad b_{II,sup} = \frac{2}{5-\psi} b_{II} = 0,5b_{II}$$

$$A_{sl,1} = 13,2 \cdot 10^{-3} \text{ m}^2, \quad I_{sl,1} = 113,17 \cdot 10^{-6} \text{ m}^4$$

$$\sigma_{cr,sl} = \frac{\pi^2 EI_{sl,1}}{A_{sl,1} a^2} = \frac{\pi^2 210 \cdot 10^9 \cdot 113,17 \cdot 10^{-6}}{13,2 \cdot 10^{-3} \cdot 4^2} = 1,111 \cdot 10^9 \text{ N/m}^2$$

There is a stress gradient along the panel that increases the critical column buckling stress. That effect was not taken into account in the given calculation, but can be easily included as the relevant information is available in handbooks.

Extrapolation of elastic critical column buckling stress to the edge of the panel

$$b_c = b_{sl,1} \quad (\psi = 1)$$

$$\sigma_{cr,c} = \frac{b_c}{b_{sl,1}} \sigma_{cr,sl} = \sigma_{cr,sl} = 1,111 \cdot 10^9 \text{ N/m}^2$$

$\sigma_{cr,c}$ is slightly larger than $\sigma_{cr,p}$ which is theoretically not possible. This results from the approximation of the mechanical model of the stiffened plate.

Slenderness of a stiffener as a column

$A_{sl,1,eff}$ is the effective cross-sectional area of the stiffener with due allowance for plate buckling, see Figure 16.7

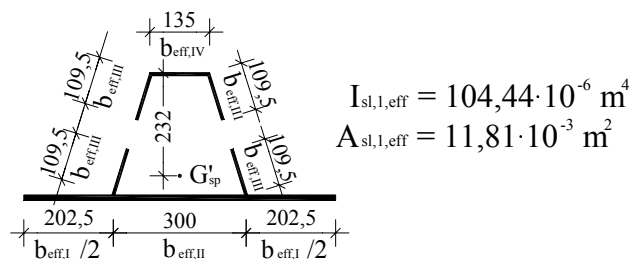


Figure 16.7: Effective cross sectional area of stiffener

$$\beta_{A,c} = \frac{A_{sl,1,eff}}{A_{sl,1}} = \frac{11,81 \cdot 10^{-3}}{13,2 \cdot 10^{-3}} = 0,895$$

$$\bar{\lambda}_c = \sqrt{\frac{\beta_{A,c} f_y}{\sigma_{cr,c}}} = \sqrt{\frac{0,895 \cdot 355 \cdot 10^6}{1,111 \cdot 10^9}} = 0,535$$

Reduction factor χ

$$i = \sqrt{\frac{I_{sl,1}}{A_{sl,1}}} = \sqrt{\frac{113,17 \cdot 10^{-6}}{13,2 \cdot 10^{-3}}} = 92,6 \cdot 10^{-3} \text{ m}$$

$e = \max(e_1, e_2)$ is the largest distance from the respective centroids of the plating and the one-sided stiffener (or of the centroids of either set of stiffeners when present on both sides) to the neutral axis of the column, see Figure 16.8.

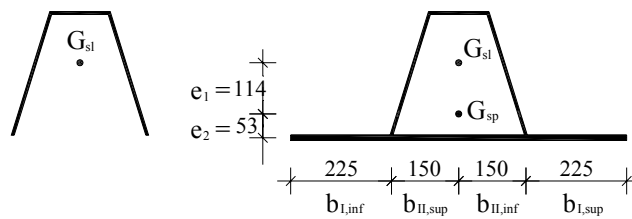


Figure 16.8: Distances e_1 and e_2

$\alpha = 0,34$ (curve b) for closed section stiffeners

$$e = \max(e_1; e_2) = \max(114 \cdot 10^{-3}; 53 \cdot 10^{-3}) = 114 \cdot 10^{-3} \text{ m}$$

$$\alpha_e = \alpha + \frac{0,09}{i/e} = 0,34 + \frac{0,09}{92,6 \cdot 10^{-3} / 114 \cdot 10^{-3}} = 0,451$$

$$\phi = 0,5 \left[1,0 + \alpha_e (\bar{\lambda}_c - 0,2) + \bar{\lambda}_c^2 \right]$$

$$\phi = 0,5 \left[1,0 + 0,451(0,535 - 0,2) + 0,535^2 \right] = 0,719$$

$$\chi_c = \frac{1}{\phi + \sqrt{\phi^2 - \bar{\lambda}_c^2}} = \frac{1}{0,719 + \sqrt{0,719^2 - 0,535^2}} = 0,834$$

Interaction between plate and column buckling

$$\xi = \frac{\sigma_{cr,p}}{\sigma_{cr,c}} - 1 = \left(\frac{1,057 \cdot 10^9}{1,111 \cdot 10^9} \right)^2 - 1 = -0,095.$$

Therefore the case $\xi = 0$ applies, see Figure 4.5.

$$\rho_c = (\rho - \chi_c) \xi (2 - \xi) + \chi_c = (1,00 - 0,834) \cdot 0 \cdot (2 - 0) + 0,834 = 0,834$$

Verification for uniform compression

$A_{c,eff}$ is the effective cross-section area in accordance with EN 1993-1-5, 4.5.1(3);

$$\begin{aligned} A_{c,eff} &= \rho_c A_{c,eff,loc} + \sum b_{edge,eff} t = \\ &= 0,834 \cdot 59,06 \cdot 10^{-3} + 0,899 \cdot 450 \cdot 10^{-3} \cdot 12 \cdot 10^{-3} = 54,111 \cdot 10^{-3} \text{ m}^2 \end{aligned}$$

Effect of shear lag

If $b_0 \leq \frac{L_e}{50}$, shear lag in flanges may be neglected.

$$L_e = 0,25(2L) = 0,25 \cdot 2 \cdot 91 = 45,5 \text{ m}$$

$$b_0 = \frac{b}{2} = 2,1\text{ m} > \frac{L_e}{50} = \frac{45,5}{50} = 0,91\text{ m} \quad \checkmark$$

$$\alpha_0 = \sqrt{1 + \frac{\sum A_{sl}}{b_0 t_f}} = \sqrt{\frac{5 \cdot 4,2 \cdot 10^{-3}}{2,1 \cdot 12 \cdot 10^{-3}}} = 1,354$$

$$\kappa = \frac{\alpha_0 b_0}{L_e} = \frac{1,345 \cdot 2,1}{45,5} = 0,062$$

$$\beta = \left(1 + 6,0 \left(\kappa - \frac{1}{2500\kappa} \right) + 1,6\kappa^2 \right)^{-1} = \left(1 + 6,0 \left(0,062 - \frac{1}{2500 \cdot 0,062} \right) + 1,6 \cdot 0,062^2 \right)^{-1}$$

$$\beta = 0,747$$

$$A_{\text{eff}} = A_{\text{c,eff}} \beta^\kappa = (54,111 \cdot 10^{-3}) \cdot 0,747^{0,062} = 53,14 \cdot 10^{-3} \text{ m}^2$$

$$A_{\text{eff}} = 53,14 \cdot 10^{-3} \text{ m}^2 \geq A_{\text{c,eff}} \beta = 54,111 \cdot 10^{-3} \cdot 0,747 = 40,4 \cdot 10^{-3} \text{ m}^2 \quad \checkmark$$

Verification for compression at the most compressed edge

$$\eta_1 = \frac{N_{\text{Ed}}}{f_y / \gamma_{M0} A_{\text{c,eff}}} = \frac{\sigma_{\text{Ed}} A}{f_y / \gamma_{M0} A_{\text{c,eff}}} = \frac{220 \cdot 10^6 \cdot 71,4 \cdot 10^3}{355 \cdot 10^6 / 1,0 \cdot 53,14 \cdot 10^{-3}} = 0,883 \leq 1,0 \quad \checkmark$$

The compression stress check was performed for the largest stress at the edge of the panel. It is allowed (EN 1993-1-5, 4.6(3)) to carry out the verification for the stress resultants at a distance 0,4a or 0,5b (whichever is smaller) from the panel end with largest stresses.

16.2.3 Minimum requirements for longitudinal stiffeners

No check of torsional buckling is needed for closed stiffeners (see 9.2.1(7) and (8) of EN 1993-1-5).

16.3 Resistance to shear

S355, $\eta=1,2$

16.3.1 Stiffened plate

I_{sl} is the second moment of area of the longitudinal stiffener about the z-axis, see Figure 16.9. For plates with two or more longitudinal stiffeners, not necessarily equally spaced, I_{sl} is the sum of the stiffness of the individual stiffeners.

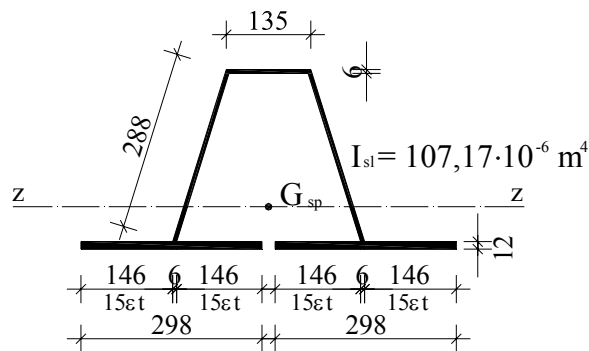


Figure 16.9: Cross section of stiffener

$$h_w = b = 4,2 \text{ m}$$

$$b_1 = 15\epsilon t = 15 \cdot 0,814 \cdot 12 \cdot 10^{-3} = 146 \cdot 10^{-3} \text{ m}$$

$$b_2 = 15\epsilon t = 15 \cdot 0,814 \cdot 12 \cdot 10^{-3} = 146 \cdot 10^{-3} \text{ m}$$

$$k_{\tau, st} = 9 \left(\frac{h_w}{a} \right)^2 \sqrt[4]{\left(\frac{\sum I_{sl}}{t^3 h_w} \right)^3} \geq \frac{2,1}{t} \sqrt[3]{\frac{\sum I_{sl}}{h_w}}$$

$$k_{\tau, st} = 9 \left(\frac{4,2}{4} \right)^2 \cdot \sqrt[4]{\left(\frac{5 \cdot 107,17 \cdot 10^{-6}}{(12 \cdot 10^{-3})^3 \cdot 4,2} \right)^3} = 249,924 \geq \frac{2,1}{12 \cdot 10^{-3}} \cdot \sqrt[3]{\frac{5 \cdot 107,17 \cdot 10^{-6}}{4,2}} = 8,8$$

$$k_{\tau} = 4,00 + 5,34 \left(\frac{h_w}{a} \right)^2 + k_{\tau, st} = 4,00 + 5,34 \left(\frac{4,2}{4} \right)^2 + 249,924 = 259,811$$

$$\bar{\lambda}_w = \frac{h_w / t}{37,4 \cdot \epsilon \cdot \sqrt{k_{\tau}}} = \frac{4,2 / (12 \cdot 10^{-3})}{37,4 \cdot 0,814 \cdot \sqrt{259,811}} = 0,713$$

16.3.2 Subpanels

Subpanel 1

$$h_{w1} = b_1 = 146 \cdot 10^{-3} \text{ m}$$

$k_{\tau1, st} = 0$ – no stiffener in the subpanel

$$k_{\tau1} = 5,34 + 4,00 \left(\frac{h_{w1}}{a} \right)^2 + k_{\tau1, st} = 5,34 + 4,00 \left(\frac{146 \cdot 10^{-3}}{4} \right)^2 = 5,391$$

$$\bar{\lambda}_{w1} = \frac{h_{w1} / t}{37,4 \cdot \epsilon \cdot \sqrt{k_{\tau1}}} = \frac{(146 \cdot 10^{-3}) / (12 \cdot 10^{-3})}{37,4 \cdot 0,814 \cdot \sqrt{5,391}} = 0,531$$

Subpanel 2

$$h_{wII} = b_{II} = 300 \cdot 10^{-3} \text{ m}$$

$k_{\tau 2, st} = 0$ – no stiffener in the subpanel

$$k_{\tau 2} = 5,34 + 4,00 \left(\frac{h_{w2}}{a} \right)^2 + k_{\tau 2, st} = 5,34 + 4,00 \left(\frac{300 \cdot 10^{-3}}{4} \right)^2 = 5,363$$

$$\bar{\lambda}_{w2} = \frac{h_{w2}/t}{37,4 \cdot \varepsilon \cdot \sqrt{k_{\tau 2}}} = \frac{(300 \cdot 10^{-3})/(12 \cdot 10^{-3})}{37,4 \cdot 0,814 \cdot \sqrt{5,363}} = 0,355$$

16.3.3 Shear buckling factor

$$\max(\bar{\lambda}_w; \bar{\lambda}_{w1}; \bar{\lambda}_{w2}) = \max(0,713; 0,531; 0,355) = \bar{\lambda}_w = 0,713 \Rightarrow$$

shear buckling of the stiffened plate is critical:

$$\frac{0,83}{\eta} = \frac{0,83}{1,2} = 0,69 \leq \bar{\lambda}_w = 0,713 < 1,08 \Rightarrow$$

$$\Rightarrow \chi_w = \frac{0,83}{\bar{\lambda}_w} = \frac{0,83}{0,713} = 1,16$$

16.3.4 Verification

$$\eta_3 = \frac{V_{Ed}}{V_{b,Rd}} = \frac{\tau_{Ed}}{\chi \frac{f_{yw}}{\gamma_{M1} \sqrt{3}}} = \frac{128 \cdot 10^6 \cdot 1,1 \cdot \sqrt{3}}{1,16 \cdot 355 \cdot 10^6} = 0,592 \leq 1,0 \quad \checkmark$$

16.4 Interaction M-V-N

A flange of a box girder should be verified using the following equation:

$$\bar{\eta}_1 + (2\bar{\eta}_3 - 1)^2 \leq 1,0 \quad (\text{EN 1993-1-5, 7.1(5)})$$

where $\bar{\eta}_1$ is calculated as in 0, but at the cross section at a distance $h_w/2$ from the interior support and $\bar{\eta}_3$ is calculated based on average shear stress in the panel (but not less than half the maximum shear stress).

Compression stress at the cross section located at a distance $h_w/2$ from the interior support:

$$\sigma_{\text{Ed}_{h_w/2}} = \left((220 - 151) \frac{4,0 - 3,8/2}{4,0} + 151 \right) \cdot 10^6 = 187,2 \cdot 10^6 \frac{\text{N}}{\text{m}^2}$$

Average shear stress in the panel:

$$\bar{\tau}_{\text{Ed}} = \left(\frac{128 - 107}{2} + 107 \right) 10^6 = 117,5 \cdot 10^6 \frac{\text{N}}{\text{m}^2} \geq \frac{\tau_{\text{max,Ed}}}{2} = \frac{128 \cdot 10^6}{2} = 64 \cdot 10^6 \frac{\text{N}}{\text{m}^2} \quad \checkmark$$

Verification of interaction within the flange

$$\bar{\eta}_1 = \frac{\sigma_{\text{Ed}} A}{f_y / \gamma_{M0} A_{\text{eff}}} = \frac{187,2 \cdot 10^6 \cdot 71,4}{355 \cdot 10^6 / 1,0 \cdot 53,14} = 0,709 \leq 1,0 \quad \checkmark$$

$$\tau_{\text{Rd}} = \chi_w \frac{f_{yw}}{\gamma_{M1} \sqrt{3}} = \frac{1,16 \cdot 355 \cdot 10^6}{1,1 \cdot \sqrt{3}} = 216 \cdot 10^6 \frac{\text{N}}{\text{m}^2}$$

$$\bar{\eta}_3 = \frac{\bar{\tau}_{\text{Ed}}}{\tau_{\text{Rd}}} = \frac{117,5}{216} = 0,544$$

$$\bar{\eta}_1 + (2\bar{\eta}_3 - 1)^2 = 0,709 + (2 \cdot 0,544 - 1)^2 = 0,717 \leq 1 \quad \checkmark$$

Additional verification of shear buckling of the subpanel, assuming the longitudinal stiffeners are rigid. The most unfavourable subpanel is Subpanel I (see 16.2.1 and 0).

$$b_1 = 450 \cdot 10^{-3} \text{ m} \Rightarrow \bar{\lambda}_{w1} = 0,531$$

$$\bar{\lambda}_{w1} = 0,531 < \frac{0,83}{\eta} = \frac{0,83}{1,2} \Rightarrow \chi_w = \eta = 1,2$$

$$\tau_{\text{Rd}} = \chi_w \frac{f_{yw}}{\gamma_{M1} \sqrt{3}} = 1,2 \frac{355 \cdot 10^6}{1,1 \cdot \sqrt{3}} = 223,6 \cdot 10^6 \frac{\text{N}}{\text{m}^2}$$

$$\bar{\eta}_3 = \frac{\bar{\tau}_{\text{Ed}}}{\tau_{\text{Rd}}} = \frac{117,5}{223,6} = 0,525 \quad \checkmark$$

17 Worked example – Plate girder

Darko Beg, P. Skuber, L. Pavlovic, P. Moze, Faculty of Civil and Geodetic Engineering, University of Ljubljana

17.1 Data

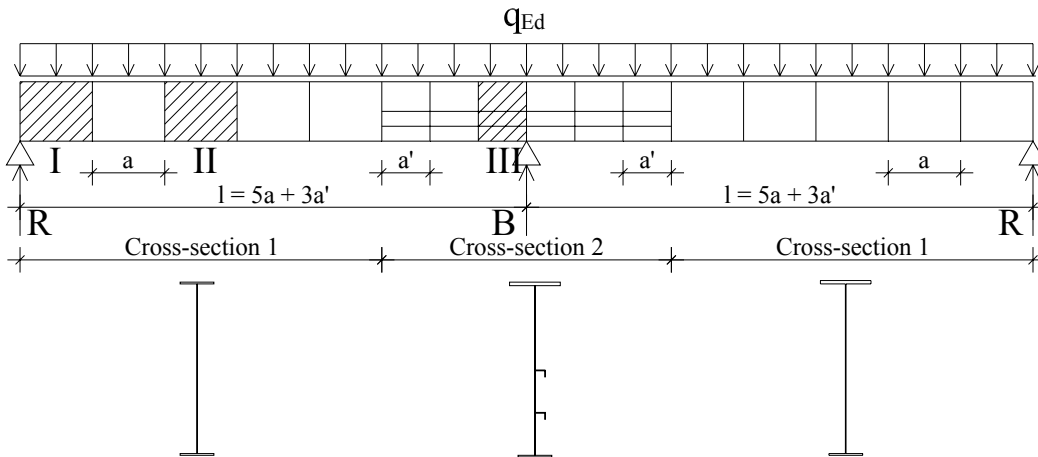


Figure 17.1: Overview and numbering of panels with cross section 1, 2 and 3

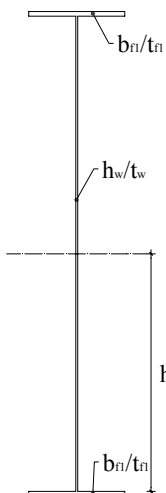
S 235 $\Rightarrow f_y = 235$ MPa

$$\varepsilon = \sqrt{\frac{235}{f_y [N/mm^2]}} = \sqrt{\frac{235}{235}} = 1$$

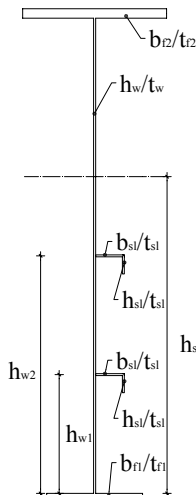
$\gamma_{M0} = 1,0$

$\gamma_{M1} = 1,0$

Cross-section 1



Cross-section 2



$a = 3$ m

$a' = 2$ m

$l = 21$ m

$q_{Ed} = 85$ kN/m

$b_{f1} / t_{f1} = 400 / 20$ mm

$b_{f2} / t_{f2} = 600 / 40$ mm

$h_w / t_w = 2000 / 8$ mm

$b_{sl} / t_{sl} = 120 / 8$ mm

$h_{sl} / t_{sl} = 80 / 8$ mm

$h_{st} / b_{st} / t_{st,w} / t_{st,f} = 180 / 180 / 10 / 20$ mm

$h_{w1} = 500$ mm

$h_{w2} = 1000$ mm

Transverse stiffener

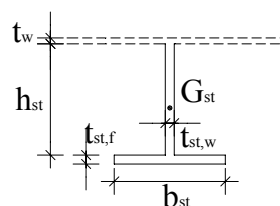


Figure 17.2: Cross sections

A two span continuous plate girder is selected in this numerical example to enable us to illustrate the design rules for the panels at the exterior and interior support as well as in the mid span. The example is not intended to show an optimal girder design but to illustrate the application of several design rules. The design loading q_{Ed} includes self-weight of the girder and all other relevant permanent and variable loads.

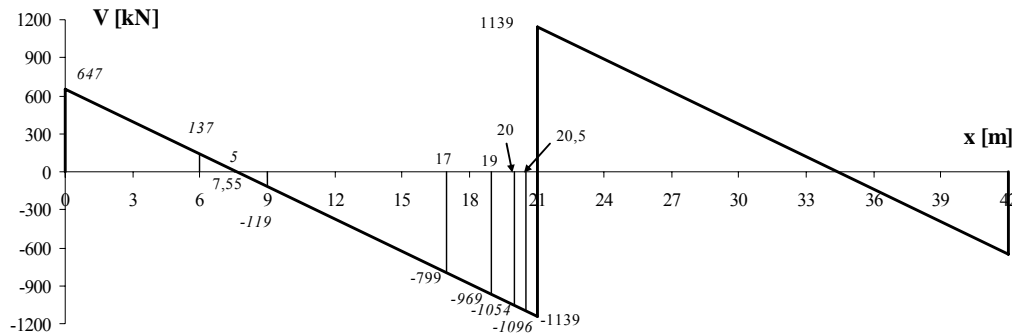


Figure 17.3: Shear force

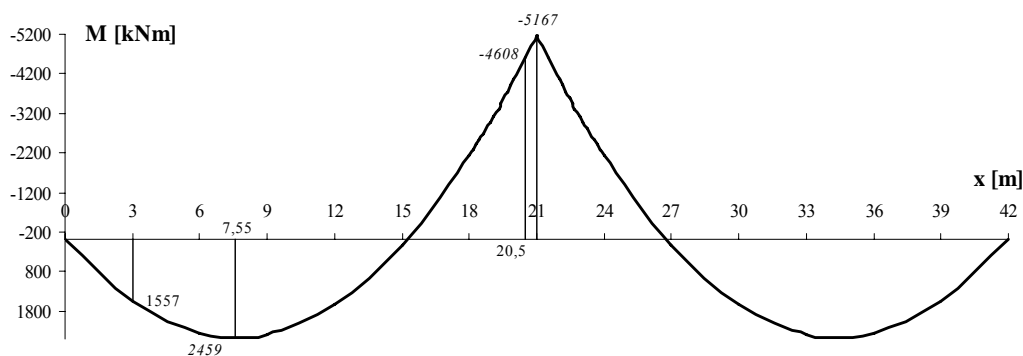


Figure 17.4: Bending moment

Shear force and bending moment were calculated by the use of Esa Prima Win version 3.30. An elastic global analysis based on gross cross-section properties was performed. All the calculations further in the text were calculated by Microsoft Excel.

17.2 Shear lag in the flanges

If $b_0 \leq \frac{L_e}{50}$, shear lag in flanges may be neglected.

17.2.1 Elastic shear lag (serviceability, fatigue)

$$L_e^{\text{midspan}} = 0,85L_1 = 0,85 \cdot 21 = 17,85 \text{ m},$$

$$L_e^{\text{support}} = 0,25(L_1 + L_2) = 0,25(21 + 21) = 10,5 \text{ m}$$

$$\text{midspan: } b_0 = \frac{b_{f1}}{2} = \frac{0,40}{2} = 0,20 \text{ m} \leq \frac{L_e}{50} = \frac{17,85}{50} = 0,357 \text{ m}, \beta_1 = 1,0 \quad \checkmark$$

support: $b_0 = \frac{b_{f1}}{2} = \frac{0,40}{2} = 0,20 \text{ m} \leq \frac{L_e}{50} = \frac{10,50}{50} = 0,21 \text{ m}, \beta_1 = 1,0 \quad \checkmark$

$$b_0 = \frac{b_{f2}}{2} = \frac{0,60}{2} = 0,30 \text{ m} \not\leq \frac{L_e}{50} = \frac{10,50}{50} = 0,21 \text{ m} \quad \boxtimes$$

$$\alpha_0 = \sqrt{1 + \frac{A_{sl}}{b_0 t}} = \sqrt{1 + 0} = 1$$

$$\kappa = \frac{\alpha_0 b_0}{L_e} = \frac{\alpha_0 b_{f2}/2}{L_e} = \frac{1 \cdot 0,30}{10,50} = 0,029$$

$$\beta_2 = \left(1 + 6,0 \left(\kappa - \frac{1}{2500\kappa} \right) + 1,6\kappa^2 \right)^{-1}$$

$$\beta = \beta_2 = \left(1 + 6,0 \left(0,029 - \frac{1}{2500 \cdot 0,029} \right) + 1,6 \cdot 0,029^2 \right)^{-1} = 0,918$$

Both flanges of cross-section 1 and the lower flange of cross-section 2 are fully effective at SLS. The upper flange of cross-section 2 is partially effective at SLS.

17.2.2 Elastic – plastic shear lag (ULS)

Only the upper flange of cross-section 2 need consideration at ULS.

$$\alpha_0 = \sqrt{1 + \frac{A_{sl}}{b_0 t}} = \sqrt{1 + 0} = 1$$

$$\kappa = \frac{\alpha_0 b_0}{L_e} = \frac{\alpha_0 b_{f2}/2}{L_e} = \frac{1 \cdot 0,30}{10,50} = 0,029$$

$$\beta = \left(1 + 6,0 \left(\kappa - \frac{1}{2500\kappa} \right) + 1,6\kappa^2 \right)^{-1}$$

$$\beta = \left(1 + 6,0 \left(0,029 - \frac{1}{2500 \cdot 0,029} \right) + 1,6 \cdot 0,029^2 \right)^{-1} = 0,918$$

$$A_{\text{eff}} = A_{f2} \beta^\kappa = A_{f2} \cdot 0,918^{0,029} = 0,998 A_{f2} \approx A_{f2}$$

Both flanges in both cross sections 1 and 2 are fully effective. \checkmark

17.3 Panel I (at the exterior support)

$$V_{\text{Ed}} = 647 \cdot 10^3 \text{ N (at the support),}$$

$$M_{\text{Ed}} = 1557 \cdot 10^3 \text{ Nm (at the end of panel I – } x = 3 \text{ m)}$$

Interaction M-V is checked with maximum values of shear force and bending moment existing in the panel, but not located in the same cross section (a conservative approach).

17.3.1 Rigid end post

The end post is designed to be rigid. Therefore it must fulfil the following criteria:

$e \geq 0,1h_w = 0,1 \cdot 2,0 = 0,20 \text{ m}$ chosen: $e = 0,20 \text{ m}$

end plate dimensions: $b_{\text{end}} / t_{\text{end}} = 320 / 15$ double sided

$A_{\text{end}} = 2 \cdot 0,16 \cdot 0,015 + 0,008 \cdot 0,015 = 4,92 \cdot 10^{-3} \text{ m}^2 \geq 4 \frac{h_w t_w^2}{e} = 4 \frac{2,00 \cdot 0,008^2}{0,20}$

$A_{\text{end}} = 4,92 \cdot 10^{-3} \text{ m}^2 \geq 2,56 \cdot 10^{-3} \text{ m}^2$

$\frac{b_{\text{end}}}{t_{\text{end}}} = \frac{0,160}{0,015} = 10,7 < 14\varepsilon = 14$ – Class 3, therefore fully effective.

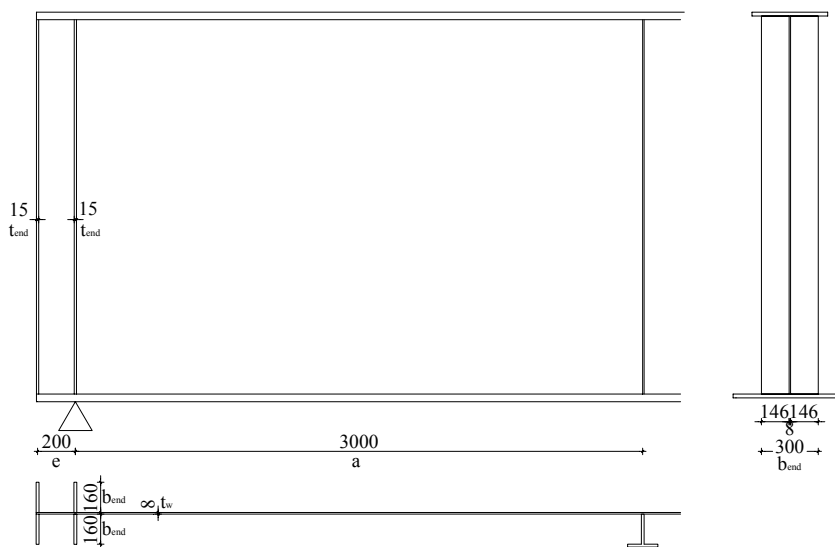


Figure 17.5: Panel I – rigid end post

17.3.2 Shear resistance

Contribution from web

$k_{\tau, \text{st}} = 0$ – no longitudinal stiffener, $\eta = 1,2$ (steel grade S235)

$\frac{a}{h_w} = \frac{3,00}{2,00} = 1,5 \Rightarrow$

$k_{\tau} = 5,34 + 4 \left(\frac{h_w}{a} \right)^2 + k_{\tau, \text{st}} = 5,34 + 4 \cdot \left(\frac{2,00}{3,00} \right)^2 + 0 = 7,118$

$\frac{h_w}{t_w} = \frac{2,00}{0,008} = 250 \geq \frac{31}{\eta} \varepsilon \sqrt{k_{\tau}} = \frac{31}{1,2} \cdot 1 \cdot \sqrt{7,118} = 69 \Rightarrow$ verification of shear

buckling is necessary

$\bar{\lambda}_w = \frac{h_w}{37,4 t_w \varepsilon \sqrt{k_{\tau}}}$

$$\bar{\lambda}_w = \frac{2,00}{37,4 \cdot 0,008 \cdot 1 \cdot \sqrt{7,118}} = 2,505 \geq 1,08 \Rightarrow \chi_w = \frac{1,37}{0,7 + \bar{\lambda}_w} = \frac{1,37}{0,7 + 2,505} = 0,427$$

$$V_{bw,Rd} = \frac{\chi_w f_{yw} h_w t_w}{\gamma_{M1} \sqrt{3}} = \frac{0,427 \cdot 235 \cdot 10^6 \cdot 2,00 \cdot 0,008}{1,1 \cdot \sqrt{3}} = 843 \cdot 10^3 \text{ N}$$

Contribution from flanges

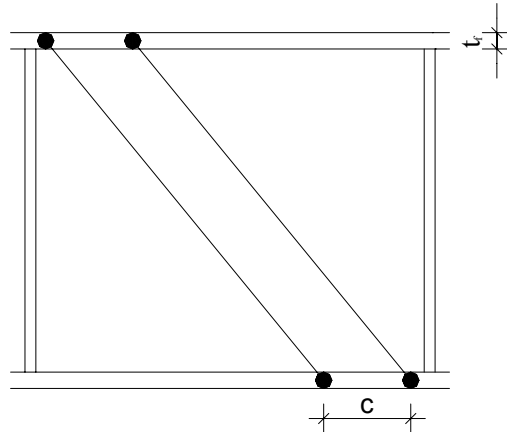


Figure 17.6: Panel I – tension band

$$c = a \left(0,25 + \frac{1,6 \cdot b_{f1} \cdot t_{f1}^2 \cdot f_{yf}}{t_w \cdot h_w^2 \cdot f_{yw}} \right) = 3,00 \left(0,25 + \frac{1,6 \cdot 0,40 \cdot 0,02^2 \cdot 235 \cdot 10^6}{0,008 \cdot 2,00^2 \cdot 235 \cdot 10^6} \right) = 0,774 \text{ m}$$

$$b_f = 0,40 \text{ m} \leq 2 \cdot 15 \epsilon t_f + t = 2 \cdot 15 \cdot 1 \cdot 0,02 + 0,008 = 0,608 \text{ m}$$

$$M_{f,Rd} = (h_w + t_{f1}) A_{f,min} \frac{f_y}{\gamma_{M0}} = (2,00 + 0,02) \cdot (0,40 \cdot 0,02) \cdot \frac{235 \cdot 10^6}{1,0} = 3798 \cdot 10^3 \text{ Nm}$$

$$V_{bf,Rd} = \frac{b_{f1} \cdot t_{f1}^2 \cdot f_{yf}}{c \cdot \gamma_{M1}} \left(1 - \left(\frac{M_{Ed}}{M_{f,Rd}} \right)^2 \right) = \frac{0,40 \cdot 0,02^2 \cdot 235 \cdot 10^6}{0,774 \cdot 1,1} \left(1 - \left(\frac{1557 \cdot 10^3}{3798 \cdot 10^3} \right)^2 \right) = 37 \cdot 10^3 \text{ N}$$

Flanges do not significantly contribute to the shear resistance; indeed $V_{bf,Rd}$ is substantially smaller than $V_{bw,Rd}$.

17.3.3 Verification for shear resistance

$$V_{b,Rd} = V_{bw,Rd} + V_{bf,Rd} \leq \frac{\eta f_{yw} h_w t_w}{\gamma_{M1} \sqrt{3}}$$

$$V_{b,Rd} = (843 + 37) \cdot 10^3 = 880 \cdot 10^3 \text{ N} \leq \frac{1,2 \cdot 235 \cdot 2 \cdot 0,008}{1,1 \cdot \sqrt{3}} \cdot 10^6 = 2368 \cdot 10^3 \text{ N} \quad \checkmark$$

$$V_{Ed} = 647 \cdot 10^3 \text{ N} \leq V_{b,Rd} = 880 \cdot 10^3 \text{ N} \quad \checkmark$$

17.3.4 Verification of bending resistance

$$M_{Ed} = 1557 \cdot 10^3 \text{ Nm} \leq M_{f,Rd} = 3798 \cdot 10^3 \text{ Nm} \quad \checkmark$$

The direct stresses may thus be transferred by the flanges only.

17.3.5 Verification of interaction M-V

Flanges take bending moment and the web takes shear force. There is no need for a verification of M-V-interaction.

17.4 Panel II (at midspan)

Cross-section of panel II is the same as panel I.

$$V_{Ed} = 137 \cdot 10^3 \text{ N (at the edge of panel II - } x = 6 \text{ m),}$$

$M_{Ed} = 2459 \cdot 10^3 \text{ Nm}$ (maximum value within the panel, at 7,55 m from the left support)

17.4.1 Verification of shear resistance

Panel II is the same as panel I and has also the same shear resistance of the web. Neglecting the contribution from the flanges because of high moments gives:

$$V_{Ed} = 137 \cdot 10^3 \text{ N} \leq V_{b,Rd} = 880 \cdot 10^3 \text{ N}$$

$V_{b,Rd}$ is calculated in Section 17.3.3.

17.4.2 Verification of bending resistance

$$M_{Ed} = 2459 \cdot 10^3 \text{ Nm} \leq M_{f,Rd} = 3798 \cdot 10^3 \text{ Nm} \quad \checkmark$$

$M_{f,Rd}$ is calculated in Section 0. The direct stresses may thus be transferred by the flanges only.

17.4.3 Interaction M-V

Flanges take bending moment and the web takes shear force. There is no need for a verification of the M-V-interaction.

17.5 Panel III (at the interior support)

$$V_{Ed} = 1139 \cdot 10^3 \text{ N (at the interior support)}$$

$M_{Ed} = -5167 \cdot 10^3 \text{ Nm}$ (at the interior support)

These are the maximum values of shear force and bending moment in the panel located in the same cross section at the interior support. For the sake of simplicity in the further design checks the absolute value of the bending moment at the interior support was used.

17.5.1 Calculation of normal stresses

Geometric characteristics are calculated ignoring the contribution of longitudinal stiffeners, which are not continuous.

$$A = b_{f1}t_{f1} + b_{f2}t_{f2} + h_w t_w = 0,4 \cdot 0,02 + 0,6 \cdot 0,04 + 2 \cdot 0,008 = 48,0 \cdot 10^{-3} \text{ m}^2$$

$$h_s = \frac{-b_{f1} \frac{t_{f1}^2}{2} + b_{f2} t_{f2} \left(h_w + \frac{t_{f2}}{2} \right) + \frac{h_w^2}{2} t_w}{A} = \frac{-0,4 \cdot \frac{0,02^2}{2} + 0,6 \cdot 0,04 \left(2 + \frac{0,40}{2} \right) + \frac{2^2}{2} \cdot 0,008}{48,0 \cdot 10^{-3}}$$

$$h_s = 1,342 \text{ m}$$

$$I = \frac{b_{f1}t_{f1}^3 + b_{f2}t_{f2}^3}{12} + b_{f1} \cdot t_{f1} \cdot \left(h_s + \frac{t_{f1}}{2} \right)^2 + b_{f2} \cdot t_{f2} \cdot \left(h_w - h_s + \frac{t_{f2}}{2} \right)^2 + \frac{t_w h_w^3}{12} + h_w \cdot t_w \cdot \left(\frac{h_w}{2} - h_s \right)^2 = 32863,87 \cdot 10^{-6} \text{ m}^4$$

$$\sigma_1 = \frac{M_{Ed}}{I/h_s} = \frac{-5167}{32863,87/1,342} \cdot 10^9 = -211 \cdot 10^6 \text{ N/m}^2 \geq \frac{-f_y}{\gamma_{M0}} = \frac{-235 \cdot 10^6}{1,1} = -214 \cdot 10^6 \text{ N/m}^2$$

$$\sigma_{s11} = \frac{M_{Ed}}{I/(h_s - h_{w1})} = \frac{-5167}{32867,87/(1,342 - 0,5)} \cdot 10^6 = -132 \cdot 10^6 \text{ N/m}^2$$

$$\sigma_{s12} = \frac{M_{Ed}}{I/(h_s - h_{w2})} = \frac{-5167}{32863,87/(1,342 - 1)} \cdot 10^9 = -54 \cdot 10^6 \text{ N/m}^2$$

$$\sigma_2 = \frac{M_{Ed}}{I/(h_s - h_w)} = \frac{-5167}{32863,87/(1,342 - 2)} \cdot 10^9 = 103 \cdot 10^6 \text{ N/m}^2 \leq \frac{f_y}{\gamma_{M0}} = 214 \cdot 10^6 \text{ N/m}^2$$

$$\psi = \frac{\sigma_2}{\sigma_1} = \frac{h_s - h_w}{h_s} = \frac{1,342 - 2}{1,342} = -0,490$$

17.5.2 Local buckling of an individual web subpanel

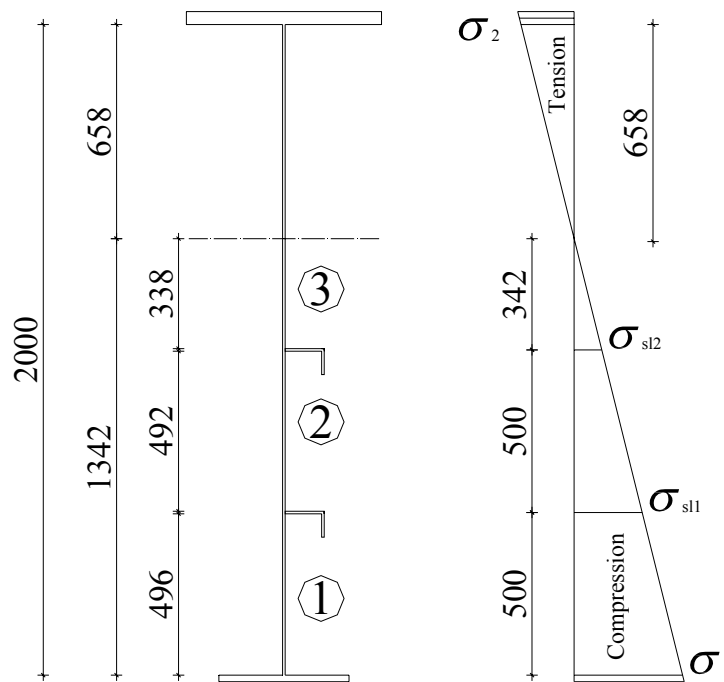


Figure 17.7: Panel III – cross section and distribution of longitudinal stresses

Web subpanel 1

$$\bar{b}_1 = h_{w1} - \frac{t_{sl}}{2} = 0,5 - \frac{0,008}{2} = 0,496 \text{ m}$$

$$\psi_1 = \frac{\sigma_{sl1}}{\sigma_1} = \frac{h_s - h_{w1}}{h_s} = \frac{1,342 - 0,5}{1,342} = 0,627$$

$$k_{\sigma 1} = \frac{8,2}{1,05 + \psi_1} = \frac{8,2}{1,05 + 0,627} = 4,890$$

$$\bar{\lambda}_{pl} = \frac{\bar{b}_1 / t_w}{28,4 \varepsilon \sqrt{k_{\sigma 1}}} = \frac{0,496 / 0,008}{28,4 \cdot 1 \cdot \sqrt{4,890}} = 0,987 > 0,673$$

$$\rho_1 = \frac{\bar{\lambda}_{pl} - 0,055(3 + \psi_1)}{\bar{\lambda}_{pl}^2} = \frac{0,987 - 0,055(3 + 0,627)}{0,987^2} = 0,808 \leq 1$$

Gross widths

$$b_{1,edge} = \frac{2}{5 - \psi_1} \bar{b}_1 = \frac{2}{5 - 0,627} \cdot 0,496 = 0,227 \text{ m}$$

$$b_{1,inf} = \frac{3 - \psi_1}{5 - \psi_1} \bar{b}_1 = \frac{3 - 0,627}{5 - 0,627} \cdot 0,496 = 0,269 \text{ m}$$

Effective widths

$$b_{1,eff} = \rho_1 \bar{b}_1 = 0,808 \cdot 0,496 = 0,401 \text{ m}$$

$$b_{1,edge,eff} = \frac{2}{5 - \psi_1} b_{1,eff} = \frac{2}{5 - 0,627} \cdot 0,401 = 0,183 \text{ m}$$

$$b_{1,inf,eff} = \frac{3 - \psi_1}{5 - \psi_1} b_{1,eff} = \frac{3 - 0,627}{5 - 0,627} \cdot 0,401 = 0,218 \text{ m}$$

$$x_{1,eff} = \bar{b}_1 - b_{1,eff} = 0,496 - 0,401 = 0,095 \text{ m}$$

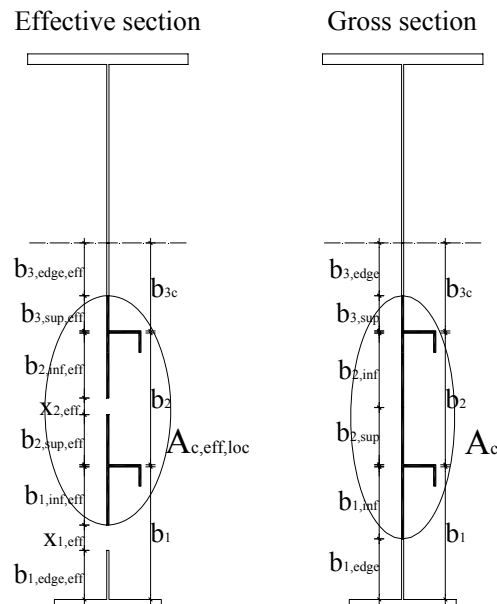


Figure 17.8: Panel III – effective and gross cross section

Web subpanel 2

$$\bar{b}_2 = h_{w2} - h_{w1} - t_{sl} = 0,50 - 0,008 = 0,492 \text{ m}$$

$$\psi_2 = \frac{\sigma_{sl2}}{\sigma_{sl1}} = \frac{h_s - h_{w2}}{h_s - h_{w1}} = \frac{1,342 - 1,000}{1,342 - 0,500} = 0,406$$

$$k_{\sigma 2} = \frac{8,2}{1,05 + \psi_2} = \frac{8,2}{1,05 + 0,406} = 5,632$$

$$\bar{\lambda}_{p2} = \frac{\bar{b}_2 / t_w}{28,4 \varepsilon \sqrt{k_{\sigma 2}}} = \frac{0,492 / 0,008}{28,4 \cdot 1 \cdot \sqrt{5,632}} = 0,912 > 0,673$$

$$\rho_2 = \frac{\bar{\lambda}_{p2} - 0,055(3 + \psi_2)}{\bar{\lambda}_{p2}^2} = \frac{0,912 - 0,055(3 + 0,406)}{0,912^2} = 0,871 \leq 1$$

The calculation of the slenderness parameter $\bar{\lambda}_{p2}$ may be done with the lower stress that occurs when subpanel 1 reaches yield stress at the most stressed edge (EN 1993-1-5, 4.4(4)).

Gross widths

$$b_{2,\text{sup}} = \frac{2}{5 - \psi_2} \bar{b}_2 = \frac{2}{5 - 0,406} \cdot 0,492 = 0,214 \text{ m}$$

$$b_{2,\text{inf}} = \frac{3 - \psi_2}{5 - \psi_2} \bar{b}_2 = \frac{3 - 0,406}{5 - 0,406} \cdot 0,492 = 0,278 \text{ m}$$

Effective widths

$$b_{2,\text{eff}} = \rho_2 \bar{b}_2 = 0,871 \cdot 0,492 = 0,429 \text{ m}$$

$$b_{2,\text{sup,eff}} = \frac{2}{5 - \psi_1} b_{2,\text{eff}} = \frac{2}{5 - 0,406} \cdot 0,429 = 0,187 \text{ m}$$

$$b_{2,\text{inf,eff}} = \frac{3 - \psi_2}{5 - \psi_2} b_{2,\text{eff}} = \frac{3 - 0,406}{5 - 0,406} \cdot 0,429 = 0,242 \text{ m}$$

$$x_{2,\text{eff}} = \bar{b}_2 - b_{2,\text{eff}} = 0,492 - 0,429 = 0,063 \text{ m}$$

Web subpanel 3

$$\bar{b}_{3c} = h_s - h_{w2} - t_{sl}/2 = 1,342 - 1,000 - \frac{0,008}{2} = 0,338 \text{ m}$$

$$\bar{b}_3 = h_w - h_{w2} - t_{sl}/2 = 2,000 - 1,000 - \frac{0,008}{2} = 0,996 \text{ m}$$

$$\psi_3 = \frac{\sigma_2}{\sigma_{sl2}} = \frac{h_s - h_w}{h_s - h_{w2}} = \frac{1,342 - 2,000}{1,342 - 1,000} = -1,924$$

$$k_{\sigma_3} = 5,98(1 - \psi_3)^2 = 5,98(1 + 1,924)^2 = 51,128$$

$$\bar{\lambda}_{p3} = \frac{\bar{b}_3 / t_w}{28,4 \varepsilon \sqrt{k_{\sigma_3}}} = \frac{0,338 / 0,008}{28,4 \cdot 1 \cdot \sqrt{51,128}} = 0,208 < 0,673$$

$$\rho_3 = 1 \quad \text{no local buckling occurs}$$

Gross widths

$$b_{3,\text{sup}} = 0,4 \bar{b}_{3c} = 0,4 \cdot 0,338 = 0,135 \text{ m}$$

$$b_{3,\text{edge}} = 0,6 \bar{b}_{3c} = 0,6 \cdot 0,338 = 0,203 \text{ m}$$

Effective widths (are the same as gross widths because $\rho_3 = 1$)

$$b_{3,\text{eff}} = \rho_3 \bar{b}_{3c} = 1 \cdot 0,338 = 0,338 \text{ m}$$

$$b_{3,\text{sup,eff}} = 0,4b_{3,\text{eff}} = 0,4 \cdot 0,338 = 0,135 \text{ m}$$

$$b_{3,\text{edge,eff}} = 0,6b_{3,\text{eff}} = 0,6 \cdot 0,338 = 0,203 \text{ m}$$

Verification of section class of longitudinal stiffeners

$$\frac{b_{\text{sl}}}{t_{\text{sl}}} = \frac{120}{8} = 15 \leq 33\varepsilon = 33 \quad \text{The flange is Class I.}$$

$$\frac{h_{\text{sl}}}{t_{\text{sl}}} = \frac{80}{8} = 10 \leq 10\varepsilon = 10 \quad \text{The web is Class I.}$$

The most slender longitudinal stiffener (upper stiffener) is thus Class 1. The other (lower) stiffener is thus also Class 1.

17.5.3 Stiffened web

Elastic critical plate buckling stress $\sigma_{\text{cr,p}}$ is calculated according to EN 1993-1-5, A.2.

Lower stiffener (see Figure 17.9):

$$A_{\text{sl,I}} = (b_{1,\text{inf}} + b_{2,\text{sup}} + t_{\text{sl}}) \cdot t_{\text{w}} + (b_{\text{sl}} + h_{\text{sl}} - t_{\text{sl}}) \cdot t_{\text{sl}}$$

$$A_{\text{sl,I}} = (0,269 + 0,214 + 0,008) \cdot 0,008 + (0,120 + 0,080 - 0,008) \cdot 0,008 = 5,464 \cdot 10^{-3} \text{ m}^2$$

$$x_{\text{sl,I}} = \frac{(h_{\text{sl}} - t_{\text{sl}}) \cdot t_{\text{sl}} \cdot \left(\frac{t_{\text{w}}}{2} + b_{\text{sl}} - \frac{t_{\text{sl}}}{2} \right) + b_{\text{sl}} t_{\text{sl}} \left(\frac{t_{\text{w}}}{2} + \frac{b_{\text{sl}}}{2} \right)}{A_{\text{sl,I}}}$$

$$x_{\text{sl,I}} = \frac{(0,080 - 0,008) \cdot 0,008 \cdot \left(\frac{0,008}{2} + 0,120 - \frac{0,008}{2} \right) + 0,120 \cdot 0,008 \left(\frac{0,008}{2} + \frac{0,120}{2} \right)}{5,464 \cdot 10^{-3}}$$

$$x_{\text{sl,I}} = 0,024 \text{ m}$$

$$I_{\text{sl,I}} = \frac{(b_{1,\text{inf}} + b_{2,\text{sup}} + t_{\text{sl}}) t_{\text{w}}^3}{12} + \frac{(h_{\text{sl}} - t_{\text{sl}}) t_{\text{sl}}^3}{12} + \frac{b_{\text{sl}}^3 t_{\text{sl}}}{12} +$$

$$+ (b_{1,\text{inf}} + b_{2,\text{sup}} + t_{\text{sl}}) t_{\text{w}} x_{\text{sl,I}}^2 + (h_{\text{sl}} - t_{\text{sl}}) t_{\text{sl}} \left(b_{\text{sl}} + \frac{t_{\text{w}}}{2} - \frac{t_{\text{sl}}}{2} - x_{\text{sl,I}} \right)^2 +$$

$$+ b_{\text{sl}} t_{\text{sl}} \left(\frac{t_{\text{w}} + b_{\text{sl}}}{2} - x_{\text{sl,I}} \right)^2$$

$$\begin{aligned}
 I_{sl,I} = & \frac{(0,269 + 0,214 + 0,008)0,008^3}{12} + \frac{(0,080 - 0,008)0,008^3}{12} + \frac{0,120^3 \cdot 0,008}{12} + \\
 & + (0,269 + 0,214 + 0,008)0,008 \cdot 0,024^2 + \\
 & + (0,080 - 0,008)0,008 \left(0,120 + \frac{0,008}{2} - \frac{0,008}{2} - 0,024 \right)^2 + \\
 & + 0,120 \cdot 0,008 \left(\frac{0,008 + 0,120}{2} - 0,024 \right)^2 = 10,28 \cdot 10^{-6} \text{ m}^4
 \end{aligned}$$

Upper stiffener (see Figure 17.9):

$$A_{sl,II} = 4,904 \cdot 10^{-3} \text{ m}^2$$

$$x_{sl,II} = 0,027 \text{ m}$$

$$I_{sl,II} = 9,92 \cdot 10^{-6} \text{ m}^4$$

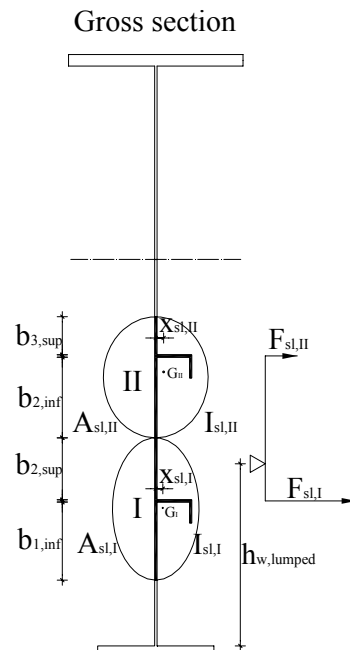


Figure 17.9: Panel III – Stiffener I and II

$$A_{sl,lumped} = A_{sl,I} + A_{sl,II} = 10,368 \cdot 10^{-3} \text{ m}^2$$

$$I_{sl,lumped} = I_{sl,I} + I_{sl,II} = 20,20 \cdot 10^{-6} \text{ m}^4$$

$$F_{sl,I} = A_{sl,I} \sigma_{sl1} = 5,464 \cdot (-132) \cdot 10^3 = -721,2 \cdot 10^3 \text{ N}$$

$$F_{sl,II} = A_{sl,II} \sigma_{sl2} = 4,904 \cdot (-54) \cdot 10^3 = -264,8 \cdot 10^3 \text{ N}$$

$$h_{w,lumped} = \frac{F_{sl,II}}{F_{sl,I} + F_{sl,II}} (h_{w2} - h_{w1}) + h_{w1} = \frac{264,8}{721,2 + 264,8} \cdot 0,500 + 0,500 = 0,632 \text{ m}$$

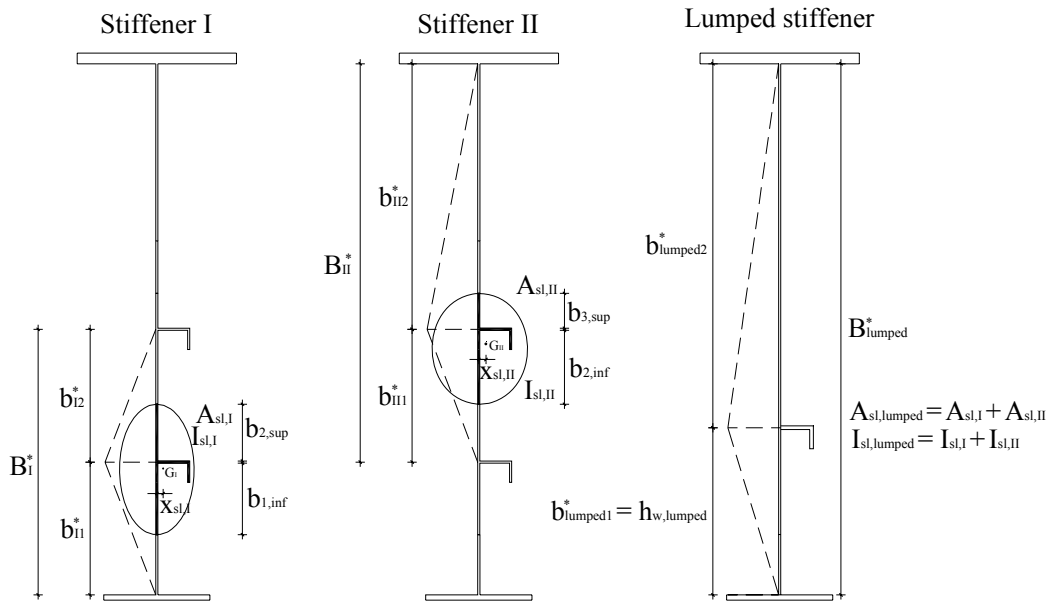


Figure 17.10: Panel III – Stiffener I and II and lumped stiffener

Case 1: Buckling of lower Stiffener

$$b_{11}^* = h_{w1} = 0,500 \text{ m}$$

$$b_{12}^* = h_{w2} - h_{w1} = 0,500 \text{ m}$$

$$B_I^* = b_{11}^* + b_{12}^* = 0,500 + 0,500 = 1,000 \text{ m}$$

$$a_{c,I} = 4,334 \sqrt{\frac{I_{sl,I} b_{11}^{*2} b_{12}^{*2}}{t_w^3 B_I^*}} = 4,334 \sqrt{\frac{10,28 \cdot 10^{-6} \cdot 0,500^2 \cdot 0,500^2}{0,008^3 \cdot 1,000}} = 4,583 \text{ m} > a' = 2 \text{ m}$$

$$\sigma_{cr,sl,I} = \frac{\pi^2 E I_{sl,I}}{A_{sl,I} a'^2} + \frac{E t_w^3 B_I^* a'^2}{4\pi^2 (1-\nu^2) A_{sl,I} b_{11}^{*2} b_{12}^{*2}}$$

$$\sigma_{cr,sl,I} = \frac{\pi^2 \cdot 210 \cdot 10^9 \cdot 10,28 \cdot 10^{-6}}{5,464 \cdot 10^{-3} \cdot 2,000^2} + \frac{210 \cdot 10^9 \cdot 0,008^3 \cdot 1,000 \cdot 2,000^2}{4\pi^2 (1-0,3^2) \cdot 5,464 \cdot 10^{-3} \cdot 0,500^2 \cdot 0,500^2}$$

$$\sigma_{cr,sl,I} = 1010 \cdot 10^6 \text{ N/cm}^2$$

$$\sigma_{cr,p,I} = \frac{h_s}{h_s - h_{w1}} \sigma_{cr,sl,I} = \frac{1,342}{1,342 - 0,500} \cdot 1010 \cdot 10^6 = 1610 \cdot 10^6 \text{ N/m}^2$$

Case 2: Buckling of upper Stiffener

$$b_{III}^* = h_{w2} - h_{w1} = 0,500 \text{ m}$$

$$b_{II2}^* = h_w - h_{w2} = 1,000 \text{ m}$$

$$B_{II}^* = b_{III}^* + b_{II2}^* = 0,500 + 1,000 = 1,500 \text{ m}$$

$$a_{c,II} = 4,334 \sqrt{\frac{I_{sl,II} b_{III}^{*2} b_{II2}^{*2}}{t_w^3 B_{II}^*}} = 4,334 \sqrt{\frac{9,92 \cdot 10^{-6} \cdot 0,500^2 \cdot 1,000^2}{0,008^3 \cdot 1,500}} = 5,804 \text{ m} > a' = 2 \text{ m}$$

$$\sigma_{cr,sl,II} = \frac{\pi^2 EI_{sl,II}}{A_{sl,II} a'^2} + \frac{Et_w^3 B_{II}^* a'^2}{4\pi^2 (1-\nu^2) A_{sl,II} b_{III}^{*2} b_{II2}^{*2}}$$

$$\sigma_{cr,sl,II} = \frac{\pi^2 \cdot 210 \cdot 10^9 \cdot 9,92 \cdot 10^{-6}}{4,904 \cdot 10^{-3} \cdot 2,000^2} + \frac{210 \cdot 10^9 \cdot 0,008^3 \cdot 1,500 \cdot 2,000^2}{4\pi^2 (1-0,3^2) \cdot 4,904 \cdot 10^{-3} \cdot 0,500^2 \cdot 1,000^2}$$

$$\sigma_{cr,sl,II} = 1063 \cdot 10^6 \text{ N/m}^2$$

$$\sigma_{cr,p,II} = \frac{h_s}{h_s - h_{w2}} \sigma_{cr,sl,II} = \frac{1,342}{1,342 - 1,000} \cdot 1063 \cdot 10^6 = 4171 \cdot 10^6 \text{ N/m}^2$$

Case 3: Buckling of lumped stiffener

$$b_{lumped1}^* = h_{w,lumped} = 0,632 \text{ m}$$

$$b_{lumped2}^* = h_w - h_{w,lumped} = 1,368 \text{ m}$$

$$B_{lumped}^* = h_w = 2,000 \text{ m}$$

$$a_{c,lumped} = 4,334 \sqrt{\frac{I_{sl,lumped} b_{lumped1}^{*2} b_{lumped2}^{*2}}{t_w^3 B_{lumped}^*}}$$

$$a_{c,lumped} = 4,334 \sqrt{\frac{20,20 \cdot 10^{-6} \cdot 0,632^2 \cdot 1,368^2}{0,008^3 \cdot 2,000}} = 8,485 \text{ m} > a' = 2,000 \text{ m}$$

$$\sigma_{cr,sl,lumped} = \frac{\pi^2 EI_{sl,lumped}}{A_{sl,lumped} a'^2} + \frac{Et_w^3 B_{lumped}^* a'^2}{4\pi^2 (1-\nu^2) A_{sl,lumped} b_{lumped1}^{*2} b_{lumped2}^{*2}}$$

$$\sigma_{cr,sl,lumped} = \frac{\pi^2 \cdot 210 \cdot 10^9 \cdot 20,20 \cdot 10^{-6}}{10,368 \cdot 10^{-3} \cdot 2,000^2} + \frac{210 \cdot 10^9 \cdot 0,008^3 \cdot 2,000 \cdot 2,000^2}{4\pi^2 \cdot 0,91 \cdot 10,368 \cdot 10^{-3} \cdot 0,632^2 \cdot 1,368^2}$$

$$\sigma_{cr,sl,lumped} = 456 \cdot 10^6 \text{ N/m}^2$$

$$\sigma_{cr,p,lumped} = \frac{h_s}{h_s - h_{w,lumped}} \sigma_{cr,sl,lumped} = \frac{1,342}{1,342 - 0,632} \cdot 1013 \cdot 10^6 = 1915 \cdot 10^6 \text{ N/m}^2$$

Critical plate buckling stress:

$$\sigma_{cr,p} = \min(\sigma_{cr,p,I}; \sigma_{cr,p,II}; \sigma_{cr,p,lumped}) = \min(1610; 4171; 1915) \cdot 10^6 = 1610 \cdot 10^6 \text{ N/m}^2$$

17.5.4 Plate type behaviour

A_c is the gross area of the compression zone of the stiffened plate except the parts of subpanels supported by an adjacent plate, see Figure 17.8 or Figure 17.11 (to be multiplied by the shear lag factor if shear lag is relevant, see in EN 1993-1-5, 3.3)

\sum_c applies to the part of the stiffened panel width that is in compression except the parts $b_{edge,eff}$, see Figure 17.8 or Figure 17.11

$A_{c,eff,loc}$ is the effective^p section areas of all the stiffeners and subpanels that are fully or partially in the compression zone except the effective parts supported by an adjacent plate element with the width $b_{edge,eff}$, see Figure 17.8 or Figure 17.11

$A_{sl,eff}$ is the sum of the effective^p section according to EN 1993-1-5, 4.4 of all longitudinal stiffeners with gross area A_{sl} located in the compression zone

$b_{c,loc}$ is the width of the compressed part of each subpanel

ρ_{loc} is the reduction factor from EN 1993-1-5, 4.4(2) for each subpanel.

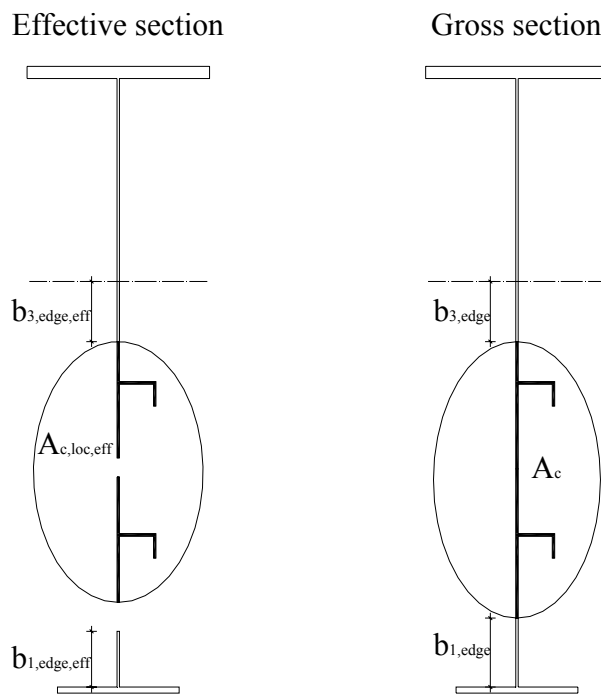


Figure 17.11: Panel III – effective and gross cross section

$$A_c = (h_s - b_{1,edge} - b_{3,edge})t_w + 2(b_{sl} + h_{sl} - t_{sl})t_{sl} =$$

$$= (1,342 - 0,227 - 0,203)0,008 + 2(0,120 + 0,08 - 0,008)0,008$$

$$A_c = 10,368 \cdot 10^{-3} \text{ m}^2$$

$$A_{c,eff,loc} = A_{sl,eff} + \sum_c \rho_{loc} b_{c,loc} t$$

$$\sum A_{sl,eff} = \sum A_{sl} = 2(b_{sl} + h_{sl} - t_{sl})t_{sl} = 2 \cdot (0,120 + 0,08 - 0,008) \cdot 0,008 = 3,072 \cdot 10^{-3} \text{ m}^2$$

$$A_{c,eff,loc} = \sum A_{sl,eff} + (b_{1,inf,eff} + b_{2,sup,eff} + b_{2,inf,eff} + b_{3,sup,eff} + 2t_{sl})t_w$$

$$A_{c,eff,loc} = 3,072 \cdot 10^{-3} + (0,218 + 0,187 + 0,242 + 0,135 + 2 \cdot 0,008) \cdot 0,008 = 9,456 \cdot 10^{-3} \text{ m}^2$$

$$\beta_{A,c}^p = \frac{A_{c,eff,loc}}{A_c} = \frac{9,456}{10,368} = 0,912$$

$$\bar{\lambda}_p = \sqrt{\frac{\beta_{A,c}^p f_y}{\sigma_{cr,p}}} = \sqrt{\frac{0,912 \cdot 235 \cdot 10^6}{1610 \cdot 10^6}} = 0,365 < 0,673 \Rightarrow$$

$$\rho = 1$$

17.5.5 Column type behaviour

The lower stiffener, that is the most compressed, is concerned.

$A_{sl,1}$ is the gross cross-sectional area of the stiffener and the adjacent parts of the plate according to Figure 17.12

$I_{sl,1}$ is the second moment of area of the stiffener, relative to the out-of-plane bending of the plate according to Figure 17.12

$A_{sl,1,eff}$ is the effective cross-sectional area of the stiffener with due allowance for plate buckling, see Figure 17.12

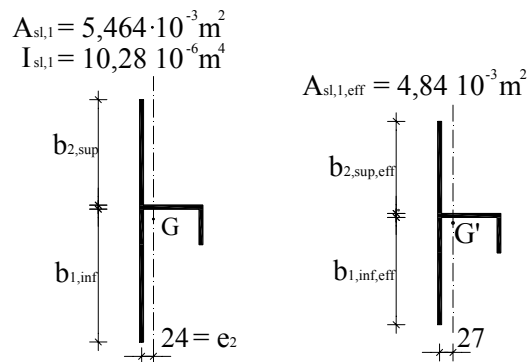


Figure 17.12: Panel III – e_1 and e_2 – lower stiffener

$$A_{sl,1,eff} = (b_{1,inf,eff} + b_{2,sup,eff} + t_{sl}) \cdot t_w + \frac{\sum A_{sl,eff}}{2}$$

$$A_{sl,1,eff} = (0,218 + 0,187 + 0,008) \cdot 0,008 + \frac{3,072 \cdot 10^{-3}}{2} = 4,840 \cdot 10^{-3} \text{ m}^2$$

$$A_{sl,1} = (b_{1,inf} + b_{2,sup} + t_{sl}) \cdot t_w + \frac{\sum A_{sl}}{2}$$

$$A_{sl,1} = (0,269 + 0,214 + 0,008) \cdot 0,008 + \frac{3,072 \cdot 10^{-3}}{2} = 5,464 \cdot 10^{-3} \text{ m}^2$$

$$I_{sl,1} = 10,28 \cdot 10^{-6} \text{ m}^4$$

$$\beta_{A,c} = \frac{A_{sl,1,eff}}{A_{sl,1}} = \frac{4,84}{5,464} = 0,886$$

$$\sigma_{cr,sl} = \frac{\pi^2 EI_{sl,1}}{A_{sl,1} a^2} = \frac{\pi^2 \cdot 210 \cdot 10^9 \cdot 10,28 \cdot 10^{-6}}{5,464 \cdot 10^{-3} \cdot 2,000^2} = 975 \cdot 10^6 \text{ N/m}^2$$

Elastic critical column buckling stress has to be extrapolated to the most compressed edge of the web.

$$\sigma_{cr,c} = \frac{h_s}{h_s - h_{w1}} \sigma_{cr,sl} = \frac{1,342}{1,342 - 0,500} \cdot 975 \cdot 10^6 = 1554 \cdot 10^6 \text{ N/m}^2$$

$$\bar{\lambda}_c = \sqrt{\frac{\beta_{A,c} f_y}{\sigma_{cr,c}}} = \sqrt{\frac{0,886 \cdot 235}{1554}} = 0,366$$

$$i = \sqrt{\frac{I_{sl,1}}{A_{sl,1}}} = \sqrt{\frac{10,28 \cdot 10^{-6}}{5,464 \cdot 10^{-3}}} = 43 \cdot 10^{-3} \text{ m}$$

$$e_2 = x_{sl1} = 24 \cdot 10^{-3} \text{ m} \quad \text{- see section 17.5.3 and Figure 17.12 and Figure 17.13}$$

$$e_1 = \frac{\frac{b_{sl}^2}{2} t_{sl} + (h_{sl} - t_{sl}) t_{sl} \left(b_{sl} - \frac{t_{sl}}{2} \right)}{(b_{sl} + h_{sl} - t_{sl}) t_{sl}} + \frac{t_w}{2} - e_2$$

$$e_1 = \frac{\frac{0,120^2}{2} 0,008 + (0,080 - 0,008) 0,008 \left(0,120 - \frac{0,008}{2} \right)}{(0,120 + 0,080 - 0,008) 0,008} + \frac{0,008}{2} + 0,0024$$

$$e_1 = 61 \cdot 10^{-3} \text{ m}$$

$$e = \max(e_1; e_2) = \max(61; 24) \cdot 10^{-3} = 61 \cdot 10^{-3} \text{ m}$$

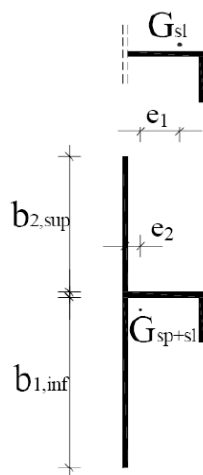


Figure 17.13: Panel III – e_1 and e_2

$\alpha = 0,49$ – curve c (open cross section stiffener)

$$\alpha_E = \alpha + \frac{0,09}{i/e} = 0,49 + \frac{0,09}{43 \cdot 10^{-3}} \cdot 61 \cdot 10^{-3} = 0,618$$

$$\phi = 0,5 \left(1 + \alpha_E (\bar{\lambda}_c - 0,2) + \bar{\lambda}_c^2 \right) = 0,5 \left(1 + 0,618 \cdot (0,366 - 0,2) + 0,366^2 \right) = 0,618$$

$$\chi_c = \left[\phi + \left(\phi^2 - \bar{\lambda}_c^2 \right)^{0,5} \right]^{-1} = \left[0,618 + \left(0,618^2 - 0,366^2 \right)^{0,5} \right]^{-1} = 0,896$$

The upper stiffener has the same cross section as the lower one, but due to vicinity to the neutral axis it is not decisive. Critical stress extrapolated to the compressed edge of the web is much higher than for the lower stiffener.

17.5.6 Interaction between plate and column buckling

$$\xi = \frac{\sigma_{cr,p}}{\sigma_{cr,c}} - 1 = \frac{1610}{1554} - 1 = 0,036$$

$$\rho_c = (\rho - \chi_c) \xi (2 - \xi) + \chi_c = (1 - 0,896) \cdot 0 \cdot (2 - 0) + 0,896 = 0,896$$

$$(1 - 0,896) \cdot 0,036 \cdot (2 - 0,036) + 0,896 = 0,903$$

17.5.7 Calculation of effective geometric characteristics

$A_{c,eff}$ is the effective^p area of the compression zone of the stiffened plate

$$A_{c,eff} = \rho_c A_{c,eff,loc} + \sum b_{edge,eff} t = 0,903 \cdot 9,456 \cdot 10^{-3} + (0,183 + 0,203) \cdot 0,008$$

$$A_{c,eff} = 11,627 \cdot 10^{-3} \text{ m}^2$$

According to EN 1993-1-5, 4.5.1(7), for the calculation of effective second moment of area of the whole I section, effective^p cross sectional area for local buckling $A_{c,eff,loc}$ may be uniformly reduced (see Figure 17.14) by multiplying the thicknesses of web and stiffeners with ρ_c .

$$t_{w,red} = \rho_c t_w = 0,903 \cdot 8 \cdot 10^{-3} \text{ m}$$

$$t_{sl,red} = \rho_c t_{sl} = 0,903 \cdot 8 \cdot 10^{-3} \text{ m}$$

$$h_{s,eff} = 1,339 \text{ m}$$

$$I_{eff} = 32626,17 \cdot 10^{-6} \text{ m}^4$$

$$W_{eff} = \frac{I_{eff}}{h_{s,eff} + t_{fl}/2} = \frac{32626,17 \cdot 10^6}{1,339 + 0,01} = 24185 \cdot 10^{-6} \text{ m}^3$$

According to EN 1993-1-5, A.2.1(4) the following requirement has to be met:

$$\sigma_{\text{com,Ed}} = \frac{M_{\text{Ed}}(h_s - h_{w1})}{I_{\text{eff}}} = \frac{5167 \cdot 10^3 (1,342 - 0,500)}{32626,17 \cdot 10^{-6}} = 133 \cdot 10^6 \text{ N/m}^2$$

$$\rho_c f_{\text{yd}} = 0,903 \frac{235 \cdot 10^6}{1,1} = 193 \cdot 10^6 \text{ N/m}^2 > \sigma_{\text{com,Ed}} = 133 \cdot 10^6 \text{ N/m}^2 \quad \checkmark$$

Otherwise further reduction of effective^p area is necessary.

17.5.8 Verification of bending resistance

Bending check at maximum moment

$$M_{\text{Rd}} = \frac{f_y}{\gamma_{\text{M0}}} W_{\text{eff}} = \frac{235 \cdot 10^6}{1,0} \cdot 24185 \cdot 10^{-6} = 5683 \cdot 10^3 \text{ Nm}$$

$$\eta_1 = \frac{M_{\text{Ed}}}{M_{\text{Rd}}} = \frac{5167 \cdot 10^3}{5683 \cdot 10^3} = 0,909 \leq 1 \quad \checkmark$$

$$\sigma_{\text{Ed,max}} = \eta_1 \frac{f_y}{\gamma_{\text{M0}}} = 0,909 \frac{235 \cdot 10^6}{1,0} = 214 \cdot 10^6 \text{ N/m}^2$$

$$\sigma_{\text{c,max}} = \sigma_{\text{Ed,max}} = 214 \cdot 10^6 \text{ N/m}^2$$

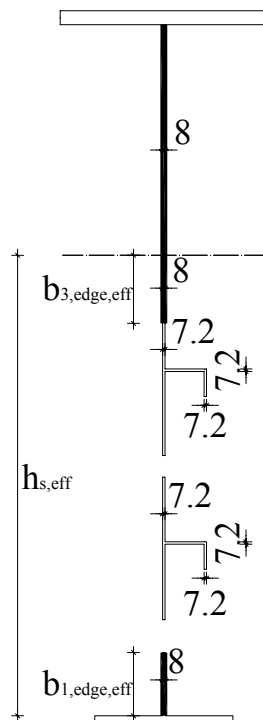


Figure 17.14: Panel III – effective geometry

Bending check at “average” bending moment in the panel

If verification at maximum bending moment cannot be fulfilled then, it is allowed to carry out the plate buckling verification of the panel for the stress resultants at a distance $\min(0,4a'; 0,5b)$ from the panel end where bending moments are the largest (EN 1993-1-5, 4.6(3)). For stiffened panels b should be taken as the maximum subpanel height.

$$x = \min(0,4a' ; 0,5(h_w - h_{w2})) = \min(0,4 \cdot 2,0 ; 0,5(2,0 - 1,0))$$

$$x = \min(0,8 ; 0,5) = 0,50 \text{ m}$$

$$M_{Ed} = 4608 \cdot 10^3 \text{ Nm}$$

$$\eta_{I1} = \frac{M_{Ed}}{\frac{f_y}{\gamma_{M0}} W_{eff}} = \frac{4608 \cdot 10^3}{\frac{235 \cdot 10^6}{1,0} \cdot 24185 \cdot 10^{-6}} = 0,881 \leq 1 \quad \checkmark$$

In this case the gross sectional resistance needs to be checked for the maximum bending moment.

$$W = \frac{I}{h_s + \frac{t_{fl}}{2}} = \frac{32863,87 \cdot 10^{-6}}{1,342 + \frac{0,02}{2}} = 24308 \cdot 10^{-6} \text{ m}^3$$

$$\eta_{I1} = \frac{M_{Ed}}{\frac{f_y}{\gamma_{M0}} W} = \frac{4608 \cdot 10^3}{\frac{235 \cdot 10^6}{1,0} \cdot 24308 \cdot 10^{-6}} = 0,807 \leq 1 \quad \checkmark$$

17.5.9 Resistance to shear

$V_{Ed} = 1139 \cdot 10^3 \text{ N}$, see Figure 17.3.

Contribution of the web

Stiffened panel

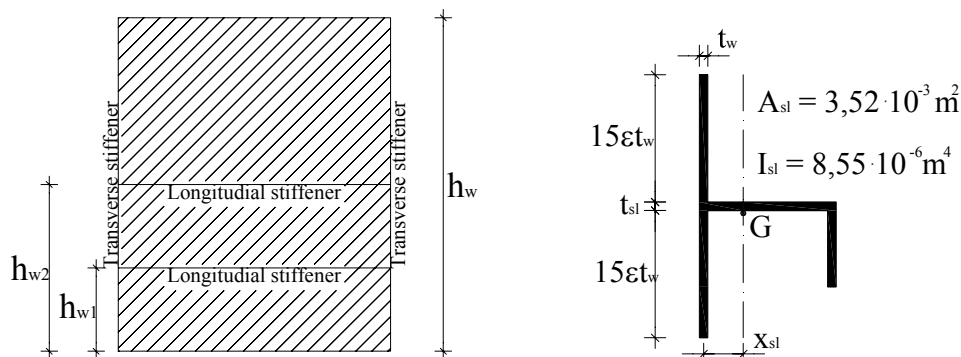


Figure 17.15: Panel III – longitudinal stiffeners

$$A_{sl} = (b_{sl} + h_{sl} - t_{sl})t_{sl} + 30\epsilon t_w^2 + t_{sl}t_w = 3,52 \cdot 10^{-3} \text{ m}^2$$

$$x_{sl} = \frac{(h_{sl} - t_{sl})t_{sl}\left(\frac{t_w}{2} + b_{sl} - \frac{t_{sl}}{2}\right) + b_{sl}t_{sl}\left(\frac{t_w + b_{sl}}{2}\right)}{A_{sl}} = 0,037 \text{ m}$$

$$I_{sl} = \frac{(30\epsilon t_w + t_{sl})t_w^3}{12} + \frac{(h_{sl} - t_{sl})t_{sl}^3}{12} + \frac{t_{sl}b_{sl}^3}{12} + (30\epsilon t_w + t_{sl})t_w x_{sl}^2 + (h_{sl} - t_{sl})t_{sl}\left(b_{sl} + \frac{t_w - t_{sl}}{2} - x_{sl}\right)^2 + b_{sl}t_{sl}\left(\frac{t_w + b_{sl}}{2} - x_{sl}\right)^2 = 8,55 \cdot 10^{-6} \text{ m}^4$$

$$\frac{a'}{h_w} = \frac{2}{2} = 1 \leq 3, \text{ two longitudinal stiffeners} \Rightarrow$$

$$k_\tau = 4,1 + \frac{6,3 + 0,18 \frac{\sum I_{sl}}{t_w^3 h_w}}{\left(\frac{a'}{h_w}\right)^2} + 2,2 \sqrt[3]{\frac{\sum I_{sl}}{t_w^3 h_w}}$$

$$k_\tau = 4,1 + \frac{6,3 + 0,18 \cdot \frac{2 \cdot 8,55 \cdot 10^{-6}}{0,008^3 \cdot 2,00}}{\left(\frac{2}{2}\right)^2} + 2,2 \cdot \sqrt[3]{\frac{2 \cdot 8,55 \cdot 10^{-6}}{0,008^3 \cdot 2,000}}$$

$$k_\tau = 19,03$$

$$\bar{\lambda}_w = \frac{h_w / t_w}{37,4\epsilon \sqrt{k_\tau}} = \frac{2,000 / 0,008}{37,4 \cdot 1 \cdot \sqrt{19,03}} = 1,532$$

Individual panel

The panel with the largest aspect ratio (at equal lengths) is critical.

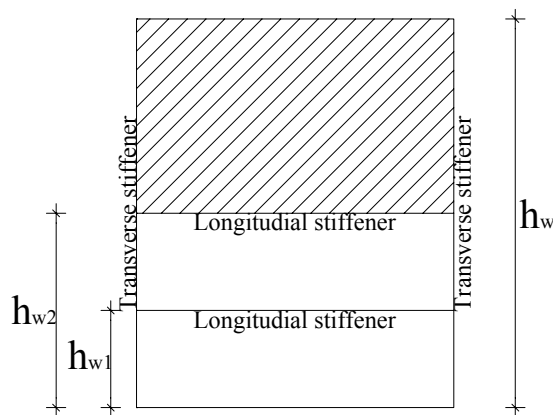


Figure 17.16: Panel III – critical panel

$k_{\tau, st} = 0$ – No stiffener within the panel.

$$\frac{a'}{h_w - h_{w2}} = \frac{2}{1} = 2 \geq 1 \Rightarrow k_{\tau} = 5,34 + 4,00 \left(\frac{h_w - h_{w2}}{a'} \right)^2 = 5,34 + 4 \left(\frac{1}{2} \right)^2 = 6,340$$

$$\bar{\lambda}_{w1} = \frac{1,000/0,008}{37,4 \cdot 1 \cdot \sqrt{6,340}} = 1,327$$

Design shear resistance

$\bar{\lambda}_w = 1,532 > \bar{\lambda}_{w1} = 1,327$ Buckling of stiffened panel is critical.

$\bar{\lambda}_w = 1,532 > 1,08 \Rightarrow$

$$\chi_w = \frac{1,37}{0,7 + \bar{\lambda}_w} = \frac{1,37}{0,7 + 1,532} = 0,614$$

$$V_{bw, Rd} = \frac{\chi_w f_{yw} h_w t_w}{\gamma_{M1} \sqrt{3}} = \frac{0,614 \cdot 235 \cdot 10^6 \cdot 2,000 \cdot 0,008}{1,1 \sqrt{3}} = 1212 \cdot 10^3 \text{ N}$$

Contribution of flanges

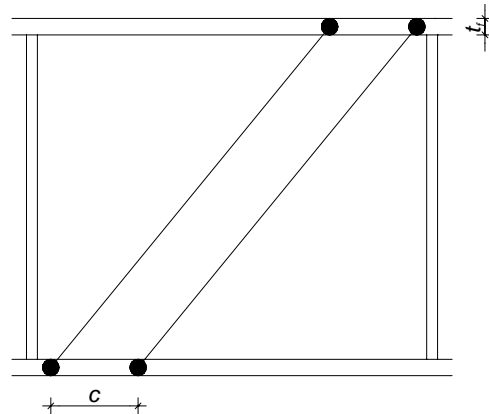


Figure 17.17: Panel III – contribution of flanges

$$M_{f, Rd} = \min(30\epsilon t_f + t_w; b_{f1}) t_f \left(h_w + \frac{t_{f1} + t_{f2}}{2} \right) \frac{f_y}{\gamma_{M0}} = b_{f1} t_{f1} \left(h_w + \frac{t_{f1} + t_{f2}}{2} \right) \frac{f_y}{\gamma_{M0}}$$

$$M_{f, Rd} = 0,400 \cdot 0,02 \cdot \left(2,000 + \frac{0,02 + 0,04}{2} \right) \frac{235 \cdot 10^6}{1,0}$$

$$M_{f, Rd} = 3816 \cdot 10^3 \text{ Nm}$$

$$M_{Ed} = 5167 \cdot 10^3 \text{ Nm} > M_{f, Rd} = 3816 \cdot 10^3 \text{ Nm}$$

and

$$M_{Ed} = M_{Rd} = 5167 \cdot 10^3 \text{ Nm (see 0)}$$

$$V_{bf, Rd} = 0$$

because the flange resistance is yet completely utilized in resisting the bending moment.

Verification of shear resistance

$$\eta = 1,2 \text{ (S235)}$$

$$V_{b,Rd} = V_{bw,Rd} + V_{bf,Rd} = 1212 \cdot 10^3 \text{ N} \leq \frac{\eta f_{yw} h_w t_w}{\gamma_{M1} \sqrt{3}} = \frac{1,2 \cdot 235 \cdot 10^6 \cdot 2 \cdot 0,008}{1,1 \cdot \sqrt{3}} = 2368 \cdot 10^3 \text{ N}$$

$$\eta_3 = \frac{V_{Ed}}{V_{b,Rd}} = \frac{1139 \cdot 10^3}{1212 \cdot 10^3} = 0,940 \leq 1,00 \quad \checkmark$$

17.5.10 Interaction M-V

Interaction should be verified at all sections other than those located at a distance less than $\frac{h_w}{2}$ from the interior support, see EN 1993-1-5, 7.1(2). For stiffened panels h_w should be taken as the maximum subpanel height.

$$V_{Ed} = 1096 \cdot 10^3 \text{ N (see Figure 17.3)}$$

$$M_{Ed} = 4608 \cdot 10^3 \text{ Nm (0,5(h}_w - h_{w2}) \text{ from the interior support - } x = 20,5 \text{ m)}$$

$$\bar{\eta}_3 = \frac{V_{Ed}}{V_{bw,Rd}} = \frac{1096}{1212} = 0,904 \geq 0,5 \quad \boxtimes$$

The interaction between M_{Ed} and V_{Ed} needs to be checked.

$$A_{full} = A + 2(b_{sl} + h_{sl} - t_{sl})t_{sl} = 51,072 \cdot 10^{-3} \text{ m}^2$$

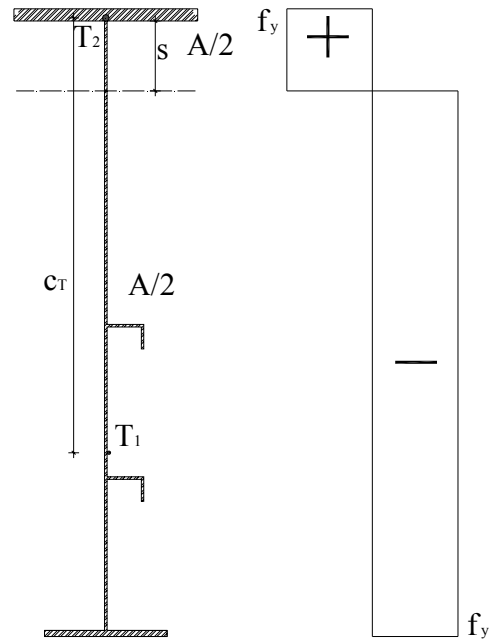


Figure 17.18: Panel III – plastic stress distribution

$$s = \frac{\frac{A_{full}}{2} - b_{f2}t_{f2}}{t_w} = 0,192 \text{ m}$$

$$c_T = \frac{b_{f1}t_{f1} \left(h_w - s + \frac{t_{f1}}{2} \right) + \frac{(h_w - s)^2 t_w}{2} + b_{f1}t_{f1} + (h_w - s)t_w + 2(b_{sl} + h_{sl} - t_{sl})t_{sl} + \frac{b_{sl}t_{sl}(2h_w - h_{w1} - h_{w2} - 2s) + (h_{sl} - t_{sl})t_{sl}(2h_w - 2s - h_{w1} - h_{w2} + h_{sl})}{b_{f1}t_{f1} + (h_w - s)t_w + 2(b_{sl} + h_{sl} - t_{sl})t_{sl}} + \frac{b_{f2}t_{f2} \left(s + \frac{t_{f2}}{2} \right) + \frac{s^2 t_w}{2}}{b_{f2}t_{f2} + s t_w}$$

$$c_T = 1,416 \text{ m}$$

$$W_{pl} = \frac{A_{full}}{2} c_T = \frac{51,072 \cdot 10^{-3}}{2} \cdot 1,416 = 36,159 \cdot 10^{-3} \text{ m}^3$$

$$M_{pl,Rd} = W_{pl} \frac{f_y}{\gamma_{M0}} = 36,159 \cdot 10^{-3} \cdot \frac{235 \cdot 10^6}{1,0} = 8497 \cdot 10^3 \text{ Nm}$$

$$M_{f,Rd} = A_{f,MIN} h_T \frac{f_y}{\gamma_{M0}} = 0,40 \cdot 0,02 \cdot 2,03 \cdot \frac{235 \cdot 10^6}{1,0} = 3816 \cdot 10^3 \text{ Nm}$$

$$\bar{\eta}_1 = \frac{M_{Ed}}{M_{pl,Rd}} = \frac{4608}{8479} = 0,542$$

$$\bar{\eta}_1 + \left(1 - \frac{M_{f,Rd}}{M_{pl,Rd}}\right) (2\bar{\eta}_3 - 1)^2$$

$$0,542 + \left(1 - \frac{3816}{8497}\right) (20,904 - 1)^2 = 0,902 \leq 1 \quad \checkmark$$

In areas of strong moment gradients this rule is usually not decisive.

17.5.11 Minimum requirements for longitudinal stiffeners

To prevent torsional buckling of stiffeners the following two checks may be performed.

Simplified check neglecting warping stiffness

$$\frac{I_t}{I_p} \geq 5,3 \frac{f_y}{E},$$

where

I_p is the polar second moment of area of the stiffener alone around the edge fixed to the plate;

I_t is the St. Venant torsional constant for the stiffener alone.

$$I_t = \frac{1}{3} \sum_i b_i t_i^3 = \frac{1}{3} (b_{sl} + h_{sl} - t_{sl}) t_{sl}^3 = \frac{0,12 + 0,08 - 0,008}{3} \cdot 0,008^3 = 32,77 \cdot 10^{-9} \text{ m}^4$$

$$I_y = \frac{t_{sl} b_{sl}^3}{3} + \frac{t_{sl}^3 (h_{sl} - t_{sl})}{12} + t_{sl} (h_{sl} - t_{sl}) \left(b_{sl} - \frac{t_{sl}}{2}\right)^2$$

$$I_y = \frac{0,008 \cdot 0,12^3}{3} + \frac{0,008^3 (0,8 - 0,008)}{12} + 0,008 \cdot (0,8 - 0,008) \left(0,12 - \frac{0,008}{2}\right)^2$$

$$I_y = 12,36 \cdot 10^{-6} \text{ m}^4$$

$$I_z = \frac{b_{sl} t_{sl}^3}{12} + \frac{t_{sl}^3 (h_{sl} - t_{sl})}{12} + t_{sl} (h_{sl} - t_{sl}) \left(\frac{h_{sl}}{2}\right)^2$$

$$I_z = \frac{0,12 \cdot 0,008^3}{12} + \frac{0,008 \cdot (0,8 - 0,008)^3}{12} + 0,008 \cdot (0,8 - 0,008) \left(\frac{0,8}{2}\right)^2 = 1,18 \cdot 10^{-6} \text{ m}^4$$

$$I_p = I_y + I_z = (12,36 + 1,18) \cdot 10^{-6} = 13,54 \cdot 10^{-6} \text{ m}^4$$

$$\frac{I_t}{I_p} = \frac{32,77 \cdot 10^{-9}}{13,54 \cdot 10^{-6}} = 0,0024 \not\geq 5,3 \frac{f_y}{E} = 0,0059 \quad \boxtimes$$

With only Saint Venant torsional stiffness taken into account minimum requirement for longitudinal stiffeners is not satisfied.

Warping stiffness is considered

If also warping stiffness is considered, the criterion is

$$\sigma_{cr} \geq \Theta \cdot f_y .$$

The recommended value of Θ is $\Theta = 6$.

The well known expression for σ_{cr} at torsional buckling reads:

$$\sigma_{cr} = \frac{1}{I_p} \left(GI_t + \frac{\pi^2 EI_w}{a^2} \right),$$

where

I_w is warping constant,

a is length of the stiffener

$$I_w = t_{sl} \frac{\left(b_{sl} - \frac{t_{sl}}{2} \right) h_{sl}^2}{2} \frac{2}{3} \left(b_{sl} - \frac{t_{sl}}{2} \right) h_{sl} = \frac{\left(b_{sl} - \frac{t_{sl}}{2} \right)^2 h_{sl}^3 t_{sl}}{3}$$

$$I_w = \frac{\left(0,12 - \frac{0,008}{2} \right)^2 0,08^3 \cdot 0,008}{3} = 18,372 \cdot 10^{-9} \text{ m}^6$$

$$\sigma_{cr} = \frac{1}{13,54 \cdot 10^{-6}} \left(80,77 \cdot 10^9 \cdot 32,77 \cdot 10^{-9} + \frac{\pi^2 210 \cdot 10^9 \cdot 18,372 \cdot 10^{-9}}{2,00^2} \right)$$

$$\sigma_{cr} = 899 \cdot 10^6 \text{ N/m}^2 \not\geq 6f_y = 6 \cdot 235 \cdot 10^6 = 1410 \cdot 10^6 \text{ N/m}^2 \quad \boxtimes$$

Minimum requirement for longitudinal stiffeners is still not satisfied.

EN 1993-1-5 does not give the formula for σ_{cr} , but to fulfil the requirement

$$\sigma_{cr} \geq 6f_y$$

the critical stress for torsional buckling of the stiffener σ_{cr} may be calculated taking into account restraining from the plating. The stiffener is considered as a column on the continuous elastic torsional support c_θ , see EN 1993-1-5, 9.2.1. Similar approach is used Annex A.2 of EN 1993-1-5 for the calculation of critical plate buckling stress for plates with one or two stiffeners. c_θ can be taken as (exact value for large number of stiffeners)

$$c_\theta = \frac{4EI_{plate}}{b} = \frac{Et^3}{3b},$$

where

b is the distance between stiffeners.

For this case the critical stress σ_{cr} is given as:

$$\sigma_{cr} = \frac{1}{I_p} \left(EI_w \frac{m^2 \pi^2}{l^2} + \frac{c_\theta l^2}{m^2 \pi^2} + GI_t \right),$$

where

m is number of buckling half waves,

l is length of the panel ($b = a$).

The minimum value of critical stress is

$$\sigma_{cr-min} = \frac{1}{I_p} \left(2\sqrt{c_\theta EI_w} + GI_t \right).$$

This formula is valid for stiffeners longer than l_{cr} .

$$l_{cr} = \pi^4 \sqrt{\frac{EI_w}{c_\theta}}.$$

For shorter stiffeners with the basic expression for σ_{cr} applies with $m = 1$.

$$c_\theta = \frac{Et_w^3}{3b} = \frac{210 \cdot 10^9 \cdot 0,008^3}{3 \cdot 0,50} = 71,68 \cdot 10^3 \text{ N}$$

$$l_{cr} = \pi^4 \sqrt{\frac{EI_w}{c_\theta}} = \pi^4 \sqrt{\frac{210 \cdot 10^9 \cdot 18,372 \cdot 10^{-9}}{71,68 \cdot 10^3}} = 1,513 \text{ m} < a' = 2,000 \text{ m}$$

$$\sigma_{cr-min} = \frac{1}{13,54 \cdot 10^{-6}} \left(2\sqrt{71,68 \cdot 10^3 \cdot 210 \cdot 10^9 \cdot 18,372 \cdot 10^{-9}} + 80,77 \cdot 10^9 \cdot 32,77 \cdot 10^{-9} \right)$$

$$\sigma_{cr-min} = 2652 \cdot 10^6 \text{ N/m}^2 \geq 6f_y = 6 \cdot 235 \cdot 10^6 = 1410 \cdot 10^6 \text{ N/m}^2 \quad \checkmark$$

Consequently, the minimum requirement for the longitudinal stiffeners is satisfied.

17.5.12 Intermediate transverse stiffeners

The transverse stiffeners are checked for the most severe conditions at the location close to the interior support. It can be easily shown that the same stiffener cross section fulfils the relevant requirements also in midspan region where the web is not stiffened with longitudinal stiffeners.

One-sided T stiffeners: $h_{st} / b_{st} / t_{st,w} / t_{st,f} = 180 / 180 / 10 / 20 \text{ mm}$ (class 3)

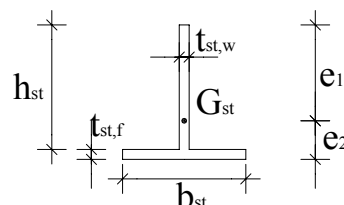


Figure 17.19: Intermediate transverse stiffener

$$A_{st} = h_{st} t_{st,w} + b_{st} t_{st,f} = 0,18 \cdot 0,01 + 0,18 \cdot 0,02 = 5,40 \cdot 10^{-3} \text{ m}^2$$

$$e_1 = \frac{\frac{h_{st}^2}{2} t_{st,w} + b_{st} t_{st,f} \left(h_{st} + \frac{t_{st,f}}{2} \right)}{A_{st}} = \frac{\frac{0,18^2}{2} 0,01 + 0,18 \cdot 0,02 \left(0,18 + \frac{0,02}{2} \right)}{5,40 \cdot 10^{-3}} = 156,7 \cdot 10^{-3} \text{ m}$$

$$e_2 = h_{st} + t_{st,f} - e_1 = 0,18 + 0,02 - 156,7 \cdot 10^{-3} = 43,3 \cdot 10^{-3} \text{ m}$$

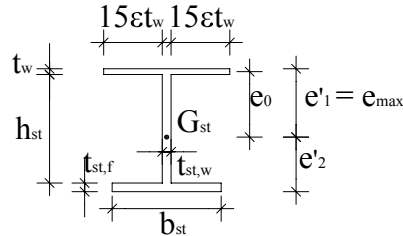


Figure 17.20: Intermediate transverse stiffener with adjacent parts

$$A'_{st} = A_{st} + (2 \cdot 15\epsilon_w + t_{st,w}) t_w = 5,4 \cdot 10^{-3} + (2 \cdot 15 \cdot 1 \cdot 0,008 + 0,01) \cdot 0,008 = 7,4 \cdot 10^{-3} \text{ m}^2$$

$$e'_1 = \frac{1}{A'_{st}} \left((2 \cdot 15\epsilon_w + t_{st,w}) \frac{t_w^2}{2} + h_{st} t_{st,w} \left(t_w + \frac{h_{st}}{2} \right) + b_{st} t_{st,f} \left(t_w + h_{st} + \frac{t_{st,f}}{2} \right) \right) =$$

$$= \frac{1}{7,4 \cdot 10^{-3}} \left((2 \cdot 15 \cdot 1 \cdot 0,008 + 0,01) \frac{0,008^2}{2} + 0,18 \cdot 0,01 \left(0,008 + \frac{0,18}{2} \right) + \right.$$

$$\left. + 0,18 \cdot 0,02 \left(0,008 + 0,18 + \frac{0,02}{2} \right) \right)$$

$$e'_1 = 121,2 \cdot 10^{-3} \text{ m}$$

$$e'_2 = t_w + h_{st} + t_{st,f} - e'_1 = 0,008 + 0,18 + 0,02 - 121,2 \cdot 10^{-3} = 86,8 \cdot 10^{-3} \text{ m}$$

$$I'_{st} = \frac{(2 \cdot 15\epsilon_w + t_{st,w}) t_w^3}{12} + \frac{h_{st}^3 t_{st,w}}{12} + \frac{b_{st,w} t_{st,f}^3}{12} + (2 \cdot 15\epsilon_w + t_{st,w}) \cdot t_w \left(e'_1 - \frac{t_w}{2} \right)^2$$

$$+ h_{st} t_{st,w} \left(e'_1 - \frac{h_{st}}{2} - t_w \right)^2 + b_{st} t_{st,f} \left(e'_2 - \frac{t_{st,f}}{2} \right)^2$$

$$I'_{st} = \frac{(2 \cdot 15 \cdot 1 \cdot 0,008 + 0,01) \cdot 0,008^3}{12} + \frac{0,18^3 \cdot 0,01}{12} + \frac{0,18 \cdot 0,02^3}{12}$$

$$+ (2 \cdot 15 \cdot 1 \cdot 0,008 + 0,01) \cdot 0,008 \left(121,2 \cdot 10^{-3} - \frac{0,008}{2} \right)^2$$

$$+ 0,18 \cdot 0,01 \left(121,2 \cdot 10^{-3} - \frac{0,18}{2} - 0,008 \right)^2 + 0,18 \cdot 0,02 \left(86,8 \cdot 10^{-3} - \frac{0,02}{2} \right)^2$$

$$I'_{st} = 54,66 \cdot 10^{-6} \text{ m}^4$$

Torsional buckling

Second moments of areas around the point of stiffener-to-web junction:

$$I_y = \frac{h_{st}^3 t_{st,w}}{12} + \frac{b_{st} t_{st,f}^3}{12} + h_{st} t_{st,w} \left(e_1 - \frac{h_{st}}{2} \right)^2 + b_{st} t_{st,f} \left(e_2 - \frac{t_{st,f}}{2} \right)^2 + A_{st} e_1^2$$

$$I_y = \frac{0,18^3 \cdot 0,01}{12} + \frac{0,18 \cdot 0,02^3}{12} + 0,18 \cdot 0,01 \left(156,7 \cdot 10^{-3} - \frac{0,18}{2} \right)^2 + 0,18 \cdot 0,02 \left(43,3 \cdot 10^{-3} - \frac{0,02}{2} \right)^2 + 5,40 \cdot 10^{-3} \cdot \left(156,7 \cdot 10^{-3} \right)^2 = 149,58 \cdot 10^{-6} \text{ m}^4$$

$$I_z = \frac{h_{st} t_{st,w}^3}{12} + \frac{b_{st}^3 h_{st,f}}{12} = \frac{0,18 \cdot 0,01^3}{12} + \frac{0,18^3 \cdot 0,02}{12} = 9,74 \cdot 10^{-6} \text{ m}^4$$

$$I_p = I_y + I_z = 149,58 \cdot 10^{-6} + 9,74 \cdot 10^{-6} = 159,32 \cdot 10^{-6} \text{ m}^4$$

$$I_w = \frac{b_{st}^3 t_{st,f}}{12} \left(h_{st} + \frac{t_{st,f}}{2} \right)^2 = \frac{0,18^3 \cdot 0,02}{12} \left(0,18 + \frac{0,02}{2} \right)^2 = 350,892 \cdot 10^{-9} \text{ m}^6$$

$$I_t = \frac{1}{3} (h_{st} t_{st,w}^3 + b_{st} t_{st,f}^3) = \frac{1}{3} (0,18 \cdot 0,01^3 + 0,18 \cdot 0,02^3) = 540 \cdot 10^{-9} \text{ m}^4$$

$$\sigma_{cr} = \frac{1}{I_p} \left(GI_t + \frac{\pi^2 EI_w}{h_w^2} \right) \geq 6 \cdot f_y$$

$$\sigma_{cr} = \frac{1}{159,32 \cdot 10^{-6}} \left(80,77 \cdot 10^9 \cdot 540 \cdot 10^{-9} + \frac{\pi^2 \cdot 210 \cdot 10^9 \cdot 350,892 \cdot 10^{-9}}{2,00^2} \right) = 1415 \cdot 10^6 \text{ N/m}^2$$

$$\sigma_{cr} = 1415 \cdot 10^6 \text{ N/m}^2 \geq 6 \cdot 235 = 1410 \cdot 10^6 \text{ N/m}^2 \quad \checkmark$$

The check of torsional buckling is decisive in this case (see the subsequent checks). However, axial forces in transverse stiffener are usually small and the check $\sigma_{cr} \geq 6f_y$ is usually very conservative. To overcome this problem the limiting slenderness may be calculated with the maximum design compressive stress $\sigma_{com,Ed}$ in the stiffener replacing f_y . In this case the torsional buckling check changes to

$$\sigma_{cr} \geq 6 \cdot \sigma_{com,Ed} \gamma_{M1}$$

Minimum requirements for transverse stiffeners (shear)

$$a'/h_w = \frac{2,00}{2,00} = 1 < \sqrt{2} \Rightarrow$$

$$I'_{st} = 54,66 \cdot 10^{-6} \text{ m}^4 \geq \frac{1,5 h_w^3 t_w^3}{a'^2} = \frac{1,5 \cdot 2,00^3 \cdot 0,008^3}{2,00^2} = 1,536 \cdot 10^{-6} \text{ m}^4$$

Transverse stiffeners act as rigid supports for web panel.

Additional compression axial force in transverse stiffener from the tension field action

$V_{Ed} = 1054 \cdot 10^3 \text{ N}$ (0,5 h_w from the edge of the panel – $x = 20 \text{ m}$, see Figure 17.3)

Slenderness parameter $\bar{\lambda}_w$ for shear is calculated in section 17.5.9 (Design shear resistance).

$$\bar{\lambda}_w = 1,532$$

Intermediate rigid stiffeners may be designed for an axial force equal to $N_{st,Ed}$ according to EN 1993-1-5, 9.3.3(3). In the case of variable shear forces the check is performed for the shear force at the distance 0,5 h_w from the edge of the panel with the largest shear force.

$$N_{st,Ed} = V_{Ed} - \frac{h_w t_w f_{yw}}{\bar{\lambda}_w^2 \gamma_{M1} \sqrt{3}} = 1054 \cdot 10^3 - \frac{2,00 \cdot 0,008 \cdot 235 \cdot 10^6}{1,532^2 \cdot 1,1 \cdot \sqrt{3}} = 213,2 \cdot 10^3 \text{ N}$$

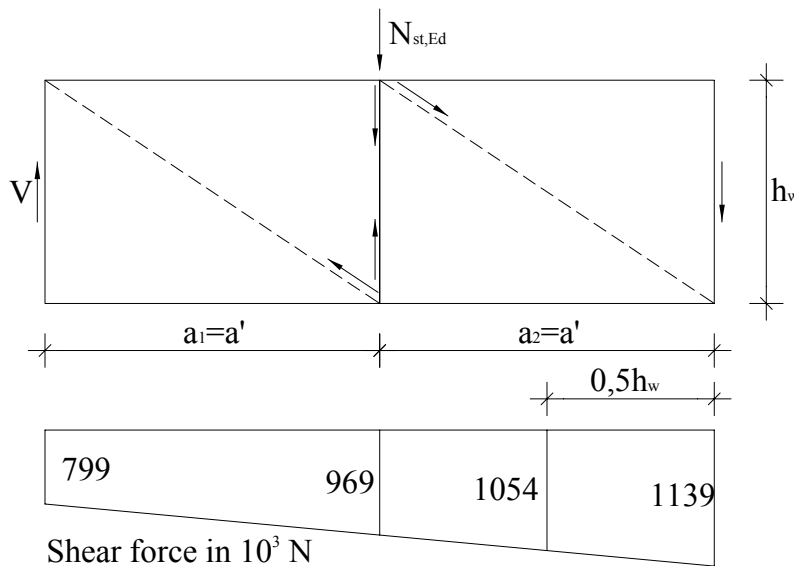


Figure 17.21: Intermediate transverse stiffener – shear force

Axial force from the deviation forces

$$\frac{\sigma_{cr,c}}{\sigma_{cr,p}} = \frac{1554 \cdot 10^6}{862 \cdot 10^6} = 1,80 \geq 1 \Rightarrow \frac{\sigma_{cr,c}}{\sigma_{cr,p}} = 1$$

$$\sigma_m = \frac{\sigma_{cr,c}}{\sigma_{cr,p}} \cdot \frac{N_{Ed}}{h_w} \left(\frac{1}{a_1} + \frac{1}{a_2} \right) = 1 \cdot \frac{N_{Ed}}{h_w} \left(\frac{1}{a_1} + \frac{1}{a_2} \right)$$

$$\sigma_{c,max} = 214 \cdot 10^6 \text{ N/m}^2 \text{ (see 17.5.8)}$$

$$N_{Ed} = \sigma_{c,max} \frac{A_{c,eff}}{2} = 214 \cdot 10^6 \frac{11,561 \cdot 10^{-3}}{2} = 1237 \cdot 10^3 \text{ N}$$

$$\sigma_m = 1 \cdot \frac{1235 \cdot 10^3}{2,00} \left(\frac{1}{2,00} + \frac{1}{2,00} \right) = 617,5 \cdot 10^3 \text{ N/m}^2$$

$$\Delta N_{st,Ed} = \frac{\sigma_m h_w^2}{\pi^2} = \frac{617,5 \cdot 10^3 \cdot 2,00^2}{\pi^2} = 250,3 \cdot 10^3 \text{ N}$$

Strength and stiffness check of the stiffener at ULS

$$\Sigma N_{st,Ed} = N_{st,Ed} + \Delta N_{st,Ed} = 213,2 \cdot 10^3 + 250,3 \cdot 10^3 = 463,5 \cdot 10^3 \text{ N}$$

Single sided transverse stiffeners are not treated explicitly in the EN 1993-1-5. In this numerical example relevant stress and displacement checks

$$\sigma_{\max} \leq f_y$$

$$w \leq \frac{h_w}{300}$$

are performed according to the interaction formula given in 9.2.1 of the commentary to EN 1993-1-5. This interaction formula is based on the second order elastic analysis and takes account of the stiffener eccentricity and simultaneous action of deviation forces and the axial forces from the tension field action.

$$N_{cr,st} = \frac{\pi^2 EI_{st}}{h_w^2} = \frac{\pi^2 \cdot 210 \cdot 10^9 \cdot 54,66 \cdot 10^{-6}}{2,00^2} = 28322 \cdot 10^3 \text{ N}$$

$$e_{\max} = e'_1 = 121,2 \cdot 10^{-3} \text{ m}$$

$$e_0 = e_{\max} - \frac{t_w}{2} = 121,2 \cdot 10^{-3} - \frac{0,008}{2} = 117,2 \cdot 10^{-3} \text{ m}$$

$$w_0 = \min \left(\frac{a_1}{300}; \frac{a_2}{300}; \frac{h_w}{300} \right) = \min \left(\frac{2,00}{300}; \frac{2,00}{300}; \frac{2,00}{300} \right) = 6,7 \cdot 10^{-3} \text{ m}$$

$$q_m = \frac{N_{st,Ed} \cdot e_0}{\sum N_{st,Ed} \cdot w_0} = \frac{213,2 \cdot 10^3 \cdot 117,2 \cdot 10^{-3}}{463,5 \cdot 10^3 \cdot 6,7 \cdot 10^{-3}} = 8,0$$

$$\sigma_{\max} = \frac{N_{st,Ed}}{A'_{st}} + \frac{\sum N_{st,Ed} e_{\max} w_0}{I'_{st}} \cdot \frac{1}{1 - \frac{\sum N_{st,Ed}}{N_{cr,st}}} (1 + 1,11 q_m) \leq \frac{f_y}{\gamma_{M1}}$$

$$\sigma_{\max} = \frac{213,2 \cdot 10^3}{7,40 \cdot 10^{-3}} + \frac{463,5 \cdot 10^3 \cdot 117,2 \cdot 10^{-3} \cdot 6,7 \cdot 10^{-3}}{54,66 \cdot 10^{-6}} \cdot \frac{1}{1 - \frac{463,5 \cdot 10^3}{28322 \cdot 10^3}} (1 + 1,11 \cdot 8,0)$$

$$\sigma_{\max} = 98,0 \cdot 10^6 \text{ N/m}^2 \leq \frac{235 \cdot 10^6}{1,1} = 213,6 \cdot 10^6 \text{ N/m}^2 \quad \checkmark$$

$$w = w_0 \frac{1}{\frac{N_{cr,st}}{\sum N_{st,Ed}} - 1} (1 + 1,25 q_m) \leq \frac{h_w}{300}$$

$$w = 6,7 \cdot 10^{-3} \frac{1}{\frac{28322 \cdot 10^3}{463,5 \cdot 10^3} - 1} (1 + 1,25 \cdot 8,0) = 1,2 \cdot 10^{-3} \text{ m} \leq \frac{2,00}{300} = 6,7 \cdot 10^{-3} \text{ m} \quad \checkmark$$

Consequently, the minimum requirement for the transverse stiffness is satisfied.

17.6 Web to flange weld

Web to flange weld may be designed for nominal shear flow:

$$v'_{II} = \frac{V_{Ed}}{h_w}, \text{ if } V_{Ed} \leq \chi_w h_w t_w \frac{f_{yw}}{\gamma_{M1} \sqrt{3}},$$

else the weld should be designed for the shear flow:

$$v'_{II} = \eta \frac{f_{yw}}{\gamma_{M1} \sqrt{3}} t_w.$$

$$V_{Ed} = 1139 \cdot 10^3 \text{ kN} \leq V_{b,Rd} = 1212 \cdot 10^3 \text{ N}$$

$$v'_{II} = \frac{1139 \cdot 10^3}{2,00} = 570 \cdot 10^3 \text{ N/m}$$

$t_w = 0,8 \text{ mm} \Rightarrow$ The throat thickness is chosen as $a_z = 3 \text{ mm}$.

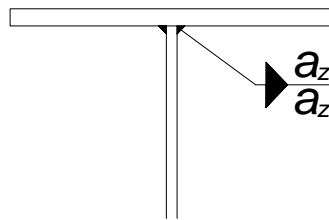


Figure 17.22: Web to flange weld

$$v_{II} = \frac{v'_{II}}{2 \cdot a_z} \leq f_{yw,d} = \frac{f_u}{\beta_w \gamma_{M2} \sqrt{3}}$$

$$v_{II} = \frac{570 \cdot 10^3}{2 \cdot 3 \cdot 10^{-3}} = 95 \cdot 10^6 \text{ N/m}^2 \leq f_{yw,d} = \frac{360 \cdot 10^6}{0,8 \cdot 1,25 \cdot \sqrt{3}} = 208 \cdot 10^6 \text{ N/m}^2 \quad \checkmark$$

17.7 Flange induced buckling

$$\frac{h_w}{t_w} = \frac{2,00}{0,008} = 250 \leq k \frac{E}{f_{yf}} \sqrt{\frac{A_w}{A_{fc}}} = 0,55 \frac{210 \cdot 10^9}{235 \cdot 10^6} \sqrt{\frac{16 \cdot 10^{-3}}{8 \cdot 10^{-3}}} = 695 \quad \checkmark$$

A_w is the cross section area of the web,

A_{fc} is the effective cross section area of the compression flange,

$$A_w = h_w \cdot t_w = 2,00 \cdot 0,008 = 16,0 \cdot 10^{-3} \text{ m}^2 \quad \text{– cross section area of the web}$$

$$A_{fc} = b_{fc} \cdot t_{fc} = 0,40 \cdot 0,02 = 8,0 \cdot 10^{-3} \text{ m}^2 \quad \text{– cross section area of the compression flange}$$

The value of the factor k should be taken as $k = 0,55$ (elastic moment resistance is utilized).

17.8 Vertical stiffener above the interior support

$$B_{Ed} = 2 \cdot 1139 = 2278 \cdot 10^3 \text{ N}$$

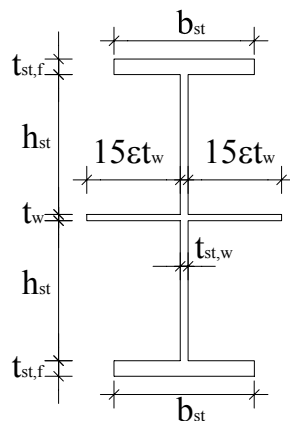


Figure 17.23: Vertical stiffener above interior support

$$A_{st,B} = (30\epsilon t_w + t_{st}) t_w + 2(t_{st,f} b_{st} + t_{st,w} h_{st})$$

$$A_{st,B} = (30 \cdot 1 \cdot 0,008 + 0,01) 0,008 + 2 \cdot (0,02 \cdot 0,18 + 0,01 \cdot 0,20)$$

$$A_{st,B} = 12,8 \cdot 10^{-3} \text{ m}^2$$

$$\sigma = \frac{B_{Ed}}{A_{st,B}} = \frac{2278 \cdot 10^3}{12,8 \cdot 10^{-3}} = 178 \cdot 10^6 \text{ N/m}^2 \leq \frac{f_y}{\gamma_{M0}} = \frac{235 \cdot 10^6}{1,0} = 235 \cdot 10^6 \text{ N/m}^2 \quad \checkmark$$

Buckling length of the stiffener:

$$l_u = 0,75h_w = 0,75 \cdot 2,00 = 1,50 \text{ m}$$

Verification of buckling design resistance of column:

$$I_{st,B} \approx \frac{b_{st} (2h_{st} + 2t_{st,f} + t_w)^3}{12} - \frac{(b_{st} - t_{st,w})(2h_{st} + t_w)^3}{12}$$

$$I_{st,B} \approx \frac{0,18(2 \cdot 0,18 + 2 \cdot 0,02 + 0,008)^3}{12} - \frac{(0,18 - 0,01)(2 \cdot 0,18 + 0,008)^3}{12} = 312,75 \cdot 10^{-6} \text{ m}^4$$

$$i_{st,B} = \sqrt{\frac{I_{st,B}}{A_{st,B}}} = \sqrt{\frac{312,75 \cdot 10^{-6}}{12,8 \cdot 10^{-3}}} = 156,3 \cdot 10^{-3} \text{ m}$$

$$\lambda = \frac{l_u}{i_{st}} = \frac{1,50}{0,1563} = 9,597 \quad \lambda_1 = 93,9\varepsilon = 93,9$$

$$\bar{\lambda} = \frac{\lambda}{\lambda_1} = \frac{9,597}{93,9} = 0,102 \quad \Rightarrow \quad \chi = 1$$

$$N_{b,Rd} = \chi A_{st,B} \frac{f_y}{\gamma_{M1}} = 1 \cdot 12,8 \cdot 10^{-3} \cdot \frac{235 \cdot 10^6}{1,1} = 2734 \cdot 10^3 \text{ N}$$

$$N_{Ed} = B_{Ed} = 2278 \cdot 10^3 \text{ N} \leq N_{b,Rd} = 2734 \cdot 10^3 \text{ N} \quad \checkmark$$

European Commission

EUR 22898 EN – Joint Research Centre

Title: Commentary and worked examples to EN 1993-1-5 "Plated structural elements"

Author(s): B. Johansson, R. Maquoi, G. Sedlacek, C. Müller, D. Beg

Luxembourg: Office for Official Publications of the European Communities

2007 – 226 pp. – 21x 29.7 cm

EUR – Scientific and Technical Research series – ISSN 1018-5593

Abstract

EN 1993-Eurocode 3 – Part 1-5 gives unified European design rules for plated structural elements made of steel which may be subject to shear lag and local and/or global plate buckling.

As these rules may be novel to many designers who so far have worked with traditional national rules this report with a commentary and worked examples gives information and guidance on the "what", the "why" and the "how" of the new European rules so that their implementation and use may be facilitated.

The report may in particular be used to confirm choices of „Nationally Determined Parameters“ and as a basis for the further harmonisation and future development of the rules.

The mission of the JRC is to provide customer-driven scientific and technical support for the conception, development, implementation and monitoring of EU policies. As a service of the European Commission, the JRC functions as a reference centre of science and technology for the Union. Close to the policy-making process, it serves the common interest of the Member States, while being independent of special interests, whether private or national.



The European Convention for Constructional Steelwork (ECCS) is the federation of the National Associations of Steelwork industries and covers a worldwide network of Industrial Companies, Universities and Research Institutes.

